2011 KRIBB Article Abstracts

Corresponding Articles Indexed in SCIE

2012. 6.

한국생명공학연구원
Korea Research Institute of Bioscience and Biotechnology

2011 KRIBB Article Abstracts

Corresponding Articles Indexed in SCIE

2012. 6.

한국생명공학연구원
Korea Research Institute of Bioscience and Biotechnology

Contents

2011
KRIBB Article Abstracts
Corresponding Articles
Indexed in SCIE

Division of Convergent BioMedical Research

- BioMedical Genomics Research Center
- BioMedical Proteomics Research Center
- Aging Research Center
- BioNanotechnology Research Center
- BioMedical Translational Research Center


KRIBB
www.kribb.re.kr

Article 1

Exploring binding sites other than the catalytic core in the crystal structure of the catalytic domain of MKP-4

Acta Crystallogr D Biol Crystall. 2011 Jan; 67(1):25-31.

Jeong DG, Yoon TS, Jung SK, Park BC, Park H, Ryu SE, Kim SJ*

*Co-corresponding: ksj@kribb.re.kr
BioMedical Proteomics Research Center

Map kinase phosphatase 4 (MKP-4), which has been implicated in signalling pathways that negatively regulate glucose uptake, belongs to the dual-specificity phosphatase (DUSP) family. An inherent property of MKPs is an ability to undergo structural rearrangement, transitioning from a partially active to a fully active conformation. Here, a 2.7 Å resolution crystal structure of the catalytic domain of MKP-4 (MKP-4C) is presented. It was determined that the MKP-4C structure seriously deviates from canonical conformations of DUSPs and this characteristic feature results in significant gaps between the catalytic core and several surrounding loops which are unique compared with other MKP counterparts that adopt an active conformation. Using virtual library screening, it was found that inhibitors bind to MKP-4C with high affinity near these gaps. Inhibitors that target other binding sites instead of the active site can be utilized to prevent transition to a fully active conformation. Compounds that are able to make contacts with these sites in MKP-4 would not only provide a beneficial increase in affinity but may also permit greater specificity relative to other protein tyrosine phosphatases.

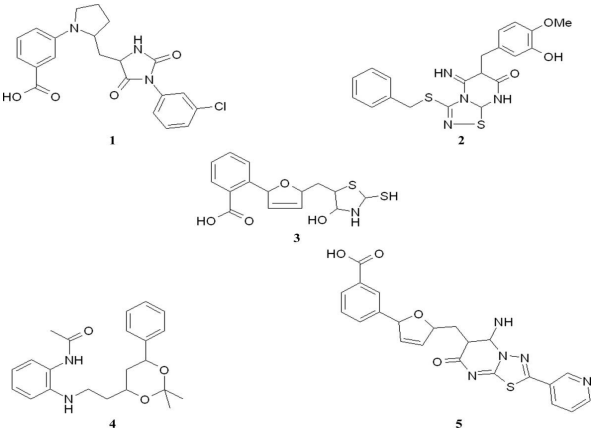

PMID: 21206059

Keywords : MAP Kinase Phosphatase 4; MKP-4; Catalytic Domain; Dual-Specificity Phosphatases; DUSP; Protein Tyrosine Phosphatases; ERK2

Article 2

Nonstick, modulus-tunable and gas-permeable replicas for mold-based, high-resolution nanolithography

Adv Funct Mater. 2011; 21(19):3681-9.

Lee BK, Cho H, Chung BH*

*Corresponding: chungbh@kribb.re.kr
BioNanotechnology Research Center

A fundamental approach to fabricating a nonstick replica mold with high performance for the manufacturing of high-resolution nanostructures using mold-based lithography is presented. Low-viscosity liquid blends consisting of methacrylate multi-functionalized silsesquioxane (SSQMA), difunctional acrylics, and a small amount of silicone diacrylate (Si-DA) with low surface tension were used as nonstick replica-mold materials. The cured SSQMA/acrylic/Si-DA networks showed a high resistance to organic solvents (<1.2 wt.%), high UV transparency (>90% at 365 nm), hydrophobicity (water contact angle >90 degrees), high modulus and wide-range modulus tunability (0.6-4.42 GPa) and small shrinkage (<3% in height). The mold materials with a nonstick property conferred by Si-DA possessed the ability to form sub-25-nm features with a high line-to-space ratio (1:1) and a high aspect ratio (4:1). In addition, a sufficiently cured replica mold with a low concentration of residual, uncross-linked (meth)acrylates was able to successfully replicate sub-25-nm features with a high line-to-space ratio (1:1) and a high aspect ratio (4:1), even if the release agent was not modified. Furthermore, replica molds can potentially be used to fabricate patterns free of bubble defects because of sufficient gas permeability.

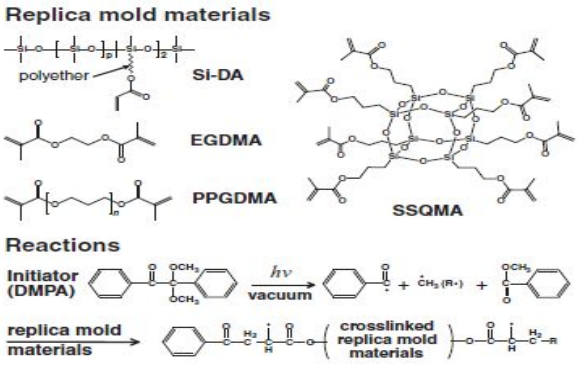

Keywords : Nanoimprint Lithography; Soft Lithography; Multifunctional Monomers; Imprint Lithography; Silicone Acrylate; Fabrication; Photopolymerization; Nanofabrication; Spectroscopy; SSQMA

Article 3

ESM-1 silencing decreased cell survival, migration, and invasion and modulated cell cycle progression in hepatocellular carcinoma

Amino Acids. 2011 Mar; 40(3):1003-13.

Kang YH, Ji NY, Lee CI, Lee HG, Kim JW, Yeom YI, Kim DG, Yoon SK, Kim JW, Park PJ, Song EY*

*Corresponding: eysong@kribb.re.kr
BioMedical Genomics Research Center

Endothelial cell-specific molecule-1 (ESM-1) is a secretory proteoglycan comprising a mature polypeptide of 165 amino acids and a single dermatan sulfate. The aim of this study was to evaluate endothelial cell-specific molecule-1 (ESM-1) as a hepatocellular carcinoma (HCC) marker and to analyze the effect of ESM-1 gene silencing in hepatocellular carcinoma cells. RT-PCR and Western Blot analysis revealed overexpression of ESM-1 in human HCC liver tissue and in serum from patients with HCC. Sandwich ELISA assay was used for quantitative analysis of ESM-1 in serum. Levels of ESM-1 were significantly elevated in the serum of patients with HCC (n = 40) as compared to serum from patients with hepatitis (AH, n = 40; CH, n = 39) or liver cirrhosis (n = 40) or from healthy subjects (n = 40). The accuracy of ESM-1 for HCC was higher than that of α-fetoprotein (AFP) according to ROC curve analysis. Expression of ESM-1 siRNA decreased cell survival through the inhibition of NF-κB pathway and induced cell cycle arrest by PTEN induction resulting in the inhibition of cyclin D1 in SK-Hep1 cells. Furthermore, ESM-1 silencing inhibited cell migration and invasion of SK-Hep1 cells. This study demonstrates that ESM-1 as a potential tumor marker is overexpressed in most tissues and serum in the presence of HCC and is involved with cell survival, cell cycle progression, migration, and invasion of hepatocellular carcinoma cells. Based on our results, we suggest that ESM-1 or a combination of ESM-1 and AFP is useful markers for diagnosis of HCC and ESM-1 may be useful therapeutic target of hepatocellular carcinoma.
PMID: 20821239

Keywords : Endothelial Cell-Specific Molecule-1; ESM-1; Hepatocellular Carcinoma; HCC; Diagnostic Marker; Cell Cycle; Cell Migration

Article 4

Combination of cysteine- and oligomerization domain-mediated protein immobilization on a surface plasmon resonance (SPR) gold chip surface

Analyst. 2011 Jun; 136(12):2506-11.

Park K, Lee JM, Jung Y, Habtemariam T, Salah AW, Fermin CD, Kim M*

*Corresponding: kimm@kribb.re.kr
BioNanotechnology Research Center

Here we report an effective method for protein immobilization on a surface plasmon resonance (SPR) gold chip, describing the combination of cysteine- and oligomerization domain-mediated immobilization of enhanced green fluorescent protein (EGFP) as a model protein for the purpose of orientation-controlled surface density packing. In order to facilitate the oligomerization of EGFP, the dimeric and trimeric constructs derived from GCN4-leucine zipper domain were chosen for multimeric EGFP assembly. For orientation-controlled immobilization of the protein, EGFP modified with cysteine residues showing excellent orientation on a gold chip was used as a starting protein, as previously reported in our earlier study (*Anal. Chem.*, 2007, 79, 2680-2687). Constructs of EGFP with oligomerization domains were genetically engineered, and corresponding fusion proteins were purified, applied to a gold chip, and then analyzed under SPR. The immobilized EGFP density on a gold chip increased according to the states of protein oligomerization, as dimeric and trimeric EGFPs displayed better adsorption capability than monomeric and dimeric forms, respectively. Fluorescence measurement corroborated the SPR results. Taken together, our findings indicated that the combination of cysteine- and oligomerization domain-mediated immobilization of protein could be used in SPR biosensor applications, allowing for an excellent orientation and high surface density simultaneously.
PMID: 21519608

Keywords : GCN4 Leucine-Zipper; Coiled-Coil; *Escherichia coli*; Microarrays; Strategies; Ectodomain; Biochips; Residues; Surface Plasmon Resonance; SPR

Article 5

Carbon nanotube-assisted enhancement of surface plasmon resonance signal

Anal Biochem. 2011 Jan; 408(2):206-11.

Lee EG, Park KM, Jeong JY, Lee SH, Baek JE, Lee HW, Jung JK, Chung BH*

*Corresponding: chungbh@kribb.re.kr
BioNanotechnology Research Center

We describe a method of amplifying the biosensing signal in surface plasmon resonance (SPR)-based immunoassays using an antibody-carbon nanotube (CNT) conjugate. As a model system, human erythropoietin (EPO) and human granulocyte macrophage colony-stimulating factor (GM-CSF) were detected by sandwich-type immunoassays using an SPR biosensor. For the amplification of the SPR signal, the CNT was conjugated with a polyclonal antibody, and then the conjugates were reacted with antibodies coupled with the target proteins. This amplification strategy increases the dynamic range of the immunoassays and enhances the detection sensitivity. The SPR immunoassays, combined with the CNT-assisted signal amplification method, provided a wide dynamic range over four orders of magnitude for both EPO and GM-CSF (0.1-1,000 ng/ml). The CNT amplification method is expected to realize the detection of picogram levels and a wide dynamic detection range of multiple proteins, enabling it to offer a robust analysis tool for the development of biopharmaceutical production.

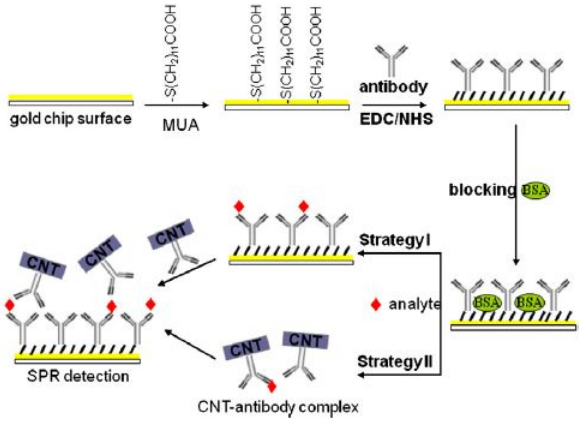

PMID: 20868647

Keywords : Surface Plasmon Resonance; SPR; Carbon Nanotube; CNT; Erythropoietin; Granulocyte Macrophage Colony-Stimulating Factor; Biosensor; Immunoassays

Article 6

Two-temperature hybridization for microarray detection of label-free microRNAs with attomole detection and superior specificity

Angew Chem Int Ed Engl. 2011 Dec; 50(52):12487-90.

Lee JM, Jung Y*

*Corresponding: ywjung@kribb.re.kr
BioNanotechnology Research Center

Two is better than one: Two short locked nucleic acid based probes were used to collectively capture and detect microRNAs by a simple two-temperature hybridization process. Intact microRNAs were directly measured down to attomolar concentrations with a high specificity and nearly four orders of magnitude of dynamic range. Single base mismatches in the microRNAs were potently discriminated from the perfectly matched targets.

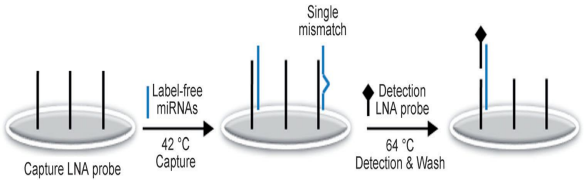

PMID: 22072424

Keywords : Biosensors; LNAs; Microarrays; microRNAs; RNA Recognition; Multiplexed Detection; Biomarkers

Article 7

Epigenomic analysis of aberrantly methylated genes in colorectal cancer identifies genes commonly affected by epigenetic alterations

Ann Surg Oncol. 2011 Aug; 18(8):2338-47.

Kim YH, Lee HC, Kim SY, Yeom YI, Ryu KJ, Min BH, Kim DH, Son HJ, Rhee PL, Kim JJ, Rhee JC, Kim HC, Chun HK, Grady WM, Kim YS*

*Corresponding: yongsung@kribb.re.kr
BioMedical Genomics Research Center

BACKGROUND: Determination of the profile of genes that are commonly methylated aberrantly in colorectal cancer (CRC) will have substantial value for diagnostic and therapeutic applications. However, there is limited knowledge of the DNA methylation pattern in CRC.
MATERIALS AND METHODS: We analyzed the methylation profile of 27,578 CpG sites spanning more than 14,000 genes in CRC and in the adjacent normal mucosa with bead-chip array-based technology.
RESULTS: We identified 621 CpG sites located in promoter regions and CpG islands that were greatly hypermethylated in CRC compared to normal mucosa. The genes on chromosome 18 showed promoter hypermethylation most frequently. According to gene ontology analysis, the most common biologically relevant class of genes affected by methylation was the class associated with the cadherin signaling pathway. Compared to the genome-wide expression array, mRNA expression was more likely to be downregulated in the genes demonstrating promoter hypermethylation, even though this was not statistically significant. We validated ten CpG sites that were hypermethylated (*ADHFE1, BOLL, SLC6A15, ADAMTS5, TFPI2, EYA4, NPY, TWIST1, LAMA1, GAS7*) and 2 CpG sites showing hypomethylation (*MAEL, SFT2D3*) in CRC compared to the normal mucosa in the array studies using pyrosequencing. The methylation status measured by pyrosequencing was consistent with the methylation array data.
CONCLUSIONS: Methylation profiling based on bead-chip arrays is an effective method for screening aberrantly methylated genes in CRC. In addition, we identified novel methylated genes that are candidate diagnostic or prognostic markers for CRC.
PMID: 21298349

Keywords : CpG Island Methylation; Fecal Occult Blood; DNA Methylation; Colon Cancer; Colorectal Cancer; CRC; Hmlh1 Promoter; Crypt Foci; Barretts-Esophagus

Article 8

Recent advances in protein tyrosine phosphatase detection using chemical probes

Anticancer Agents Med Chem. 2011 Jan; 11(1):54-63.

Lee K, Kang HJ, Xia Y, Chung SJ*

*Corresponding: sjchung@kribb.re.kr
BioNanotechnology Research Center

Protein tyrosine phosphatases (PTPs) are key regulatory enzymes in signal transduction pathways and their aberrancy has been implicated in various diseases such as cancers, metabolic syndrome, and autoimmune disorders. In spite of its great importance, determination of the functional significance of PTPs remains a major challenge, and efficient methodologies are needed to specifically delineate PTP functions. Besides the strategy to use potent and selective PTP inhibitors to study the physiological roles of the enzymes, measurement of PTP activities using specific PTP substrates or activity-based probes (ABPs) has been reported. This review focused on the recent development of small molecular probes to detect PTP activities, consisting of five sub-categories: 1. Conventional fluorescent substrates; 2. Ratiometric fluorescent PTP substrates; 3. Fluorescence substrates with selectivity to a single PTP or a class of PTPs; 4. ABPs specific for PTPs; and 5. A real-time imaging of PTP-substrate complex using a small molecule PTP probe which, offers a measurement of a real-time activity of a certain PTP in cells.

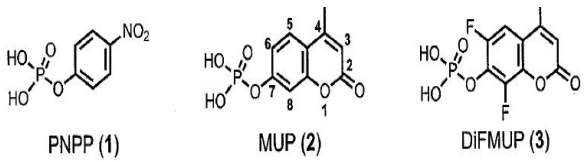

PMID: 21235434

Keywords : DiFMUP; In-gel Assay; Phosphotyrosine; Dual-Specificity PTP (DUSP); Forster Resonance Energy Transfer (FRET); 4-fluoromethylphenylphosphate (FMPP); 2-fluoromethylphosphotyrosine (FMPT)

Article 9

Genome-wide identification of chemosensitive single nucleotide polymorphism markers in gastric cancer

Anticancer Res. 2011 Dec; 31(12):4329-38.

Ha YJ, Yoon SN, Jeon YJ, Cho DH, Roh SA, Kim BS, Kim HJ, Kim SY, Kim YS*, Kim JC

*Co-corresponding: yongsung@kribb.re.kr
BioMedical Genomics Research Center

A chemosensitive single nucleotide polymorphism (SNP) discovery schema is presented that utilizes (i) genome-wide SNP screening, with a human SNP array and an *in vitro* chemosensitivity assay, in 93 patients with gastric cancer (GC), and (ii) biological utility assessment using cell viability assays of transfected GC cells. Cytotoxicity analysis showed that most of the MKN1 and SNU638 clones transfected with the G allele of Deoxyribonuclease II beta (DNASE2B) rs3738573 were more sensitive to docetaxel than those with the C allele ($p \leq 0.001$-0.029) and most of the AGS and SNU638 clones transfected with the T allele of 5-hydroxytryptamine receptor IE (HTRIE) rs3828741 were more sensitive to paclitaxel than those with the C allele ($p \leq 0.001$-0.019). Our findings show that the two novel markers, DNASE2B rs3738573 and HTR1E rs3828741, have potential for improving the prediction of chemosensitivity of GC patients.
PMID: 22199298

Keywords : Single Nucleotide Polymorphisms (SNPs); SNP Screening; Gastric Cancer; Chemosensitivity; Docetaxel; DNASE2B; HTRIE

Article 10

Translocation and oligomerization of Bax is regulated independently by activation of p38 MAPK and caspase-2 during MN9D dopaminergic neurodegeneration

Apoptosis. 2011 Nov; 16(11):1087-100.

Oh CK, Han BS*, Choi WS, Youdim MB, Oh YJ

*Co-first: bshan@kribb.re.kr
BioMedical Proteomics Research Center

Bax is translocated into the mitochondrial membrane and oligomerized therein to initiate mitochondrial apoptotic signaling. Our previous study indicated that reactive oxygen species (ROS)-mediated activation of mitogen-activated protein kinase (MAPK) and caspase is critically involved in 6-hydroxydopamine (6-OHDA)-mediated neurodegeneration. Here, we specifically attempted to examine whether and how these death signaling pathways may be linked to Bax translocation and oligomerization. We found that 6-OHDA treatment triggered translocation and oligomerization of Bax onto the mitochondria in MN9D dopaminergic neuronal cells. These events preceded cytochrome c release into the cytosol. Cross-linking assay revealed that co-treatment with a ROS scavenger or a pan-caspase inhibitor inhibited 6-OHDA-induced Bax oligomerization. Among several candidates of ROS-activated MAPKs and caspases, we found that co-treatment with PD169316 or VDVAD specifically inhibited 6-OHDA-induced Bax oligomerization, suggesting critical involvement of p38 MAPK and caspase-2. Consequently, overexpression of a dominant negative form of p38 MAPK or a shRNA-mediated knockdown of caspase-2 indeed inhibited 6-OHDA-induced Bax oligomerization. However, activation of p38 MAPK and caspase-2 was independently linked to oligomerization of Bax. This specificity was largely confirmed with a Bax 6A7 antibody known to detect activated forms of Bax on the mitochondria. Taken together, our data suggest that there is an independent amplification loop of Bax translocation and oligomerization via caspase-2 and p38 MAPK during ROS-mediated dopaminergic neurodegeneration.
PMID: 21739275

Keywords : Bax oligomerization; Caspase-2; p38 MAPK; 6-Hydroxydopamine; Etoposide-induced Apoptosis; Parkinsons-Disease; Bcl-2 Proteins

Article 11

Aberrant up-regulation of *LAMB3* and *LAMC2* by promoter demethylation in gastric cancer

Biochem Biophys Res Commun. 2011 Mar; 406(4):539-45.

Kwon OH, Park JL, Kim M, Kim JH, Lee HC, Kim HJ, Noh SM, Song KS, Yoo HS, Paik SG, Kim SY*, Kim YS*

*Co-corresponding: kimsy@kribb.re.kr yongsung@kribb.re.kr
BioMedical Genomics Research Center

The *LAMB3* and *LAMC2* genes encode the laminin-5 β3 and γ2 chains, respectively, which are parts of laminin-5, one of the major components of the basement membrane zone. Here, we report the frequent up-regulation of *LAMB3* and *LAMC2* by promoter demethylation in gastric cancer. Gene expression data analysis showed that *LAMB3* and *LAMC2* were up-regulated in various tumor tissues. Combined analyses of DNA methylation and gene expression of both genes in gastric cancer cell lines and tissues showed that DNA hypomethylation was associated with the up-regulation of both genes. Treatment with a methylation inhibitor induced *LAMB3* and *LAMC2* expression in gastric cancer cell lines in which both genes were silenced. By chromatin immunoprecipitation assay, we showed the activation histone mark H3K4me3 was associated with the expression of both genes. The expression level of *LAMB3* affected multiple malignant phenotypes in gastric cancer cell lines. These results suggest that epigenetic activation of *LAMB3* and *LAMC2* may play an important role in gastric carcinogenesis.
PMID: 21345334

Keywords : Demethylation; Malignant Phenotype; Gastric Carcinogenesis; C-Myc; Hypomethylation; *LAMB3*; *LAMC2*

Article 12

Interaction of a putative BH3 domain of clusterin with anti-apoptotic Bcl-2 family proteins as revealed by NMR spectroscopy

Biochem Biophys Res Commun. 2011 May; 408(4):541-7.

Lee DH, Ha JH, Kim Y, Bae KH, Park JY, Choi WS, Yoon HS, Park SG, Park BC, Yi GS, Chi SW*

*Co-corresponding: swchi@kribb.re.kr
BioMedical Proteomics Research Center

Clusterin (CLU) is a multifunctional glycoprotein that is overexpressed in prostate and breast cancers. Although CLU is known to be involved in the regulation of apoptosis and cell survival, the precise molecular mechanism underlying the pro-apoptotic function of nuclear CLU (nCLU) remains unclear. In this study, we identified a conserved BH3 motif in C-terminal coiled coil (CC2) region of nCLU by sequence analysis and characterized the molecular interaction of the putative nCLU BH3 domain with anti-apoptotic Bcl-2 family proteins by nuclear magnetic resonance (NMR) spectroscopy. The chemical shift perturbation data demonstrated that the nCLU BH3 domain binds to pro-apoptotic BH3 peptide-binding grooves in both Bcl-X(L) and Bcl-2. A structural model of the Bcl-X(L)/nCLU BH3 peptide complex reveals that the binding mode is remarkably similar to those of other Bcl-X(L)/BH3 peptide complexes. In addition, mutational analysis confirmed that Leu323 and Asp328 of nCLU BH3 domain, absolutely conserved in the BH3 motifs of BH3-only protein family, are critical for binding to Bcl-X(L). Taken altogether, our results suggest a molecular basis for the pro-apoptotic function of nCLU by elucidating the residue specific interactions of the BH3 motif in nCLU with anti-apoptotic Bcl-2 family proteins.
PMID: 21527247

Keywords : Clusterin; Apoptosis; BH3 domain; NMR; Bcl-2 family protein; BH3-Only Proteins; Oxidative Stress

Article 13

The activation of p38 MAPK primarily contributes to UV-induced RhoB expression by recruiting the c-Jun and p300 to the distal CCAAT box of the RhoB promoter

Biochem Biophys Res Commun. 2011 Jun; 409(2):211-6.

Ahn J, Choi JH, Won M, Kang CM, Gyun MR, Park HM, Kim CH, Chung KS*

*Co-corresponding: kschung@kribb.re.kr
BioMedical Genomics Research Center

The Ras-related small GTP-binding protein RhoB is rapidly induced in response to genotoxic stresses caused by ionizing radiation. It is known that UV-induced RhoB expression results from the binding of activating transcription factor 2 (ATF2) via NF-Y to the inverted CCAAT box (-23) of the RhoB promoter. Here, we show that the association of c-Jun with the distal CCAAT box (-72) is primarily involved in UV-induced RhoB expression and p38 MAPK regulated RhoB induction through the distal CCAAT box. UV-induced RhoB expression and apoptosis were markedly attenuated by pretreatment with the p38 MAPK inhibitor. siRNA knockdown of RhoB, ATF2 and c-Jun resulted in decreased RhoB expression and eventually restored the growth of UV-irradiated Jurkat cells. In the reporter assay using luciferase under the RhoB promoter, inhibition of RhoB promoter activity by the p38 inhibitor and knockdown of c-Jun using siRNA occurred through the distal CCAAT box. Immunoprecipitation and DNA affinity protein binding assays revealed the association of c-Jun and p300 via NF-YA and the dissociation of histone deacetylase 1 (HDAC1) via c-Jun recruitment to the CCAAT boxes of the RhoB promoter. These results suggest that the activation of p38 MAPK primarily contributes to UV-induced RhoB expression by recruiting the c-Jun and p300 proteins to the distal CCAAT box of the RhoB promoter in Jurkat cells.
PMID: 21565167

Keywords : UV-light; RhoB; c-Jun; CCAAT box; p38 MAPK; p300; Radiation-induced Apoptosis; Growth-factor

Article 14

Steatosis induced by the accumulation of apolipoprotein A-I and elevated ROS levels in H-ras12V transgenic mice contributes to hepatic lesions

Biochem Biophys Res Commun. 2011 Jun; 409(3):532-8.

Wang AG, Moon HB, Chae JI, Kim JM, Kim YE, Yu DY*, Lee DS

*Co-corresponding: dyyu10@kribb.re.kr
Aging Research Center

Hepatic steatosis is considered to have an important impact on liver tumorigenesis, despite a lack of clear experimental evidence. Histopathological analysis of H-ras12V transgenic mice showed liver lesions on a steatosis background had significantly higher incidence than on a non-steatosis background. Further investigation showed that apolipoprotein A-I was elevated and accumulated around fatty vacuoles. This elevated level of apolipoprotein A-I was coupled with an elevated level of H-ras12V protein and ROS. In conclusion, our results suggest that the expression of H-ras12V oncogene leads to elevated levels of ROS and apolipoprotein A-I that contribute to steatosis. The steatosis, in turn, promotes the development of hepatic lesions induced by H-ras12V oncogene.

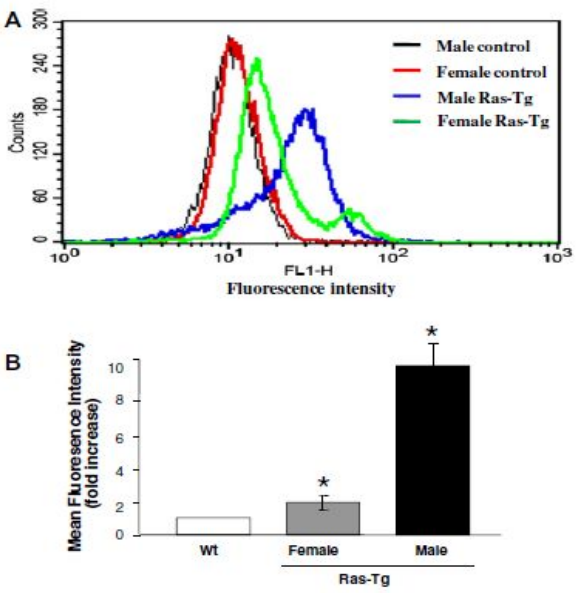

PMID: 21600874

Keywords : Steatosis; Apolipoprotein A-I; Hepatic lesions; H-ras12V; Transgenic Mice; Fatty Liver-disease; C Virus-infection

Article 15

Simultaneous *in vivo* tracking of dendritic cells and priming of an antigen-specific immune response

Biomaterials. 2011 Sep; 32(26):6254-63.

Noh YW, Jang YS, Ahn KJ, Lim YT, Chung BH*

*Co-corresponding: chungbh@kribb.re.kr
BioNanotechnology Research Center

We report the fabrication of a one-pot antigen system that delivers antigen to dendritic cells (DCs) and tracks their *in vivo* migration after injection. Multifunctional polymer nanoparticles containing ovalbumin protein, magnetic resonance imaging contrast agents (iron oxide nanoparticles), and near-infrared fluorophores (indocyanine green, ICG), MPN-OVA, were prepared using a double emulsion method. The MPN-OVA was efficiently taken up by the dendritic cells and subsequently localized in the lysosome. Flow cytometry analysis revealed an increase in the uptake of OVA antigen by MPN-OVA at 37 °C, when compared with soluble OVA protein. We found that MPN-OVA had no effect on DC surface expression of MHC class I, costimulatory (CD80, CD86) or adhesion (CD54) molecules or the ability of DCs to mature in response to LPS. Following the uptake of MPN-OVA, exogenous OVA antigen was delivered to the cytoplasm, and OVA peptides were presented on MHC class I molecules, which enhanced OVA antigen-specific cross-presentation to OT-1 T cells and CD8OVA1.3 T cell hybridoma *in vitro*. The immunization of mice with MPN-OVA-treated DCs induced OVA-specific CTL activity in draining lymph nodes. The presence of MPN allowed us to monitor the migration of DCs via lymphatic drainage using NIR fluorescence imaging, and the homing of DCs into the lymph nodes was imaged using MRI. This system has potential for use as a delivery system to induce T cell priming and to image DC-based immunotherapies.

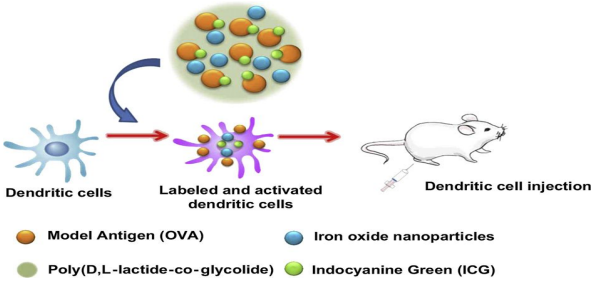

PMID: 21620470

Keywords : Polymer nanoparticles; Dendritic cells; Dual-modality imaging; Antigen Delivery; Immunity; Cytotoxic T-lymphocytes; Imaging Contrast Agents

Article 16

Splitting and self-assembling of far-red fluorescent protein with an engineered beta strand peptide: application for alpha-synuclein imaging in mammalian cells

Biomaterials. 2011 Dec; 32(34):9051-8.

Keem JO, Lee IH, Kim SY, Jung Y*, Chung BH*

*Co-corresponding: ywjung@kribb.re.kr chungbh@kribb.re.kr
BioNanotechnology Research Center

We introduce the strategic development of self-assembling peptide/protein fragments based on the far-red fluorescent protein mPlum. The first beta strand (mPlum 1, 18 amino acids) of mPlum was engineered to spontaneously bind with the rest of the protein (mPlum 2-11, next 10 beta strands) and to form a native chromophore. The target beta strand mPlum 1 was separated from mPlum 2-11 and linked via a flexible peptide linker, resulting in fluorescently inactive circularly permuted mPlum protein (CpmPlum). *In vitro* evolution of this CpmPlum to a fluorescently active form and the subsequent splitting of the engineered mPlum 1 peptide afforded self-assembling mPlum fragments. Recombinantly expressed and synthetically prepared beta strand peptides were successfully assembled with the remaining mPlum protein *in vitro* and in cells. This developed pair of peptide/protein fragments was effectively used for peptide tag detection of alpha-synuclein in mammalian cells. Sequential expression of self-assembling mPlum fragments offered an entirely genetically encoded sensing system of naturally unfolded alpha-synuclein.

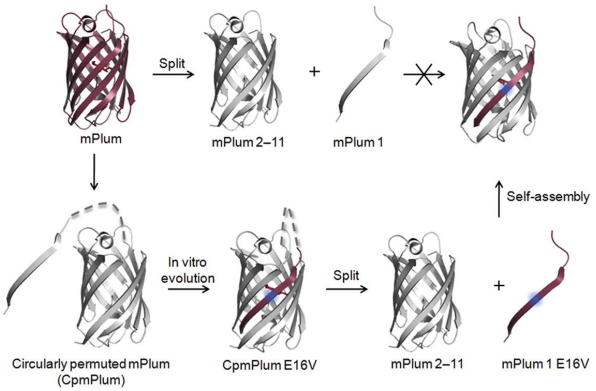

PMID: 21880361

Keywords : Fluorescent protein; Protein Engineering; Split protein; Molecular evolution; Biosensors; Complementation Assay; GFP

Article 17

Cosmomycin C inhibits signal transducer and activator of transcription 3 (STAT3) pathways in MDA-MB-468 breast cancer cell

Bioorg Med Chem. 2011 Dec; 19(24):7582-9.

Kim J, Lee YJ, Shin DS, Jeon SH, Son KH, Han DC, Jung SN, Oh TK, Kwon BM*

*Corresponding: kwonbm@kribb.re.kr
BioMedical Genomics Research Center

The signal transducer and activator of transcription 3 (STAT3) is constitutively activated in cancer cells. Therefore, blocking the aberrant activity of STAT3 in tumor cells is a validated therapeutic strategy. To discover novel inhibitors of STAT3 activity, we screened against microbial natural products using a dual-luciferase assay. Using the microbial metabolome library, we identified cosmomycin C (CosC), which was isolated from the mycelium extract of *Streptomyces* sp. KCTC19769, as a STAT3 pathway inhibitor. CosC inhibited STAT3 (Tyr705) phosphorylation and subsequent nuclear translocation in MDA-MB-468 breast cancer cells. CosC-mediated inhibition of STAT3 signaling pathway was confirmed by suppressed expression of STAT3 downstream target proteins including cyclin D1, Bcl-xL, survivin, Mcl-1, and VEGF in CosC-treated MDA-MB-468 cells. Flow cytometry showed that CosC caused accumulation in the G(0)-G(1) phase of the cell cycle and induced apoptosis via PARP cleavage and caspase-3 activation. Based on these findings, CosC may be a potential candidate for modulation of STAT3 pathway.

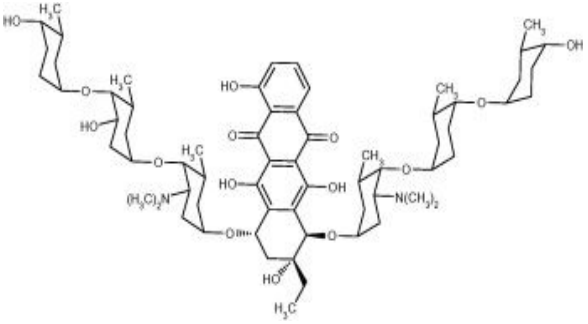

PMID: 22071520

Keywords : Cosmomycin; Signal transducer and activator of transcription 3 (STAT3); Apoptosis; Antitumor; Breast cancer; DNA-Binding Properties; Kinase Pathway

Article 18

2-Hydroxycurcuminoid induces apoptosis of human tumor cells through the reactive oxygen species-mitochondria pathway

Bioorg Med Chem Lett. 2011 Jan; 21(2):747-51.

Han YM, Shin DS, Lee YJ, Ismail IA, Hong SH, Han DC*, Kwon BM*

*Co-corresponding: dchan@kribb.re.kr kwonbm@kribb.re.kr
BioMedical Genomics Research Center

2-Hydroxycinnamaldehyde (HCA) and curcumin have been reported to have antitumor effects against various human tumor cells *in vitro* and *in vivo* by generation of ROS. Aldehyde-free HCA analogs were synthesized based on the structure of curcumin, which we have called 2-hydroxycurcuminoids. The hydroxyl group of curcuminoids enhances the ability to generate ROS. 2-Hydroxycurcuminoid (HCC-7) strongly inhibited the growth of SW620 colon tumor cells with a GI(50) value of 7μM, while the parent compounds, HCA and curcumin, displayed GI(50) values of 12 and 30μM, respectively. HCC-7 was found to induce apoptosis through the reactive oxygen species-mitochondria pathway and cell cycle arrest at G2/M phase.

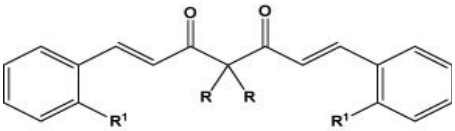

PMID: 21183341

Keywords : Hydroxycinnamaldehyde; Curcuminoid; Apoptosis; Reactive Oxygen Species; Chronic Lymphocytic-leukemia; Curcumin Analogs

Article 19

Biological evaluation of KRIBB3 analogs as a microtubule polymerization inhibitor

Bioorg Med Chem Lett. 2011 Feb; 21(3):977-9.

Lee S*, Kim JN, Lee HK, Yoon KS, Shin KD, Kwon BM, Han DC*

*Co-corresponding: sangku@kribb.re.kr dchan@kribb.re.kr
BioMedical Genomics Research Center

A series of KRIBB3 analogs were synthesized by modifying substituents at aryl moieties of KRIBB3 for examining structure-activity relationships, and their inhibitory activities on microtubule polymerization were evaluated. The presence of free phenolic hydrogens in aryl moieties of KRIBB3 analogs plays an important role in inhibition of microtubule polymerization.

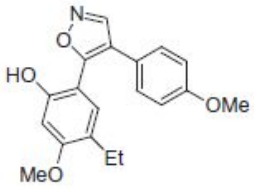

KRIBB3

PMID: 21215627

Keywords : Microtubule; Cancer; Anti-mitotic; Isoxazole; Inhibition; Apoptosis

Article 20

Butamben derivatives enhance BMP-2-stimulated commitment of C2C12 cells into osteoblasts with induction of voltage-gated potassium channel expression

Bioorg Med Chem Lett. 2011 Dec; 21(24):7363-6.

Kim HJ, Park M, Han YM, Kwon BM*, Kim SH

*Co-corresponding: kwonbm@kribb.re.kr
BioMedical Genomics Research Center

As the primary step for 'drug repositioning', we evaluated the effect of 2000 drugs and drug candidates on the commitment of bi-potential mesenchymal precursor C2C12 cells into osteoblasts in the presence of bone morphogenetic protein (BMP)-2 and found that butamben enhanced BMP-2-stimulated induction of alkaline phosphatase, a biomarker of osteoblastogenesis. Investigating the underlying mechanism of its anabolic actions, we found anabolic action of its derivative (compound 4) relies on BMP-2 signaling and mRNA induction of BMPs and voltage-gated potassium channels.

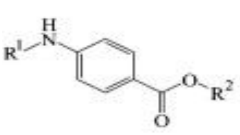

Compound	R^1	R^2
1	-H	$-CH_3$
2	-H	$-CH(CH_3)_2$
3 (Butamben)	-H	$-(CH_2)_3CH_3$
4	$-COCH_3$	$-(CH_2)_3CH_3$

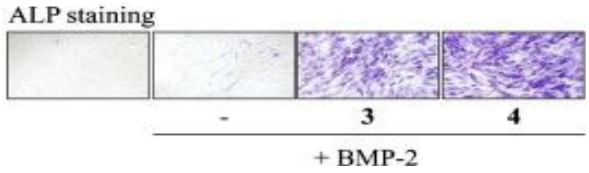

PMID: 22041064

Keywords : Drug Repositioning; Butamben; Osteoblastogenesis; Bone Morphogenetic Protein; Voltage-gated Potassium Channel; P38

Article 21

Improving Pb2+ detection using DNAzyme-based fluorescence sensors by pairing fluorescence donors with gold nanoparticles

Biosens Bioelectron. 2011 Jan; 26(5):2125-9.

Kim JH, Han SH, Chung BH*

*Corresponding: chungbh@kribb.re.kr
BioNanotechnology Research Center

For previously reported fluorescence Pb(2+) sensors, DNAzymes have lead to a significant increase in Pb(2+) detecting sensitivity and specificity. However, these sensors suffer from incomplete fluorescence quenching and require additional steps for annealing DNAzymes and substrates as well as for removing the uncoupled substrates. In this study, we successfully overcome these issues by immobilizing the substrate nucleic acids on gold nanoparticles through thiol linkages. The immobilization of the substrate molecules to the gold nanoparticles lead to almost-complete fluorescence quenching and fast Pb(2+) detection, without altering the Pb(2+) specificity of the DNAzymes. After optimizing the concentration of DNAzymes, reaction time and pH, we could detect Pb(2+) as low as 5 nM within 20 min without the preliminary and the post treatments. Considering the multi-color-fluorescence quenching capability of gold nanoparticles and the to-be-developed functional nucleic acids for other metal ions, this study could extend the application of DNAzymes to the detection of multiple heavy metal ions.

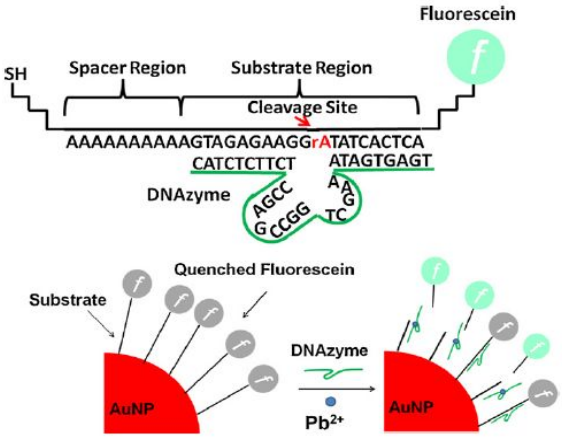

PMID: 20888751

Keywords : DNAzyme; Gold nanoparticles; Lead Ions; Sensor; Fluorescence Energy Transfer; Multiplexing; Colorimetric Detection

Article 22

Naked eye detection of mutagenic DNA photodimers using gold nanoparticles

Biosens Bioelectron. 2011 Jan; 26(5):2805-9.

Kim JH, Chung BH*

*Corresponding: chungbh@kribb.re.kr
BioNanotechnology Research Center

We developed a method to detect mutagenic DNA photodimers by the naked eye using gold nanoparticles. The stability of gold nanoparticles in a high ionic strength solution is maintained by straight ssDNA adsorbed physically on the AuNPs. However, we found that UV-irradiated DNA was less adsorptive onto gold nanoparticles because of a conformational change of UV-irradiated DNA. The accumulated deformation of the DNA structure by multiple-dimer formation triggered aggregation of the gold nanoparticles mixed with the UV-irradiated DNA and thus red to purple color changes of the mixture, which allowed colorimetric detection of the DNA photodimers by the naked eye. No fragmented mass and reactive oxygen species production under the UVB irradiation confirmed that the aggregation of gold nanoparticles was solely attributed to the accumulated deformation of the UV irradiated DNA. The degree of gold nanoparticles-aggregation was dependent on the UVB irradiated time and base compositions of the UV-irradiated oligonucleotides. In addition, we successfully demonstrated how to visually qualify the photosensitizing effect of chemical compounds in parallel within only 10 min by applying this new method. Since our method does not require any chemical or biochemical treatments or special instruments for purifying and qualifying the DNA photolesions, it should provide a feasible tool for the studies of the UV-induced mutagenic or carcinogenic DNA dimers and accelerate screening of a large number of drug candidates.

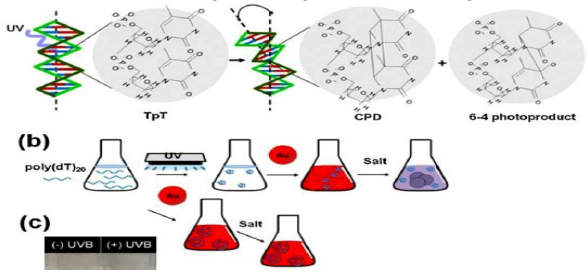

PMID: 21159501

Keywords : DNA; Gold nanoparticles; Sensors; Pyrimidine Dimer; Photosensitizer; Colorimetric Detection; Cell Carcinoma; Skin-Cancer

Article 23

The affinity ratio--its pivotal role in gold nanoparticle-based competitive colorimetric aptasensor

Biosens Bioelectron. 2011 Jun; 26(10):4058-63.

Kim YS, Kim JH*, Kim IA, Lee SJ, Gu MB

*Co-first: joong@kribb.re.kr
BioNanotechnology Research Center

We present an important role of the ratio of affinities in unmodified gold nanoparticles-based colorimetric aptasensor reactions. An affinity ratio, representing the competitive interactions among aptamers, targets, and unmodified gold nanoparticles (umAuNPs), was found to be an important factor for the sensitivity (the performance), where the affinity ratio is the affinity of the aptamer to targets divided by the affinity to umAuNPs ($K_{dAuNP}/K_{dTarget}$). In this study, the five different aptamers having different affinity ratios to both umAuNPs and targets are used, and the degree of color change is well correlated with its affinity ratio. This result is verified by using a tetracycline binding aptamer (TBA) showing different affinities to its three derivatives, tetracycline, oxytetracycline and doxycycline. Based on this model, the sensitivity of umAuNPs based colorimetric detection for ibuprofen can be enhanced simply through reducing the ibuprofen binding aptamer's affinity to umAuNP by using bis (p-sulfonatophenyl) phenylphosphine as an AuNP-capping ligand, instead of using the citrate. As a result, a clear color change is observed even at a 20-fold less amount of ibuprofen. This study presents that the performance (detection sensitivity) of umAuNPs-based colorimetric aptasensors could be improved by simply adjusting the affinity ratio of the aptamers to targets and umAuNPs, without knowing the conformational changes of aptamers upon the target binding or needing any modification of aptamer sequences.

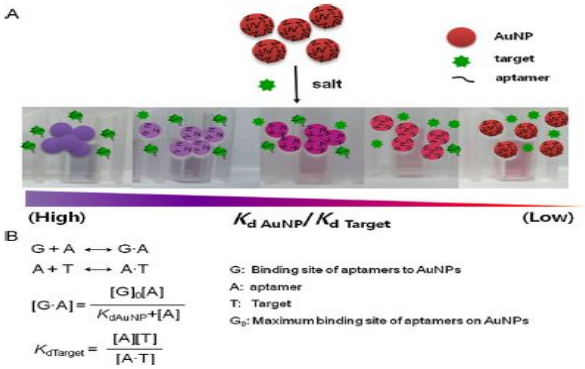

PMID: 21514814

Keywords : Aptamers; Competitive Interactions; Biosensor; Gold nanoparticles; Nanomaterials; DNA Aptamers; Oxytetracycline; Reagentless

Article 24

Label-free electrochemical detection of human α -thrombin in blood serum using ferrocene-coated gold nanoparticles

Biosens Bioelectron. 2011 Oct; 28(1):454-8.

Kwon D, Jeong H, Chung BH*

*Corresponding: chungbh@kribb.re.kr
BioNanotechnology Research Center

This paper describes a novel approach to label-free electrochemical detection of human α-thrombin in human blood serum that utilizes ferrocene-coated gold nanoparticles (Fc-AuNPs). Human α-thrombin was specifically bound by the thiolated aptamers immobilized on the electrode. Positively charged Fc-AuNPs were electrostatically bound to the negatively charged aptamers. In principle, a high current peak should be observed in the absence of interactions between the aptamers and the human α-thrombin. This behavior indicates maximum adsorption of Fc-AuNPs by the negatively charged aptamers on the electrode surface. In contrast, when the thrombin-aptamer complex is formed, a low signal is expected because of the blocking capacities of the protein, which hinders the electrostatic binding of the Fc-AuNPs. The electrochemical signal, recorded by cyclic voltammetry and differential pulse voltammetry, indicates whether interactions between aptamers and proteins have occurred. There is a good correlation between the ferrocene oxidation peak intensity readings from our thrombin sensing system and the thrombin concentration, within the range of 1.2 μM-12 pM.

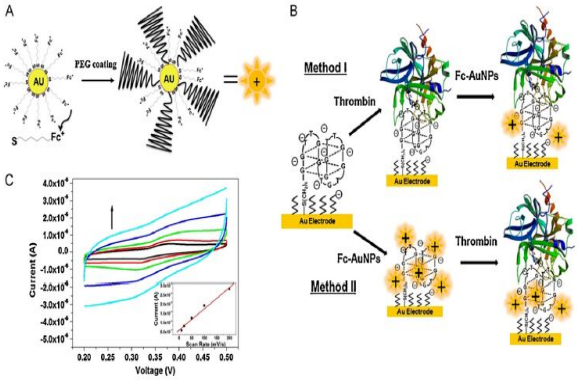

PMID: 21802275

Keywords : Label-free; Gold nanoparticles; Aptasensor; Electrochemistry; DNA Aptamer; Thrombin; Biosensor

Article 25

Functional characterization of the ER stress induced X-box-binding protein-1 (Xbp-1) in the porcine system

BMC Mol Biol. 2011 May; 12:25.

Zhang JY, Lee KS, Kim JS, Song BS, Jin DI, Koo DB, Yu K*

*Co-corresponding: kweonyu@kribb.re.kr
Aging Research Center

BACKGROUND: The unfolded protein response (UPR) is an evolutionary conserved adaptive reaction for increasing cell survival under endoplasmic reticulum (ER) stress conditions. X-box-binding protein-1 (Xbp1) is a key transcription factor of UPR that activates genes involved in protein folding, secretion, and degradation to restore ER function. The UPR induced by ER stress was extensively studied in diseases linked to protein misfolding and aggregations. However, in the porcine system, genes in the UPR pathway were not investigated. In this study, we isolated and characterized the porcine *Xbp1* (*pXbp1*) gene in ER stress using porcine embryonic fibroblast (PEF) cells and porcine organs. ER stress was induced by the treatment of tunicamycin and cell viability was investigated by the MTT assay. For cloning and analyzing the expression pattern of *pXbp1*, RT-PCR analysis and Western blot were used. Knock-down of *pXbp1* was performed by the siRNA-mediated gene silencing.
RESULTS: We found that the *pXbp1* mRNA was the subject of the IRE1α-mediated unconventional splicing by ER stress. Knock-down of *pXbp1* enhanced ER stress-mediated cell death in PEF cells. In adult organs, *pXbp1* mRNA and protein were expressed and the spliced forms were detected.
CONCLUSIONS: It was first found that the UPR mechanisms and the function of pXbp1 in the porcine system. These results indicate that pXbp1 plays an important role during the ER stress response like other animal systems and open a new opportunity for examining the UPR pathway in the porcine model system.
PMID: 21605464

Keywords : Endoplasmic-Reticulum Stress; Transcription Factor Xbp-1; Messenger-RNA; Nuclear Transfer; Transmembrane Protein; Targeted Disruption; Diabetes-Mellitus; Cell-Survival

Article 26

Discovery of novel inhibitors of dual-specificity phosphatase Pyst2 with structure-based virtual screening

Bull Korean Chem Soc. 2011; 32(7):2167-8.

Park H, Jeon JY, Ryu SE, Kim SJ*

*Co-corresponding: ksj@kribb.re.kr
BioMedical Proteomics Research Center

Protein tyrosine phosphatases (PTPs) are a family of the regulatory enzymes that are responsible for the dephosphorylation of phosphotyrosine residues in the protein substrates. Pyst2 was known to be overexpressed in leukemia and other malignant cells. Of the 85,000 compounds subject to the virtual screening with docking simulations, 100 top-scored compounds were selected as virtual hits. 92 of them were available from the compound supplier and were tested for inhibitory activity against Pyst2 by in vitro enzyme assay. As a result, we identified 2 compounds that inhibited the catalytic activity of Pyst2 by more than 50% at the concentration of 50 μM.

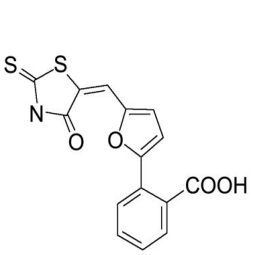

1

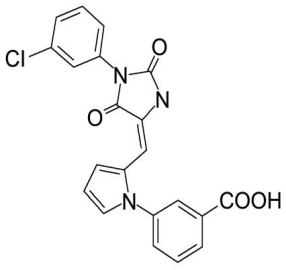

2

Keywords : Pyst2 Phosphatase; Virtual Screening; Inhibitor; Docking; Solvation; Genetic Algorithm; Leukemia; MAP

Article 27

Identification of two Eya2 phosphatase inhibitors from virtual screening with docking simulations

Bull Korean Chem Soc. 2011; 32(11):4086-8.

Park H, Yu KR, Kim SJ*

*Corresponding: ksj@kribb.re.kr
BioMedical Proteomics Research Center

Protein tyrosine phosphatases (PTPs) serve as a hallmark in the signal transductions through the hydrolysis of the phosphorylated tyrosine residue on various protein substrates. Eyes absent PTPs (Eya's) differ from the other PTPs in that they use an aspartate residue and a metal ion as the nucleophile and the Lewis acid catalyst in the catalytic reactions. Eya's may be involved in a variety of cancers and played a critical role in tumorigenesis. Of the 85,000 compounds subject to the virtual screening with docking simulations, 100 top-scored compounds were selected as virtual hits. 87 of them were available from the compound supplier and were tested for inhibitory activity against Eya2 phosphatase by in vitro enzyme assay. This inhibition assay was performed in duplicates at all concentrations of the inhibitors and the average values were used as data points. As a result, we identified two compounds that inhibited the catalytic activity of Eya2 by more than 50% at the concentration of 25 μM. We have identified two new novel inhibitors of Eya2 phosphatase by means of the structure-based virtual screening with docking simulations. These inhibitors exhibit a significant potency with IC50 values of 13.7 and 24.1 μM and have a proper ligand groups to be coordinated to the active-site Mg2+ ion.

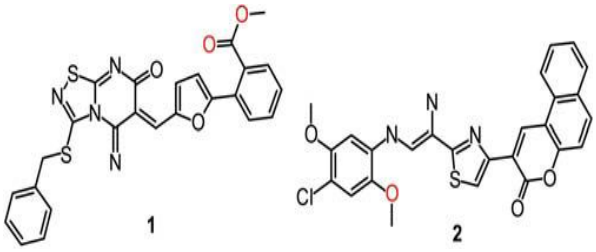

1 2

Keywords : Eya2 Phosphatase; Virtual Screening; Inhibitor; Docking; Cancer

Article 28

Up-regulation and clinical significance of serine protease kallikrein 6 in colon cancer

Cancer. 2011 Jun; 117(12):2608-19.

Kim JT, Song EY, Chung KS, Kang MA, Kim JW, Kim SJ, Yeom YI, Kim JH, Kim KH, Lee HG*

*Corresponding: hglee@kribb.re.kr
BioMedical Genomics Research Center

BACKGROUND: Kallikrein-related peptidase 6 (KLK6) encodes a trypsin-like serine protease that is up-regulated in several cancers, although the putative functions of KLK6 in cancer have not been elucidated. In the current study, overexpression of KLK6 was identified in colon cancer, and the possibility that KLK6 may be a suitable candidate as a tumor marker was examined.
METHODS: Messenger RNA (mRNA) transcript levels and protein up-regulation of KLK6 in colon cancer tissues was examined using reverse transcriptase-polymerase chain reaction, immunohistochemistry, and clinicopathologic analyses. Cell proliferation, invasiveness, and antiapoptotic activity were determined in colon cancer cells that were transfected with small-interfering RNA (siRNA) of *KLK6*.
RESULTS: *KLK6* mRNA was up-regulated significantly in tumor tissues compared with nontumor regions. KLK6 protein was strongly expressed in adenocarcinomas but was not expressed in normal mucosa or in premalignant dysplastic lesions. Sera from patients with colon cancer revealed an increase in KLK6 secretion (0.25 μg/mL; P = .031) compared with noncancer cells (0.19 μg/mL). Clinicopathologic and immunohistochemical studies of 143 patients with colon cancer revealed a significant correlation between KLK6 expression and Dukes disease stage (P = .005). High KLK6 expression was associated significantly with shorter overall (P = .001) and recurrence-free survival (P = .001). The rates of proliferation and invasiveness were decreased by 50% in cells that were transfected with *KLK6* siRNA. The overexpression of KLK6 led to decreased activity of the E-cadherin promoter.
CONCLUSIONS: KLK6 was up-regulated significantly in tissues and sera from patients with colon cancer and was associated closely with a poor prognosis, suggesting that KLK6 may be used as a potential biomarker and a therapeutic target for colon cancer.
PMID: 21656738

Keywords : Kallikrein-Related Peptidase 6; Invasiveness; Immunohistochemistry; Colon Cancer; Potential Serum Biomarker; Prostate-Specific Antigen; Zyme/Protease M/Neurosin

Article 29

Differential antiproliferation effect of 2'-benzoyloxycinnamaldehyde in K-ras-transformed cells via downregulation of thiol antioxidants

Cancer Sci. 2011 Jan; 102(1):212-8.

Ock J, Lee HA, Ismail IA, Lee HJ, Kwon BM*, Suk K, Lee WH, Hong SH, Kim SH

*Co-corresponding: kwonbm@kribb.re.kr
BioMedical Genomics Research Center

2'-Benzoyloxycinnamaldehyde (BCA), one of the derivatives of 2'-hydroxycinnamaldehyde (HCA) isolated from the bark of *Cinnamomum cassia*, induces apoptosis in human cancer cells. We found that BCA induces stronger antiproliferative effects in K-ras-transformed cells (RK3E-ras) than in isogenic non-transformed cells (RK3E). Treatment of RK3E-ras with BCA resulted in increased ROS generation and depletion of intracellular glutathione, whereas BCA-treated RK3E showed no significant increase in the ROS level with concurrent increase in intracellular glutathione (GSH). Thiol antioxidants recovered cell proliferation inhibition caused by BCA in both cell lines, while non-thiol antioxidants failed to recover cell death. BCA decreased metallothionein (MT) expression in RK3E-ras, while inducing remarkable MT expression in RK3E. The increase of intracellular GSH in RK3E is partially caused by differential induction of γ-glutamylcysteine synthetase (γ-GCS) due to BCA treatment. To evaluate the upstream pathway for differential expression of γ-GCS and MT, we analyzed early DJ-1 (PARK7) and NF-E2 p45-related factor 2 (Nrf2) changes after BCA treatment. In RK3E, DJ-1 expression considerably increased for 3 h with concurrent induction of Nrf2, whereas in RK3E-ras cells BCA decreased these protein levels. Based on these findings, it seems that the therapeutic selectivity of BCA in RK3E-ras results from decreased thiol antioxidants via decreased DJ-1 and Nrf2 expression.

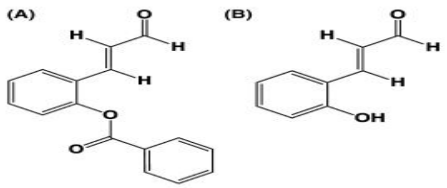

PMID: 21091848

Keywords : Cancer-Chemotherapy; Glutathione; Dj-1; 2'-Hydroxycinnamaldehyde; Metallothionein; Induction; Apoptosis; Tumor; Cinnamaldehydes

Article 30

Upregulation of RhoB via c-Jun N-terminal kinase signaling induces apoptosis of the human gastric carcinoma NUGC-3 cells treated with NSC12618

Carcinogenesis. 2011 Mar; 32(3):254-61.

Kim BK, Kim HM, Chung KS, Kim DM, Park SK, Song A, Won KJ, Lee K, Oh YK, Lee K, Song KB, Simon JA, Han G, Won M*

*Corresponding: misun@kribb.re.kr
BioMedical Genomics Research Center

RhoB expression is reduced in most invasive tumors, with loss of RhoB expression correlating significantly with tumor stage. Here, we demonstrate that upregulation of RhoB by the potent anticancer agent NSC126188 induces apoptosis of NUGC-3 human gastric carcinoma cells. The crucial role of RhoB in NSC126188-induced apoptosis is indicated by the rescue of NUGC-3 cells from apoptosis by knockdown of RhoB. In the presence of NSC126188, c-Jun N-terminal kinase (JNK) signaling was activated, and the JNK inhibitor SP600125 reduced RhoB expression and suppressed the apoptosis of NUGC-3 cells. Knockdowns of mitogen-activated protein kinase kinase (MKK) 4/7, JNK1/2 and c-Jun downregulated RhoB expression and rescued cells from apoptotic death in the presence of NSC126188. The JNK inhibitor SP600125 suppressed transcriptional activation of RhoB in the presence of NSC126188, as indicated by a reporter assay that used luciferase under the RhoB promoter. The ability of NSC126188 to increase luciferase activity through both the p300-binding site and the inverted CCAAT sequence (iCCAAT box) suggests that JNK signaling to upregulate RhoB expression is mediated through both the p300-binding site and the iCCAAT box. However, the JNK inhibitor SP600125 did not inhibit the upregulation of RhoB by farnesyltransferase inhibitor (FTI)-277. The p300-binding site did not affect activation of the RhoB promoter by FTI-277 in NUGC-3 cells, suggesting that the transcriptional activation of RhoB by NSC126188 occurs by a different mechanism than that reported for FTIs. Our data indicate that NSC126188 increases RhoB expression via JNK-mediated signaling through a p300-binding site and iCCAAT box resulting in apoptosis of NUGC-3 cells.

PMID: 21084431

Keywords : Farnesyltransferase Inhibitors; Fission Yeast; Cancer; Transformation; Ras; Suppression; Activation; Invasion

Article 31

Structure-based virtual screening approach to the discovery of novel inhibitors of eyes absent 2 phosphatase with various metal chelating moieties

Chem Biol Drug Des. 2011 Oct; 78(4):642-50.

Park H, Jung SK, Yu KR, Kim JH, Kim YS, Ko JH, Park BC, Kim SJ*

*Corresponding: ksj@kribb.re.kr
BioMedical Proteomics Research Center

Despite a series of persuasive experimental evidence for the involvement of eyes absent protein tyrosine phosphatases in various human cancers, no small-molecule inhibitor has been reported so far. We have identified seven novel inhibitors of eyes absent homologue 2 (Eya2) with IC(50) values ranging from 1 to 70 μm by the virtual screening with docking simulations and enzyme inhibition assay. Atomic charges of the active-site Mg(2+) ion complex are calculated to enhance the accuracy of docking simulations. The newly discovered inhibitors are structurally diverse and have various chelating groups for the Mg(2+) ion. The interactions with the amino acid residues responsible for the stabilizations of the inhibitors in the active site of Eya2 are addressed in detail.

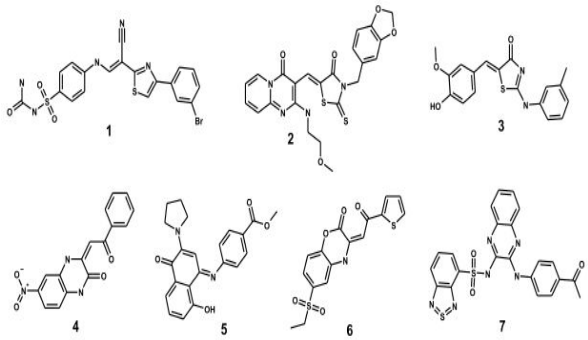

PMID: 21777393

Keywords : Chelating Group; Docking; Eyes Absent Protein Tyrosine Phosphatase; Inhibitor; Virtual Screening; Transcription Factor; Genetic Algorithm; Dephosphorylation; Sulfonamide

Article 32

Electric detection of target DNA by fabricating gold nanowire bridges on planar nanogap electrodes

Chem Commun (Camb). 2011 May; 47(20):5756-8.

Cho H, Kim SK, Jung Y, Jung J, Chung BH*

*Corresponding: chungbh@kribb.re.kr
BioNanotechnology Research Center

We described the electrical detection of target DNA on nanogap electrodes by fabricating DNA-templated conducting gold nanobridges connecting two electrodes. For the electrical detection of target DNA (partial avian influenza virus/H1N1/HA sequence) prepared *via* asymmetric PCR, we fabricated DNA-templated conducting gold nanowire bridges on planar nanogap electrodes using positively charged gold nanoparticles. The devices have potential applications in self-assembled nanoscale electronic circuits. The electrical signals of the DNA bridges were successfully amplified by the formation of DNA-templated conducting gold nanowires.

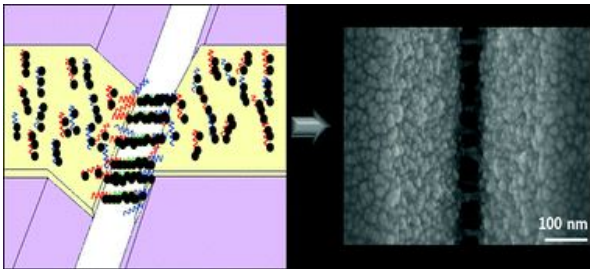

PMID: 21499634

Keywords : Electrochemical-Behavior; Hybridization; Nanowire Bridges; Planar Nanogap Electrodes; Gold Nanoparticles

Article 33

A label-free, direct and noncompetitive FRET immunoassay for ochratoxin A based on intrinsic fluorescence of an antigen and antibody complex

Chem Commun (Camb). 2011 Aug; 47(32):9098-100.

Li T, Jeon KS, Suh YD, Kim MG*

*Corresponding: mgkim@kribb.re.kr
BioNanotechnology Research Center

Ochratoxin A (OTA) is one of the most common foodcontaminating mycotoxins and a potent toxin produced by several species of *Aspergillus ochraceus* and *Penicillium verrucosum*. A label-free, direct and noncompetitive homogeneous immunoassay, in which ochratoxin A (OTA) coupled with the anti-OTA antibody participates in fluorescence resonance energy transfer (FRET), was developed for the detection of OTA with great specificity and a detection limit of 1 ng mL(-1). The investigation has led to the development of a novel, label-free, direct and noncompetitive antibody-based FRET immunoassay system for the sensitive and specific detection of OTA in artificial samples. The procedure does not involve washing steps and it can be performed in a 20 min period. The FRET immunoassay system has been applied to the analysis of OTA in wheat grain samples. Finally, the strategy used in this effort has the potential of being applied to the development of other label-free immunoassay techniques that can be used as on-site screening tools for the simple and rapid detection of OTA.

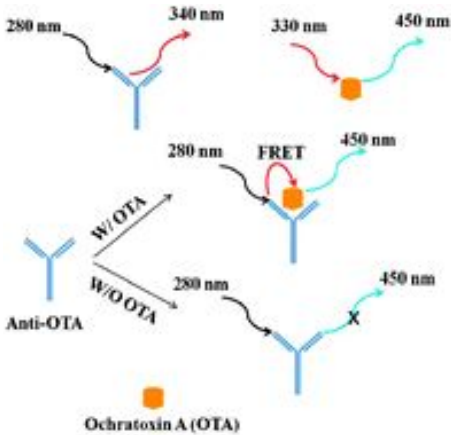

PMID: 21727957

Keywords : Resonance Energy-Transfer; Monoclonal-Antibody; Serum-Albumin; Immunosensor; Mycotoxins; Strip

Article 34

Photoreversible cellular imaging using photochrome-conjugated fullerene silica nanoparticles

Chem Commun (Camb). 2011 Oct; 47(38):10668-70.

Jeong J, Yun E, Choi Y, Jung HY, Chung SJ, Song NW, Chung BH*

*Corresponding: chungbh@kribb.re.kr
BioNanotechnology Research Center

Photochromic compound-conjugated fluorescent fullerene-silica nanoparticles prepared by the reverse-microemulsion method was utilized for photoswitchable cellular imaging by repeatable irradiation of ultraviolet and visible light. We prepared photoreversibly switchable photoluminescent nanoparticles through the conjugation of an amine-functionalised photochrome, C60, and silica by the reverse microemulsion method. The PL of the nanoparticles was reversibly and repeatedly switched on and off upon UV and visible light irradiation through the intermolecular energy transfer between the photo-induced transformation of PC and C60–O–Si, the PL species. The quenching efficiency (about 50%) of PC-FSNP by UV irradiation in both a pristine solution and an intracellular environment was comparable to that of other photoreversible switching systems. This nanosystem consisted of a photoswitchable molecule and a rigid, photostable and biocompatible photoluminescent moiety could be used for photoreversible analysis during cellular imaging and detection of target molecules in a complex biological system with a high signal-to-noise ratio.

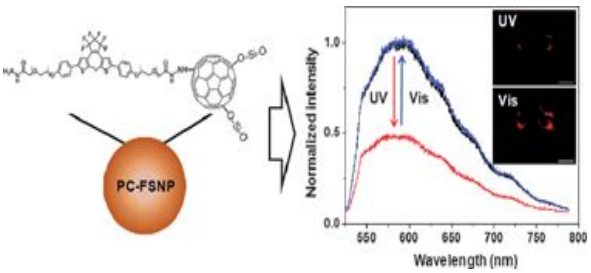

PMID: 21887422

Keywords : Diarylethenes; Switches; Fluorescent Fullerene-Silica Nanoparticles; Reverse-Microemulsion Method; Cellular Imaging

Article 35

Novel chemosensitive single-nucleotide polymorphism markers to targeted regimens in metastatic colorectal cancer

Clin Cancer Res. 2011 Mar; 17(5):1200-9.

Kim JC, Kim SY, Cho DH, Ha YJ, Choi EY, Kim CW, Roh SA, Kim TW, Ju H, Kim YS*

*Corresponding: yongsung@kribb.re.kr
BioMedical Genomics Research Center

PURPOSE: Methods for predicting individual responsiveness to targeted chemotherapy are urgently needed, considering the frequent resistance and extremely high cost.
EXPERIMENTAL DESIGN: A chemosensitive single-nucleotide polymorphism (SNP) discovery schema is presented that utilizes (i) genome-wide SNP screening with a human SNP array and an *in vitro* chemosensitivity assay in 118 colorectal cancers, (ii) clinical association analysis in the other 98 patients who had received chemotherapy for metastatic cancer, and (iii) biological utility assessment using cell viability assays of transfected colorectal cancer (CRC) cells.
RESULTS: Nine SNPs related to bevacizumab and cetuximab regimen sensitivity were chosen during screening. Overall responses for bevacizumab regimens revealed that patients carrying the *TT* genotype at *ANXA11 rs1049550* or at least one G allele at *LINS1 rs11247226* seemed greater chemosensitive than those carrying at least one C allele or the *AA* genotype, respectively ($P < 0.05$). For cetuximab regimens, patients carrying the *GG* genotype at *DFNB31 rs2274159* or *LIFR rs3729740* seemed greater chemosensitive than those carrying at least one A allele ($P = 0.025$ and $P = 0.07$). Cytotoxicity analyses showed that all RKO and HCT116 CRC clones transfected with the *G* allele at *LIFR rs3729740* and the *C* allele at *ISX rs361863* were more sensitive to cetuximab regimens than those with the A and T allele, respectively ($P \leq 0.001$-0.024).
CONCLUSIONS: Chemosensitive SNP markers were identified using a novel three-step process. The candidate marker *LIFR rs3729740* and possibly *ISX rs361863* will hopefully predict responsive patients to cetuximab regimens, although further validation is needed in large cohorts.

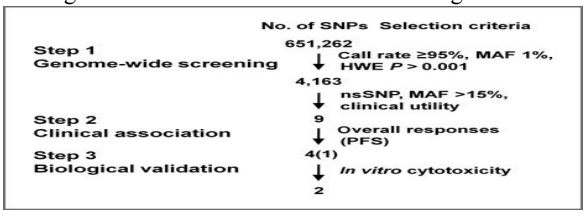

PMID: 21239504

Keywords : Leukemia Inhibitory Factor; Whole-Genome Association; Chemotherapy; Cetuximab; Identification; Resistance; Tumors

Article 36

Development of a fluorescent microsphere immunoassay for cystatin B (CSTB) in serum of patients with hepatocellular carcinoma

Clin Chem Lab Med. 2011 Jan; 49(1):151-5.

Ji NY, Kang YH, Park MY, Lee CI, Kim MK, Kim DG, Kim JW, Song EY*

*Corresponding: eysong@kribb.re.kr
BioMedical Genomics Research Center

BACKGROUND: Serum cystatin B (CSTB) concentrations have been reported to be increased in patients with hepatocellular carcinoma compared to concentrations seen in normal subjects. In this study, we developed a "fluorescent microsphere immunoassay" (FMI) capable of specifically detecting CSTB in serum.
METHODS: The FMI used a microparticle conjugated polyclonal antibody to CSTB and biotinylated monoclonal antibody as capture protein and probe protein, respectively. The results were obtained using the Bio-Plex^{200} system.
RESULTS: The dose-response relationship between CSTB and fluorescent intensity showed linearity in the range 0-1000 pg/mL and 7 pg/mL, sensitivity lower than 11.2 pg/mL. This result revealed that the FMI system was more sensitive than enzyme-linked immunoassay (ELISA). Additionally, the FMI system used smaller sample volumes compared to ELISA.
CONCLUSIONS: We measured CSTB with both the FMI and an ELISA procedure and compared the two methods. The CSTB concentrations in serum specimens as measured with the FMI assay system were similar to those measured with ELISA. Thus, the new FMI using the Bio-Plex system may be useful for detection of CSTB in human serum.
PMID: 20961191

Keywords : Cystatin B; ELISA; Fluorescent Microsphere Immunoassay; Hepatocellular Carcinoma; Serum; Cytokines; Cysteine; Epm1

Article 37

Sequential patterning of two fluorescent streptavidins assisted by photoactivatable biotin on an aminodextran-coated surface

Colloids Surf B Biointerfaces. 2011 Oct; 87(1):67-72.

Ahn J, Shin YB, Chang WS, Kim MG*

*Corresponding: mgkim@kribb.re.kr
BioNanotechnology Research Center

Sequential patterning of two fluorescent streptavidins (SAvs) was carried out using photopatterning of photoactivatable biotin (photobiotin) on an aminodextran surface, which was crucial for the minimization of non-specific binding. Photobiotin was bound by photoreaction to the amine groups of aminodextran. Water contact angle at each step during the preparation of the aminodextran surface was measured to investigate the hydrophilicity of the surfaces. The specific and nonspecific binding of a fluorescent SAv was investigated for the aminodextran surface and the amine-silane surface. The aminodextran surface almost entirely prevented nonspecific binding of a fluorescent SAv and was successfully used for sequential patterning of two fluorescent SAvs. The addition of ethanolamine (40 mM) in the photobiotin solution diminished blurring of pattern shape. To decrease pattern size, the UV light was focused on the aminodextran surface in an inverted microscope system. Under optimized conditions, two fluorescent SAvs array of approximately 25 μm size was obtained using a shadow mask of 100 μm hole size in the inverted microscope system.

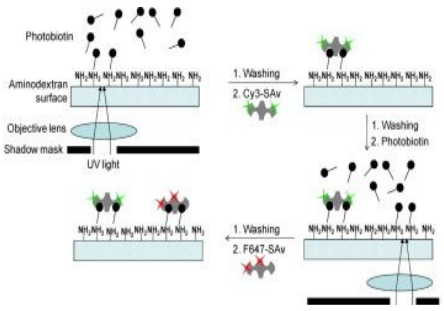

PMID: 21664802

Keywords : Aminodextran Surface; Photobiotin; Photopatterning; Sequential Patterning; Fluorescent Streptavidin; Plasmon Resonance Sensors; Avidin; Chip

Article 38

Epigenetic regulation of *microRNA-10b* and targeting of oncogenic *MAPRE1* in gastric cancer

Epigenetics. 2011 Jun; 6(6):740-51.

Kim K, Lee HC, Park JL, Kim M, Kim SY, Noh SM, Song KS, Kim JC, Kim YS*

*Corresponding: yongsung@kribb.re.kr
BioMedical Genomics Research Center

MicroRNAs act as negative regulators of gene expression, and the altered expression of microRNAs by epigenetic mechanisms is strongly implicated in carcinogenesis. Here we report that the microRNA-10b gene (*miR-10b*) was silenced in gastric cancer cells by promoter methylation. In this study, using a methylation array and bisulfate pyrosequencing analysis, we found that *miR-10b* promoter CpGs were heavily methylated in gastric cancers. Clinicopathologic data showed that *miR-10b* methylation increased with patient age and occurred significantly more frequently in intestinal-type (28/44, 64%) than in diffuse-type (22/56, 39%) gastric cancers (P = 0.016). In addition, *miR-10b* methylation was also associated with an increase in expression of the oncogene that encodes microtubule-associated protein, RP/EB family, member 1 (*MAPRE1*; P = 0.004), which was identified as a potential *miR-10b* target. After 5-aza-2'-deoxycytidine treatment of gastric cancer cells, *miR-10b* methylation was significantly decreased, and expression of *miR-10b* and *HOXD4*, which is 1 kb downstream of *miR-10b*, was greatly restored. Moreover, decreased *MAPRE1* expression coincided with increased *miR-10b* expression, suggesting that *miR-10b* targets *MAPRE1* transcription. We also found that transfection with precursor *miR-10b* into gastric cancer cells dramatically decreased *MAPRE1* mRNA and protein, resulting in a significant decrease in colony formation and cell growth rates. Thus, we show a tumor-suppressive role for *miR-10b* in gastric carcinogenesis. *miR-10b* methylation may be a useful molecular biomarker for assessing the risk of gastric cancer development, and modulation of *miR-10b* may represent a therapeutic approach for treating gastric cancer.

PMID: 21562367

Keywords : Gastric Cancer; *Mir-10B*; CpG Methylation; Hoxd4; *Mapre1*; Tumor-Suppressor Gene; Human Solid Tumors; DNA Methylation; Breast-Cancer; Protein Eb1

Article 39

Crystal structure of constitutively monomeric *E. coli* Hsp33 mutant with chaperone activity

FEBS Lett. 2011 Feb; 585(4):664-70.

Chi SW, Jeong DG, Woo JR, Lee HS, Park BC, Kim BY, Erikson RL, Ryu SE, Kim SJ*

*Co-corresponding: ksj@kribb.re.kr
BioMedical Proteomics Research Center

Heat shock protein 33 (Hsp33) from *Escherichia coli* is a redox-regulated molecular chaperone that protects cells from oxidative stress. To understand the molecular basis for the monomer-dimer switch in the functional regulation of *E. coli* Hsp33, we generated a constitutively monomeric Hsp33 by introducing the Q151E mutation in the dimeric interface and determined its crystal structure. The overall scaffold of the monomeric $Hsp33_{1-235}$ (Q151E) mutant is virtually the same as that of the dimeric form, except that there is no domain swapping. The measurement of chaperone activity to thermally denatured luciferase showed that the constitutively monomeric Hsp33 mutant still retains chaperone activity similar to that of wild-type $Hsp33_{1-235}$, suggesting that a Hsp33 monomer is sufficient to interact with slowly unfolded substrate.

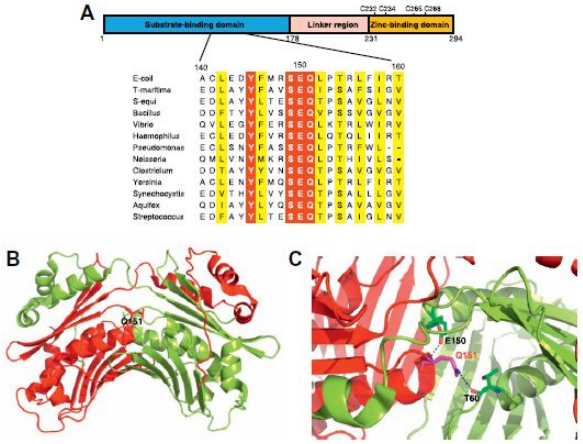

PMID: 21266175

Keywords : Heat Shock Protein 33 (Hsp33); Chaperone; Domain-Swapping; Redox-Sensitive; Switch Domain

Article 40

Identification of DNA methylation markers for lineage commitment of *in vitro* hepatogenesis

Hum Mol Genet. 2011 Jul; 20(14):2722-33.

Kim M, Kang TW, Lee HC, Han YM, Kim H, Shin HD, Cheong HS, Lee D, Kim SY, Kim YS*

*Corresponding: yongsung@kribb.re.kr
BioMedical Genomics Research Center

Hepatocytes that have differentiated from human embryonic stem cells (hESCs) have great potential for the treatment of liver disease as well as for drug testing. Moreover, *in vitro* hepatogenesis is a powerful model system for studying the molecular mechanisms underlying liver development. DNA methylation is an important epigenetic mechanism that influences differential gene expression during embryonic development. We profiled gene expression and DNA methylation of three cell states of *in vitro* hepatogenesis-hESC, definitive endoderm and hepatocyte-using microarray analysis. Among 525 state-specific expressed genes, 67 showed significant negative correlation between gene expression and DNA methylation. State-specific expression and methylation of target genes were validated by quantitative reverse transcription-polymerase chain reaction and pyrosequencing, respectively. To elucidate genome-scale methylation changes beyond the promoter, we also performed high-throughput sequencing of methylated DNA captured by the MBD2 protein. We found dynamic methylation changes in intergenic regions of the human genome during differentiation. This study provides valuable methylation markers for the lineage commitment of *in vitro* hepatogenesis and should help elucidate the molecular mechanisms underlying stem cell differentiation and liver development.

PMID: 21505074

Keywords : Embryonic Stem-Cells; Functional Hepatic Cells; Liver Development; Gene-Expression; Hepatocytes; Transcription; Pluripotent

Article 41

Chemopreventive effect of *Curcuma longa* Linn on liver pathology in HBx transgenic mice

Integr Cancer Ther. 2011 Jun; 10(2):168-77.

Kim J, Ha HL, Moon HB, Lee YW, Cho CK, Yoo HS, Yu DY*

*Corresponding: dyyu10@kribb.re.kr
Aging Research Center

Unlike other forms of hepatocellular carcinoma (HCC), HCC induced by hepatitis B virus (HBV) infection shows a poor prognosis after conventional therapies. HBV induces liver cirrhosis and HCC. Many researchers have made efforts to find new substances that suppress the activity of HBV. *Curcuma longa* Linn (CLL) has been used for traditional medicine and food in Asia, especially in India, and has shown chemopreventive effects in a HBV-related *in vitro* model. This *in vivo* study was designed to seek the chemopreventive effects of CLL and its mechanisms. CLL mixture concentrated with dextrose water by boiling was lyophilized. CLL extracts were administrated to HBV X protein (HBx) transgenic mice aged 4 weeks for 2 to 4 weeks and aged 6 months for 3 months. After administration, histological changes in the liver tissue and expression of HBx-related genes were investigated. CLL-treated mice showed less visceral fat, a smaller liver/body weight ratio and delayed liver pathogenesis. Proliferating cell nuclear antigen (PCNA) expression was also increased in CLL-treated HBx transgenic mice, indicating regeneration of damaged liver tissue. CLL treatment decreased expression of HBx and increased p21 and cyclin D1 in livers of HBx transgenic mice. In addition, p-p53 was increased after CLL treatment. These results suggest that CLL can have beneficial effects on the early and late stages of liver pathogenesis, preventing and delaying liver carcinogenesis. This drug should be considered as a potential chemopreventive agent for HBV-related hepatocarcinogenesis.

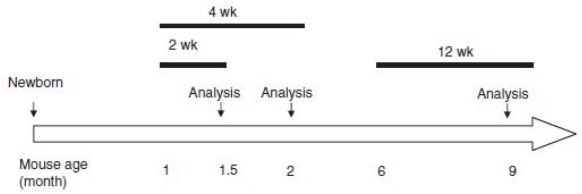

PMID: 21190953

Keywords : Chemopreventive Effect; HBV X Protein (HBx); *Curcuma Longa* Linn (CLL); Hepatocellular Carcinoma; p53; Hepatic Steatosis; Apoptosis; Epidemiology

Article 42

Human *ZNF312b* oncogene is regulated by Sp1 binding to its promoter region through DNA demethylation and histone acetylation in gastric cancer

Int J Cancer. 2011; 129(9):2124-33.

Song IS, Ha GH, Kim JM, Jeong SY, Lee HC, Kim YS, Kim YJ, Kwon TK, Kim NS*

*Corresponding: nskim37@kribb.re.kr
BioMedical Genomics Research Center

In a previous study, human *ZNF312b* was identified as a cell proliferation-associated oncogene *via* the K-ras/extracellular signal-regulated kinase cascade in gastric cancer. However, the mechanism concerning its transcriptional activation remains unknown. Here, we show that DNA methylation and histone acetylation of the *ZNF312b* promoter function as a switch for ZNF312b transcriptional activation in gastric cancer. The transcription level of *ZNF312b* was increased by treatment with a demethylating agent, 5-aza-2'-deoxycytidine, and the histone deacetylase inhibitor sodium butyrate, in several human cancer cell lines including gastric cancer. Consistent with these results, epigenetic analysis, such as pyrosequencing, bisulfate sequencing, and methyl-specific PCR (MSP), showed that the expression level of *ZNF312b* is highly dependent on the degree of DNA methylation in gastric cancer cell lines. In addition, by ChIP assay using anti-acetyl/methyl H3K9 antibodies, histone acetylation was shown to mediate the expression of the *ZNF312b* gene. Interestingly, ChIP assay using the Sp1 antibody revealed that the binding of transcription factor Sp1 to the *ZNF312b* promoter for its transcriptional activation requires DNA demethylation and histone acetylation. Moreover, a knockdown of *Sp1* resulted in a decrease in ERK-mediated proliferation *via* down-regulation of the *ZNF312b* gene in gastric cancer cells. Taken together, these results suggest that the aberrant expression of *ZNF312b* promotes gastric tumorigenesis through epigenetic modification of its promoter region and provides a molecular mechanism for *ZNF312b* expression to contribute to the progression of gastric cancer.

PMID: 21170990

Keywords : Epigenetics; *ZNF312b*; DNA Methylation; Histone Modification; Sp1; Gastric Cancer; Zinc-Finger Gene; Transcription

Article 43

NSC126188, a piperazine alkyl derivative, induces apoptosis via upregulation of RhoB in HeLa cells

Invest New Drugs. 2011 Oct; 29(5):853-60.

Kim BK, Kim DM, Chung KS, Park SK, Choi SJ, Song A, Lee K, Lee CW, Song KB, Han G, Simon J, Kim HM, Won M*

*Co-corresponding: misun@kribb.re.kr
BioMedical Genomics Research Center

We describe here a piperazine alkyl derivative, NSC126188, which induced apoptosis of HeLa cells by upregulating RhoB expression. NSC126188 caused multi-septation of fission yeast and hypersensitized a Δ*rho3* mutant, which implicates the involvement of functional human homolog RhoB. The treatment of cells with NSC126188 induced apoptosis and a dramatic increase in RhoB expression. In addition, RhoB knockdown using siRNA rescued cells from apoptosis, indicating a crucial role of RhoB in NSC126188-induced apoptosis. In a reporter assay using luciferase and EGFP under control of the RhoB promoter, NSC126188 increased both luciferase activity and the expression of EGFP, implicating transcriptional activation of RhoB by NSC126188. Furthermore, NSC126188 demonstrated *in vivo* anti-tumor activity, inhibiting tumor growth by 66.8% in a nude mouse xenograft using PC-3 human prostate cancer cells. These results suggest that NSC126188 is a potential lead compound and that upregulation of RhoB is associated with NSC126188-induced apoptosis.

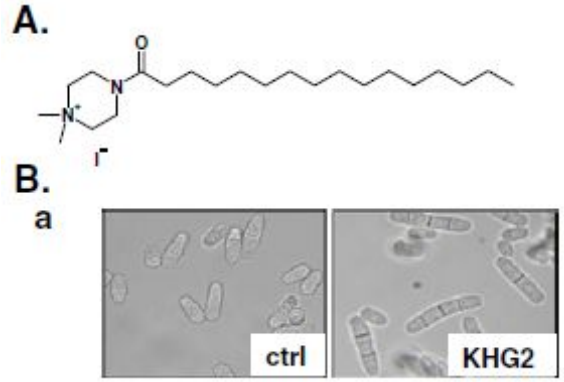

PMID: 20432054

Keywords : NSC126188; Apoptosis; RhoB; Anti-Cancer Compound; Piperazine Alkyl Derivative; Fission Yeast; Farnesyltransferase Inhibitors; Schizosaccharomyces-Pombe

Article 44

Molecular mimicry-based repositioning of nutlin-3 to anti-apoptotic Bcl-2 family proteins

J Am Chem Soc. 2011 Feb; 133(5):1244-7.

Ha JH, Won EY, Shin JS, Jang M, Ryu KS, Bae KH, Park SG, Park BC, Yoon HS, Chi SW*

*Co-corresponding: swchi@kribb.re.kr
BioMedical Proteomics Research Center

The identification of off-target binding of drugs is a key to repositioning drugs to new therapeutic categories. Here we show the universal interactions of the p53 transactivation domain (p53TAD) with various anti-apoptotic Bcl-2 family proteins via a mouse double minute 2 (MDM2) binding motif, which play an important role in transcription-independent apoptotic pathways of p53. Interestingly, our structural studies reveal that the anti-apoptotic Bcl-2 family proteins and MDM2 share a similar mode of interaction with the p53TAD. On the basis of this close molecular mimicry, our NMR results demonstrate that the potent MDM2 antagonists Nutlin-3 and PMI bind to the anti-apoptotic Bcl-2 family proteins in a manner analogous to that with the p53TAD.

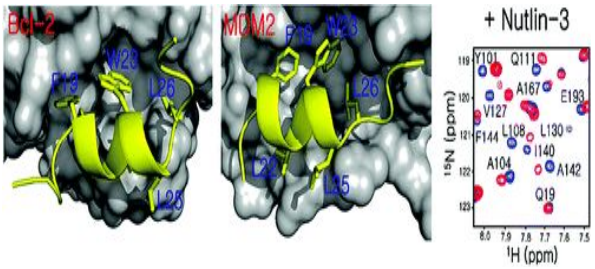

PMID: 21210687

Keywords : Structural Basis; Terminal Domain; P53; MDM2; Activation; Transcription; Mitochondria; Bax

Article 45

A simple technique for consistently obtaining large single crystals of hen egg-white lysozyme in a concentration gradient of $NiCl_2$

J Appl Crystallogr. 2011; 44:252-3.

Magay E, Yoon TS*

*Corresponding: yoonts@kribb.re.kr
BioMedical Proteomics Research Center

A simple protocol is reported for consistently obtaining large single crystals of hen egg-white lysozyme (HEWL) greater than 2 mm in the longest dimension. Comparative crystallization experiments with different sources of HEWL showed that the simple addition of glass capillaries, `crystal hangers', reduced excessive nucleation and resulted in large single crystals regardless of the commercial source of HEWL.

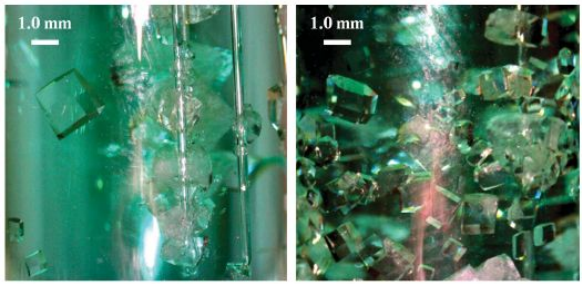

Keywords : Hen Egg-White Lysozyme (HEWL); Crystallization; Neutron Diffraction; Crystallography; $NiCl_2$

Article 46

KRIBB11 inhibits HSP70 synthesis through inhibition of heat shock factor 1 function by impairing the recruitment of positive transcription elongation factor b to the *hsp70* promoter

J Biol Chem. 2011 Jan; 286(3):1737-47.

Yoon YJ, Kim JA, Shin KD, Shin DS, Han YM, Lee YJ, Lee JS, Kwon BM*, Han DC*

*Co-corresponding: kwonbm@kribb.re.kr dchan@kribb.re.kr
BioMedical Genomics Research Center

Heat shock factor 1 (HSF1) is the master switch for heat shock protein (HSP) expression in eukaryotes. A synthetic chemical library was screened to identify inhibitors of HSF1 using a luciferase reporter under the control of a heat shock element. A compound named KRIBB11 (N^2-(1*H*-indazole-5-yl)-N^6-methyl-3-nitropyridine-2,6-diamine) was identified for its activity in abolishing the heat shock-induced luciferase activity with an IC_{50} of 1.2 μmol/liter. When the cells were exposed to heat shock in the presence of KRIBB11, the induction of HSF1 downstream target proteins such as HSP27 and HSP70 was blocked. In addition, treatment of HCT-116 cells with KRIBB11 induced growth arrest and apoptosis. Markers of apoptosis, such as cleaved poly(ADP-ribose) polymerase, were detected after KRIBB11 treatment. Biotinyl-KRIBB11 was synthesized as an affinity probe for the identification of KRIBB11 target proteins. Using affinity chromatography and competition assays, KRIBB11 was shown to associate with HSF1 *in vitro*. Chromatin immunoprecipitation analysis showed that KRIBB11 inhibited HSF1-dependent recruitment of p-TEFb (positive transcription elongation factor b) to the *hsp70* promoter. Finally, intraperitoneal treatment of nude mice with KRIBB11 at 50 mg/kg resulted in a 47.4% ($p < 0.05$) inhibition of tumor growth without body weight loss. Immunoblotting assays showed that the expression of HSP70 was lower in KRIBB11-treated tumor tissue than in control tissues. Because HSPs are expressed at high levels in a wide range of tumors, these results strengthen the rationale for targeting HSF1 in cancer therapy.

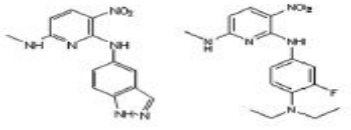

PMID: 21078672

Keywords : Non-Oncogene Addiction; DNA-Binding Activity; Gene-Expression; Hydrogen-Peroxide; HSP90 Inhibitors; Cancer-Cells; Factor HSF1; Phosphorylation; Stress

Article 47

TRIM32 protein sensitizes cells to tumor necrosis factor (TNFα)-induced apoptosis via its RING domain-dependent E3 ligase activity against X-linked inhibitor of apoptosis (XIAP)

J Biol Chem. 2011 Jul; 286(29):25729-38.

Ryu YS, Lee Y, Lee KW, Hwang CY, Maeng JS, Kim JH, Seo YS, You KH, Song B, Kwon KS*

*Corresponding: kwonks@kribb.re.kr
Aging Research Center

TRIM32, which belongs to the tripartite motif (TRIM) protein family, has the RING finger, B-box, and coiled-coil domain structures common to this protein family, along with an additional NHL domain at the C terminus. TRIM32 reportedly functions as an E3 ligase for actin, a protein inhibitor of activated STAT y (PIASy), dysbindin, and c-Myc, and it has been associated with diseases such as muscular dystrophy and epithelial carcinogenesis. Here, we identify a new substrate of TRIM32 and propose a mechanism through which TRIM32 might regulate apoptosis. Our overexpression and knockdown experiments demonstrate that TRIM32 sensitizes cells to TNFα-induced apoptosis. The RING domain is necessary for this pro-apoptotic function of TRM32 as well as being responsible for its E3 ligase activity. TRIM32 colocalizes and directly interacts with X-linked inhibitor of apoptosis (XIAP), a well known cancer therapeutic target, through its coiled-coil and NHL domains. TRIM32 overexpression enhances XIAP ubiquitination and subsequent proteasome-mediated degradation, whereas TRIM32 knockdown has the opposite effect, indicating that XIAP is a substrate of TRIM32. *In vitro* reconstitution assay reveals that XIAP is directly ubiquitinated by TRIM32. Our novel results collectively suggest that TRIM32 sensitizes TNFα-induced apoptosis by antagonizing XIAP, an anti-apoptotic downstream effector of TNFα signaling. This function may be associated with TRIM32-mediated tumor suppressive mechanism.

PMID: 21628460

Keywords : NF-Kappa-B; Dystrophy Type 2H; Coiled-Coil Protein; Ubiquitin Ligase; Antiviral Activity; Caspase Activity; Opitz-Syndrome; Finger; Iap

Article 48

Hepatitis B virus X protein regulates hepatic glucose homeostasis via activation of inducible nitric oxide synthase

J Biol Chem. 2011 Aug; 286(34):29872-81.

Shin HJ, Park YH, Kim SU, Moon HB, Park do S, Han YH, Lee CH, Lee DS, Song IS, Lee DH, Kim M, Kim NS, Kim DG, Kim JM, Kim SK, Kim YN, Kim SS, Choi CS, Kim YB, Yu DY*

*Co-corresponding: dyyu10@kribb.re.kr
Aging Research Center

Dysregulation of liver functions leads to insulin resistance causing type 2 diabetes mellitus and is often found in chronic liver diseases. However, the mechanisms of hepatic dysfunction leading to hepatic metabolic disorder are still poorly understood in chronic liver diseases. The current work investigated the role of hepatitis B virus X protein (*HBx*) in regulating glucose metabolism. We studied HBx-overexpressing (*HBx*Tg) mice and *HBx*Tg mice lacking inducible nitric oxide synthase (iNOS). Here we show that gene expressions of the key gluconeogenic enzymes were significantly increased in HepG2 cells expressing HBx (HepG2-*HBx*) and in non-tumor liver tissues of hepatitis B virus patients with high levels of *HBx* expression. In the liver of *HBx*Tg mice, the expressions of gluconeogenic genes were also elevated, leading to hyperglycemia by increasing hepatic glucose production. However, this effect was insufficient to cause systemic insulin resistance. Importantly, the actions of HBx on hepatic glucose metabolism are thought to be mediated via iNOS signaling, as evidenced by the fact that deficiency of iNOS restored HBx-induced hyperglycemia by suppressing the gene expression of gluconeogenic enzymes. Treatment of HepG2-*HBx* cells with nitric oxide (NO) caused a significant increase in the expression of gluconeogenic genes, but JNK1 inhibition was completely normalized. Furthermore, hyperactivation of JNK1 in the liver of *HBx*Tg mice was also suppressed in the absence of iNOS, indicating the critical role for JNK in the mutual regulation of HBx- and iNOS-mediated glucose metabolism. These findings establish a novel mechanism of HBx-driven hepatic metabolic disorder that is modulated by iNOS-mediated activation of JNK.

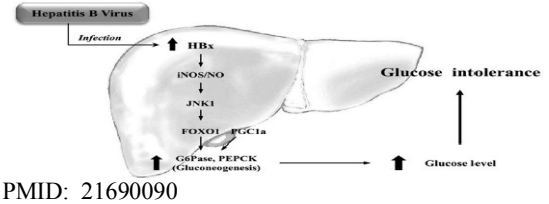

PMID: 21690090

Keywords : Chronic Viral-Hepatitis; Insulin Sensitivity; Transgenic Mice; Liver-Cancer; Kappa-B; Transcription; Hepatocytes; Gluconeogenesis

Article 49

Serum cancer biomarker discovery through analysis of gene expression data sets across multiple tumor and normal tissues

J Biomed Inform. 2011 Dec; 44(6):1076-85.

Jin H, Lee HC, Park SS, Jeong YS, Kim SY*

*Corresponding: kimsy@kribb.re.kr
BioMedical Genomics Research Center

The development of convenient serum bioassays for cancer screening, diagnosis, prognosis, and monitoring of treatment is one of top priorities in cancer research community. Although numerous biomarker candidates have been generated by applying high-throughput technologies such as transcriptomics, proteomics, and metabolomics, few of them have been successfully validated in the clinic. Better strategies to mine omics data for successful biomarker discovery are needed. Using a data set of 22,794 tumor and normal samples across 23 tissues, we systematically analyzed current problems and challenges of serum biomarker discovery from gene expression data. We first performed tissue specificity analysis to identify genes that are both tissue-specific and up-regulated in tumors compared to controls, but identified few novel candidates. Then, we designed a novel computation method, the multiple normal tissues corrected differential analysis (MNTDA), to identify genes that are expected to be significantly up-regulated even after their expressions in other normal tissues are considered, and, in a simulation study, showed that the multiple normal tissues corrected differential analysis outperformed the single tissue differential analysis combined with tissue specificity analysis. By applying the multiple normal tissues corrected differential analysis, we identified some genes as novel biomarker candidates. However, the number of potential candidates was disappointingly small, exemplifying the difficulty of finding serum cancer biomarkers. We discussed a few important points that should be considered during biomarker discovery from omics data.
PMID: 21872680

Keywords : Cancer Serum Biomarker; Tissue Specificity Analysis; Multiple Normal Tissues Corrected Differential Analysis; Malignant-Melanoma; Prostate-Cancer; Prognostic-Significance; DNA Methylation

Article 50

Genome-wide identification of possible methylation markers chemosensitive to targeted regimens in colorectal cancers

J Cancer Res Clin Oncol. 2011 Oct; 137(10):1571-80.

Kim JC, Lee HC, Cho DH, Choi EY, Cho YK, Ha YJ, Choi PW, Roh SA, Kim SY, Kim YS*

*Corresponding: yongsung@kribb.re.kr
BioMedical Genomics Research Center

PURPOSE: Few efficient methylation markers of chemosensitivity have been discovered. The genome-wide analysis of methylation markers is needed to identify chemosensitive candidates to targeted therapy.
METHODS: This study describes a two-step process to select chemosensitive candidates of methylation genes. A genome-wide screening of methylation genes was performed using a Beadarray and an *in vitro* chemosensitivity assay of 119 colorectal cancers (CRCs). Ten candidate genes identified during the initial screening were verified by biological utility assessment using cell viability assays of transfected CRC cells.
RESULTS: Five methylation genes related to sensitivity to bevacizumab regimens (*RASSF1, MMP25, KCNQ1, ESR1*, and *GALR2*) or cetuximab regimens (*SCL18A2, GPX7, NID2, IGFBP3*, and *ALX4*) were chosen during the first step. A viability assay revealed that GALR2-overexpressing HCT116 cells were significantly more chemosensitive to bevacizumab regimens than control cells (P = 0.022 and 0.019 for bevacizumab with FOLFIRI and FOLFOX, respectively), concurrently verified on a caspase-3 activity assay. GPX7- or ALX4-overexpressed RKO cells were significantly less viable to cetuximab regimens compared to control cells (GPX7: P = 0.027 each for cetuximab with FOLFIRI and FOLFOX; ALX4: P = 0.049 and 0.003 for cetuximab with FOLFIRI and FOLFOX, respectively), but caspase-3 activity was not prominent in GPX7-overexpressed RKO cells.
CONCLUSIONS: Two novel genes, *GALR2* and *ALX4*, have been identified as chemosensitive methylation candidates to bevacizumab and cetuximab regimens, respectively. As our study did not include a clinical association study, the two candidates should be validated in large clinical cohorts, hopefully predicting responsive patients to targeted regimens.
PMID: 21850381

Keywords : Colorectal Cancer; Targeted Chemotherapy; Chemosensitive Marker; Genome-Wide; DNA Methylation; Resistance; Therapies; Carcinoma

Article 51

Enzymatic tailoring for precise control of plasmonic resonance absorbance of gold nanoparticle assemblies

J Colloid Interface Sci. 2011 Aug; 360(2):335-40.

Kim JH, Kim JW, Chung BH*

*Corresponding: chungbh@kribb.re.kr
BioNanotechnology Research Center

We report an enzymatic method to control the plasmon resonance absorbance of gold nanoparticle (AuNP) arrays assembled on hyaluronic acids. While multiple electrostatic interactions between cysteamine on the AuNPs and the carboxylic acid residues in the whole intact hyaluronic acid induced the formation of large aggregates, precise control of the plasmon absorbance was possible by tailoring the size of the bio-polymeric templates with hyaluronidase, almost over the entire range of the resonant coupling wavelengths. It was possible to precisely tune the position of the second plasmon absorbance by manipulating the amount of the template and the enzymatic hydrolysis time. Finally, we were able to produce a chain-like array of AuNPs, which was nearly one dimensional, with a maximum shift of up to 189 nm in the plasmon absorbance at the optimal hydrolysis time of the templates. This enzymatic method can be used as a useful tool to tailor the plasmonic properties of the nanostructures required for specific applications.

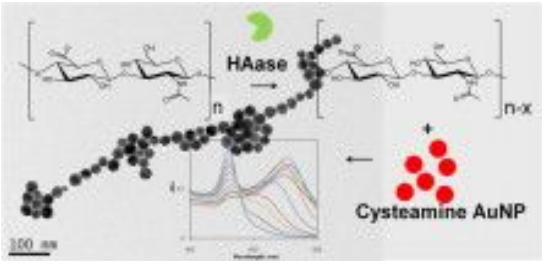

PMID: 21621790

Keywords : Gold Nanoparticles; Surface Plasmonic Resonance; One Dimensional Array; Hyalurnoic Acid; Hyaluronidase; Aggregation; Colloids

Article 52

RKIP downregulation induces the HBx-mediated Raf-1 mitochondrial translocation

J Microbiol Biotechnol. 2011 May; 21(5):525-8.

Kim SY, Park SG, Jung H, Chi SW, Yu DY, Lee SC, Bae KH*

*Corresponding: khbae@kribb.re.kr
BioMedical Proteomics Research Center

The Raf-1 kinase inhibitory protein (RKIP) can regulate multiple key signaling pathways. Specifically, RKIP binds to Raf-1 kinase and inhibits the Ras-Raf-1-MEK1/2- ERK1/2 pathway. Additionally, Raf-1 has been shown to translocate to mitochondria and thereby protect cells from stress-mediated apoptosis. Recently, HBx was found to stimulate the mitochondrial translocation of Raf-1, contributing to the anti-apoptotic effect. We found that RKIP was downregulated during HBx-mediated hepatocarcinogenesis. In this study, we show that RKIP bound to Raf-1 and consequently inhibited the translocation of Raf-1 into mitochondria. This promoted the apoptosis of cells treated with apoptotic stimulus. Thus, the downregulation of RKIP increased the level of free Raf-1 and thereby elevated the mitochondrial translocation of Raf-1 during HBx-mediated hepatocarcinogenesis. The elevated Raf-1 mitochondrial translocation induced the increased anti-apoptotic effect and subsequently promoted HBx-mediated hepatocarcinogenesis.

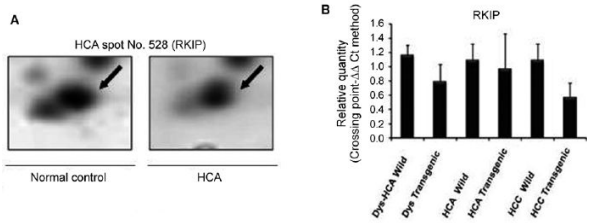

PMID: 21617351

Keywords : Hepatitis B Virus X; Hepatocarcinogenesis; Raf-1; RKIP; Kinase Inhibitory Protein; Virus-X-Protein; Induced Apoptosis

Article 53

Direct nanopatterning of silsesquioxane/poly(ethylene glycol) blends with high stability and nonfouling properties

Macromol Biosci. 2011 May; 11(5):600-6.

Lee BK, Kawai T, Chung BH*

*Co-corresponding: chungbh@kribb.re.kr
BioNanotechnology Research Center

A free-radical-polymerizable SSQ/PEG blend with direct patternability has been proposed as an ideal nonfouling material for nanostructure-based biomedical applications. Cured SSQ/PEG networks show an UV transparency of >90% at 365 nm, high resistance to organic/aqueous solutions, hydrophilicity and Young's moduli of 1.898-2.815 GPa. SSQ/PEG patterns with 25-nm linewidths, 25-nm spacing, and an aspect ratio of 4:1 were directly fabricated on transparent substrates by UV embossing, and cured SSQ/PEG networks with long-term stability under chemical, thermal, and biological stress showed strong resistance to the nonspecific adsorption of biomolecules. These characteristics may offer a new strategy for the development of a number of medical nanodevice applications such as labs-on-a-chip.

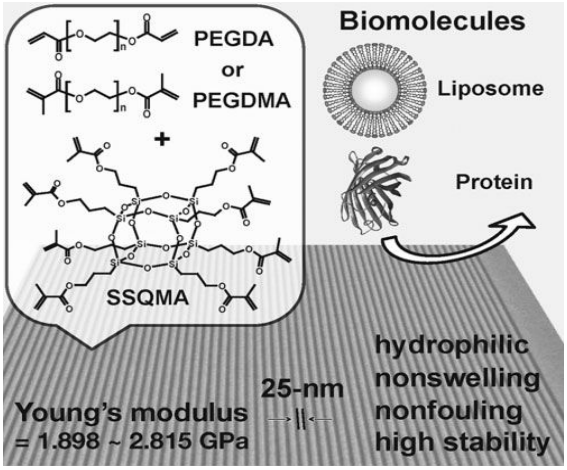

PMID: 21188687

Keywords : Crosslinking; Direct Nanopatterning; Mechanical Properties; Nonfouling Materials; Silsesquioxanes; Self-Assembled Monolayers; Surface Modification; Protein Adsorption

Article 54

RPTPμ tyrosine phosphatase promotes adipogenic differentiation via modulation of p120 catenin phosphorylation

Mol Biol Cell. 2011 Dec; 22(24):4883-91.

Kim WK, Jung H, Kim EY, Kim do H, Cho YS, Park BC, Park SG, Ko Y, Bae KH*, Lee SC*

*Co-corresponding: khbae@kribb.re.kr lesach@kribb.re.kr
BioMedical Proteomics Research Center

Adipocyte differentiation can be regulated by the combined activity of protein tyrosine kinases (PTKs) and protein tyrosine phosphatases (PTPs). In particular, PTPs act as key regulators in differentiation-associated signaling pathways. We recently found that receptor-type PTPμ (RPTPμ) expression is markedly increased during the adipogenic differentiation of 3T3-L1 preadipocytes and mesenchymal stem cells. Here, we investigate the functional roles of RPTPμ and the mechanism of its involvement in the regulation of signal transduction during adipogenesis of 3T3-L1 cells. Depletion of endogenous RPTPμ by RNA interference significantly inhibited adipogenic differentiation, whereas RPTPμ overexpression led to an increase in adipogenic differentiation. Ectopic expression of p120 catenin suppressed adipocyte differentiation, and the decrease in adipogenesis by p120 catenin was recovered by introducing RPTPμ. Moreover, RPTPμ induced a decrease in the cytoplasmic p120 catenin expression by reducing its tyrosine phosphorylation level, consequently leading to enhanced translocation of Glut-4 to the plasma membrane. On the basis of these results, we propose that RPTPμ acts as a positive regulator of adipogenesis by modulating the cytoplasmic p120 catenin level. Our data conclusively demonstrate that differentiation into adipocytes is controlled by RPTPμ, supporting the utility of RPTPμ and p120 catenin as novel target proteins for the treatment of obesity.

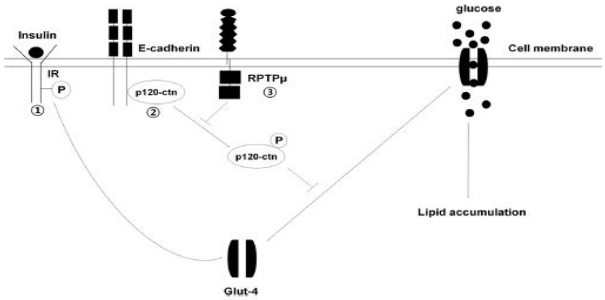

PMID: 21998202

Keywords : Cell-Cell Adhesion; Adipocyte Differentiation; Beta Catenin; 3T3-L1 Preadipocytes; Signaling System; Lipid-Metabolism; Kinases; Dephosphorylates

Article 55

The S-nitrosylation of glyceraldehyde-3-phosphate dehydrogenase 2 is reduced by interaction with glutathione peroxidase 3 in *Saccharomyces cerevisiae*

Mol Cells. 2011 Mar; 31(3):255-9.

Lee PY, Bae KH, Jeong DG, Chi SW, Moon JH, Kang S, Cho S, Lee SC, Park BC*, Park SG*

*Co-corresponding: parkbc@kribb.re.kr sgpark@kribb.re.kr
BioMedical Proteomics Research Center

Glutathione peroxidases (Gpxs) are the key anti-oxidant enzymes found in *Saccharomyces cerevisiae*. Among the three Gpx isoforms, glutathione peroxidase 3 (Gpx3) is ubiquitously expressed and modulates the activities of redox-sensitive thiol proteins involved in various biological reactions. By using a proteomic approach, glyceraldehyde-3-phosphate dehydrogenase 2 (GAPDH2; EC 1.2.1.12) was found as a candidate protein for interaction with Gpx3. GAPDH, a key enzyme in glycolysis, is a multi-functional protein with multiple intracellular localizations and diverse activities. To validate the interaction between Gpx3 and GAPDH2, immunoprecipitation and a pull-down assay were carried out. The results clearly showed that GAPDH2 interacts with Gpx3 through its carboxyl-terminal domain both *in vitro* and *in vivo*. Additionally, Gpx3 helps to reduce the S-nitrosylation of GAPDH upon nitric oxide (NO) stress; this subsequently increases cellular viability. On the basis of our findings, we suggest that Gpx3 protects GAPDH from NO stress and thereby contributes to the maintenance of homeostasis during exposure to NO stress.
PMID: 21229323

Keywords : Apoptosis; GAPDH2; Glutathione Peroxidase 3; Nitosylation; Oxidative Stress; Nitric-Oxide

Article 56

Identification of proteins differentially expressed in gastric cancer cells with high metastatic potential for invasion to lymph nodes

Mol Cells. 2011 Jun; 31(6):563-71.

Lee do H, Lee Y, Ryu J, Park SG, Cho S, Lee JJ, Choi C, Park BC*

*Corresponding: parkbc@kribb.re.kr
BioMedical Proteomics Research Center

In a search for proteins involved in cancer metastasis, we analyzed proteomes of the human gastric cancer cell OCUM-2M and its metastatic subline OCUM-2MLN. We observed that aspartate aminotransferase (AAT), D-site binding protein (DBP), and anterior gradient protein 2 (AGR2) are differentially expressed in metastatic OCUM-2MLN cells. Measurement of protein expression in clinical samples indicated that DBP and AAT are also down-regulated in metastatic adenocarcinoma. Additionally, urokinase-type tissue plasminogen activator is up-regulated in OCUM-2MLN cells and also in metastatic gastric cancer samples. Collectively, these results raise a possibility that AAT, DBP and AGR2 are functionally implicated in the invasiveness of gastric cancer cells.
PMID: 21533548

Keywords : AAT; AGR2; DBP; Gastric Cancer; Metastasis; Proteome; Mass-Spectrometry; Breast-Cancer; Estrogen-Receptor; Tumor Progression; Gene Xag-2

Article 57

Peroxiredoxin II preserves cognitive function against age-linked hippocampal oxidative damage

Neurobiol Aging. 2011 Jun; 32(6):1054-68.

Kim SU, Jin MH, Kim YS, Lee SH, Cho YS, Cho KJ, Lee KS, Kim YI, Kim GW, Kim JM, Lee TH, Lee YH, Shong M, Kim HC, Chang KT, Yu DY*, Lee DS

*Co-corresponding: dyyu10@kribb.re.kr
Aging Research Center

Reactive oxygen species (ROS), routinely produced in biological reactions, contribute to both normal aging and age-related decline in cognitive function. However, little is known regarding the involvement of specific antioxidants in the underlying mechanism(s). Here, we examined if peroxiredoxin II (Prx II) scavenges intracellular ROS that cause age-dependent mitochondrial decay in hippocampal CA1 pyramidal neurons and subsequent impairment of learning and memory. Age-dependent mitochondrial ROS generation and long-term potentiation (LTP) decline were more prominent in hippocampal neurons in Prx II(-/-) than in wild-type mice. Additionally, Prx II(-/-) mice failed to activate synaptic plasticity-related cellular signaling pathways involving CREB, CaMKII, and ERK, or to maintain functional integrity of their mitochondria. Dietary vitamin E alleviated Prx II deficiency-related deficits, including mitochondrial decay and CREB signaling, resulting in restoration of the abrupt cognitive decline in aged Prx II(-/-) mice. These results suggest that Prx II help maintain hippocampal synaptic plasticity against age-related oxidative damage.
PMID: 19577336

Keywords : Reactive Oxygen Species; Peroxiredoxin; Hippocampus; Aging; Mitochondria; Long-Term Potentiation; Alzheimers-Disease; Vitamin-E; Neurotrophic Factor

Article 58

ADGO 2.0: interpreting microarray data and list of genes using composite annotations

Nucleic Acids Res. 2011 Jul; 39(W):W302-6.

Chi SM, Kim J, Kim SY*, Nam D

*Co-corresponding: kimsy@kribb.re.kr
BioMedical Genomics Research Center

ADGO 2.0 is a web-based tool that provides composite interpretations for microarray data comparing two sample groups as well as lists of genes from diverse sources of biological information. Some other tools also incorporate composite annotations solely for interpreting lists of genes but usually provide highly redundant information. This new version has the following additional features: first, it provides multiple gene set analysis methods for microarray inputs as well as enrichment analyses for lists of genes. Second, it screens redundant composite annotations when generating and prioritizing them. Third, it incorporates union and subtracted sets as well as intersection sets. Lastly, users can upload their own gene sets (e.g. predicted miRNA targets) to generate and analyze new composite sets. The first two features are unique to ADGO 2.0. Using our tool, we demonstrate analyses of a microarray dataset and a list of genes for T-cell differentiation. The new ADGO is available at http://www.btool.org/ADGO2.
PMID: 21624890

Keywords : High-Throughput Data; Complex Functionality; Enrichment Analysis; Set Enrichment; Genome; Tools

Article 59

Factors influencing the detection of the *BRAF* T1799A mutation in papillary thyroid carcinoma

Oncol Rep. 2011 Jun; 25(6):1639-44.

Kim HS, Kim JO, Lee DH, Lee HC, Kim HJ, Kim JH, Jang YS, Lee JM, Kim SY, Kim YS*

*Corresponding: yongsung@kribb.re.kr
BioMedical Genomics Research Center

The *BRAF* T1799A mutation is a heterozygous point mutation and its reported prevalence in papillary thyroid carcinoma (PTC) has varied from 29 to 83%, with an overall mean of 44%. In Korea, the reported mutation rate reached 83% in PTC and 52% in micropapillary carcinoma. We hypothesized that the differences in prevalence may be influenced by the methods of mutation analysis, the sizes of tumor and ethnic differences. Three types of DNA samples from the same PTC mass (0.4-1.6 cm, mean 0.83 cm sized) per each patient (n=17) were isolated. The first type was obtained from frozen PTC tissues using laser-captured microdissection (Frozen-laser, n=17), the second was obtained from frozen tissue by manual tumor margin dissection using a blade (Frozen-blade, n=17) and the third was obtained from formalin-fixed, paraffin-embedded tissue by manual margin dissection (Paraffin-blade, n=15, 2 failed). The mutation rates of the three-matched DNA samples were compared by the SNP mode and AQ mode of pyrosequencing, and direct DNA sequencing. Both the AQ mode of pyrosequencing and the direct DNA sequencing detected the *BRAF* T1799A mutation in 100% of the 'Frozen-laser' samples, but the mutation was omitted in 1/17 of the 'Frozen-blade' samples and in 5/15 of the 'Paraffin-blade' samples, while the former was more rapid and objective than the latter. The SNP mode of pyrosequencing variably detected the mutation from 40 to 100%, and it showed the lowest sensitivity. Our results indicate that the reported prevalence of the *BRAF* T1799A mutation in PTC can be underestimated due the mutation analysis methods, and especially in small PTCs. The *BRAF* T1799A mutation may be an early and essential carcinogenic event in nearly all Korean PTCs, and even in micro-PTCs. For the accurate detection of the *BRAF* T1799A mutation from small PTCs, fresh or frozen tissues and more cautious microdissection are required, and the AQ mode of pyrosequencing assay is preferred.

PMID: 21431280

Keywords : Papillary Thyroid Carcinoma; *BRAF* Mutation; Lcm; Pyrosequencing; Braf(V600E) Mutation; Microcarcinoma; Diagnosis; Nodules; Ret/Ptc

Article 60

Structural and functional analysis of substrate recognition by the 250s loop in amylomaltase from *Thermus brockianus*

Proteins. 2011 Feb; 79(2):633-44.

Jung JH, Jung TY, Seo DH, Yoon SM, Choi HC, Park BC, Park CS, Woo EJ*

*Co-corresponding: ejwoo@kribb.re.kr
BioMedical Proteomics Research Center

Amylomaltase, or 4-α-glucanotransferase (EC 2.4.1.25), is involved in glycogen and maltooligosaccharide metabolism in microorganisms, catalyzing both the hydrolysis and transfer of an α-1,4-oligosacchraride to other sugar molecules. In this study, we determined the crystal structure of amylomaltase from *Thermus brockianus* at a resolution of 2.3 Å and conducted a biochemical study to understand the detailed mechanism for its activity. Careful comparison with previous amylomaltase structures showed a pattern of conformational flexibility in the 250s loop with higher B-factor. Amylomaltase from *T. brockianus* exhibited a high transglycosylation factor for glucose and a lower value for maltose. Mutation of Gln256 resulted in increased K_m for maltotriose and a sharp decrease of the transglycosylation factor for maltose, suggesting the involvement of Gln 256 in substrate binding between subsites +1 and +2. Mutation of Phe251 resulted in significantly lower glucose production but increased maltose production from maltopentose substrates, showing an altered substrate-binding affinity. The mutational data suggest the conformational flexibility of the loop may be involved in substrate binding in the GH77 family. Here, we present an action model of the 250s loop providing the molecular basis for the involvement of residues Phe251, Gln256, and Trp258 in the hydrolysis and transglycosylation activities in amylomaltase.

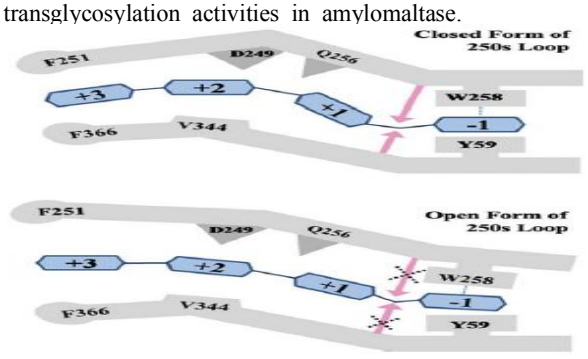

PMID: 21117235

Keywords : Amylomaltase; 250S Loop; Substrate Binding Sites; *Thermus brockianus*; Large Cyclic Glucans; Glycosyl Hydrolases; Pyrococcus-Furiosus; Cycloamylose

Article 61

Crystal structure of a novel mitogen-activated protein kinase phosphatase, SKRP1

Proteins. 2011 Nov; 79(11):3242-6.

Wei CH, Ryu SY, Jeon YH, Yoon MY, Jeong DG, Kim SJ*, Ryu SE

*Co-corresponding: ksj@kribb.re.kr
BioMedical Proteomics Research Center

Dual specificity protein tyrosine phosphatases (DUSPs) are important signal transduction enzymes and control activity of various map kinases. We determined the crystal structure of SKRP1 in a very high resolution that revealed a conserved overall PTP catalytic domain structure and three prominent ion molecules including two sulfates and one phosphate. Two sulfate ions seem to mimic the phosphoryl groups of pTyr and pThr of SKRP1 substrates. The extra phosphate ion in the active site pocket entrance has not been seen in other PTP structures and may play a role in the activity regulation of SKRP1 by providing a pseudosubstrate binding site. The SKRP1 structure should be useful for elucidating the biological function of SKRP1 together with future biochemical studies including mapping of binding sites for JNK signaling pathway proteins such as MKK7 and ASK1.

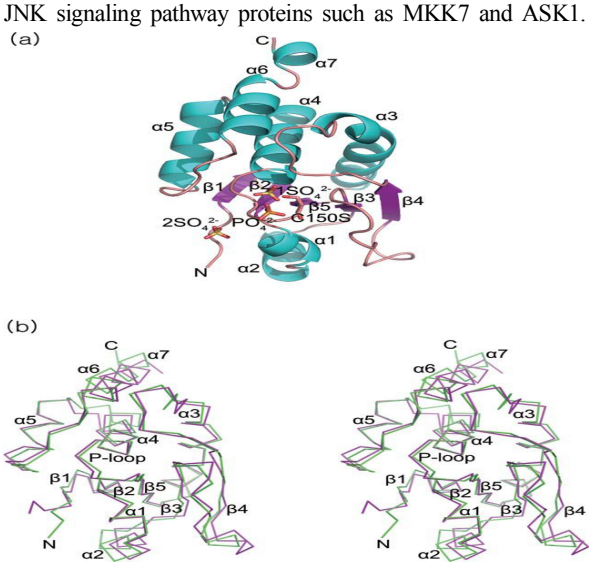

PMID: 21989941

Keywords : SKRP1; DUSP; Protein Tyrosine Phosphatase; Crystal Structure; High-Resolution Structure; JNK Signaling

Article 62

Monitoring of adipogenic differentiation at the single-cell level using atomic force microscopic analysis

Spectrosc-Biomed Appl. 2011; 26(6):329-35.

Kwon YN, Kim WK, Lee SH, Kim K, Kim EY, Ha TH, Han H, Bae KH*

*Corresponding: khbae@kribb.re.kr
BioMedical Proteomics Research Center

Adipogenesis plays an important role in energy homeostasis by storing excess energy as lipid droplets. However, these reservoirs are implicated in a host of major human health problems, such as obesity. Elucidation of the mechanisms underlying adipogenesis is thus crucial to overcome these problems. The preadipocyte cell lines represent an optimal model to examine adipogenesis. Cells differentiate into adipocytes with various speeds of conversion and fat accumulation. Here, we have presented a novel method for detecting adipogenic differentiation at the single-cell level using atomic force microscopic analysis. Data obtained with this method revealed a good correlation between membrane stiffness and the degree of adipogenic differentiation. Although we could not determine the underlying cause for membrane stiffness reduction during adipogenic differentiation, the technique clearly offers advantages over the existing detection systems, such as lipid drop staining and extraction. Furthermore, the degree of adipogenic differentiation at the single-cell level can be detected with this method.

Keywords : Adipogenesis; AFM; Adipocyte Differentiation; Stiffness; Mesenchymal Stem-Cells; Tyrosine Phosphatase; FAT

2011
KRIBB Article Abstracts
Corresponding Articles
Indexed in SCIE

Division of Biosytems Research

- Systems & Synthetic Biology Research Center
- Green Bio Research Center
- Industrial Bio-materials Research Center
- Environmental Biotechnology Research Center

Korea Research Institute of Bioscience and Biotechnology


KRIBB
www.kribb.re.kr

Article 63

Exceptional production of both prodigiosin and cycloprodigiosin as major metabolic constituents by a novel marine bacterium, *Zooshikella rubidus* S1-1

Appl Environ Microbiol. 2011 Jul; 77(14):4967-73.

Lee JS, Kim YS, Park S, Kim J, Kang SJ, Lee MH, Ryu S, Choi JM, Oh TK*, Yoon JH*

*Co-corresponding: otk@kribb.re.kr jhyoon@kribb.re.kr
Systems & Synthetic Biology Research Center

A Gram-negative, red-pigment-producing marine bacterial strain, designated S1-1, was isolated from the tidal flat sediment of the Yellow Sea, Korea. On the basis of phenotypic, phylogenetic, and genetic data, strain S1-1 (KCTC 11448BP) represented a new species of the genus *Zooshikella*. Thus, we propose the name *Zooshikella rubidus* sp. nov. Liquid chromatography and mass spectrometry of the red pigments produced by strain S1-1 revealed that the major metabolic compounds were prodigiosin and cycloprodigiosin. In addition, this organism produced six minor prodigiosin analogues, including two new structures that were previously unknown. To our knowledge, this is the first description of a microorganism that simultaneously produces prodigiosin and cycloprodigiosin as two major metabolites. Both prodigiosin and cycloprodigiosin showed antimicrobial activity against several microbial species. These bacteria were approximately 1.5-fold more sensitive to cycloprodigiosin than to prodigiosin. The metabolites also showed anticancer activity against human melanoma cells, which showed significantly more sensitivity to prodigiosin than to cycloprodigiosin. The secondary metabolite profiles of strain S1-1 and two reference bacterial strains were compared by liquid chromatography-mass spectrometry. Multivariate statistical analyses based on secondary metabolite profiles by liquid chromatography-mass spectrometry indicated that the metabolite profile of strain S1-1 could clearly be distinguished from those of two phylogenetically related, prodigiosin-producing bacterial strains.

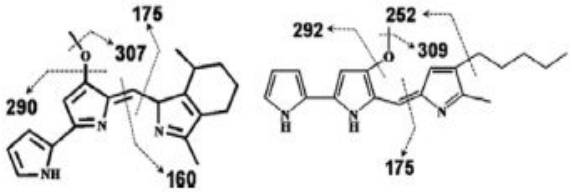

PMID: 21642414

Keywords : Hahella-Chejuensis KCTC-2396; *Zooshikella rubidus*; Gene-Cluster; Serratia-Marcescens; Mass-Spectrometry; H+/Cl-Symporter; Sp-Nov.; Biosynthesis; Hydrochloride

Article 64

Features and applications of bacterial sialidases

Appl Microbiol Biotechnol. 2011 Jul; 91(1):1-15.

Kim S, Oh DB, Kang HA, Kwon O*

*Corresponding: oskwon@kribb.re.kr
Systems & Synthetic Biology Research Center

Sialidases, or neuraminidases (EC 3.2.1.18), belong to a class of glycosyl hydrolases that release terminal *N*-acylneuraminate residues from the glycans of glycoproteins, glycolipids, and polysaccharides. In bacteria, sialidases can be used to scavenge sialic acids as a nutrient from various sialylated substrates or to recognize sialic acids exposed on the surface of the host cell. Despite the fact that bacterial sialidases share many structural features, their biochemical properties, especially their linkage and substrate specificities, vary widely. Bacterial sialidases can catalyze the hydrolysis of terminal sialic acids linked by the α(2,3)-, α(2,6)-, or α(2,8)-linkage to a diverse range of substrates. In addition, some of these enzymes can catalyze the transfer of sialic acids from sialoglycans to asialoglycoconjugates via a transglycosylation reaction mechanism. Thus, some bacterial sialidases have been applied to synthesize complex sialyloligosaccharides through chemoenzymatic approaches and to analyze the glycan structure. In this review article, the biochemical features of bacterial sialidases and their potential applications in regioselective hydrolysis reactions as well as sialylation by transglycosylation for the synthesis of sialylated complex glycans are discussed.

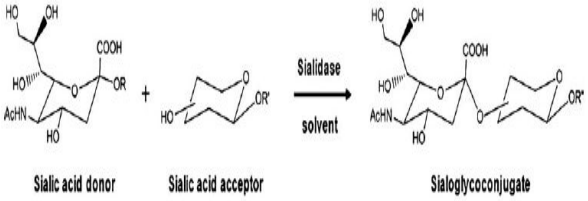

PMID: 21544654

Keywords : Sialidase; *In vitro* Trans-Sialylation; Sialoglycoconjugate; Chemoenzymatic Synthesis; Sialic Acid; *Streptococcus pneumoniae*; Corynebacterium-Diphtheriae

Article 65

Flavonoids biotransformation by bacterial non-heme dioxygenases, biphenyl and naphthalene dioxygenase

Appl Microbiol Biotechnol. 2011 Jul; 91(2):219-28.

Seo J*, Kang SI, Kim M, Han J, Hur HG

*First: jyseo@kribb.re.kr
Systems & Synthetic Biology Research Center

This review details recent progresses in the flavonoid biotransformation by bacterial non-heme dioxygenases, biphenyl dioxygenase (BDO), and naphthalene dioxygenase (NDO), which can initially activate biphenyl and naphthalene with insertion of dioxygen in stereospecfic and regiospecific manners. Flavone, isoflavone, flavanone, and isoflavanol were biotransformed by BDO from *Pseudomonas pseudoalcaligenes* KF707 and NDO from *Pseudomonas* sp. strain NCIB9816-4, respectively. In general, BDO showed wide range of substrate spectrum and produced the oxidized products, whereas NDO only metabolized flat two-dimensional substrates of flavone and isoflavone. Furthermore, biotransformation of B-ring skewed substrates, flavanone and isoflavanol, by BDO produced the epoxide products, instead of dihydrodiols. These results support the idea that substrate-driven reactivity alteration of the Fe-oxo active species may occur in the active site of non-heme dioxygenases. The study of flavonoid biotransformation by structurally-well defined BDO and NDO will provide the substrate structure and reactivity relationships and eventually establish the production of non-plant-originated flavonoids by means of microbial biotechnology.

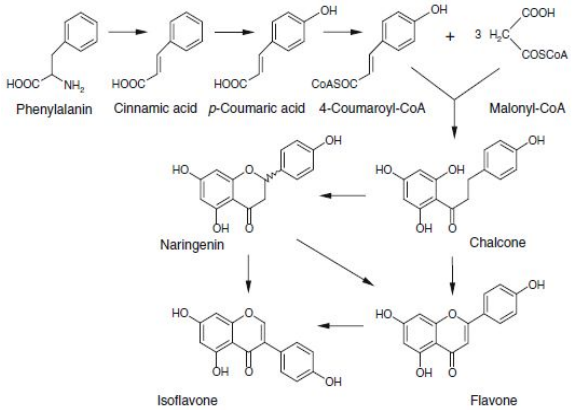

PMID: 21626021

Keywords : Biotransformation; Biphenyl Dioxygenase; Naphthalene Dioxygenase; Flavonoid; Polyphenol; *Aspergillus niger*; Gene-Cluster; Biosynthesis

Article 66

Evidences for correlation between the reduced VCAM-1 expression and hyaluronan synthesis during cellular senescence of human mesenchymal stem cells

Biochem Biophys Res Commun. 2011 Jan; 404(1):463-9.

Jung EM, Kwon O, Kwon KS, Cho YS, Rhee SK, Min JK*, Oh DB*

*Co-corresponding: jekmin@kribb.re.kr dboh@kribb.re.kr
Systems & Synthetic Biology Research Center

Mesenchymal stem cells (MSCs) undergo cellular senescence during *in vitro* expansion culture, which accompanies the loss of migration and homing abilities. In this study, we analyzed expression levels of several surface markers of human MSCs at different passages of expansion culture. It has been shown that expression of vascular cell adhesion molecule-1 (VCAM-1) was most markedly decreased among the tested markers in the senescent MSCs. Interestingly the reduced VCAM-1 expression could be restored by applying hyaluronan, a major glycosaminoglycan ligand of CD44, to the culture. It was found that the hyaluronan level in extracellular and pericellular matrices was greatly reduced in the senescent MSCs, mainly due to the decreased expression of hyaluronan synthases, suggesting a correlation between the reduced VCAM-1 expression and hyaluronan synthesis. In fact, when hyaluronan synthases were knock-downed by siRNA transfection, the VCAM-1 expression was also reduced. Our results indicate that VCAM-1 expression in the senescent MSCs was down-regulated because of the reduced synthesis of hyaluronan. Thus, we suggest that hyaluronan supplementation in expansion culture of MSCs would compensate adverse effects induced by its decreased synthesis and subsequently enhance cell adhesion and migration abilities.

PMID: 21144825

Keywords : Mesenchymal Stem Cells; VCAM-1 (CD106); Hyaluronan; CD44; Senescence; Crosslinking; Bone-Marrow; ICAM-1

Article 67

Phellinstatin, a new inhibitor of enoyl-ACP reductase produced by the medicinal fungus *Phellinus linteus*

Bioorg Med Chem Lett. 2011 Mar; 21(6):1716-8.

Cho JY, Kwon YJ, Sohn MJ, Seok SJ, Kim WG*

*Corresponding: wgkim@kribb.re.kr
Environmental Biotechnology Research Center

A new trimeric hispidin derivative, phellinstatin, was isolated from a culture broth of the medicinal fungus *Phellinus linteus* and its structure was established by various spectral analysis. Phellinstatin strongly inhibited *Staphylococcus aureus* enoyl-ACP reductase with an IC_{50} of 6 μM and also showed antibacterial activity against *S. aureus* and MRSA.

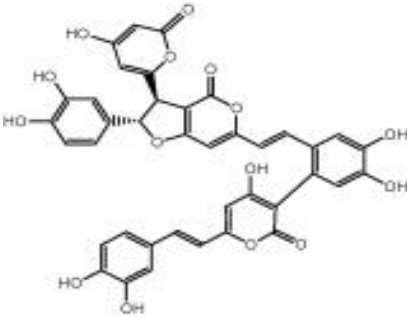

PMID: 21316961

Keywords : Hispidin; Enoyl-ACP Reductase; Inhibitor; Antibacterial; *Staphylococcus aureus*; *Phellinus linteus*; Inonotus-Xeranticus; Igniarius

Article 68

Ethanol fermentation from Jerusalem artichoke powder using *Saccharomyces cerevisiae* KCCM50549 without pretreatment for inulin hydrolysis

Bioresour Technol. 2011 Jan; 102(2):2109-11.

Lim SH, Ryu JM, Lee H, Jeon JH, Sok DE, Choi ES*

*Corresponding: choi4162@kribb.re.kr
Systems & Synthetic Biology Research Center

A strain of *Saccharomyces cerevisiae*, KCCM50549, was found to efficiently ferment the inulin-containing carbohydrates in Jerusalem artichoke without acidic or enzymatic pretreatment prior to fermentation. *S. cerevisiae* KCCM50549 could utilize almost completely the fructo-oligosaccharides present in Jerusalem artichoke (up to degree of polymerization (DP) of 15), in contrast to the other *S. cerevisiae* strain such as NCYC625 that fermented the fructo-oligosaccharides with DP of up to around six. Inulin-fermenting *S. cerevisiae* KCCM50549 produced c.a. 1.6 times more ethanol from Jerusalem artichoke compared with *S. cerevisiae* NCYC625. Direct ethanol fermentation of Jerusalem artichoke flour at 180 g/L without any supplements or pretreatments by *S. cerevisiae* KCCM50549 in a 5 L jar fermentor yielded 36.2 g/L of ethanol within 36 h. The conversion efficiency of inulin-type sugars to ethanol was 70% of the theoretical ethanol yield.

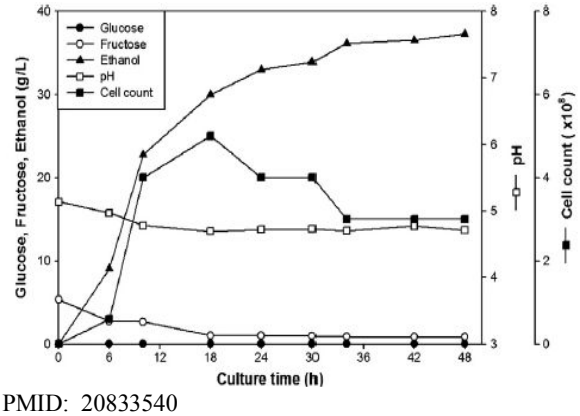

PMID: 20833540

Keywords : *Saccharomyces cerevisiae*; Ethanol; Jerusalem artichoke; Inulin

Article 69

Harvest of *Scenedesmus* sp. with bioflocculant and reuse of culture medium for subsequent high-density cultures

Bioresour Technol. 2011 Feb; 102(3):3163-8.

Kim DG, La HJ, Ahn CY, Park YH, Oh HM*

*Corresponding: heemock@kribb.re.kr
Environmental Biotechnology Research Center

The optimal flocculating conditions for harvesting high-density cultures of *Scenedesmus* sp. were investigated using inorganic coagulants and the bioflocculant produced by *Paenibacillus polymyxa* AM49. The flocculated medium as nutrients for subsequent algal cultivation was also tested. Consecutive treatment with 8.5 mM CaCl(2) and 0.2 mM FeCl(3) as coagulants and 1% bioflocculant from the culture broth of *P. polymyxa* AM49 showed the highest flocculating activity of up to 95% for high density algal cultures. The medium flocculated with the coagulants and bioflocculant showed less than 8% decrease in the growth yield in the subsequent algal cultivation. Furthermore, a 20% or 50% fresh BG11 medium supplement allowed the flocculated medium to maintain a high growth yield in subsequent algal cultivation. These results suggest that the flocculation method presented here is efficient and bio-friendly, and allows the reuse of the flocculated medium, thereby contributing to the economic cultivation and harvest of microalgae.

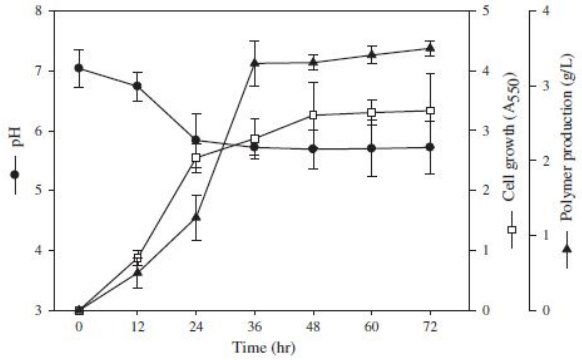

PMID: 21094603

Keywords : Bioflocculant; Flocculation; Harvest; Reuse of Medium; *Scenedesmus* sp.; Biopolymer; Microalgae; Biodiesel

Article 70

Cloning and characterization of a modular GH5 β-1,4-mannanase with high specific activity from the fibrolytic bacterium *Cellulosimicrobium* sp. strain HY-13

Bioresour Technol. 2011 Oct; 102(19):9185-92.

Kim DY, Ham SJ, Lee HJ, Cho HY, Kim JH, Kim YJ, Shin DH, Rhee YH, Son KH*, Park HY*

*Co-corresponding: sonkh@kribb.re.kr hypark@kribb.re.kr
Industrial Bio-materials Research Center

The gene (1272-bp) encoding a β-1,4-mannanase from a gut bacterium of *Eisenia fetida*, *Cellulosimicrobium* sp. strain HY-13 was cloned and expressed in *Escherichia coli*. The recombinant β-1,4-mannanase (rManH) was approximately 44.0 kDa and has a catalytic GH5 domain that is 65% identical to that of the *Micromonospora* sp. β-1,4-mannosidase. The enzyme exhibited the highest catalytic activity toward mannans at 50 °C and pH 6.0. rManH displayed a high specific activity of 14,711 and 8498 IU mg^{-1} towards ivory nut mannan and locust bean gum, respectively; however it could not degrade the structurally unrelated polysaccharides, mannobiose, or *p*-nitrophenyl sugar derivatives. rManH was strongly bound to ivory nut mannan, Avicel, chitosan, and chitin but did not attach to curdlan, insoluble oat spelt xylan, lignin, or poly(3-hydroxybutyrate). The superior biocatalytic properties of rManH suggest that the enzyme can be exploited as an effective additive in the animal feed industry.

PMID: 21767948

Keywords : *Cellulosimicrobium* sp Strain HY-13; *Eisenia fetida*; Gut Bacterium; High Specific Activity; beta-1,4-Mannanase; Sequence-Analysis; Gene Cloning; Enzyme

Article 71

Generation of catalytic protein particles in *Escherichia coli* cells using the cellulose-binding domain from *Cellulomonas fimi* as a fusion partner

Biotechnol Bioproc Eng. 2011; 16(6):1173-9.

Choi SL, Lee SJ, Ha KS, Song JJ, Rhee YH, Lee SG*

*Corresponding: sglee@kribb.re.kr
Systems & Synthetic Biology Research Center

The cellulose-binding domain (CBD) of a *Cellulomonas fimi* exo-glucanase was translationally fused with β-glucuronidase (GusA) from *Escherichia coli* and β-glycosidase (BglA) from *Thermus caldophilus*, respectively. Two fusion proteins (GusA-CBD and BglA-CBD) were expressed as insoluble aggregates in cells and isolated by centrifugation of the cell lysates. Interestingly, activity assays revealed that > 90% of the catalytic activity of both proteins was localized in the insoluble fractions. For example, the GusA-CBD particles exhibited 21 units per mg protein, which corresponded to 19% specific activity of the highly purified soluble GusA. The specific activity increased further up to 42 units per mg protein when treated with either sonication or chaotropic L-arginine. These results demonstrate that fusion with CBD family II may activate catalytic protein particles in *E. coli* cells, and that internal proteins of the particles are also active. Finally, the protein particles were tested in repeated batch operations after being cross-linked with chemicals, indicating that they have potential as a new preparation for immobilized biocatalysts.

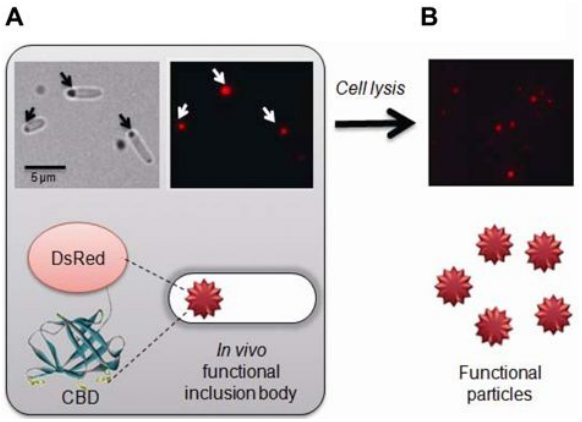

Keywords : Cellulose-Binding Domain (CBD); Protein Particles; Vivo Enzyme Immobilization; *Escherichia coli*; Beta-Glycosidase; Beta-Glucuronidase; Crystal-Structure

Article 72

Predicting tissue-specific expressions based on sequence characteristics

BMB Rep. 2011 Apr; 44(4):250-5.

Paik H, Ryu T, Heo HS, Seo SW, Lee D, Hur CG*

*Co-corresponding: hurlee@kribb.re.kr
Green Bio Research Center

In multicellular organisms, including humans, understanding expression specificity at the tissue level is essential for interpreting protein function, such as tissue differentiation. We developed a prediction approach via generated sequence features from overrepresented patterns in housekeeping (HK) and tissue-specific (TS) genes to classify TS expression in humans. Using TS domains and transcriptional factor binding sites (TFBSs), sequence characteristics were used as indices of expressed tissues in a Random Forest algorithm by scoring exclusive patterns considering the biological intuition; TFBSs regulate gene expression, and the domains reflect the functional specificity of a TS gene. Our proposed approach displayed better performance than previous attempts and was validated using computational and experimental methods.

Expressed tissue	Pattern*	TRANSFAC Description†	TRANSFAC Score†
Liver	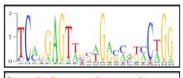	· HNF-1 (M01011) · TCat presented liver- specific TFBS	2.2
Kidney		· Zic3 · M00450 · GL1 protein related · Related to renal morphogenesis (33)	1.5
Brain	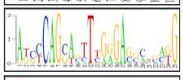	· M00138 · Brain octamer-protein related TFBS	2.3
Brain	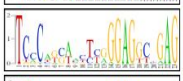	· Olf-1 · M00261 · DNA binding site for direct neuronal express	2.2
Lung	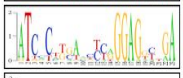	· STAT (M00224) · Unknown lung-specific TFBS	2.1
GI tract		· Muscle initiator (M00321) · Unknown GI tract- specific TFBS	1.8
Testis		· Spz1 (M00446) · Novel bHLH-Zip protein, testis-specific expressions	1.5

PMID: 21524350

Keywords : Domain; Housekeeping; Random Forest; Tissue-specific; Transcription Factor Binding Site; CpG Islands; Liver; Cirrhosis

Article 73

DNA barcodes for two scale insect families, mealybugs (Hemiptera: Pseudococcidae) and armored scales (Hemiptera: Diaspididae)

Bull Entomol Res. 2011 Aug; 101(4):429-34.

Park DS, Suh SJ, Hebert PD, Oh HW*, Hong KJ

*Co-corresponding: hwoh@kribb.re.kr
Industrial Bio-materials Research Center

Although DNA barcode coverage has grown rapidly for many insect orders, there are some groups, such as scale insects, where sequence recovery has been difficult. However, using a recently developed primer set, we recovered barcode records from 373 specimens, providing coverage for 75 species from 31 genera in two families. Overall success was >90% for mealybugs and >80% for armored scale species. The G·C content was very low in most species, averaging just 16.3%. Sequence divergences (K2P) between congeneric species averaged 10.7%, while intra-specific divergences averaged 0.97%. However, the latter value was inflated by high intra-specific divergence in nine taxa, cases that may indicate species overlooked by current taxonomic treatments. Our study establishes the feasibility of developing a comprehensive barcode library for scale insects and indicates that its construction will both create an effective system for identifying scale insects and reveal taxonomic situations worthy of deeper analysis.
PMID: 21272395

Keywords : DNA Barcoding; COI; Mealybug; Armored Scale; NUMTs; G.C Content; Evolution; ;Endosymbionts; Sequences

Article 74

Construction of an efficient *in vitro* system for analysis of transcription from Sigma 54-dependent *pspA* promoter

Bull Korean Chem Soc. 2011; 32(6):2129-31.

Han K, Bak G, Uhm KN, Kim KS*, Lee Y

*Co-corresponding: sunny06@kribb.re.kr
Systems & Synthetic Biology Research Center

IbsC is a small toxin protein in *Escherichia coli*, whose expression is repressed by a cis-acting small noncoding RNA, SibC. Overexpression of IbsC or the absence of SibC transcription induces the expression of both psp operon (*pspABCDE*) and *pspG* gene encoding phage shock proteins. The *psp* operon is transcribed from *pspA* promoter by RNA polymerase holoenzyme containing the alternative stress-responsive sigma factor 54. We prepared an S150 fraction from *E. coli* lysates as an *in vivo*-mimic transcription machinery for the *pspA* induction by IbsC. Our results show that the pRS56 fusion was appropriately constructed for efficient analysis of *in vitro* transcription from the σ 54-specific *pspA* promoter. The *in vitro* transcription system including the utilization of S100 we set up in this study can be used to analyze factors involved in transcription induction of *pspA* by IbsC.

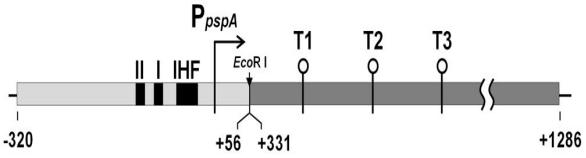

Keywords : Transcription; Sigma 54; *pspA* Promoter; *rnpB* Terminator; Shock Protein Operon; *Escherichia coli*; Sequences; RNAs; Sib

Article 75

Efficient synthesis of octyl-β-d-galactopyranoside by *Bacillus* spore-displayed β-galactosidase using an amphiphilic 1,2-dimethoxyethane co-solvent

Enzyme Microb Technol. 2011 Mar; 48(3):232-8.

Bae J, Choi EH, Pan JG*

*Corresponding: jgpan@kribb.re.kr
Systems & Synthetic Biology Research Center

For enzymatic synthesis of octyl-β-d-galactopyranoside (octyl-gal) from lactose and n-octanol, *Escherichia coli* β-galactosidase (β-Gal) was expressed and displayed on the surfaces of *Bacillus subtilis* spores. The spore-displayed β-Gal was found to be stable when an amphiphilic 1,2-dimethoxyethane (DME) was used as a co-solvent; the transgalactosylation efficiency and octyl-gal conversion were optimal at 50% (v/v) DME. In addition, the product was maximally obtained from 100mM lactose in a phosphate buffer/n-octanol/DME (25/25/50, v/v) mixture. By increasing the agitation speed and the amount of spores displaying β-Gal, a yield of 33.7 mM octyl-gal was obtained over 24h in a batch mode, which is much higher than in other octyl-gal bioconversion processes, such as those involving lipid-coating, reverse micelles, or whole cells. On the other hand, intermittent addition of spore-displayed β-Gal and/or lactose in the reaction medium had no effect on the octyl-gal yield. The synthesized octyl-gal was hydrolyzed by the spore-displayed β-Gal, and a high concentration of octyl-gal competitively inhibited the enzymes (K_i value of 10.8mM). In summary, we demonstrate that octyl-gal synthesis by spore-displayed β-Gal in non-aqueous medium can be significantly improved with the use of DME as a co-solvent.
PMID: 22112905

Keywords : Octyl Galactoside; Spore Display; Beta-Galactosidase; Transgalactosylation; Monoglyme; Co-Solvent; Enzymatic-Synthesis; Catalyzed Synthesis; Alkyl Glucoside; Glycosides

Article 76

A highly active endo-β-1,4-mannanase produced by *Cellulosimicrobium* sp. strain HY-13, a hemicellulolytic bacterium in the gut of *Eisenia fetida*

Enzyme Microb Technol. 2011 Apr; 48(4-5):365-70.

Kim DY, Ham SJ, Lee HJ, Kim YJ, Shin DH, Rhee YH, Son KH*, Park HY*

*Co-corresponding: sonkh@kribb.re.kr hypark@kribb.re.kr
Industrial Bio-materials Research Center

A xylanolytic gut bacterium isolated from *Eisenia fetida*, *Cellulosimicrobium* sp. strain HY-13, produced an extracellular glycoside hydrolase capable of efficiently degrading mannose-based substrates such as locust bean gum, guar gum, mannotetraose, and mannopentaose. The purified mannan-degrading enzyme (ManK, 34,926 Da) from strain HY-13 was found to have an N-terminal amino acid sequence of DEATTDGLHVVDD, which has not yet been identified. Under the optimized reaction conditions of 50°C and pH 7.0, ManK exhibited extraordinary high specific activities of 7109 IU/mg and 5158 IU/mg toward locust bean gum and guar gum, respectively, while the enzyme showed no effect on sugars substituted with *p*-nitrophenol and various non-mannose carbohydrates. Thin layer chromatography revealed that the enzyme degraded locust bean gum to mannobiose and mannotetraose. No detectable amount of mannose was produced from hydrolytic reactions with the substrates. ManK strongly attached to Avicel, β-cyclodextrin, lignin, and poly(3-hydroxybutyrate) granules, but not bound to chitin, chitosan, curdlan, or insoluble oat spelt xylan. The aforementioned characteristics of ManK suggest that it is a unique endo-β-1,4-mannanase without additional carbohydrolase activities, which differentiates it from other well-known carbohydrolases.
PMID: 22112951

Keywords : *Cellulosimicrobium* sp Strain HY-13; *Eisenia fetida*; Gut Bacterium; Highly Active Endo-beta-1,4-mannanase; Mannan-degrading Enzyme; Cellulomonas-Fimi; Endo-Beta-1,4-Xylanase

Article 77

Adsorption immobilization of *Escherichia coli* phytase on probiotic *Bacillus polyfermenticus* spores

Enzyme Microb Technol. 2011 Jun; 49(1):66-71.

Cho EA, Kim EJ, Pan JG*

*Corresponding: jgpan@kribb.re.kr
Systems & Synthetic Biology Research Center

The immobilization of enzymes on edible matrix supports is of great importance for developing stabilized feed enzymes. In this study, probiotic *Bacillus* spores were explored as a matrix for immobilizing *Escherichia coli* phytase, a feed enzyme releasing phosphate from phytate. Because *Bacillus* spore is inherently resistant to heat, solvents and drying, they were expected to be a unique matrix for enzyme immobilization. When mixed with food-grade *Bacillus polyfermenticus* spores, phytases were adsorbed to their surface and became immobilized. The amount of phytase attached was 28.2 ± 0.7 mg/g spores, corresponding to a calculated activity of 63,960 U/g spores; however, the measured activity was 41,120±990.1U/g spores, reflecting a loss of activity upon adsorption. Immobilization increased the half life (t(1/2)) of the enzyme three- to ten-fold at different temperatures ranging from 60 to 90°C. Phytase was bound to the spore surface to the extent that ultrasonication treatment was not able to detach phytases from spores. Desorption of spore-immobilized phytase was only achieved by treatment with 1M NaCl, 10% formic acid in 45% acetonitrile, SDS, or urea, suggesting that adsorption of phytase to the spore might be via hydrophobic and electrostatic interactions. We propose here that *Bacillus* spore is a novel immobilization matrix for enzymes that displays high binding capacity and provides food-grade safety.

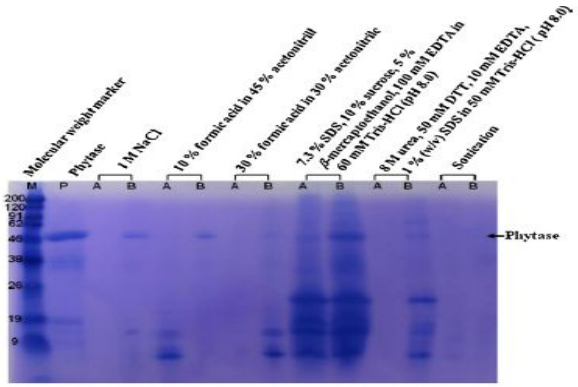

PMID: 22112273

Keywords : Adsorption Immobilization; Phytase; Thermostability; *Bacillus* spore; Generally Recognized-As-Safe (Gras); Feed Enzyme; Catalytic-Activity; Surface Display; Hydrophobicity

Article 78

Decolorization of indigo carmine by laccase displayed on *Bacillus subtilis* spores

Enzyme Microb Technol. 2011 Jun; 49(1):100-4.

Cho EA, Seo J, Lee DW, Pan JG*

*Corresponding: jgpan@kribb.re.kr
Systems & Synthetic Biology Research Center

Blue multicopper oxidases, laccases displayed on the surface of *Bacillus* spores were used to decolorize a widely used textile dyestuff, indigo carmine. The laccase-encoding gene of *Bacillus subtilis*, *cotA*, was cloned and expressed in *B. subtilis* DB104, and the expressed enzyme was spontaneously localized on *Bacillus* spores. *B. subtilis* spores expressing laccase exhibited maximal activity for the oxidation of 2,2'-azino-bis (3-ethylthiazoline-6-sulfonate) (ABTS) at pH 4.0 and 80°C, and for the decolorization of indigo carmine at pH 8.0 and 60°C. The displayed enzyme retained 80% of its original activity after pre-treatment with organic solvents such as 50% acetonitrile and n-hexane for 2h at 37°C. The apparent K_m of the enzyme displayed on spores was 443±124 μM for ABTS with a V_{max} of 150 ± 16 U/mg spores. Notably, 1mg of spores displaying *B. subtilis* laccase (3.4 × 10(2)U for ABTS as a substrate) decolorized 44.6 μg indigo carmine in 2h. The spore reactor (0.5 g of spores corresponding to 1.7×10(5)U in 50 mL) in a consecutive batch recycling mode decolorized 223 mg indigo carmine/L to completion within 42 h at pH 8.0 and 60°C. These results suggest that laccase displayed on *B. subtilis* spores can serve as a powerful environmental tool for the treatment of textile dye effluent.

PMID: 22112278

Keywords : Fungal Laccase; Spore Display; Decolorization; Indigo Carmine; *Bacillus subtilis*; Surface Display; T1 Copper Site; Trametes-Versicolor; Endospore Coat

Article 79

2-Aminobenzoic acid of *Bacillus* sp. BS107 as an ISR determinant against *Pectobacterium carotovorum* subsp. *carotovotrum* SCC1 in tobacco

Eur J Plant Pathol. 2011; 129(3):371-8.

Yang S, Park M, Kim I, Kim Y, Yang J, Ryu CM*

*Co-corresponding: cmryu@kribb.re.kr
Systems & Synthetic Biology Research Center

Root drench-treatment of tobacco seedlings with *Bacillus* sp. BS107 (BS107) suppressed disease development caused by the pathogen *Pectobacterium carotovorum* subsp. *carotovotrum* SCC1 (SCC1). A determinant of BS107 involved in induced systemic resistance (ISR) against SCC1 was isolated from cell-free culture. ISR bioassay-guided isolation was involved in determining active fractions during chromatography. Mass spectrometry and NMR analyses of the isolated metabolite identified 2-aminobenzoic acid (2-AB) as a main ISR determinant. 2-AB at 2.3 mM suppressed significantly disease development and exhibited no direct contact inhibition of pathogen. Reverse Transcriptase (RT)-PCR analyses of tobacco leaves revealed up-regulation of the induced resistance marker genes such as *PR1a, PR1c, PR2* and *PR4* by application of 2-AB on the root. Among aminobenzoic acids tested, 2- and 4-aminobenzoic acids showed ISR activity against soft-rot pathogen, but 3-aminobenzoic acid did not. This is the first report that 2-AB exhibits the ISR against SCC1in tobacco. BS107 can play a role in promoting plant defences by secretion of bacterial determinants including 2-AB for elicitation of ISR.

Keywords : Aminobenzoic Acid; *Bacillus* sp; BS107; Induced Systemic Resistance; Soft-rot Disease; Syringae pv. Tabaci; Mosaic-Virus; *Arabidopsis thaliana*; Plant Defenses

Article 80

The most abundant polyphenol of soyleaves, coumestrol, displays potent α-glucosidase inhibitory activity

Food Chem. 2011 Jun; 126(3):1057–63.

Yuk HJ, Lee JH, Curtis-Long MJ, Lee JW, Kim YS, Ryu HW, Park CG, Jeong TS*, Park KH

*Co-corresponding: tsjeong@kribb.re.kr
Industrial Bio-materials Research Center

The leaves of soybean (*Glycine max*) were extracted into four different polar solvents: ethylacetate, butanol, ethanol and water. The ethylacetate extract (EE) showed the lowest IC50 value against α-glucosidase (70.1 μg/ml). To investigate the compounds responsible for this effect, activity guided fractionation of soybean leaves by chromatography yielded seven phenolic compounds which were identified as formononetin (1), afromosin (2), coumestrol (3), isotrifoliol (4), phaseol (5), glyceofuran (6) and a new compound, glyceollin V (7). Importantly, coumestrol 3 was not only the most potent component with IC50 = 6.0 μM, but also the most abundantpolyphenol in soybean leaves. There was shown to be an increasing inhibition across the developmental stage of the plant, which correlated strongly with an increase in compound 3 in the leaves. In fact, we have shown it can comprise up to 65% of the polyphenols in the leaves by HPLC analysis.

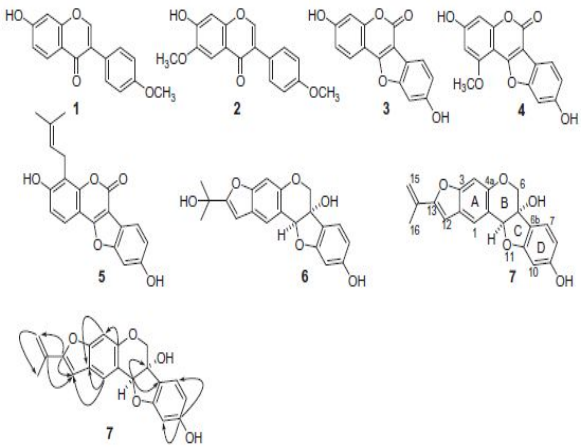

Keywords : Alpha-Clucosidase; Soy Leaf; Isoflavones; Pterocarpans; Coumestrol; Phytoestrogens; Cultivars; Seed

Article 81

Prediction of cancer prognosis with the genetic basis of transcriptional variations

Genomics. 2011 Jun; 97(6):350-7.

Paik H*, Lee E, Park I, Kim J, Lee D

*First: hyojung@kribb.re.kr
Green Bio Research Center

Phenotypes of diseases, including prognosis, are likely to have complex etiologies and be derived from interactive mechanisms, including genetic and protein interactions. Many computational methods have been used to predict survival outcomes without explicitly identifying interactive effects, such as the genetic basis for transcriptional variations. We have therefore proposed a classification method based on the interaction between genotype and transcriptional expression features (CORE-F). This method considers the overall "genetic architecture," referring to genetically based transcriptional alterations that influence prognosis. In comparing the performance of CORE-F with the ensemble tree, the best-performing method predicting patient survival, we found that CORE-F outperformed the ensemble tree (mean AUC, 0.85 vs. 0.72). Moreover, the trained associations in the CORE-F successfully identified the genetic mechanisms underlying survival outcomes at the interaction-network level.

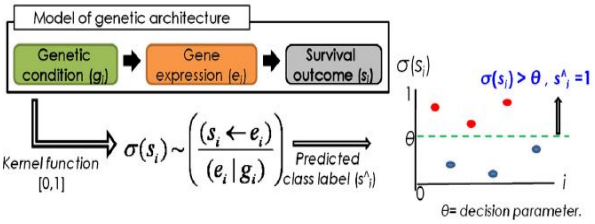

PMID: 21419214

Keywords : Genetic Architecture; Genotype; Transcriptional Variation; Survival Prediction; Ovarian-Cancer; Classification; Regression; Network

Article 82

Correlations between environmental factors and toxic and non-toxic *Microcystis* dynamics during bloom in Daechung Reservoir, Korea

Harmful Algae. 2011; 10(2):188-93.

Joung SH, Oh HM, Ko SR, Ahn CY*

*Corresponding: cyahn@kribb.re.kr
Environmental Biotechnology Research Center

While it has been known that toxic and non-toxic *Microcystis* coexist in lakes and their relative proportions vary depending on environmental factors, the main driving force for such variations is still unclear. Therefore, this study attempted to verify the environmental factors related to the dynamics of the abundance of toxic and non-toxic *Microcystis* in the Daechung Reservoir, Korea. Water samples were collected at weekly intervals from June to October, 2006. *Microcystis* was a dominant cyanobacterial genus during this period. The proportion of toxic *Microcystis* genotypes was quantified using a real-time PCR with 2 primer sets for the *cpcBA*-IGS and *mcyJ* genes to determine the total *Microcystis* and potentially toxic genotypes, respectively. Cell densities of toxic and non-toxic *Microcystis* were strongly related, implying that their growth may be governed by the same environmental factors. Although nontoxic *Microcystis* was generally dominant over potentially toxic genotypes, the toxic proportion briefly predominated during the *Microcystis* bloom. While the phosphorus concentration was the fundamental regulating factor for cyanobacterial proliferation, the proportion changes of potentially toxic *Microcystis* genotypes were more closely related with the water temperature ($P < 0.01$), suggesting that eutrophication together with global warming could lead to more frequent toxic blooms.

Keywords : Bloom; Cyanobacterium Microcystis; Microcystin; Toxic Genotypes; Real-time PCR; Phycocyanin Intergenic Spacer; Synthetase Gene; Flanking Regions; Aeruginosa

Article 83

Flavobacterium ponti sp. nov., isolated from seawater

Int J Syst Evol Microbiol. 2011 Jan; 61(1):81-5.

Yoon JH*, Park S, Kang SJ, Oh SJ, Myung SC, Kim W

*First: jhyoon@kribb.re.kr
Systems & Synthetic Biology Research Center

A Gram-stain-negative, non-flagellated, non-gliding, yellow-pigmented and rod-shaped bacterial strain, designated GSW-R14^T, was isolated from seawater of Geoje Island in the South Sea, Korea. Strain GSW-R14^T grew optimally at 25 °C, at pH 7.0-8.0 and in the presence of 2 % (w/v) NaCl. Phylogenetic analyses based on 16S rRNA gene sequences showed that strain GSW-R14^T belonged to the genus *Flavobacterium*, joining *Flavobacterium gelidilacus* LMG 21477^T by a bootstrap resampling value of 100 %. Strain GSW-R14^T exhibited 97.6 % 16S rRNA gene sequence similarity to F. gelidilacus LMG 21477^T and similarities of 91.2-95.2 % to other members of the genus Flavobacterium. Strain GSW-R14^T contained MK-6 as the predominant menaquinone. The fatty acid profile of strain GSW-R14^T was similar to that of *F. gelidilacus* LMG 21477^T. The DNA G+C content of strain GSW-R14^T was 31.4 mol% and its DNA-DNA relatedness with *F. gelidilacus* LMG 21477^T was 31 %. Strain GSW-R14^T could be distinguished from *F. gelidilacus* and the other species of the genus *Flavobacterium* by its phylogenetic and genetic distinctiveness and by several phenotypic properties. On the basis of these data, strain GSW-R14^T is considered to represent a novel species of the genus *Flavobacterium*, for which the name *Flavobacterium ponti* sp. nov. is proposed; the type strain is GSW-R14^T (=KCTC 22802^T =CCUG 58402^T).
PMID: 20154326

Keywords : Bacterial Systematics; Identification; Strains; Phylogenetic Analyses; *Flavobacterium ponti*; *F. gelidilacus*

Article 84

Roseovarius marinus sp. nov., isolated from seawater

Int J Syst Evol Microbiol. 2011 Feb; 61(2):427-32.

Jung YT, Lee JS, Oh KH, Oh TK, Yoon JH*

*Corresponding: jhyoon@kribb.re.kr
Systems & Synthetic Biology Research Center

A Gram-stain-negative, non-motile, ovoid- to rod-shaped bacterium, designated HDW-9^T, belonging to the class *Alphaproteobacteria*, was isolated from seawater of the Yellow Sea, Korea. Strain HDW-9^T grew optimally at pH 7.0-8.0, at 30 °C and with 2-3 % (w/v) NaCl. Neighbour-joining, maximum-likelihood and maximum-parsimony phylogenetic trees based on 16S rRNA gene sequences showed that strain HDW-9^T clustered with *Roseovarius crassostreae* CV919-312^T, with which it exhibited 95.5 % 16S rRNA gene sequence similarity. Strain HDW-9^T exhibited 92.5-94.7 % 16S rRNA gene sequence similarity with the other type strains of species of the genus *Roseovarius*. Strain HDW-9^T contained Q-10 as the predominant ubiquinone and $C_{18:1}$ ω7c as the major fatty acid. The DNA G+C content was 58.3 mol%. Differential phenotypic properties distinguished strain HDW-9^T from the other members of the genus Roseovarius. Strain HDW-9^T is considered to represent a novel species of the genus *Roseovarius*, for which the name *Roseovarius marinus* sp. nov. is proposed. The type strain is HDW-9^T (=KCTC 22805^T =CCUG 58403^T).
PMID: 20348324

Keywords : Roseobacter Clade; Bacteria; Bacteriochlorophyll; Identification; Sequences; Sediment; *Roseovarius marinus*

Article 85

Ohtaekwangia koreensis gen. nov., sp. nov. and *Ohtaekwangia kribbensis* sp. nov., isolated from marine sand, deep-branching members of the phylum *Bacteroidetes*

Int J Syst Evol Microbiol. 2011 May; 61(5):1066-72.

Yoon JH*, Kang SJ, Lee SY, Lee JS, Park S

*Corresponding: jhyoon@kribb.re.kr
Systems & Synthetic Biology Research Center

Two Gram-stain-negative, non-motile, non-spore-forming, rod-shaped bacterial strains, designated 3B-2^T and 10AO^T, were isolated from a sand sample collected from the west coast of the Korean peninsula by using low-nutrient media, and their taxonomic positions were investigated in a polyphasic study. The strains did not grow on marine agar. They grew optimally at 30 °C and pH 6.5-7.5. Strains 3B-2^T and 10AO^T shared 97.5 % 16S rRNA gene sequence similarity and mean level of DNA-DNA relatedness of 12 %. In phylogenetic trees based on 16S rRNA gene sequences, strains 3B-2^T and 10AO^T, together with several uncultured bacterial clones, formed independent lineages within the evolutionary radiation encompassed by the phylum *Bacteroidetes*. Strains 3B-2^T and 10AO^T contained MK-7 as the predominant menaquinone and iso-$C_{15:0}$ and $C_{16:1}\omega5c$ as the major fatty acids. The DNA G+C contents of strains 3B-2^T and 10AO^T were 42.8 and 44.6 mol%, respectively. Strains 3B-2^T and 10AO^T exhibited very low levels of 16S rRNA gene sequence similarity (<85.0 %) to the type strains of recognized bacterial species. These data were sufficient to support the proposal that the novel strains should be differentiated from previously known genera of the phylum *Bacteroidetes*. On the basis of the data presented, we suggest that strains 3B-2^T and 10AO^T represent two distinct novel species of a new genus, for which the names *Ohtaekwangia koreensis* gen. nov., sp. nov. (the type species; type strain 3B-2^T = KCTC 23018^T = CCUG 58939^T) and *Ohtaekwangia kribbensis* sp. nov. (type strain 10AO^T = KCTC 23019^T = CCUG 58938^T) are proposed.
PMID: 20511453

Keywords : Urchin Strongylocentrotus-intermedius; Emended Description; Bacterial Systematics; Soil Bacteria; Pure Culture; Microorganisms; *Ohtaekwangia koreensis*; *Ohtaekwangia kribbensis*

Article 86

Lysobacter dokdonensis sp. nov., isolated from soil

Int J Syst Evol Microbiol. 2011 May; 61(5):1089-93.

Oh KH, Kang SJ, Jung YT, Oh TK, Yoon JH*

*Corresponding: jhyoon@kribb.re.kr
Systems & Synthetic Biology Research Center

A Gram-negative, non-motile, rod-shaped bacterial strain, DS-58^T, was isolated from a soil sample from Dokdo, an island of Korea, and its taxonomic position was investigated. Phylogenetic analysis based on 16S rRNA gene sequences showed that strain DS-58^T fell within the family *Xanthomonadaceae*. The isolate showed 96.9 % 16S rRNA gene sequence similarity with its closest phylogenetic neighbour, *Lysobacter niastensis* GH41-7^T, and 93.4-95.7 % 16S rRNA gene sequence similarity with other members of the genus *Lysobacter*. Strain DS-58^T contained Q-8 as the predominant ubiquinone and iso-$C_{16:0}$, iso-$C_{15:0}$ and iso-$C_{17:1}\omega9c$ as the major fatty acids. The DNA G+C content was 68.1 mol%. Strain DS-58^T could be distinguished phenotypically from type strains of closely related species of the genus *Lysobacter* and phylogenetically from all members of the genus *Lysobacter*. On the basis of phenotypic, chemotaxonomic and phylogenetic data, strain DS-58^T is considered to represent a novel species of the genus *Lysobacter*, for which the name *Lysobacter dokdonensis* sp. nov. is proposed. The type strain is DS-58^T (= KCTC 12822^T = DSM 17958^T).
PMID: 20525815

Keywords : Greenhouse Soils; Ginseng Field; Genus; Identification; Rhizosphere; Bacteria; *Lysobacter dokdonensis*

Article 87

Ruegeria faecimaris sp. nov., isolated from a tidal flat sediment

Int J Syst Evol Microbiol. 2011 May; 61(5):1182-8.

Oh KH, Jung YT, Oh TK, Yoon JH*

*Corresponding: jhyoon@kribb.re.kr
Systems & Synthetic Biology Research Center

A Gram-negative-staining, non-motile and rod-shaped bacterial strain, HD-28^T, was isolated from a tidal flat of the Yellow Sea, Korea. Strain HD-28^T grew optimally at pH 7.0-8.0 and 30 °C in the presence of 2-3 % (w/v) NaCl. Phylogenetic analyses based on 16S rRNA gene sequences showed that strain HD-28^T was most closely related to species of the genus *Ruegeria* and exhibited 95.5-96.9 % 16S rRNA gene sequence similarity to the type strains of *Ruegeria* species. A neighbour-joining phylogenetic tree based on *gyrB* gene sequences also showed that strain HD-28^T fell within the cluster comprising recognized species of the genus *Ruegeria*, showing 77.5-83.9 % sequence similarity. Strain HD-28^T contained Q-10 as the predominant ubiquinone and $C_{18:1}\omega7c$ as the major fatty acid. The major polar lipids detected in strain HD-28^T were phosphatidylcholine, phosphatidylglycerol, an unidentified aminolipid and two unidentified lipids. The DNA G+C content was 57.9 mol%. Differential phenotypic properties, together with phylogenetic distinctiveness, demonstrated that strain HD-28^T could be distinguished from recognized species of the genus *Ruegeria*. On the basis of phenotypic, chemotaxonomic and phylogenetic data, strain HD-28^T is considered to represent a novel species of the genus *Ruegeria*, for which the name *Ruegeria faecimaris* sp. nov. is proposed. The type strain is HD-28^T (= KCTC 23044^T = CCUG 58878^T).
PMID: 20562248

Keywords : Gen.-Nov.; Comb. Nov.; Bacteria; Reclassification; Silicibacter; Mobilis; Strains; Pelagia; *Ruegeria faecimaris*

Article 88

Paraperlucidibaca baekdonensis gen. nov., sp. nov., isolated from seawater

Int J Syst Evol Microbiol. 2011 Jun; 61(6):1382-5.

Oh KH, Lee SY, Lee MH, Oh TK, Yoon JH*

*Corresponding: jhyoon@kribb.re.kr
Systems & Synthetic Biology Research Center

A Gram-negative, non-spore-forming, rod-shaped bacterial strain, RL-2^T, was isolated from seawater of the East Sea in Korea and was subjected to a polyphasic taxonomic study. Strain RL-2^T grew optimally at pH 7.5-8.0, at 20 °C and in the absence of NaCl. Phylogenetic trees based on 16S rRNA gene sequence analysis showed that strain RL-2^T forms a cluster with *Perlucidibaca piscinae* IMCC1704^T and various uncultured and unidentified gammaproteobacteria. Strain RL-2^T exhibited 16S rRNA gene sequence similarity values of 96.1 % to *Perlucidibaca piscinae* IMCC1704^T and 93.7-99.7 % to the uncultured bacterial clones belonging to the cluster and an unidentified gammaproteobacterium. The fatty acid profile of strain RL-2^T was similar to that of *Perlucidibaca piscinae* IMCC1704^T, but the predominant ubiquinone type (Q-11) of strain RL-2^T was different from that (Q-8) of *Perlucidibaca piscinae* IMCC1704^T. The DNA G+C content of strain RL-2^T was 61.3 mol%. On the basis of phylogenetic, chemotaxonomic and phenotypic data, strain RL-2^T is considered to represent a novel species of a new genus in the family *Moraxellaceae*, for which the name *Paraperlucidibaca baekdonensis* gen. nov., sp. nov. is proposed. The type strain of *Paraperlucidibaca baekdonensis* is RL-2^T (= KCTC 23145^T = CCUG 59307^T).
PMID: 20601489

Keywords : Bacteria; Identification; *Moraxellaceae*; Psychrobacter; Sea; *Paraperlucidibaca baekdonensis*

Article 89

Mucilaginibacter boryungensis sp. nov., isolated from soil

Int J Syst Evol Microbiol. 2011 Jul; 61(7):1549-53.

Kang SJ, Jung YT, Oh KH, Oh TK, Yoon JH*

*Corresponding: jhyoon@kribb.re.kr
Systems & Synthetic Biology Research Center

A Gram-stain-negative, non-motile, non-spore-forming bacterial strain, BDR-9^T, was isolated from soil collected from Boryung on the west coast of the Korean peninsula, and its taxonomic position was investigated by using a polyphasic study. Strain BDR-9^T grew optimally at 25 °C, at pH 6.0-7.5 and in the absence of NaCl. Phylogenetic analyses based on 16S rRNA gene sequences revealed that strain BDR-9^T fell within the clade comprising species of the genus *Mucilaginibacter* within the phylum *Bacteroidetes*. 16S rRNA gene sequence similarity values between strain BDR-9^T and the type strains of species of the genus *Mucilaginibacter* were in the range 94.0-95.6 %. Strain BDR-9^T contained MK-7 as the predominant menaquinone and iso-$C_{15:0}$ and $C_{16:1}\omega7c$ and/or iso-$C_{15:0}$ 2-OH as the major fatty acids. The DNA G+C content was 44.3 mol%. Differential phenotypic properties and phylogenetic distinctiveness of strain BDR-9^T demonstrated that this strain is distinguishable from species of the genus *Mucilaginibacter*. On the basis of phenotypic, chemotaxonomic and phylogenetic data, strain BDR-9^T is considered to represent a novel species of the genus *Mucilaginibacter*, for which the name *Mucilaginibacter boryungensis* sp. nov. is proposed. The type strain is BDR-9^T (= KCTC 23157^T = CCUG 59599^T).
PMID: 20656810

Keywords : Bacteria; Identification; Soil; Polyphasic Study; Phylogenetic Analyses; *Mucilaginibacter boryungensis*

Article 90

Thalassomonas agariperforans sp. nov., an agarolytic bacterium isolated from marine sand

Int J Syst Evol Microbiol. 2011 Nov; 61(11):2573-6.

Park S, Choi WC, Oh TK, Yoon JH*

*Corresponding: jhyoon@kribb.re.kr
Systems & Synthetic Biology Research Center

A Gram-staining-negative, motile, agarolytic bacterium, designated M-M1^T, was isolated from marine sand obtained from Geoje Island, South Sea, Korea, and its taxonomic position was investigated using a polyphasic taxonomic approach. Strain M-M1^T grew optimally at pH 7.0-8.0, at 30 °C and in the presence of 2 % (w/v) NaCl. It did not grow in the presence of >7 % (w/v) NaCl. Phylogenetic analysis based on 16S rRNA gene sequences showed that strain M-M1^T fell within the clade comprising members of the genus *Thalassomonas*, clustering with *Thalassomonas agarivorans* TMA1^T, *Thalassomonas loyana* CBMAI 722^T and *Thalassomonas ganghwensis* JC2041^T, with which it exhibited 16S rRNA gene sequence similarity values of 96.4, 96.0 and 94.9 % respectively. Strain M-M1^T exhibited 94.7-95.2 % 16S rRNA gene sequence similarity to the other species of the genus *Thalassomonas*. Strain M-M1^T contained Q-8 as the predominant ubiquinone and $C_{16:1}\omega7c$ and/or iso-$C_{15:0}$ 2-OH, $C_{16:0}$ and $C_{18:1}\omega7c$ as the major fatty acids. The DNA G+C content was 44.2 mol%. Strain M-M1^T could be differentiated from phylogenetically related species of the genus *Thalassomonas* by differences in some phenotypic properties. On the basis of the phenotypic, chemotaxonomic and phylogenetic data, strain M-M1^T is considered to represent a novel species of the genus *Thalassomonas*, for which the name *Thalassomonas agariperforans* sp. nov. is proposed. The type strain is M-M1^T (= KCTC 23343^T = CCUG 60020^T).
PMID: 21131503

Keywords : Identification; Sediment; Marine Sand; Agarolytic Bacterium; Polyphasic Taxonomic Approach; *Thalassomonas agariperforans*

Article 91

Oceanisphaera ostreae sp. nov., isolated from seawater of an oyster farm, and emended description of the genus *Oceanisphaera* Romanenko et al. 2003

Int J Syst Evol Microbiol. 2011 Dec; 61(12):2880-4.

Choi WC, Kang SJ, Jung YT, Oh TK, Yoon JH*

*Corresponding: jhyoon@kribb.re.kr
Systems & Synthetic Biology Research Center

A Gram-stain-negative, motile, non-spore-forming and short rod- or rod-shaped bacterial strain, T-w6^T, was isolated from seawater of an oyster farm in the South Sea, Korea. Strain T-w6^T grew optimally at 25 °C and in the presence of 2% (w/v) NaCl. Phylogenetic analyses based on 16S rRNA gene sequences revealed that strain T-w6^T joined the cluster comprising *Oceanisphaera* species with a bootstrap resampling value of 90.8%, and this cluster joined the clade comprising members of the genera Oceanimonas and Zobellella with a bootstrap resampling value of 100%. Strain T-w6^T exhibited 16S rRNA gene sequence similarity of 95.9 and 96.6% to the type strains of *Oceanisphaera litoralis* and *Oceanisphaera donghaensis*, respectively. Strain T-w6^T and the type strains of *Oceanisphaera litoralis* and *Oceanisphaera donghaensis* had Q-8 as the predominant ubiquinone and iso-$C_{15:0}$ 2-OH and/or $C_{16:1}\omega7c$, $C_{18:1}\omega7c$ and $C_{16:0}$ as the major fatty acids. The major polar lipids were phosphatidylglycerol and phosphatidylethanolamine. The DNA G+C content of strain T-w6^T was 56.6 mol%. Mean DNA-DNA relatedness of strain T-w6^T with *Oceanisphaera litoralis* DSM 15406^{T}and *Oceanisphaera donghaensis* KCTC 12522^T was 13 and 10%, respectively. Phenotypic properties of strain T-w6^T demonstrated that this strain could be distinguished from the other *Oceanisphaera* species. On the basis of the data presented, strain T-w6^T is considered to represent a novel species of the genus *Oceanisphaera*, for which the name *Oceanisphaera ostreae* sp. nov. is proposed; the type strain is T-w6^T (=KCTC 23422^T =CCUG 60525^T). An emended description of the genus *Oceanisphaera* is also presented.
PMID: 21257693

Keywords : Halophilic Bacterium; Identification; Strains; Sea; Phylogenetic Analyses; *Oceanisphaera ostreae*;

Article 92

Creation of metal-independent hyperthermophilic L-arabinose isomerase by homologous recombination

J Agric Food Chem. 2011 Dec; 59(24):12939-47.

Hong YH, Lee DW*, Pyun YR, Lee SH

*Co-first: leehicam@kribb.re.kr
Systems & Synthetic Biology Research Center

Hyperthermophilic L-arabinose isomerases (AIs) are useful in the commercial production of D-tagatose as a low-calorie bulk sweetener. Their catalysis and thermostability are highly dependent on metals, which is a major drawback in food applications. To study the role of metal ions in the thermostability and catalysis of hyperthermophilic AI, four enzyme chimeras were generated by PCR-based hybridization to replace the variable N- and C-terminal regions of hyperthermophilic *Thermotoga maritima* AI (TMAI) and thermophilic *Geobacillus stearothermophilus* AI (GSAI) with those of the homologous mesophilic *Bacillus halodurans* AI (BHAI). Unlike Mn(2+)-dependent TMAI, the GSAI- and TMAI-based hybrids with the 72 C-terminal residues of BHAI were not metal-dependent for catalytic activity. By contrast, the catalytic activities of the TMAI- and GSAI-based hybrids containing the N-terminus (residues 1-89) of BHAI were significantly enhanced by metals, but their thermostabilities were poor even in the presence of Mn(2+), indicating that the effects of metals on catalysis and thermostability involve different structural regions. Moreover, in contrast to the C-terminal truncate (Δ20 residues) of GSAI, the N-terminal truncate (Δ7 residues) exhibited no activity due to loss of its native structure. The data thus strongly suggest that the metal dependence of the catalysis and thermostability of hyperthermophilic AIs evolved separately to optimize their activity and thermostability at elevated temperatures. This may provide effective target regions for engineering, thereby meeting industrial demands for the production of D-tagatose.

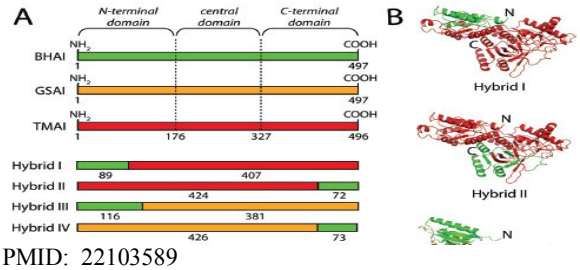

PMID: 22103589

Keywords : L-Arabinose Isomerase; Metal; Thermostability; Chimera; D-Tagatose; D-Galactose; Thermotoga-Neapolitana; Xylose Isomerase; Rhamnose Isomerase; Stearothermophilus

Article 93

Aquastatin C, a new glycoaromatic derivative from *Sporothrix* sp. FN611

J Antibiot. 2011 Feb; 64(2):213-6.

Kwon YJ, Sohn MJ, Kim WG*

*Corresponding: wgkim@kribb.re.kr
Environmental Biotechnology Research Center

Bacterial fatty acid synthesis (FAS) is an attractive antibacterial target. The bacterial fatty acid system (FAS II) uses discrete monofunctional enzymes, whereas mammalian fatty acid synthase (FAS I) is mediated by a single multifunctional enzyme–ACP complex. The enoyl-ACP reductase inhibitors may prove to be interesting lead compounds for the development of effective antibacterial drugs. We previously isolated aquastatin A from a fungal strain Sporothrix sp. AT 28. Aquastatin B was obtained by acid hydrolysis from aquastatin A. Aquastatin C is a rare metabolite incorporating one aromatic ring with a sugar and an aliphatic chain. Aquastatin C is a new glycoaromatic derivative of aquastatin A. Aquastatin C completely lost inhibitory activity of aquastatin A against bacterial enoyl-ACP reductases, such as S. aureus FabI, S. pneumoniae FabK and M. tuberculosis InhA. Also aquastatin C did not inhibited bacterial growth of S. aureus, methicillin-resistant S. aureus and S. pneumonia. These results could provide new insights into the development of a selective mechanism-based antibacterial agent with targeting FabI.

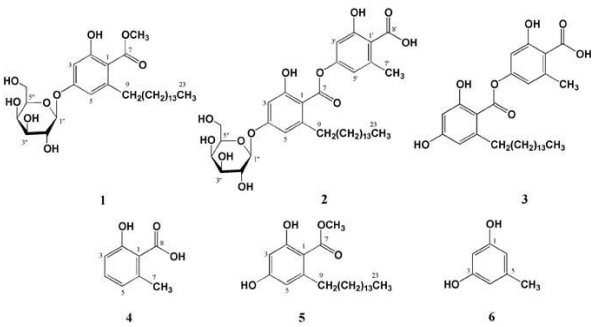

PMID: 21139622

Keywords : Antibacterial; Aquastatin; Enoyl-ACP Reductase; *Sporothrix*; *Staphylococcus aureus*; Cyclic-Nucleotide Phosphodiesterase; Inhibitor; KS-502

Article 94

Effect of nitrogen limitation on oleic acid biosynthesis in *Botryococcus braunii*

J Appl Phycol. 2011; 23(6):1031-7.

Choi GG, Kim BH, Ahn CY, Oh HM*

*Corresponding: heemock@kribb.re.kr
Environmental Biotechnology Research Center

The influence of nitrogen (N) deficiency on the cell growth and intracellular lipid production of the alga *Botryococcus braunii* UTEX 572 was investigated. Biomass concentration and lipid content of *B. braunii* cultivated in modified Chu-13 medium containing 0.04, 0.37, and 3.66 mM nitrate were 0.23-0.38 g L(-1) and 36-63% of dry cell weight, respectively. The specific growth rate of *B. braunii* reached a constant of 0.185 day(-1) during cultivation with an initial nitrate feed of 3.66 mM. The maximum lipid content of *B. braunii* was 63% with 0.04 mM nitrate. However, the maximum lipid productivity of 0.019 g L(-1) day(-1) was achieved with 0.37 mM nitrate. The level of oleic acid, an important component of biodiesel, was higher at 86% of the total fatty acids under N-limited conditions (0.04 mM nitrate) compared to 69% under N-sufficient conditions (3.66 mM nitrate). Furthermore, expression of the stearoyl-ACP desaturase gene (*sad*) encoding a stearoyl-ACP desaturase involved in the synthesis of oleic acid was 2.6-fold higher under N-limited conditions than under N-sufficient conditions.

Keywords : Biodiesel; *Botryococcus braunii*; Nitrogen Limitation; Oleic Acid; Sad; Stearoyl-ACP Desaturase; Lipid-Accumulation; Isochrysis-Galbana; Rt-PCR; Microalgae

Article 95

Complete genome sequence of the polycyclic aromatic hydrocarbon-degrading bacterium *Alteromonas* sp. strain SN2

J Bacteriol. 2011 Aug; 193(16):4292-3.

Jin HM, Jeong H, Moon EJ, Math RK, Lee K, Kim HJ, Jeon CO, Oh TK*, Kim JF

*Co-corresponding: otk@kribb.re.kr
Systems & Synthetic Biology Research Center

Alteromonas species are functionally important in the recovery of marine habitats from pollution. *Alteromonas* sp. strain SN2, able to metabolize polycyclic aromatic hydrocarbons, was isolated from a crude oil-contaminated sea-tidal flat. Here we report the complete 4.97-Mb genome sequence and annotation of strain SN2. This genomic sequence was determined using the Roche/454 technology. These will advance the understanding of strain SN2's adaptation to the sea-tidal flat ecosystem and its pollutant metabolic versatility.
PMID: 21705606

Keywords : Organic-Matter; RNA Genes; Sea; Aromatic Hydrocarbons; Bacterium; Pollutant Metabolic Versatility; *Alteromonas* sp.

Article 96

Draft genome sequence of the *Paenibacillus polymyxa* type strain (ATCC 842^T), a plant growth-promoting bacterium

J Bacteriol. 2011 Sep; 193(18):5026-7.

Jeong H*, Park SY, Chung WH, Kim SH, Kim N, Park SH, Kim JF

*Co-corresponding: hyjeong@kribb.re.kr
Systems & Synthetic Biology Research Center

Paenibacillus polymyxa is an endospore-forming Gram-positive soil bacterium that is well-known for its ability to promote plant growth. Here we report the draft genome sequence of *P. polymyxa* ATCC 842^T, the type strain of the species *P. polymyxa*, and the family *Paenibacillaceae*. The genome of *P. polymyxa* ATCC 842^T was sequenced using an Illumina genome analyzer platform. Genome annotation was performed using the RAST server and the AutoFACT software. The *P. polymyxa* genome contains a repertoire of biosynthetic genes for antibiotics and hydrolytic enzymes that account for its beneficial effects in the rhizosphere to the host plants it associates with. The genome information provided here will allow further study of the plant growth-promoting activity of *P. polymyxa* species at the genomic level.

PMID: 21742878

Keywords : Ribosomal-RNA; *Bacillus*; Identification; E681; Rhizobacterium; Biosynthesis; Ecology; Plant Growth; *Paenibacillus polymyxa*

Article 97

Genome sequence of an ammonia-oxidizing soil archaeon, "*Candidatus* Nitrosoarchaeum koreensis" MY1

J Bacteriol. 2011 Oct; 193(19):5539-40.

Kim BK, Jung MY, Yu DS, Park SJ, Oh TK, Rhee SK, Kim JF*

*Corresponding: jfk@kribb.re.kr
Systems & Synthetic Biology Research Center

Ammonia-oxidizing archaea are ubiquitous microorganisms which play important roles in global nitrogen and carbon cycle on earth. Here we present the high-quality draft genome sequence of an ammonia-oxidizing archaeon, "*Candidatus* Nitrosopumilus koreensis" MY1, that dominated an enrichment culture of a soil sample from the rhizosphere. The genome sequence of MY1 was determined by next generation sequencing technologies. MY1 keeps a number of genes to cope with oxidative stress and antibiotic resistance genes. MY1 is thought to have a citrate transporter for citrate utilization and NiFe-hydrogenase genes related to energy metabolism to survive competition in the rhizosphere. Its genome contains genes for survival in the rhizosphere environment as well as those for carbon fixation and ammonium oxidation to nitrite.

PMID: 21914867

Keywords : Ammonia-oxidizing Archaea; Marine Crenarchaeota; Rhizosphere; Bacteria; Nitrification; Assimilation; Sea; *Nitrosoarchaeum koreensis*

Article 98

Crystal structure of the human N-Myc downstream-regulated gene 2 protein provides insight into its role as a tumor suppressor

J Biol Chem. 2011 Apr; 286(14):12450-60.

Hwang J, Kim Y, Kang HB, Jaroszewski L, Deacon AM, Lee H, Choi WC, Kim KJ, Kim CH, Kang BS, Lee JO, Oh TK, Kim JW*, Wilson IA, Kim MH*

*Co-corresponding: wjkim@kribb.re.kr mhk8n@kribb.re.kr
Systems & Synthetic Biology Research Center

Considerable attention has recently been paid to the N-Myc downstream-regulated gene (*NDRG*) family because of its potential as a tumor suppressor in many human cancers. Primary amino acid sequence information suggests that the NDRG family proteins may belong to the α/β-hydrolase (ABH) superfamily; however, their functional role has not yet been determined. Here, we present the crystal structures of the human and mouse NDRG2 proteins determined at 2.0 and 1.7 Å resolution, respectively. Both NDRG2 proteins show remarkable structural similarity to the ABH superfamily, despite limited sequence similarity. Structural analysis suggests that NDRG2 is a nonenzymatic member of the ABH superfamily, because it lacks the catalytic signature residues and has an occluded substrate-binding site. Several conserved structural features suggest NDRG may be involved in molecular interactions. Mutagenesis data based on the structural analysis support a crucial role for helix α6 in the suppression of TCF/β-catenin signaling in the tumorigenesis of human colorectal cancer, via a molecular interaction.

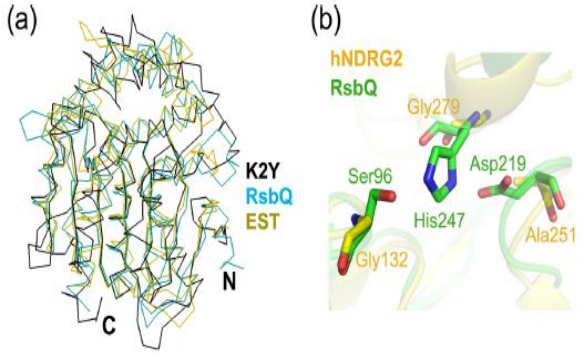

PMID: 21247902

Keywords : Colon-Carcinoma Cells; Beta Catenin; Tumor Suppressor; Metastasis Suppressor; Colorectal Cancer; Prostate Cancer; Down Regulation; C-Myc; NDRG2

Article 99

Whitefly infestation of pepper plants elicits defence responses against bacterial pathogens in leaves and roots and changes the below-ground microflora

J Ecol. 2011; 99(1):46-56.

Yang JW, Yi HS, Kim H, Lee B, Lee S, Ghim SY, Ryu CM*

*Corresponding: cmryu@kribb.re.kr
Systems & Synthetic Biology Research Center

Upon facing biotic stresses, plants orchestrate defence mechanisms via internal and external mechanisms that are mediated by signalling molecules such as salicylic acid, jasmonic acid, ethylene and various other volatile compounds. Although pathogen- and chemical-induced plant resistance has been studied extensively within the same plant compartment, the effects of above-ground (AG) insect-elicited plant defence on the resistance expression in roots and the below-ground (BG) microbial community are not well understood. We assessed the effect of AG whitefly (*Bemisia tabaci*) attack on the elicitation of induced resistance against a leaf pathogen, *Xanthomonas axonopodis* pv. *vesicatoria*, a soil-borne pathogen, *Ralstonia solanacearum*, and on BG modifications of the rhizosphere microflora in peppers (*Capsicum annuum*). Symptom development caused by the two bacterial pathogens on leaves and roots was significantly reduced in whitefly-exposed plants as compared to controls. A combined treatment with benzothiadiazole (BTH) and whitefly caused an additive effect on induced resistance, indicating that whitefly-induced plant defence can utilize salicylic acid (SA)-dependent signalling. To obtain further genetic evidence of this phenomenon, we evaluated the gene expression of *Capsicum annuum pathogenesis-related protein* (*CaPR*) *1*, *CaPR4, CaPR10* and *Ca protease inhibitor II*, and observed increased expression after BTH and/or whitefly treatment indicating that AG whitefly infestation elicited SA and jasmonic acid signalling in AG and BG. Since the expression pattern of PR genes in the roots differed, we assessed microbial diversity in plants treated with BTH and/or whitefly. In addition to eliciting BG defence responses, a whitefly infestation of the leaves augmented the population of root-associated Gram-positive bacteria and fungi, which may have positively affected plant growth and induced systemic resistance. Whitefly feeding reduced plant size, which usually occurs as a consequence of the high costs of direct resistance induction. Our results demonstrate that whitefly-induced resistance against bacterial pathogens can cross the AG-BG border and may cause further indirect benefits on future plant development, because it can positively affect the association or plant roots with putatively beneficial microorganisms.

Keywords : Above-Ground; Below-Ground; Plant Growth; Rhizobacteria; Plant-Herbivore Interactions; *Ralstonia solanacearum*; Whitefly; *Xanthomonas axonopodis*

Article 100

Shewanella upenei sp. nov., a lipolytic bacterium isolated from bensasi goatfish *Upeneus bensasi*

J Microbiol. 2011 Jun; 49(3):381-6.

Kim KK, Kim YO, Park S, Kang SJ, Nam BH, Kim DN, Oh TK, Yoon JH*

*Corresponding: jhyoon@kribb.re.kr
Systems & Synthetic Biology Research Center

A Gram-staining-negative, motile, non-spore-forming and rod-shaped bacterial strain, 20-23R^T, was isolated from intestine of bensasi goatfish, *Upeneus bensasi*, and its taxonomic position was investigated by using a polyphasic study. Phylogenetic analyses based on 16S rRNA gene sequences revealed that strain 20-23R^T belonged to the genus *Shewanella*. Strain 20-23R^T exhibited 16S rRNA gene sequence similarity values of 99.5, 99.2, and 97.5% to *Shewanella algae* ATCC 51192^T, *Shewanella haliotis* DW01^T, and *Shewanella chilikensis* JC5^T, respectively. Strain 20-23R^T exhibited 93.1-96.0% 16S rRNA gene sequence similarity to the other *Shewanella* species. It also exhibited 98.3-98.4% *gyrB* sequence similarity to the type strains of S. algae and *S. haliotis*. Strain 20-23R^T contained simultaneously both menaquinones and ubiquinones; the predominant menaquinone was MK-7 and the predominant ubiquinones were Q-8 and Q-7. The fatty acid profiles of strain 20-23R^T, *S. algae* KCTC 22552^T and *S. haliotis* KCTC 12896^T were similar; major components were iso-$C_{15:0}$, $C_{16:1}$, $C_{16:0}$ ω7c and/or iso-$C_{15:0}$ 2-OH and $C_{17:1}$ ω8c. The DNA G+C content of strain 20-23R^T was 53.9 mol%. Differential phenotypic properties and genetic distinctiveness of strain 20-23R^T, together with the phylogenetic distinctiveness, revealed that this strain is distinguishable from recognized *Shewanella* species. On the basis of the data presented, strain 20-23R^T represents a novel species of the genus *Shewanella*, for which the name *Shewanella upenei* sp. nov. is proposed. The type strain is 20-23R^T (=KCTC 22806^T =CCUG 58400^T). PMID: 21717322

Keywords : *Shewanella upenei*; *Upeneus bensasi*; Taxonomy; New Species; Polyunsaturated Fatty-Acid; Sediments; Marine-Bacteria; Systematics

Article 101

Identification of the genes involved in 1-deoxynojirimycin synthesis in *Bacillus subtilis* MORI 3K-85

J Microbiol. 2011 Jun; 49(3):431-40.

Kang KD, Cho YS, Song JH, Park YS, Lee JY, Hwang KY, Rhee SK, Chung JH, Kwon O*, Seong SI

*Co-corresponding: oskwon@kribb.re.kr
Systems & Synthetic Biology Research Center

1-Deoxynojirimycin (DNJ), a D-glucose analogue with a nitrogen atom substituting for the ring oxygen, is a strong inhibitor of intestinal α-glucosidase. DNJ has several promising biological activities, including its antidiabetic, antitumor, and antiviral activities. Nevertheless, only limited amounts of DNJ are available because it can only be extracted from some higher plants, including the mulberry tree, or purified from the culture broth of several types of soil bacteria, such as *Streptomyces* sp. and *Bacillus* sp. In our previous study, a DNJ-producing bacterium, *Bacillus subtilis* MORI, was isolated from the traditional Korean fermented food Chungkookjang. In the present study, we report the identification of the DNJ biosynthetic genes in *B. subtilis* MORI 3K-85 strain, a DNJ-overproducing derivate of the *B. subtilis* MORI strain generated by γ-irradiation, xhe genomic DNA library of *B. subtilis* MORI 3K-85 was constructed in *Escherichia coli*, and clones showing α -glucosidase inhibition activity were selected. After DNA sequencing and a series of subcloning, we were able to identify a putative Operon which consists of *gabT1, yktc1*, and *gutB1* genes predicted to encode putative transaminase, phosphatase, and oxidoreductase, respectively. When a recombinant plasmid containing this Operon sequence was transformed into an *E. coli* strain, the resulting transformant was able to produce DNJ into the culture medium. Our results indicate that the gabT1, yktc1, and gutB1 genes are involved in the DNJ biosynthetic pathway in *B. subtilis* MORI, suggesting the possibility of employing these genes to establish a large-scale microbial DNJ overproduction system through genetic engineering and process optimization.
PMID: 21717329

Keywords : *Bacillus subtilis* MORI 3K-85; Genomic DNA Library Screening; 1-deoxynojirimycin (DNJ); Alpha-glucosidase Inhibitor; Gene Cloning; Biosynthesis; Inhibitor; Glycosylation

Article 102

Detection of a unique fibrinolytic enzyme in *Aeromonas sp.* JH1

J Microbiol. 2011 Dec; 49(6):1018-21.

Cho HY*, Seo MJ, Park JU, Kang BW, Kim GY, Joo WH, Lee YC, Cho YS, Jeong YK

*Corresponding: hycho@kribb.re.kr
Industrial Bio-materials Research Center

A fibrinolytic enzyme was found in a Gram-negative bacterium, *Aeromonas* sp. JH1. SDS-PAGE and fibrinzymography showed that it was a 36 kDa, monomeric protein. Of note, the enzyme was highly specific for fibrinogen molecules and the hydrolysis rate of fibrinogen subunits was highest for α, β, and γ chains in that order. The first 15 amino acids of N-terminal sequence were X-D-A-T-G-P-G-G-N-V-X-T-G-K-Y, which was distinguishable from other fibrinolytic enzymes. The optimum pH and temperature of the enzyme were approximately 8.0 and 40°C, respectively. Therefore, these results provide a fibrinolytic enzyme with potent thrombolytic activity from the *Aeromonas* genus.
PMID: 22203567

Keywords : Amidolytic Activity; *Aeromonas sp* JH1; Fibrinogen Subunits; Fibrinolytic Enzyme; N-Terminal Amino Acid Sequence; Serine-Protease

Article 103

Evaluation of environmental factors on cyanobacterial bloom in eutrophic reservoir using artificial neural networks

J Phycol. 2011; 47(3):495-504.

Ahn CY, Oh HM*, Park YS

*Corresponding: heemock@kribb.re.kr
Environmental Biotechnology Research Center

Cyanobacterial blooms are a common issue in eutrophic freshwaters, and some cyanobacteria produce toxins, threatening the health of humans and livestock. Microcystin, a representative cyanobacterial hepatotoxin, is frequently detected in most Korean lakes and reservoirs. This study developed predictive models for cyanobacterial bloom using artificial neural networks (ANNs; self-organizing map [SOM] and multilayer perceptron [MLP]), including an evaluation of related environmental factors. Fourteen environmental factors, as independent variables for predicting the cyanobacteria density, were measured weekly in the Daechung Reservoir from spring to autumn over 5 years (2001, 2003-2006). Cyanobacterial density was highly associated with environmental factors measured 3 weeks earlier. The SOM model was efficient in visualizing the relationships between cyanobacteria and environmental factors, and also for tracing temporal change patterns in the environmental condition of the reservoir. And the MLP model exhibited a good predictive power for the cyanobacterial density, based on the environmental factors of 3 weeks earlier. The water temperature and total dissolved nitrogen were the major determinants for cyanobacteria. The water temperature had a stronger influence on cyanobacterial growth than the nutrient concentrations in eutrophic waters. Contrary to general expectations, the nitrogen compounds played a more important role in bloom formation than the phosphorus compounds.

Keywords : Artificial Neural Network; Algal Bloom; Cyanobacteria; Multilayer Perceptron; Prediction Model; Self-Organizing Map; Microcystis-Aeruginosa; River

Article 104

Identification of the high-temperature response genes from *Porphyra seriata* (rhodophyta) expression sequence tags and enhancement of heat tolerance of *Chlamydomonas* (chlorophyta) by expression of the *Porphyra HTR2* gene

J Phycol. 2011; 47(4):821-28.

Kim E, Park HS, Jung Y, Choi DW, Jeong WJ*, Park HS, Hwang MS, Park EJ, Gong YG

*Co-first: wonjoong@kribb.re.kr
Green Bio Research Center

Temperature is one of the major environmental factors that affect the distribution, growth rate, and life cycle of intertidal organisms, including red algae. In an effort to identify the genes involved in the high-temperature tolerance of *Porphyra*, we generated 3,979 expression sequence tags (ESTs) from gametophyte thalli of *P. seriata* Kjellm. under normal growth conditions and high-temperature conditions. A comparison of the ESTs from two cDNA libraries allowed us to identify the high temperature response (*HTR*) genes, which are induced or up-regulated as the result of high-temperature treatment. Among the *HTRs, HTR2* encodes for a small polypeptide consisting of 144 amino acids, which is a noble nuclear protein. *Chlamydomonas* expressing the *Porphyra HTR2* gene shows higher survival and growth rates than the wild-type strain after high-temperature treatment. These results suggest that *HTR2* may be relevant to the tolerance of high-temperature stress conditions, and this *Porphyra* EST data set will provide important genetic information for studies of the molecular basis of high-temperature tolerance in marine algae, as well as in *Porphyra*.

Keywords : Expression Sequence Tags; High-Temperature Response Gene; *HTR2*; *Porphyra seriata*; Shock Proteins; Abiotic Stress; *Arabidopsis*; Transcriptome; Yezoensis

Article 105

Metabolic engineering of *Escherichia coli* for alpha-farnesene production

Metabol Eng. 2011; 13(6):648-55.

Wang C, Yoon SH, Jang HJ, Chung YR, Kim JY, Choi ES*, Kim SW

*Co-corresponding: choi4162@kribb.re.kr
Systems & Synthetic Biology Research Center

Sesquiterpenes are important materials in pharmaceuticals and industry. Metabolic engineering has been successfully used to produce these valuable compounds in microbial hosts. However, the microbial potential of sesquiterpene production is limited by the poor heterologous expression of plant sesquiterpene synthases and the deficient FPP precursor supply. In this study, we engineered *E. coli* to produce alpha-farnesene using a codon-optimized alpha-farnesene synthase and an exogenous MVA pathway. Codon optimization of alpha-farnesene synthase improved both the synthase expression and alpha-farnesene production. Augmentation of the metabolic flux for FPP synthesis conferred a 1.6- to 48.0-fold increase in alpha-farnesene production. An additional increase in alpha-farnesene production was achieved by the protein fusion of FPP synthase and alpha-farnesene synthase. The engineered *E. coli* strain was able to produce 380.0 mg/L of alpha-farnesene, which is an approximately 317-fold increase over the initial production of 1.2 mg/L.

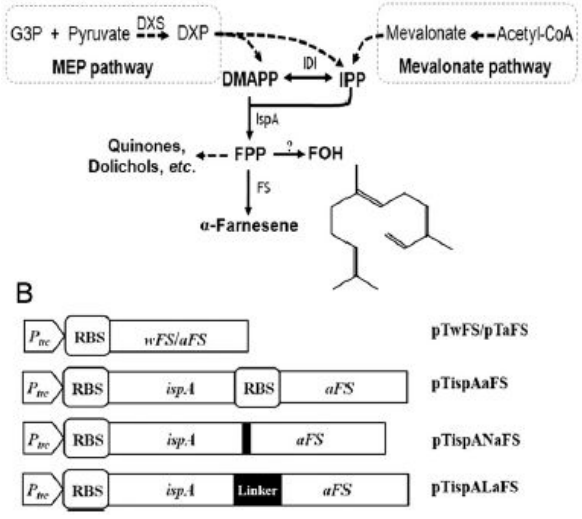

Keywords : Alpha-Farnesene; FPP Synthesis; Mevalonate Pathway; Codon Optimization; Protein Fusion; Octaprenyl Diphosphate Synthase; Isoprenoid Biosynthesis

Article 106

A novel family VII esterase with industrial potential from compost metagenomic library

Microb Cell Fact. 2011; 10:41.

Kang CH, Oh KH, Lee MH, Oh TK, Kim BH, Yoon JH*

*Co-corresponding: jhyoon@kribb.re.kr
Systems & Synthetic Biology Research Center

BACKGROUND: Among the vast microbial genomic resources now available, most microbes are unculturable in the laboratory. A culture-independent metagenomic approach is a novel technique that circumvents this culture limitation. For the screening of novel lipolytic enzymes, a metagenomic library was constructed from compost, and the clone of *estCS2* was selected for lipolytic properties on a tributyrin-containing medium.
RESULTS: The *estCS2* sequence encodes a protein of 570 amino acid residues, with a predicted molecular mass of 63 kDa, and based on amino acid identity it most closely matches (45%) the carboxylesterase from *Haliangium ochraceum* DSM 14365. EstCS2 belong to family VII, according to the lipolytic enzyme classification proposed by Arpigny and Jaeger, and it retains the catalytic triad Ser245-Glu363-His466 that is typical of an α/β hydrolase. The Ser245 residue in the catalytic triad of EstCS2 is located in the consensus active site motif GXSXG. The EstCS2 exhibits strong activity toward *p*-nitrophenyl caproate (C6), and it is stable up to 60°C with an optimal enzymatic activity at 55°C. The maximal activity is observed at pH 9, and it remains active between pH 6-10. EstCS2 shows remarkable stability in up to 50% (v/v) dimethyl sulfoxide (DMSO) or dimethylformamide (DMF). The enzyme has the ability to cleave sterically hindered esters of tertiary alcohol, as well as to degrade polyurethanes, which are widely used in various industries.
CONCLUSIONS: The high stability of EstCS2 in organic solvents and its activity towards esters of ketoprofen and tertiary alcohols, and in polyurethane suggests that it has potential uses for many applications in biotransformation and bioremediation.
PMID: 21619698

Keywords : Compost Metagenomic Library; Bacterial Lipases; Tertiary Alcohols; Sequence; Enzymes; Biocatalysis; Classification; Polyurethane

Article 107

Arabidopsis TTR1 causes LRR-dependent lethal systemic necrosis, rather than systemic acquired resistance, to Tobacco ringspot virus

Mol Cells. 2011 Nov; 32(5):421-9.

Nam M, Koh S, Kim SU, Domier LL, Jeon JH, Kim HG, Lee SH, Bent AF, Moon JS*

*Corresponding: jsmoon@kribb.re.kr
Green Bio Research Center

Most Arabidopsis ecotypes display tolerance to the *Tobacco ringspot virus* (TRSV), but a subset of Arabidopsis ecotypes, including Estland (Est), develop lethal systemic necrosis (LSN), which differs from the localized hypersensitive responses (HRs) or systemic acquired resistance (SAR) characteristic of incompatible reactions. Neither viral replication nor the systemic movement of TRSV was restricted in tolerant or sensitive *Arabidopsis* ecotypes; therefore, the LSN phenotype shown in the sensitive ecotypes might not be due to viral accumulation. In the present study, we identified the Est *TTR1* gene (tolerance to *Tobacco ringspot virus 1*) encoding a TIR-NBS-LRR protein that controls the ecotype-dependent tolerant/sensitive phenotypes by a map-based cloning method. The tolerant Col-0 ecotype *Arabidopsis* transformed with the sensitive Est *TTR1* allele developed an LSN phenotype upon TRSV infection, suggesting that the Est *TTR1* allele is dominant over the tolerant *ttr1* allele of Col-0. Multiple sequence alignments of 10 tolerant ecotypes from those of eight sensitive ecotypes showed that 10 LRR amino acid polymorphisms were consistently distributed across the *TTR1/ttr1* alleles. Site-directed mutagenesis of these amino acids in the LRR region revealed that two sites, L956S and K1124Q, completely abolished the LSN phenotype. VIGS study revealed that *TTR1* is dependent on SGT1, rather than EDS1. The LSN phenotype by *TTR1* was shown to be transferred to *Nicotiana benthamiana*, demonstrating functional conservation of *TTR1* across plant families, which are involved in SGT-dependent defense responses, rather than EDS1-dependent signaling pathways.
PMID: 22057987

Keywords : *Arabidopsis*; Lethal Systemic Necrosis; TIR-NBS-LRR; *Tobacco Ringspot Virus*; Tolerance; Disease Resistance; Mosaic-Virus; Sgt1; Rar1

Article 108

Bilateral inhibition of HAUSP deubiquitinase by a viral interferon regulatory factor protein

Nat Struct Mol Biol. 2011 Nov; 18(12):1336-44.

Lee HR, Choi WC, Lee S, Hwang J, Hwang E, Guchhait K, Haas J, Toth Z, Jeon YH, Oh TK*, Kim MH*, Jung JU

*Co-corresponding: otk@kribb.re.kr mhk8n@kribb.re.kr
Systems & Synthetic Biology Research Center

Herpesvirus-associated ubiquitin-specific protease (HAUSP) regulates the stability of p53 and the p53-binding protein MDM2, implicating HAUSP as a therapeutic target for tuning p53-mediated antitumor activity. Here we report the structural analysis of HAUSP with Kaposi's sarcoma-associated herpesvirus viral interferon (IFN) regulatory factor 4 (vIRF4) and the discovery of two vIRF4-derived peptides, vif1 and vif2, as potent and selective HAUSP antagonists. This analysis reveals a bilateral belt-type interaction that results in inhibition of HAUSP. The vif1 peptide binds the HAUSP TRAF domain, competitively blocking substrate binding, whereas the vif2 peptide binds both the HAUSP TRAF and catalytic domains, robustly suppressing its deubiquitination activity. Peptide treatments comprehensively blocked HAUSP, leading to p53-dependent cell-cycle arrest and apoptosis in culture and to tumor regression in xenograft mouse model. Thus, the virus has developed a unique strategy to target the HAUSP-MDM2-p53 pathway, and these virus-derived short peptides represent biologically active HAUSP antagonists.

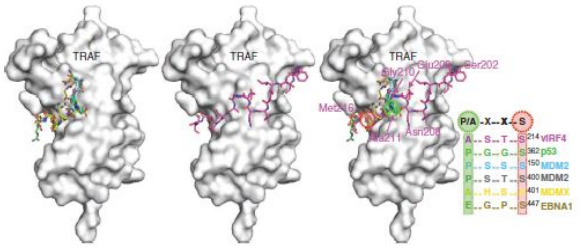

PMID: 22056774

Keywords : Sarcoma-Associated Herpesvirus; Ubiquitin-Specific Protease; *In vivo*; Nuclear Antigen; DNA Damage; P53; Lymphomas; MDM2; Destabilization

Article 109

An improved method for *Agrobacterium*-mediated genetic transformation from cotyledon explants of *Brassica juncea*

Plant Biotechnol, 2011; 28(1):17-23.

Bhuiyan MSU, Min SR, Jeong WJ, Sultana S, Choi KS, Lim YP, Song WY, Lee Y, Liu JR*

*Corresponding: jrliu@kribb.re.kr
Green Bio Research Center

An efficient *Agrobacterium*-mediated genetic transformation method was established for *Brassica juncea* by investigating several factors responsible for successful gene transfer. Four-day-old cotyledon explants from *in vitro* grown seedlings were co-cultivated with *Agrobacterium* strain GV3101 harboring the binary vector EnPCAMBIA1302-YCF1, which contained the hygromycin phosphotransferase (*HPT*) gene as a selectable marker and the yeast cadmium factor 1 (*YCF1*) gene. Two days co-cultivation period on shoot induction medium (MS medium supplemented with 0.1 mg l(-1) alpha-naphthaleneacetic acid, 1.0 mg l(-1) 6-benzyladenine, and 2.0 mg l(-1) silver nitrate) containing 20 mg l(-1) acetosyringone and five days delaying exposure of explants to selective agent enhanced transformation efficiency significantly. A three-step selection strategy was developed to select hygromycin resistant shoots. Hygromycin-resistant shoots were subsequently rooted on root induction medium. Rooted plantlets were transferred to pot-soil, hardened, and grown in a greenhouse until maturity. Using the optimized transformation procedure, transformation efficiency reached at 16.2% in this study. Southern blot analysis was performed to confirm that transgenes (*HPT* and *YCF1*) were stably integrated into the plant genome. All transgenic plants showed single-copy of transgene integration in the host genome. Segregation analysis of T_1 progeny showed that the transgenes were stably integrated and transmitted to the progeny in a Mendelian fashion.

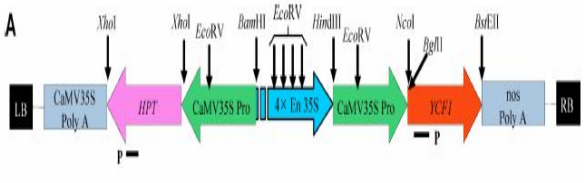

Keywords : Cotyledon Explants; Co-Cultivation; Genetic Transformation; Hygromycin; Indian Mustard; Shoot Regeneration; Transgenic Plants; Tolerance; Tumefaciens

Article 110

Transgenic poplar expressing *Arabidopsis NDPK2* enhances growth as well as oxidative stress tolerance

Plant Biotechnol J, 2011 Apr; 9(3):334-47.

Kim YH, Kim MD, Choi YI, Park SC, Yun DJ, Noh EW, Lee HS, Kwak SS*

*Corresponding: sskwak@kribb.re.kr
Environmental Biotechnology Research Center

Nucleoside diphosphate kinase 2 (NDPK2) is known to regulate the expression of antioxidant genes in plants. Previously, we reported that overexpression of *Arabidopsis NDPK2* (*AtNDPK2*) under the control of an oxidative stress-inducible *SWPA2* promoter in transgenic potato and sweetpotato plants enhanced tolerance to various abiotic stresses. In this study, transgenic poplar (*Populus alba* × *Poplus glandulosa*) expressing the *AtNDPK2* gene under the control of a *SWPA2* promoter (referred to as SN) was generated to develop plants with enhanced tolerance to oxidative stress. The level of *AtNDPK2* expression and NDPK activity in SN plants following methyl viologen (MV) treatment was positively correlated with the plant's tolerance to MV-mediated oxidative stress. We also observed that antioxidant enzyme activities such as ascorbate peroxidase, catalase and peroxidase were increased in MV-treated leaf discs of SN plants. The growth of SN plants was substantially increased under field conditions including increased branch number and stem diameter. SN plants exhibited higher transcript levels of the auxin-response genes *IAA2* and *IAA5*. These results suggest that enhanced *AtNDPK2* expression affects oxidative stress tolerance leading to improved plant growth in transgenic poplar.

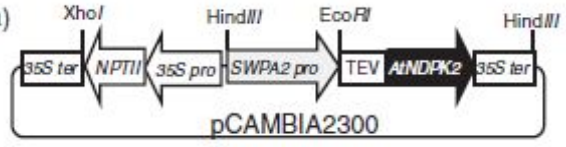

PMID: 20649941

Keywords : Antioxidant Enzyme; Auxin; Nucleoside Diphosphate Kinase 2; *Arabidopsis NDPK2*; *AtNDPK2*; Stress-Inducible Promoter; Transgenic Poplar; Sweet-Potato

Article 111

A novel light-dependent selection marker system in plants

Plant Biotechnol J, 2011 Apr; 9(3):348-58.

Koh S, Kim H, Kim J, Goo E, Kim YJ, Choi O, Jwa NS, Ma J, Nagamatsu T, Moon JS*, Hwang I

*Co-corresponding: jsmoon@kribb.re.kr
Green Bio Research Center

Photosensitizers are common in nature and play diverse roles as defense compounds and pathogenicity determinants and as important molecules in many biological processes. Toxoflavin, a photosensitizer produced by *Burkholderia glumae*, has been implicated as an essential virulence factor causing bacterial rice grain rot. Toxoflavin produces superoxide and H_2O_2 during redox cycles under oxygen and light, and these reactive oxygen species cause phytotoxic effects. To utilize toxoflavin as a selection agent in plant transformation, we identified a gene, *tflA*, which encodes a toxoflavin-degrading enzyme in the *Paenibacillus polymyxa* JH2 strain. TflA was estimated as 24.56 kDa in size based on the amino acid sequence and is similar to a ring-cleavage extradiol dioxygenase in the *Exiguobacterium* sp. 255-15; however, unlike other extradiol dioxygenases, Mn(2+) and dithiothreitol were required for toxoflavin degradation by TflA. Here, our results suggested toxoflavin is a photosensitizer and its degradation by TflA serves as a light-dependent selection marker system in diverse plant species. We examined the efficiencies of two different plant selection systems, toxoflavin/*tflA* and hygromycin/hygromycin phosphotransferase (*hpt*) in both rice and *Arabidopsis*. The toxoflavin/*tflA* selection was more remarkable than hygromycin/*hpt* selection in the high-density screening of transgenic *Arabidopsis* seeds. Based on these results, we propose the toxoflavin/*tflA* selection system, which is based on the degradation of the photosensitizer, provides a new robust nonantibiotic selection marker system for diverse plants.

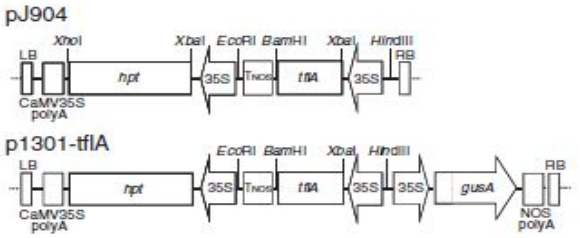

PMID: 20731786

Keywords : Photosensitizer; Toxoflavin; *TflA*; Selection Marker System; Rice; *Arabidopsis*; Transgenic Plants; Cercosporin; *Agrobacterium*

Article 112

VaSpoU1 (SpoU gene) may be involved in organelle rRNA/tRNA modification in *Viscum album*

Plant Biotechnol Rep, 2011; 5(3):289-95.

Ahn JW, Kim SW, Liu JR, Jeong WJ*

*Corresponding: wonjoong@kribb.re.kr
Green Bio Research Center

The SpoU family of proteins catalyzes the methylation of transfer RNAs (tRNAs) and ribosomal RNAs (rRNAs). We characterized a putative tRNA/rRNA methyltransferase, VaSpoU1 of the SpoU family, from *Viscum album* (mistletoe). VaSpoU1 and other plant SpoU1s exhibit motifs of the SpoU methylase domain that are conserved with bacterial and yeast SpoU methyltransferases. *VaSpoU1* transcripts were detected in the leaves and stems of *V. album*. VaSpoU1-GFP fusion proteins localized to both chloroplasts and mitochondria in *Arabidopsis* protoplasts. Sequence analysis similarly predicted that the plant SpoU1 proteins would localize to chloroplasts and mitochondria. Interestingly, mitochondrial localization of VaSpoU1 was inhibited by the deletion of a putative N-terminal presequence in *Arabidopsis* protoplasts. Therefore, VaSpoU1 may be involved in tRNA and/or rRNA methylation in both chloroplasts and mitochondria.

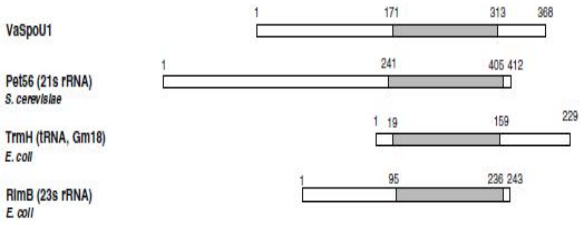

Keywords : Methyltransferase; SpoU Family; Subcellular Localization; AdoMet (S-adenosyl-(L) methionine); SpoU Methylase Domain; *VaSpoU1*; rRNA; tRNA

Article 113

Overexpression of a yeast cadmium factor 1 (*YCF1*) enhances heavy metal tolerance and accumulation in *Brassica juncea*

Plant Cell Tiss Organ Cult. 2011; 105(1):85-91.

Bhuiyan MSU, Min SR, Jeong WJ, Sultana S, Choi KS, Song WY, Lee Y, Lim YP, Liu JR*

*Corresponding: jrliu@kribb.re.kr
Green Bio Research Center

A yeast cadmium factor 1 (YCF1) is a member of the ATP-binding cassette (ABC) transporter family associated with multi-drug resistance, and it is localized at the vacuolar membrane in *Saccharomyces cerevisiae*. To determine ability to increase heavy metal tolerance and accumulation, *YCF1* was introduced into *Brassica juncea* plants by *Agrobacterium*-mediated genetic transformation. *YCF1* gene presence in transgenic plants was demonstrated by polymerase chain reaction (PCR). Reverse transcriptase-PCR analysis confirmed *YCF1* gene expression in the transgenic plants, but the degree of *YCF1* expression varied among the lines. *YCF1* overexpression in *B. juncea* conferred enhanced tolerance to cadmium (Cd[II]) and lead (Pb[II]) stress. Transgenic *B. juncea* seedlings showed 1.3- to 1.6-fold tolerance to Cd stress and 1.2- to 1.4-fold tolerance to Pb stress compared to wild type (WT) plants (per gram fresh weight). Most importantly, the shoot tissues of transgenic seedlings contained about 1.5- to 2-fold higher Cd(II) and Pb(II) levels than those of WT, demonstrating significantly increased accumulation of both Cd(II) and Pb(II) in transgenic plants.

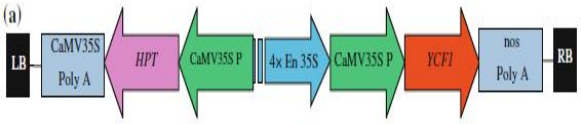

Keywords : *Brassica juncea*; Phytoremediation; Heavy Metal; ABC Transporter; Yeast Cadmium Factor 1; Accumulation; Transgenic Plants; *YCF1*

Article 114

Overexpression of *AtATM3* in *Brassica juncea* confers enhanced heavy metal tolerance and accumulation

Plant Cell Tiss Organ Cult. 2011; 107(1):69-77.

Bhuiyan MSU, Min SR, Jeong WJ, Sultana S, Choi KS, Lee Y, Liu JR*

*Corresponding: jrliu@kribb.re.kr
Green Bio Research Center

AtATM3, a member of the ATP-binding cassette transporter family, is localized at the mitochondrial membrane of *Arabidopsis thaliana* and is involved in the biogenesis of Fe-S clusters and iron homeostasis in plants. Through *Agrobacterium*-mediated genetic transformation, the *AtATM3* gene driven by the cauliflower mosaic virus 35S promoter (CaMV35S) was introduced into *Brassica juncea* (Indian mustard), a plant species suitable for phytoremediation, with the aim of improving heavy metal tolerance and accumulation in plants. The presence of the *AtATM3* gene in transgenic plants was confirmed by polymerase chain reaction (PCR). Reverse transcriptase-PCR analysis confirmed *AtATM3* expression in transgenic plants, but the level of *AtATM3* expression varied between lines. *AtATM3* overexpression in *B. juncea* conferred enhanced tolerance to cadmium [Cd(II)] and lead [Pb(II)] stresses. Importantly, the shoot tissues of transgenic seedlings contained about 1.5- to 2.5-fold higher Cd(II) and Pb(II) levels than wild type (WT) seedlings, demonstrating significantly-increased accumulation of both Cd(II) and Pb(II) in transgenic plants. The enhanced capacity of heavy metal tolerance and accumulation by *AtATM3* transgenic plants was attributed to higher *BjGSHII* (*B. juncea* glutathione synthetase II) and *BjPCS1* (phytochelatin synthase 1) expression levels induced by *AtATM3* overexpression. In addition, *AtATM3* overexpression regulated the expression of several metal transporters in the transgenic *B. juncea* plants under heavy metal stress conditions. Therefore, *AtATM3* transgenic plants are more tolerant of and can accumulate more heavy metals to enhance phytoremediation of contaminated soils.

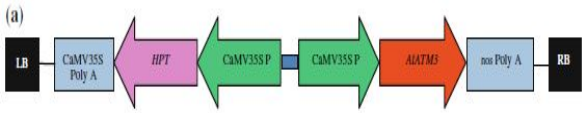

Keywords : ABC transporter; *AtATM3*; Biomass; *Brassica juncea*; Phytoremediation; Indian Mustard; *Arabidopsis thaliana*; Transgenic Plants

Article 115

A rapid, simple method for the genetic discrimination of intact *Arabidopsis thaliana* mutant seeds using metabolic profiling by direct analysis in real-time mass spectrometry

Plant Methods. 2011 Jun; 7:14.

Kim SW, Kim HJ, Kim JH, Kwon YK, Ahn MS, Jang YP, Liu JR*

*Corresponding: jrliu@kribb.re.kr
Green Bio Research Center

BACKGROUND: Efficient high throughput screening systems of useful mutants are prerequisite for study of plant functional genomics and lots of application fields. Advance in such screening tools, thanks to the development of analytic instruments. Direct analysis in real-time (DART)-mass spectrometry (MS) by ionization of complex materials at atmospheric pressure is a rapid, simple, high-resolution analytical technique. Here we describe a rapid, simple method for the genetic discrimination of intact *Arabidopsis thaliana* mutant seeds using metabolic profiling by DART-MS.
RESULTS: To determine whether this DART-MS combined by multivariate analysis can perform genetic discrimination based on global metabolic profiling, intact *Arabidopsis thaliana* mutant seeds were subjected to DART-MS without any sample preparation. Partial least squares-discriminant analysis (PLS-DA) of DART-MS spectral data from intact seeds classified 14 different lines of seeds into two distinct groups: Columbia (Col-0) and Landsberg erecta (Ler) ecotype backgrounds. A hierarchical dendrogram based on partial least squares-discriminant analysis (PLS-DA) subdivided the Col-0 ecotype into two groups: mutant lines harboring defects in the phenylpropanoid biosynthetic pathway and mutants without these defects. These results indicated that metabolic profiling with DART-MS could discriminate intact *Arabidopsis* seeds at least ecotype level and metabolic pathway level within same ecotype.
CONCLUSION: The described DART-MS combined by multivariate analysis allows for rapid screening and metabolic characterization of lots of *Arabidopsis* mutant seeds without complex metabolic preparation steps. Moreover, potential novel metabolic markers can be detected and used to clarify the genetic relationship between *Arabidopsis* cultivars. Furthermore this technique can be applied to predict the novel gene function of metabolic mutants regardless of morphological phenotypes.
PMID: 21658279

Keywords : *Arabidopsis thaliana*; Direct Analysis in Real-Time Mass Spectrometry (DART-MS); Partial Least Squares-Discriminant Analysis (PLS-DA); Seed; Flavonoid Biosynthesis; Multivariate-Analysis

Article 116

Potential for augmentation of fruit quality by foliar application of *Bacilli* spores on apple tree

Plant Pathol J. 2011; 27(2):164-9.

Ryu CM, Shin JN, Qi W, Mei RH, Kim EJ, Pan JG*

*Corresponding: jgpan@kribb.re.kr
Systems & Synthetic Biology Research Center

Previous studies have addressed the management of phyllosphere pathogens by leaf and root-associated microbes. The present study evaluated the effect of the foliar application of three strains of *Bacillus* spp. on plant growth and fruit quality. The application of a bacilli spore preparation significantly improved leaf growth parameters such as leaf thickness and photosynthesis capacity, indicating that bacilli treatment directly promoted leaf growth. In addition, foliar treatment resulted in an improvement in the key indicators of fruit quality including water, glucose, and sucrose contents. The present results suggest that foliar spraying of beneficial bacilli is a potential treatment of wide application for the improvement of apple quality. Foliar application of bacilli preparation as effective plant growth-promoting rhizobacteria broadens the spectrum of their availability for orchard application.

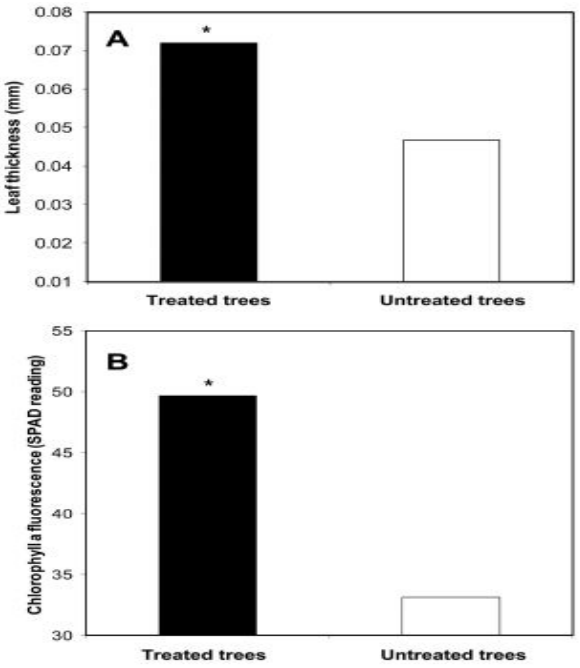

Keywords : Apple; Bacilli; Foliar Application; Fruit Quality; PGPR; Plant-Growth; *Arabidopsis*; Phyllosphere; Induced Systemic Resistance; *Pseudomonas fluorescens*

Article 117

Overexpression of 2-cysteine peroxiredoxin enhances tolerance to methyl viologen-mediated oxidative stress and high temperature in potato plants

Plant Physiol Biochem. 2011 Aug; 49(8):891-7.

Kim MD, Kim YH, Kwon SY, Jang BY, Lee SY, Yun DJ, Cho JH, Kwak SS, Lee HS*

*Corresponding: hslee@kribb.re.kr
Environmental Biotechnology Research Center

Oxidative stress is one of the major causative factors for injury to plants exposed to environmental stresses. Plants have developed diverse defense mechanisms for scavenging oxidative stress-inducing molecules. The antioxidative enzyme 2-cysteine peroxiredoxin (2-Cys Prx) removes peroxides and protects the photosynthetic membrane from oxidative damage. In this study, transgenic potato (*Solanum tuberosum* L. cv. Atlantic) expressing *At2-Cys Prx* under control of the oxidative stress-inducible *SWPA2* promoter or enhanced CaMV 35S promoter (referred to as SP and EP plants, respectively) was generated using *Agrobacterium*-mediated transformation. The transgenic plants were tested for tolerance to stress. Following treatment with 3 μM methyl viologen (MV), leaf discs from SP and EP plants showed approximately 33 and 15% less damage than non-transformed (NT) plants. When 300 μM MV was sprayed onto whole plants, the photosynthetic activity of SP plants decreased by 25%, whereas that of NT plants decreased by 60%. In addition, SP plants showed enhanced tolerance to high temperature at 42 °C. After treatment at high temperature, the photosynthetic activity of SP plants decreased by about 7% compared to plants grown at 25 °C, whereas it declined by 31% in NT plants. These results indicate that transgenic potato can efficiently regulate oxidative stress from various environmental stresses via overexpression of *At2-Cys Prx* under control of the stress-inducible *SWPA2* promoter.

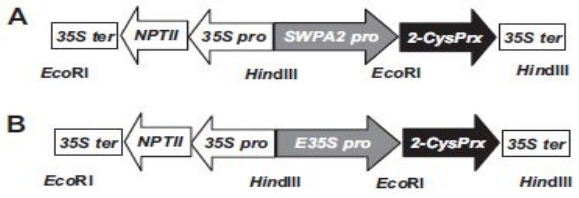

PMID: 21620719

Keywords : 2-Cys Prx; High Temperature; Oxidative Stress; Photosynthetic Activity; *Solanum tuberosum*; Transgenic Tobacco; Superoxide-Dismutase; Ascorbate Peroxidase; Sweet-Potato; *Arabidopsis*

Article 118

SCOF-1-expressing transgenic sweetpotato plants show enhanced tolerance to low-temperature stress

Plant Physiol Biochem. 2011 Dec; 49(12):1436-41.

Kim YH, Kim MD, Park SC, Yang KS, Jeong JC, Lee HS, Kwak SS*

*Corresponding: sskwak@kribb.re.kr
Environmental Biotechnology Research Center

Low-temperature stress represents one of the principal limitations affecting the distribution and productivity of many plant species, including crops such as sweetpotato. Transgenic sweetpotato (*Ipomoea batatas* L. cv. Yulmi) plants expressing the soybean cold-inducible zinc finger protein (SCOF-1) under control of an oxidative stress-inducible peroxidase (*SWPA2*) promoter (referred to as SF plants), were developed and evaluated for enhanced tolerance to low-temperature conditions. Following 4 °C treatment of SF plants, *SCOF-1* expression correlated positively with tolerance to low-temperature stress at the leaf disc level. Increased *SCOF-1* expression also correlated with enhanced tolerance to different low-temperature treatments at the whole plant level. SF plants treated with low-temperature stress (4 or 10 °C for 30 h) exhibited less of a reduction in photosynthetic activity and lipid peroxidation levels than non-transgenic (NT) plants. Furthermore, the photosynthetic activity and lipid peroxidation levels of SF plants recovered to near pre-stress levels after 12 h of recovery at 25 °C. In contrast, these activities remained at a reduced level in NT plants after the same recovery period. Thus, this study has shown that low-temperature stress in sweetpotato can be efficiently modulated by overexpression of *SCOF-1*.

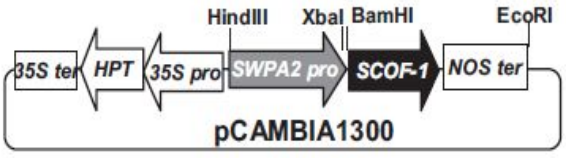

PMID: 22078381

Keywords : Low-temperature Stress; Soybean Cold-Inducible Zinc Finger Protein; Stress-Inducible Promoter; Transgenic Sweetpotato; Oxidative Stress; Freezing Tolerance; Resistance

Article 119

Sweetpotato late embryogenesis abundant 14 (*IbLEA14*) gene influences lignification and increases osmotic- and salt stress-tolerance of transgenic calli

Planta. 2011 Mar; 233(3):621-34.

Park SC, Kim YH, Jeong JC, Kim CY, Lee HS, Bang JW, Kwak SS*

*Corresponding: sskwak@kribb.re.kr
Environmental Biotechnology Research Center

Late embryogenesis abundant 14 (*LEA14*) cDNA was isolated from an EST library prepared from dehydration-treated fibrous roots of sweetpotato (*Ipomoea batatas*). Quantitative RT-PCR revealed a variety of different *IbLEA14* expression patterns under various abiotic stress conditions. *IbLEA14* expression was strongly induced by dehydration, NaCl and abscisic acid treatments in sweetpotato plants. Transgenic sweetpotato non-embryogenic calli harboring *IbLEA14* overexpression or RNAi vectors under the control of *CaMV 35S* promoter were generated. Transgenic calli overexpressing *IbLEA14* showed enhanced tolerance to drought and salt stress, whereas RNAi calli exhibited increased stress sensitivity. Under normal culture conditions, lignin contents increased in *IbLEA14*-overexpressing calli because of the increased expression of a variety of monolignol biosynthesis-related genes. Stress treatments elicited higher expression levels of the gene encoding cinnamyl alcohol dehydrogenase in *IbLEA14*-overexpressing lines than in control or RNAi lines. These results suggest that *IbLEA14* might positively regulate the response to various stresses by enhancing lignification.

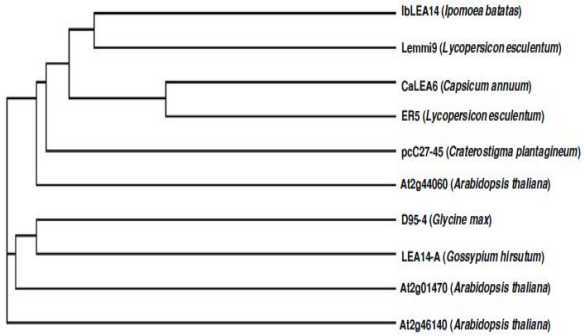

PMID: 21136074

Keywords : Abiotic Stress; Late Embryogenesis Abundant Protein; Ipomoea; Lignin; Transgenic Callus; Dehydration Tolerance; Plant Transformation; Lignin Biosynthesis

Article 120

Host-dependent suppression of RNA silencing mediated by the viral suppressor p19 in potato

Planta. 2011 Nov; 234(5):1065-72.

Ahn JW, Lee JS, Davarpanah SJ, Jeon JH, Park YI, Liu JR, Jeong WJ*

*Corresponding: wonjoong@kribb.re.kr
Green Bio Research Center

p19 protein encoded by *tomato bushy stunt virus* (TBSV) is known as a suppressor of RNA silencing via inhibition of small RNA-guided cleavage in plants. In this study, we generated TBSVp19-expressing patatin-RNAi transgenic potatoes to identify the inhibitory mechanisms of RNA silencing mediated by TBSVp19. In TBSVp19-expressing patatin-RNAi lines, reduction of *patatin*-derived siRNA accumulation and complementation of *patatin* transcripts were detected in comparison with the non-TBSVp19-expressing patatin-RNAi line, suggesting that TBSVp19 suppresses the siRNA-mediated silencing pathway. Interestingly, no apparent effect on the accumulation of miRNA168 and other miRNAs was detected in TBSVp19-expressing lines; previous studies reported that p19 induced the accumulation of both miRNA168 and its target *Argonaute 1* (*AGO1*) mRNA, but suppressed AGO1 translation via up-regulation of miRNA168 in *Arabidopsis*. In addition, the expression of *Argonaute 1* (*AGO1-1* and *AGO1-2*) and *Dicer-like 1* (*DCL1*) was not significantly altered in p19-expressing lines. Interestingly, no translational inhibition of AGO1 mediated by p19 was detected. These results suggest that p19 suppresses siRNA-mediated silencing in potato, but may not affect miRNA-mediated silencing, possibly due to the host-dependent manner of p19 activity.

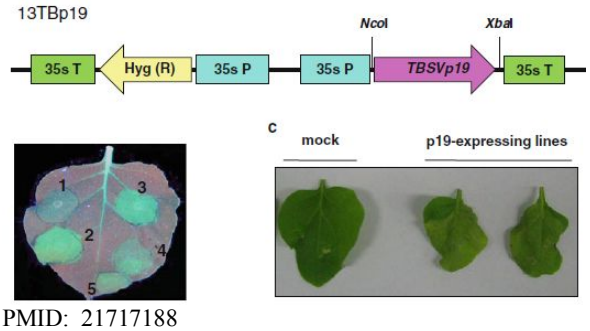

PMID: 21717188

Keywords : microRNA (miRNA); RNA-induced Silencing Complexes (RISCs); Short Interfering RNA (siRNA); *Tomato Bushy Stunt Virus* p19 (TBSVp19); Transient Gene-Expression

Article 121

Microbial production of farnesol (FOH): Current states and beyond

Process Biochem. 2011; 46(6):1221-9.

Wang C, Kim JY, Choi ES*, Kim SW

*Co-corresponding: choi4162@kribb.re.kr
Systems & Synthetic Biology Research Center

Farnesol (FOH) recently has been paid close attention because of its intrinsic properties as a cosmetic, pharmaceutical and industrial material. However, extraction from natural sources and chemical synthesis often suffer from the low yield and purity. Metabolic engineering of microorganisms for FOH production is an alternative way to meet the ever-growing demands. Several efforts have been done to make it possible to produce FOH from microorganisms including *S. cerevisiae* and *E. coil*. With developments of systems biology and synthetic biology, an optimal industrial microorganism can be expected to produce FOH cost-effectively. This review aims to give an update on the various facets of FOH synthesis pathway including the features of involved genes and enzymes, and recent progresses on FOH production. Combining traditional metabolic engineering with these new fascinating molecular, systems biology and synthetic biology tools will provide a better understanding of FOH biosynthesis and a great potential of microbial production.

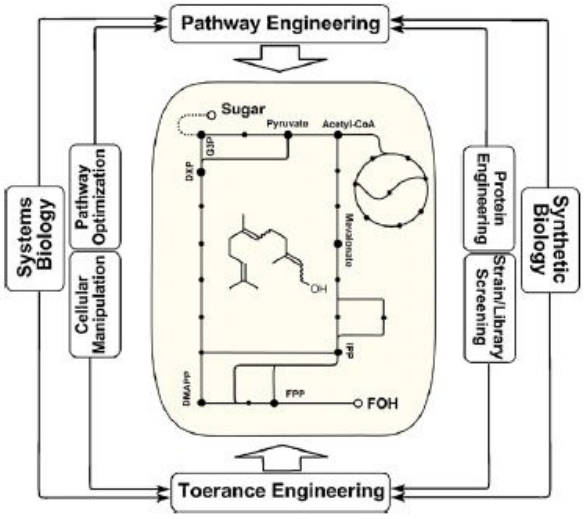

Keywords : Farnesol; Metabolic Engineering; Microbial Production; FPP Synthase; Phosphatases; Quorum-Sensing Molecule; Hmg-Coa Reductase; Isoprenoid Biosynthesis; Prenyl Alcohols

2011
KRIBB Article Abstracts
Corresponding Articles
Indexed in SCIE

Division of Bioresource Infrastructure

- Biological Resource Center
- Genome Resource Center
- Laboratory Animal Center
- International Biological Material Research Center

Korea Research Institute of Bioscience and Biotechnology


KRIBB
www.kribb.re.kr

Article 122

Detection of bacteria in normal adult nasal cavity based on polymerase chain reaction-denaturing gradient gel electrophoresis

Am J Rhinol Allergy. 2011 Jan; 25(1):e18-22.

Cho JH, Jung MY, Kim JK, Chang YH*

*Corresponding: yhchang@kribb.re.kr
Biological Resource Center

BACKGROUND: This study investigated the bacterial diversity in a normal adult nasal cavity using polymerase chain reaction-denaturing gradient gel electrophoresis (PCR-DGGE) of 16S ribosomal RNA (rRNA) gene fragments and compared the results with those of a culture-based method.
METHODS: We swabbed the inferior turbinate from 19 normal volunteers. The transport media was divided by two, one for bacterial culture and another direct extraction for bacterial DNA. PCR-DGGE was performed from the bacterial DNA and all of the sequences were compared with the reference organism by using the BLAST program (a genome database of GenBank in the National Center for Biotechnology Information, Bethesda, MD).
RESULTS: All 224 colonies were obtained from 19 samples by using a culture-based method; however, only 9 kinds of bacteria were detected. Staphylococcus epidermidis was the most frequently detected bacteria, and *Staphylococcus aureus* was the second most. The detection rates of other bacteria were very low. On the other hand, the PCR-DGGE from direct DNA extraction revealed 34 different bands that corresponded to 23 different kinds of bacteria. There were nine genera, viz., *Staphylococcus, Bacillus, Enterobacter, Corynebacterium, Actinobacterium, Hafnia, Moraxella, Dolosigranulum*, and *Clostridium*. Among them, unspecific *Staphylococcus* species and *Enterobacter aerogenes* were detected most frequently.
CONCLUSION: Compared with the previous culture-based method, PCR-DGGE can detect much more diversity of bacteria in the nasal cavity.

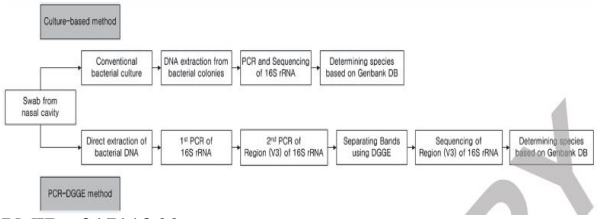

PMID: 21711966

Keywords : Normal Maxillary Sinuses; Middle Meatus; Chronic Rhinosinusitis; Healthy-Subjects; Flora; Sinusitis; Culture; Interference

Article 123

Hepatoprotective effect of *Platycodon grandiflorum* against chronic ethanol-induced oxidative stress in C57BL/6 mice

Ann Nutr Metab. 2011; 58(3):224-31.

Noh JR, Kim YH, Gang GT, Hwang JH, Kim SK, Ryu SY, Kim YS, Lee HS, Lee CH*

*Corresponding: chullee@kribb.re.kr
Laboratory Animal Center

AIMS: This study was carried out to evaluate the hepatoprotective effect of *Platycodon grandiflorum* (PG) in ethanol (EtOH)-induced liver damage.
METHODS AND RESULTS: PG treatment (both the total extract and saponin fraction) significantly blocked EtOH-induced oxidative stress through the preservation of activities of antioxidant enzymes in HepG2 cells. Furthermore, while the administration of EtOH to C57BL/6 mice for 6 weeks induced liver damage, along with a significant increase in plasma glutamic oxalacetic transaminase, glutamic pyruvic transaminase, hepatic triglyceride and thiobarbituric acid reactive substance levels, PG treatment significantly decreased glutamic oxalacetic transaminase, glutamic pyruvic transaminase, hepatic triglyceride and thiobarbituric acid reactive substance levels compared with the EtOH-treated control group ($p < 0.05$). Histological observation by hematoxylin-eosin and oil red O staining in the liver showed more effective inhibition of lipid accumulation in PG-treated groups, as compared to the EtOH-treated control group. Additionally, PG treatments appeared to enhance the activities of superoxide dismutase and catalase in the liver ($p < 0.05$).
CONCLUSION: These results suggest that PG has a protective effect against EtOH-induced oxidative damage, possibly by inhibition of lipid accumulation and peroxidation through the enhancement of the antioxidant defense system. PG might be useful as a therapeutically potent natural ingredient for the prevention of chronic EtOH-induced oxidative stress and liver damage.

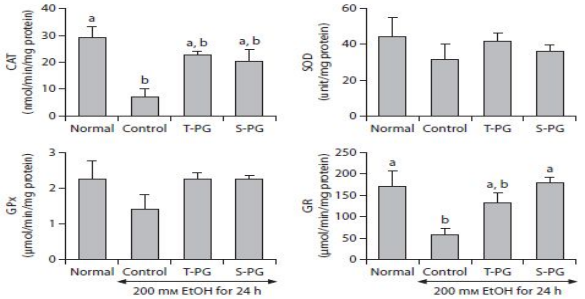

PMID: 21811061

Keywords : *Platycodon grandiflorum*; Ethanol; Hepatoprotection; Antioxidant Effect; Alcoholic Liver-Disease; Glutathione Peroxidase; Induced Hepatotoxicity; Superoxide-Dismutase; Saponins

Article 124

Antiatherogenic effect of antioxidant polyphenols from *Phellinus baumii* in apolipoprotein E-deficient mice

Ann Nutr Metab. 2011; 59(2-4):145-53.

Noh JR, Lee IK, Kim YH, Gang GT, Hwang JH, Ly SY, Yun BS, Lee CH*

*Co-corresponding: chullee@kribb.re.kr
Laboratory Animal Center

AIMS: The present study was carried out to investigate the antiatherosclerotic effect of antioxidant polyphenols from *Phellinus baumii* (PBE) in apolipoprotein E-deficient (apoE-/-) mice.
METHODS AND RESULTS: apoE-/- mice were randomly divided into three groups: mice on a normal chow diet comprised the normal group, mice on an atherogenic diet plus vehicle were the control group, and mice on an atherogenic diet plus PBE (500 mg/kg) comprised the PB500 group. After 8 weeks of treatment, the plasma lipids and cytokine levels were measured. Although no significant differences were found in cholesterol levels among groups, the triglyceride level was significantly decreased in the PBE-treated group compared with the control group. Plasma tumor necrosis factor (TNF)-α and interleukin (IL)-6 levels were reduced by PBE treatment. Real-time PCR analysis of the aorta showed that PBE significantly prevented the upregulation of the vascular cell adhesion molecule (VCAM)-1, intercellular adhesion molecule (ICAM)-1, TNF-α, IL-6, and IL-1β expression. Furthermore, reduced macrophage infiltration, lipid accumulation and atherosclerotic lesions were observed in the aortic sinus and en face of the whole aorta in PBE-fed apoE-/- mice compared with atherogenic diet-fed control mice.
CONCLUSIONS: Collectively, the findings of the present study suggest that the antiatherosclerotic effect of PBE is probably related to the inhibition of adhesion molecule and cytokine expression resulting in amelioration of lesion development.
PMID: 22142871

Keywords : *Phellinus baumii*; Antioxidant Polyphenols; Apolipoprotein E-Deficient Mice; Atherosclerosis; Adhesion Molecule; Lipopolysaccharide; Gilvus; VCAM-1

Article 125

Gilvimarinus agarilyticus sp. nov., a new agar-degrading bacterium isolated from the seashore of Jeju Island

Anton Leeuw Int J G. 2011 Jun; 100(1):67-73.

Kim BC, Kim MN, Lee KH, Kim HS, Min SR, Shin KS*

*Corresponding: ksshin@kribb.re.kr
Biological Resource Center

An agarolytic bacterium, designated as strain M5c^T, was isolated from sea sand in Jeju Island, Korea. This isolate was Gram-negative, positive for catalase and oxidase, rod and motile by means of monotrichous flagella. Strain M5c^T has translucent or dark ivory colonies, forms a dent on an agar plate under colonies, and grows in the presence of 1-12% (w/v) NaCl and at 10-37°C. This isolate hydrolyzes agar, alginic acid, carboxymethyl (CM)-cellulose and starch. Phylogenetic analysis based on 16S rRNA gene sequences showed that strain M5c^T can be considered as a species within the genus *Gilvimarinus*, being most closely related to *Gilvimarinus chinensis* QM42^T, with a 16S rRNA gene sequence similarity of 95.6%. The major cellular fatty acids were C16:1ω7c and/or iso-C15:0 2OH (33.5%), C16:0 (26.5%) and C18:1ω7c (14.1%). The DNA G+C content was 53.8 mol%. Based on these polyphasic data, strain M5c^T should be classified as a novel species, for which the name *Gilvimarinus agarilyticus* sp. nov. is proposed. The type strain for the novel species is M5c^T (= KCTC 23325^T = NCAIM B 02425^T).

PMID: 21340651

Keywords : *Gilvimarinus agarilyticus*; Agar; Phylogeny; Taxonomy; 16S rRNA; Marine Bacterium; Sequences; Neoagarobiose

Article 126

Homologous overexpression of *omcZ*, a gene for an outer surface c-type cytochrome of *Geobacter sulfurreducens* by single-step gene replacement

Biotechnol Lett. 2011 Oct; 33(10):2043-8.

Park I, Kim BC*

*Corresponding: bckim@kribb.re.kr
Biological Resource Center

The electron transfer pathway of *Geobacter sulfurreducens* has been intensively studied because of its ability of electron transfer to extracellular electron acceptors, such as Fe(III) and on electrode. However, the absence of overexpression system of *G. sulfurreducens* is one of the main obstacles for studying the physiology of *G. sulfurreducens*. OmcZ, an outer membrane-related c-type cytochrome of *G. sulfurrducens*, was homologously overexpressed via genomic integration. Quantitative RT-PCR analysis showed that the *omcZ* transcript in the knock-in strain was sixfold more abundant than in the wild type. Notably, *omcZ* expression appears to downregulate the expression level of OmcS, another outer membrane-related c-type cytochrome of *G. sulfurreducens*, based on the comparisons of total protein and transcript levels. This is the first report of the successful genetic overexpression system for studying functional genomics of *G. sulfurreducens*.

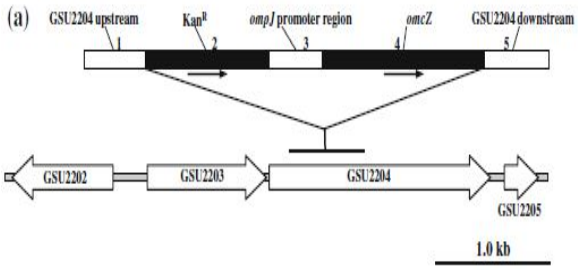

PMID: 21698445

Keywords : Cytochromes; *Geobacter Sulfurreducens*; Knock-In; *Omcz*; *Omcs*; Overexpression; Subsurface; Electrodes

Article 127

SigCS base: an integrated genetic information resource for human cerebral stroke

BMC System Biol. 2011; 5:S10.

Park YK, Bang OS, Cha MH, Kim J, Cole JW, Lee D, Kim YJ*

*Co-corresponding: yjkim8@kribb.re.kr
Genome Resource Center

Background: To understand how stroke risk factors mechanistically contribute to stroke, the genetic components regulating each risk factor need to be integrated and evaluated with respect to biological function and through pathway-based algorithms. This resource will provide information to researchers studying the molecular and genetic causes of stroke in terms of genomic variants, genes, and pathways.

Methods: Reported genetic variants, gene structure, phenotypes, and literature information regarding stroke were collected and extracted from publicly available databases describing variants, genome, proteome, functional annotation, and disease subtypes. Stroke related candidate pathways and etiologic genes that participate significantly in risk were analyzed in terms of canonical pathways in public biological pathway databases. These efforts resulted in a relational database of genetic signals of cerebral stroke, SigCS base, which implements an effective web retrieval system.

Results: The current version of SigCS base documents 1943 non-redundant genes with 11472 genetic variants and 165 non-redundant pathways. The web retrieval system of SigCS base consists of two principal search flows, including: 1) a gene-based variant search using gene table browsing or a keyword search, and, 2) a pathway-based variant search using pathway table browsing. SigCS base is freely accessible at http://sysbio.kribb.re.kr/sigcs.

Conclusions: SigCS base is an effective tool that can assist researchers in the identification of the genetic factors associated with stroke by utilizing existing literature information, selecting candidate genes and variants for experimental studies, and examining the pathways that contribute to the pathophysiological mechanisms of stroke.

Keywords : Ischemic-Stroke; Risk-Factor; Arteriovenous-Malformations; Hemorrhagic Stroke; Genome; Classification; Database; Countries; Aneurysms; Epidemic

Article 128

Activation of NAD(P)H:quinone oxidoreductase ameliorates spontaneous hypertension in an animal model via modulation of eNOS activity

Cardiovasc Res. 2011 Aug; 91(3):519-27.

Kim YH, Hwang JH, Noh JR, Gang GT, Kim do H, Son HY, Kwak TH, Shong M, Lee IK, Lee CH*

*Corresponding: chullee@kribb.re.kr
Laboratory Animal Center

AIMS: Hypertension is one of the most common human diseases worldwide, and extensive research efforts are focused upon the identification and utilizing of novel therapeutic drug targets. Nitric oxide (NO) produced by endothelial NO synthase (eNOS) is an important regulator of blood pressure (BP). β-Lapachone (βL), a well-known substrate of NAD(P)H:quinone oxidoreductase (NQO1), increases the cellular NAD(+)/NADH ratio via the activation of NQO1. In this study, we evaluated whether βL-induced activation of NQO1 modulates BP in an animal model of hypertension.
METHODS AND RESULTS: Spontaneously hypertensive rats (SHR), primary human aortic endothelial cells (HAEC), and endothelial cell lines were used to investigate the hypotensive effect of βL and its mode of action. βL treatment stimulated endothelium-dependent vascular relaxation in response to acetylcholine in aorta of SHR and dramatically lowered BP in SHR, but the hypotensive effect was completely blocked by eNOS inhibition with ω -nitro-l-arginine methyl ester. Aortic eNOS phosphorylation and eNOS protein expression were significantly increased in βL-treated SHR. *In vitro* studies revealed that βL treatment elevated the intracellular NAD(+)/NADH ratio and concentration of free Ca(2+) ([Ca(2+)]i), and resulted in Akt/AMP-activated protein kinase/eNOS activation. These effects were abolished by NQO1 siRNA and [Ca(2+)]i inhibition through a ryanodine receptor blockade.
CONCLUSION: This study is the first to demonstrate that NQO1 activation has a hypotensive effect mediated by eNOS activation via cellular NAD(+)/NADH ratio modulation in an animal model. These results provide strong evidence suggesting NQO1 might be a new therapeutic target for hypertension.
PMID: 21502369

Keywords : eNOS; Hypertension; NAD(+)/NADH Ratio; NQO1; Beta-Lapachone; Blood-Pressure; Calcium-Concentration; Calorie Restriction; Smooth-Muscle; Redox State

Article 129

Joostella atrarenae sp. nov., a novel member of the *Flavobacteriaceae* originating from the black sea sand of Jeju Island

Curr Microbiol. 2011 Feb; 62(2):606-11.

Kim BC, Lee KH, Kim MN, Jung MY, Chang YH, Lee J, Shin KS*

*Corresponding: ksshin@kribb.re.kr
Biological Resource Center

Strain M1-2^T was isolated from the black sand from the seashore of Jeju Island, Republic of Korea and was classified using a polyphasic taxonomic approach. Strain M1-2^T appeared as Gram-negative, motile rods that could grow in the presence of 1-10% (w/v) NaCl and at temperatures ranging from 4 to 37°C. This isolate has catalase and oxidase activity and hydrolyses aesculin, DNA and L: -tyrosine. Based on phylogenetic analysis using 16S rRNA gene sequences, strain M1-2^T belongs to the genus *Joostella* and is clearly distinct from the other described species of this genus, *Joostella marina* (type strain En5^T). The 16S rRNA gene sequence similarity level between M1-2^T and *J. marina* En5^T is 97.2%, and the DNA-DNA relatedness value between the two strains is 23.9%. Strain M1-2^T contains MK-6 as the major menaquinone and iso-$C_{15:0}$, summed feature 3 ($C_{16:1}$ ω7c and/or iso-$C_{15:0}$ 2OH) and iso-$C_{17:0}$ 3OH as major cellular fatty acids. The DNA G + C content is 32.3 mol%. These data suggest that strain M1-2^T should be classified as a novel species, for which the name *Joostella atrarenae* sp. nov. is proposed. The type strain for the novel species is M1-2^T (= KCTC 23194^T = NCAIM B.002413^T).

PMID: 20820783

Keywords : Performance Liquid-Chromatography; Family *Flavobacteriaceae*; Deoxyribonucleic-Acid; Bacterial Systematics; Emended Description; Sequences; *Joostella atrarenae*

Article 130

Photobacterium atrarenae sp. nov. a novel bacterium isolated from sea sand

Curr Microbiol. 2011 Nov; 63(5):433-8.

Kim BC, Poo H, Kim MN, Lee KH, Lee J, Rhee MS, Shin KS*

*Corresponding: ksshin@kribb.re.kr
Biological Resource Center

The gram-reaction-negative, motile, facultatively anaerobic, catalase-positive, oxidase-positive bacterial strain M3-4^T was isolated from black sea sand and subjected to a taxonomic study. Cells of strain M3-4^T have monotrichous flagella, grow optimally at 37°C and at pH 7-8 in the presence of 1-4% (w/v) NaCl and hydrolyze casein, starch and L: -tyrosine. According to phylogenetic analyses using 16S rRNA gene sequences, strain M3-4^T belongs to the genus *Photobacterium* and is most closely related to *Photobacterium rosenbergii* LMG 22223^T (97.4%) and *P. gaetbulicola* KCTC 22804^T(96.6%). The DNA-DNA relatedness value between M3-4^T and *P. rosenbergii* LMG 22223^T was 21.5%. The DNA G+C mol% of strain M3-4^T was 53.6. The major cellular fatty acid of strain M3-4^T was a summed feature 3 consisting of $C_{16:1}$ ω7c and/or iso-$C_{15:0}$ 2-OH (35.0%), followed by $C_{16:0}$ (25.4%) and $C_{18:1}$ω7c (16.8%). These data suggest that strain M3-4^T represents a novel species in genus *Photobacterium*, for which the name *P. atrarenae* sp. nov. is proposed. The type strain is M3-4^T (= KCTC 23265^T = NCAIM B 02414^T).
PMID: 21861148

Keywords : Tidal Flat Sediment; Deoxyribonucleic-Acid; Marine Bacterium; Sequences; Relatedness; Trees; *Photobacterium atrarenae*

Article 131

Hepatoprotective effects of chestnut (*Castanea crenata*) inner shell extract against chronic ethanol-induced oxidative stress in C57BL/6 mice

Food Chem Toxicol. 2011 Jul; 49(7):1537-43.

Noh JR, Kim YH, Gang GT, Hwang JH, Lee HS, Ly SY, Oh WK, Song KS, Lee CH*

*Corresponding: chullee@kribb.re.kr
Laboratory Animal Center

This study was carried out to evaluate the protective effects of chestnut inner shell extract (CISE) on chronic ethanol-induced oxidative stress in liver. Mice were fed a control liquid diet (Normal-control), liquid diet containing ethanol alone (EtOH+Vehicle), or were administered CISE and ethanol (EtOH+CISE) for 6 weeks. Administration of ethanol induced liver damage with significant increase of plasma GOT, GPT, hepatic triglyceride (TG) and thiobarbituric acid reactive substance (TBARS) levels. By contrast, co-treatment of CISE with ethanol significantly decreased the activities of GOT and GPT in the plasma, and hepatic TG and TBARS levels. Histological observations were consistent with the result obtained from hepatic lipid quantification. Moreover, CISE treatment with ethanol decreased CYP2E1 expression and increased activities of catalase and superoxide dismutase, which were significantly inhibited by treatment with ethanol alone. To determine the active compound of CISE, fractionation of CISE was conducted and scoparone and scopoletin were identified as main compounds. These compounds were also shown to inhibit the ethanol-induced reduction in antioxidant enzyme activity in an *in vitro* model system. These results suggest that CISE has protective effects against ethanol-induced oxidative damage, possibly by inhibition of lipid accumulation, peroxidation and increase of antioxidant defense system in the liver.

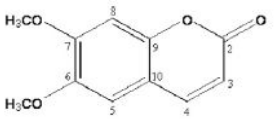

Scoparone

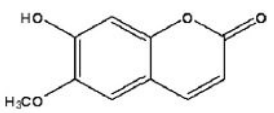

Scopoletin

PMID: 21457746

Keywords : Chestnut Inner Shell; Ethanol; Hepatoprotection; Antioxidants; Oxidative Stress; Alcoholic Liver-Disease; High-Fat Diet; Glutathione Peroxidase; Lipid-Peroxidation;

Article 132

Major chimpanzee-specific structural changes in sperm development-associated genes

Funct Integr Genomics. 2011 Sep; 11(3):507-17.

Kim RN, Kim DW, Choi SH, Chae SH, Nam SH, Kim DW, Kim A, Kang A, Park KH, Lee YS, Hirai M, Suzuki Y, Sugano S, Hashimoto K, Kim DS, Park HS*

*Corresponding: hspark@kribb.re.kr
Genome Resource Center

A comprehensive analysis of transcriptional structures of chimpanzee sperm development-associated genes is of significant interest for deeply understanding sperm development and male reproductive process. In this study, we sequenced 7,680 clones from a chimpanzee testis full-length cDNA library and obtained 1,933 nonredundant high-quality full-length cDNA sequences. Comparative analysis between human and chimpanzee showed that 78 sperm development-associated genes, most of which were yet uncharacterized, had undergone severe structural changes (mutations at the start/stop codons, INDELs, alternative splicing variations and fusion forms) on genomic and transcript levels throughout chimpanzee evolution. Specifically, among the 78 sperm development-associated genes, 39 including *ODF2, UBC,* and *CD59* showed markedly chimpanzee-specific structural changes. Through dN/dS analysis, we found that 56 transcripts (including seven sperm development-associated genes) had values of greater than one when comparing human and chimpanzee DNA sequences, whereas the values were less than one when comparing humans and orangutans. Gene ontology annotation and expression profiling showed that the chimpanzee testis transcriptome was enriched with genes that are associated with chimpanzee male germ cell development. Taken together, our study provides the first comprehensive molecular evidence that many chimpanzee sperm development-associated genes had experienced severe structural changes over the course of evolution on genomic and transcript levels.

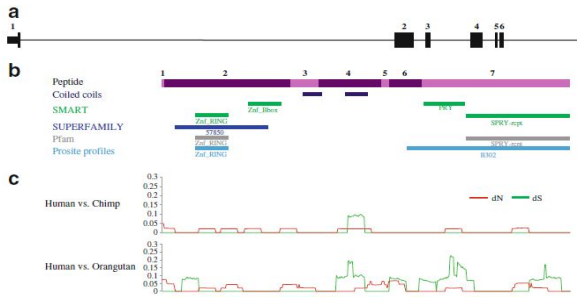

PMID: 21484476

Keywords : Structural Changes; Chimpanzee; Testis; Sperm Development; Gene Ontology; Primates; Sequence

Article 133

Expression of the Protective Antigen for PEDV in Transgenic Duckweed, *Lemna minor*

Horticult Environ Biotech. 2011; 52(5):511-5.

Ko SM, Sun HJ, Oh MJ, Song IJ, Kim MJ, Sin HS, Goh CH, Kim YW, Lim PO, Lee HY, Kim SW*

*Co-corresponding: kimsw@kribb.re.kr
Biological Resource Center

Duckweeds are small, floating aquatic plants with a number of useful characteristics, including edibility, fast-growing, and a clonal proliferation. Duckweed is also fed to animals as a diet complement because of its high nutritional value. Porcine epidemic diarrhea virus (PEDV) is a major causative agent of fatal diarrhea in piglets and is a serious problem in the hog-raising industry. In this study, we assessed the feasibility of producing a protective antigen for the PEDV spike protein 1 using duckweed, *Lemna minor*. Stably transformed *Lemna* were obtained by co-cultivation with *A. tumefaciens* EHA105 harboring the PEDV spike protein gene. Transgene integration and expression of the PEDV spike protein 1 gene were confirmed by genomic PCR and RT-PCR and western blot analysis of transgenic *Lemna*, respectively. This is the first report of the expression of a vaccine antigen against an animal infectious disease in duckweed.

Keywords : Aquatic Plant; Porcine Diarrhea; Spike Protein; Transformation; Vaccine; Synthetic Neutralizing Epitope; Epidemic Diarrhea Virus; Tobacco

Article 134

Paenibacillus xylanisolvens sp. nov., a xylan-degrading bacterium from soil

Int J Syst Evol Microbiol. 2011 Jan; 61(1):160-4.

Khianngam S, Tanasupawat S, Akaracharanya A, Kim KK, Lee KC, Lee JS*

*Co-corresponding: jslee@kribb.re.kr
Biological Resource Center

A xylan-degrading bacterium, strain X11-1^T, was isolated from soil collected in Nan province, Thailand. The strain was characterized based on its phenotypic and genotypic characteristics. Strain X11-1^T was a Gram-stain-positive, facultatively anaerobic, spore-forming, rod-shaped bacterium. It contained meso-diaminopimelic acid in the cell-wall peptidoglycan. The major menaquinone was MK-7, anteiso-$C_{15:0}$ (56.6 %) and $C_{16:0}$ (14.0 %) were the predominant cellular fatty acids and diphosphatidylglycerol, phosphatidylmonomethylethanolamine, phosphatidylethanolamine and phosphatidylglycerol were the major phospholipids. The DNA G+C content was 51.6 mol%. Phylogenetic analysis using 16S rRNA gene sequences showed that strain X11-1^T was affiliated to the genus *Paenibacillus* and was closely related to *Paenibacillus naphthalenovorans* KACC 11505^T and *Paenibacillus validus* CCM 3894^T, with 96.5 % sequence similarity. Therefore, the strain represents a novel species of the genus *Paenibacillus*, for which the name *Paenibacillus xylanisolvens* sp. nov. is proposed. The type strain is X11-1^T (=KCTC 13042^T =PCU 311^T =TISTR 1829^T).
PMID: 20190026

Keywords : Xylanolytic Bacterium; Phoenix-Dactylifera; Genus *Paenibacillus*; Emended Description; Phyllosphere; Polymyxa; Enzymes; ASH; *Paenibacillus xylanisolvens*

Article 135

Fontibacillus panacisegetis sp. nov., isolated from soil of a ginseng field

Int J Syst Evol Microbiol. 2011 Feb; 61(2):369-74.

Lee KC, Kim KK, Eom MK, Kim MJ, Lee JS*

*Corresponding: jslee@kribb.re.kr
Biological Resource Center

A facultatively anaerobic, endospore-forming bacterium, designated strain P11-6^T, was isolated from soil of a ginseng field located in Geumsan County, Republic of Korea. Cells of strain P11-6^T were Gram-stain-negative, catalase-negative, motile rods and produced semi-translucent, circular, white colonies on tryptic soy agar. The isolate contained MK-7 as the only menaquinone and anteiso-$C_{15:0}$ as the major fatty acid. Diphosphatidylglycerol, phosphatidylglycerol, phosphatidylethanolamine, an unknown aminophosphoglycolipid, an unknown aminophospholipid, two unknown phospholipids, three unknown glycolipids and three unknown lipids were detected in the polar lipid profile. The DNA G+C content of strain P11-6^T was 41.9 mol%. Phylogenetic analysis based on 16S rRNA gene sequencing showed that strain P11-6^T was most closely related to *Fontibacillus aquaticus* GPTSA 19^T (97.2 % sequence similarity) and that it formed a separate lineage with *F. aquaticus* in the family *Paenibacillaceae*. Combined phenotypic and DNA-DNA hybridization data supported the conclusion that strain P11-6^T represents a novel species in the genus *Fontibacillus*, for which the name *Fontibacillus panacisegetis* sp. nov. is proposed; the type strain is P11-6^T (=KCTC 13564^T =CECT 7605^T).
PMID: 20305061

Keywords : Coryneform Bacteria; Identification; Chromatography; Nocardia; Trees; *Fontibacillus panacisegetis*

Article 136

Vagococcus acidifermentans sp. nov., isolated from an acidogenic fermentation bioreactor

Int J Syst Evol Microbiol. 2011 May; 61(5):1123-6.

Wang L, Cui YS, Kwon CS, Lee ST, Lee JS*, Im WT

*Co-corresponding: jslee@kribb.re.kr
Biological Resource Center

A Gram-staining-positive, coccus-shaped, non-spore-forming, facultatively anaerobic bacterium, designated AC-1^T, was isolated from an acidogenic fermentation bioreactor treating food wastewater. On the basis of 16S rRNA gene sequence analysis, strain AC-1^T was shown to belong to the genus *Vagococcus*. The closest phylogenetic relatives were *Vagococcus elongatus* PPC9^T (97.4 % 16S rRNA gene sequence similarity), *Vagococcus penaei* CD276^T (96.7 %) and *Vagococcus carniphilus* ATCC BAA-640^T (96.6 %). The major fatty acids were $C_{18:1}\omega9c$ (24.8 %) and $C_{16:0}$ (19.5 %) and the G+C content of genomic DNA was 44.2 mol%, which supported the affiliation of strain AC-1^T to the genus *Vagococcus*. Strain AC-1^T and *V. elongatus* DSM 21480^T exhibited 11 % DNA-DNA relatedness. Physiological and biochemical tests differentiated strain AC-1^T from the type strains of recognized species of the genus *Vagococcus*. Therefore, strain AC-1^T is considered to represent a novel species, for which the name *Vagococcus acidifermentans* sp. nov. is proposed. The type strain is AC-1^T (= KCTC 13418^T = LMG 24798^T).
PMID: 20543153

Keywords : Deoxyribonucleic-Acid; Sequences; Bacteria; Acidogenic Fermentation Bioreactor; *Vagococcus acidifermentans*

Article 137

Bacillus luteolus sp. nov., a halotolerant bacterium isolated from a salt field

Int J Syst Evol Microbiol. 2011 Jun; 61(6):1344-9.

Shi R, Yin M, Tang SK, Lee JC, Park DJ, Zhang YJ, Kim CJ*, Li WJ

*Co-corresponding: changjin@kribb.re.kr
Biological Resource Center

A novel Gram-stain-positive, motile, strictly aerobic bacterium, designated YIM 93174^T, was isolated from a salt field in Korea. Cells of this strain were rod-shaped and formed pale tangerine colonies and grew at pH 6.0-8.0 (optimal growth at pH 7.0), at 15-45 °C (optimum 28-37 °C) and at salinities of 0-10 % (w/v) NaCl (optimum 0-2 % NaCl). Some phenotypic characters allowed differentiation of strain YIM 93174^T from its nearest phylogenetic relatives. Comparative 16S rRNA gene sequence analysis showed that strain YIM 93174^T belongs to the genus *Bacillus*, exhibiting the highest level of sequence similarity with the type strain of *Bacillus humi* (95.7 %), followed by those of *Bacillus alkalitelluris* (94.9 %) and *Bacillus litoralis* (94.5 %). The major fatty acids were iso-$C_{15:0}$, anteiso-$C_{15:0}$ and iso-$C_{16:0}$. The cell-wall peptidoglycan was of the A1γ type, containing meso-diaminopimelic acid as the diagnostic diamino acid. The genomic DNA G+C content was 36.9 mol% and the predominant respiratory quinone was MK-7. The major polar lipids of strain YIM 93174^T were diphosphatidylglycerol, phosphatidylglycerol, phosphatidylethanolamine, phosphatidylinositol, phosphatidylinositol mannoside and two unknown phospholipids. On the basis of the evidence from this polyphasic study, strain YIM 93174^T represents a novel species of the genus *Bacillus*, for which the name *Bacillus luteolus* sp. nov. is proposed, with YIM 93174^T (= DSM 22388^T = KCTC 13210^T = CCTCC AA 208068^T) as the type strain.
PMID: 20584813

Keywords : Moderately Halophilic Bacterium; Deoxyribonucleic-Acid; Gen. Nov.; China; Lake; Soil; Georgenia; Sequences; Trees; *Bacillus luteolus*

Article 138

Reclassification of *Paenibacillus ginsengisoli* as a later heterotypic synonym of *Paenibacillus anaericanus*

Int J Syst Evol Microbiol. 2011 Sep; 61(9):2101-6.

Kim KK, Lee KC, Lee JS*

*Corresponding: jslee@kribb.re.kr
Biological Resource Center

The type strains of the species *Paenibacillus ginsengisoli* (KCTC 13931(T)) and *Paenibacillus anaericanus* (DSM 15890(T)) were compared in order to clarify the taxonomic relationship of the two species. On the basis of 16S rRNA and *rpoB* gene sequence comparisons, the two strains shared 99.9 and 99.6 % similarity, respectively. The mean DNA-DNA relatedness value was 77 % and the genomic DNA G+C contents were 43.2 and 42.2 mol%, respectively. Phenotypic data, including fatty acid patterns and acid-production, enzyme-activity and substrate-utilization profiles, showed no pronounced differences between the type strains of the two species. These genotypic and phenotypic data suggest that the two taxa constitute a single species. According to Rules 38 and 42 of the *Bacteriological Code*, they should be united under the name *Paenibacillus anaericanus*, with the name *Paenibacillus ginsengisoli* as a later heterotypic synonym.
PMID: 20870883

Keywords : sp nov.; Genus *Paenibacillus*; South Korea; Bacterium; Soil; Identification; Hybridization; 16S rRNA; rpoB; *Paenibacillus ginsengisoli*; *Paenibacillus anaericanus*

Article 139

Wickerhamomyces ochangensis sp. nov., an ascomycetous yeast isolated from the soil of a potato field

Int J Syst Evol Microbiol. 2011 Oct; 61(10):2543-6.

Shin KS*, Bae KS, Lee KH, Park DS, Kwon GS, Lee JB

*Corresponding: ksshin@kribb.re.kr
Biological Resource Center

A novel ascomycetous yeast, designated strain N7a-Y2^T, was isolated from soil collected in a potato field in Ochang, Korea, and its taxonomic position was studied. A neighbour-joining tree based on the D1/D2 domain of large-subunit rRNA gene sequences revealed that the isolate was a member of the *Wickerhamomyces* clade and that it was closely related to *Wickerhamomyces bisporus, Candida quercuum, Candida ulmi and Wickerhamomyces alni*. Strain N7a-Y2^T formed Saturn-shaped ascospores in unconjugated and persistent asci. D1/D2 domain 26S rRNA gene sequence divergences of 11.0-21.1 % between strain N7a-Y2^T and other members of the *Wickerhamomyces* clade indicate that the strain represents a novel species of the genus *Wickerhamomyces*, for which the name *Wickerhamomyces ochangensis* sp. nov. is proposed. The type strain is N7a-Y2^T (= KCTC 17870^T = CBS 11843^T).
PMID: 21057051

Keywords : Genetically Modified Crops; Sequences; Benefits; Pichia; Ascomycetous Yeast; *Wickerhamomyces ochangensis*

Article 140

Genome sequence of *Leuconostoc fallax* KCTC 3537

J Bacteriol. 2011 Jan; 193(2):588-9.

Nam SH, Choi SH, Kang A, Kim DW, Kim DS, Kim RN, Kim A, Park HS*

*Corresponding: hspark@kribb.re.kr
Genome Resource Center

Leuconostoc fallax is known to be present during the manufacturing process of kimchi, the best-known traditional Korean dish. Here, we present the draft genome sequence of the type strain *Leuconostoc fallax* KCTC 3537 (1,638,971 bp, with a G+C content of 37.5%), which consists of 30 large contigs (>100 bp in size).
PMID: 21075921

Keywords : RNA Genes; Resource; Database; DNA; *Leuconostoc fallax*

Article 141

Genome Sequence of *Weissella cibaria* KACC 11862

J Bacteriol. 2011 Feb; 193(3):797-8.

Kim DS, Choi SH, Kim DW, Nam SH, Kim RN, Kang A, Kim A, Park HS*

*Corresponding: hspark@kribb.re.kr
Genome Resource Center

Weissella cibaria KACC 11862 is a Gram-positive, heterofermentative, *Leuconostoc*-like lactic acid bacterium that is widely distributed in Korean traditional foods such as kimchi. Here we report the draft genome sequence of the type strain, *W. cibaria* KACC 11862 (1,599 known genes, 80 RNA genes), which consists of 72 large contigs (>100 bp in size).
PMID: 21097615

Keywords : RNA Genes; Kimchi; DNA; *Weissella cibaria*

Article 142

Genome Sequence of *Leuconostoc gelidum* KCTC 3527, Isolated from Kimchi

J Bacteriol. 2011 Feb; 193(3):799-800.

Kim DS, Choi SH, Kim DW, Kim RN, Nam SH, Kang A, Kim A, Park HS*

*Corresponding: hspark@kribb.re.kr
Genome Resource Center

Leuconostoc gelidum KCTC 3527 is found mainly in vegetables and plays an important role in vegetable fermentation, including that of Korean traditional kimchi. Here we announce the draft genome sequence of *Leuconostoc gelidum* KCTC 3527, isolated from Korean traditional kimchi, and describe major findings from its annotation.
PMID: 21131494

Keywords : RNA Genes; Kimchi; DNA; *Leuconostoc gelidum*

Article 143

Genome sequence of *Lactobacillus coryniformis* subsp. *coryniformis* KCTC 3167

J Bacteriol. 2011 Feb; 193(4):1014-5.

Nam SH, Choi SH, Kang A, Kim DW, Kim DS, Kim RN, Kim A, Park HS*

*Corresponding: hspark@kribb.re.kr
Genome Resource Center

Lactobacillus coryniformis subsp. *coryniformis* is known to be present during the manufacturing process of kimchi, the best-known traditional Korean dish. Here, we present the draft genome sequence of *Lactobacillus coryniformis* subsp. *coryniformis* type strain KCTC 3167 (2,964,752 bp, with a G+C content of 42.8%), which consists of 55 scaffolds.
PMID: 21148735

Keywords : RNA Genes; Resource; Database; DNA; *Lactobacillus coryniformis*

Article 144

Genome sequence of *Leuconostoc inhae* KCTC 3774, isolated from Kimchi

J Bacteriol. 2011 Mar; 193(5):1278-9.

Kim DS, Choi SH, Kim DW, Kim RN, Nam SH, Kang A, Kim A, Park HS*

*Corresponding: hspark@kribb.re.kr
Genome Resource Center

Leuconostoc inhae strain KCTC 3774 is a Gram-positive, non-spore-forming, heterofermentative, spherical or lenticular lactic acid bacterium. Here we announce the draft genome sequence of *Leuconostoc inhae* KCTC 3774, isolated from traditional Korean kimchi, and describe major findings from its annotation.
PMID: 21183671

Keywords : RNA Genes; Kimchi; DNA; Bacterial Community; sp nov; *Leuconostoc inhae*

Article 145

Genome sequence of *Lactobacillus animalis* KCTC 3501

J Bacteriol. 2011 Mar; 193(5):1280-1.

Nam SH, Choi SH, Kang A, Kim DW, Kim RN, Kim A, Kim DS, Park HS*

*Corresponding: hspark@kribb.re.kr
Genome Resource Center

Lactobacillus animalis is one of the most prevalent lactic acid bacteria present during the manufacturing process of kimchi, the best-known traditional Korean dish. Here, we present the draft genome sequence of *Lactobacillus animalis* type strain KCTC 3501 (1,882,795 bp, with a G+C content of 41.1%), which consists of 7 scaffolds.
PMID: 21183665

Keywords : RNA Genes; Kimchi; Resource; Database; DNA; *Lactobacillus animalis*

Article 146

Genome sequence of *Lactobacillus farciminis* KCTC 3681

J Bacteriol. 2011 Apr; 193(7):1790-1.

Nam SH, Choi SH, Kang A, Kim DW, Kim RN, Kim A, Kim DS, Park HS*

*Corresponding: hspark@kribb.re.kr
Genome Resource Center

Lactobacillus farciminis is one of the most prevalent lactic acid bacterial species present during the manufacturing process of kimchi, the best-known traditional Korean dish. Here, we present the draft genome sequence of the type strain *Lactobacillus farciminis* KCTC 3681 (2,498,309 bp, with a G+C content of 36.4%), which consists of 5 scaffolds.
PMID: 21257766

Keywords : RNA Genes; Kimchi; Resource; Database; DNA; *Lactobacillus farciminis*

Article 147

Draft genome sequence of *Kocuria rhizophila* P7-4

J Bacteriol. 2011 Aug; 193(16):4286-7.

Kim WJ, Kim YO, Kim DS, Choi SH, Kim DW, Lee JS, Kong HJ, Nam BH, Kim BS, Lee SJ, Park HS*, Chae SH

*Co-corresponding: hspark@kribb.re.kr
Genome Resource Center

We report the draft genome sequence of *Kocuria rhizophila* P7-4, which was isolated from the intestine of *Siganus doliatus* caught in the Pacific Ocean. The 2.83-Mb genome sequence consists of 75 large contigs (>100 bp in size) and contains 2,462 predicted protein-coding genes.
PMID: 21685281

Keywords : SP. Nov.; RNA Genes; DNA; *Kocuria rhizophila*

Article 148

Genome sequence of *Acinetobacter* sp. strain P8-3-8, isolated from *Fistularia commersonii* in Vietnam

J Bacteriol. 2011 Aug; 193(16):4288-9.

Kim YO, Kim WJ, Choi SH, Kim DS, Kim DW, Lee JS, Kong HJ, Nam BH, Kim BS, Lee SJ, Park HS*, Chae SH

*Co-corresponding: hspark@kribb.re.kr
Genome Resource Center

Acinetobacter sp. strain P8-3-8 is an aerobic, Gram-negative marine bacterium isolated from the intestine of the bluespotted cornetfish (*Fistularia commersonii*). Here, we present the draft genome sequence of *Acinetobacter* sp. P8-3-8 (3,905,565 bp, with a G+C content of 37.6%) containing 3,621 putative coding sequences. The genome data reveal a high density of genes encoding transcriptional regulators involved in anaerobic respiration.
PMID: 21685286

Keywords : RNA Genes; SP ADP1; DNA; *Acinetobacter*; *Fistularia commersonii*

Article 149

Genome sequence of *Leuconostoc pseudomesenteroides* KCTC 3652

J Bacteriol. 2011 Aug; 193(16):4299.

Kim DW, Choi SH, Kang A, Nam SH, Kim RN, Kim A, Kim DS, Park HS*

*Corresponding: hspark@kribb.re.kr
Genome Resource Center

We announce the genome sequence of one of the most prevalent lactic acid bacteria present during the manufacturing process of cane juice, the type strain *Leuconostoc pseudomesenteroides* KCTC 3652 (3,244,985 bp, with a G+C content of 38.3%), which consists of 1,160 large contigs (>100 bp in size). All of the contigs were assembled by the Newbler Assembler 2.3 software program (454 Life Sciences).
PMID: 21705609

Keywords : RNA Genes; DNA; Lactic Acid Bacteria; Newbler Assembler; *Leuconostoc pseudomesenteroides*

Article 150

Draft genome sequence of *Lactobacillus zeae* KCTC 3804

J Bacteriol. 2011 Sep; 193(18):5023.

Kim DW, Choi SH, Kang A, Nam SH, Kim DS, Kim RN, Kim A, Park HS*

*Corresponding: hspark@kribb.re.kr
Genome Resource Center

We announce the draft genome sequence of the type strain *Lactobacillus zeae* KCTC 3804 (3,110,326 bp, with a G+C content of 47.8%), which is one of the most prevalent lactic acid bacteria present during the processing of raw cow's milk. The genome consists of 113 large contigs (>100 bp). All of the contigs were assembled by Newbler Assembler 2.3 (454 Life Science).
PMID: 21868802

Keywords : RNA Genes; DNA; Lactic Acid Bacteria; Newbler Assembler; *Lactobacillus zeae*

Article 151

Draft genome sequence of *Lactobacillus mali* KCTC 3596

J Bacteriol. 2011 Sep; 193(18):5037.

Kim DW, Choi SH, Kang A, Nam SH, Kim DS, Kim RN, Kim A, Park HS*

*Corresponding: hspark@kribb.re.kr
Genome Resource Center

We announce the draft genome sequence of the type strain *Lactobacillus mali* KCTC 3596 (2,652,969 bp, with a G+C content of 36.0%), which is one of the most prevalent lactic acid bacteria present during the manufacturing process of apple juice. The genome consists of 122 large contigs (>100 bp). All of the contigs were assembled by Newbler Assembler 2.3 (454 Life Science).
PMID: 21742889

Keywords : RNA Genes; DNA; Lactic Acid Bacteria; Newbler Assembler; *Lactobacillus mali*

Article 152

Genome sequence of *Lactobacillus cypricasei* KCTC 13900

J Bacteriol. 2011 Sep; 193(18):5053-4.

Kim DS, Choi SH, Kim DW, Kim RN, Nam SH, Kang A, Kim A, Park HS*

*Corresponding: hspark@kribb.re.kr
Genome Resource Center

Lactobacillus cypricasei KCTC 13900 is important in the generation of particular flavors and in other ripening processes associated with specific cheeses. Here, we announce the draft genome sequence of *Lactobacillus cypricasei* KCTC 13900, isolated from cheeses, and describe major findings from its annotation.
PMID: 21742864

Keywords : RNA Genes; Cheese; DNA; Lactic Acid Bacteria; *Lactobacillus cypricasei*

Article 153

Genome sequence of *Lactobacillus suebicus* KCTC 3549

J Bacteriol. 2011 Oct; 193(19):5532-3.

Nam SH, Choi SH, Kang A, Kim DW, Kim RN, Kim DS, Kim A, Park HS*

*Corresponding: hspark@kribb.re.kr
Genome Resource Center

Lactobacillus suebicus is important in the generation of particular flavors and in other ripening processes associated with apple mash. Here, we present the draft genome sequence of the type strain *Lactobacillus suebicus* KCTC 3549 (2,656,936 bp, with a G+C content of 39.0%), which consists of 143 large contigs (>100 bp).
PMID: 21914862

Keywords : RNA Genes; Resource; Database; DNA; *Lactobacillus suebicus*

Article 154

Draft genome sequence of *Lactobacillus malefermentans* KCTC 3548

J Bacteriol. 2011 Oct; 193(19):5537.

Kim DW, Choi SH, Kang A, Nam SH, Kim DS, Kim RN, Kim A, Park HS*

*Corresponding: hspark@kribb.re.kr
Genome Resource Center

We announce the draft genome sequence of the type strain *Lactobacillus malefermentans* KCTC 3548 (2,003,922 bp, with a G+C content of 41.1%), which is one of the most prevalent lactic acid bacteria present during the manufacturing process of beer; the genome consists of 172 large contigs (>100 bp in size). All of the contigs were assembled by using Newbler Assembler 2.3 (454 Life Science).
PMID: 21914865

Keywords : RNA Genes; DNA; Lactic Acid Bacteria; Newbler Assembler; *Lactobacillus malefermentans*

Article 155

Genome sequence of *Lactobacillus versmoldensis* KCTC 3814

J Bacteriol. 2011 Oct; 193(19):5589-90.

Kim DS, Choi SH, Kim DW, Kim RN, Nam SH, Kang A, Kim A, Park HS*

*Corresponding: hspark@kribb.re.kr
Genome Resource Center

Lactobacillus versmoldensis KCTC 3814 was isolated from raw fermented poultry salami. The species was present in high numbers and frequently dominated the lactic acid bacteria (LAB) populations of the products. Here, we announce the draft genome sequence of *Lactobacillus versmoldensis* KCTC 3814, isolated from poultry salami, and describe major findings from its annotation.
PMID: 21914893

Keywords : RNA Genes; DNA; Lactic Acid Bacteria; *Lactobacillus versmoldensis*

Article 156

Genome sequence of *Leuconostoc carnosum* KCTC 3525

J Bacteriol. 2011 Nov; 193(21):6100-1.

Nam SH, Kim A, Choi SH, Kang A, Kim DW, Kim RN, Kim DS, Park HS*

*Corresponding: hspark@kribb.re.kr
Genome Resource Center

We announce the draft genome sequence of the type strain *Leuconostoc carnosum* KCTC 3525 (3,234,408 bp with a G+C content of 40.9%), one of the most prevalent lactic acid bacteria present during the manufacturing process of vacuum-packaged meats, which consists of 2,407 large contigs (>500 bp in size). The genome sequence was obtained by a whole-genome shotgun strategy using Roche 454 GS (FLX Titanium) pyrosequencing, and all of the reads were assembled using Newbler Assembler 2.3.
PMID: 21994929

Keywords : RNA Genes; Resource; DNA; Lactic Acid Bacteria; Newbler Assembler; *Leuconostoc carnosum*

Article 157

A *Phellinus baumii* extract reduces obesity in high-fat diet-fed mice and absorption of triglyceride in lipid-loaded mice

J Med Food. 2011 Mar; 14(3):209-18.

Noh JR, Lee IK, Ly SY, Yang KJ, Gang GT, Kim YH, Hwang JH, Yun BS, Lee CH*

*Co-corresponding: chullee@kribb.re.kr
Laboratory Animal Center

This study evaluated the anti-obesity effects of *Phellinus baumii* extract (PBE) in high-fat diet (HFD)-fed mice. Male 8-week-old C57BL/6 mice were randomly divided into four groups: control, normal chow diet plus vehicle; HFD-control, high-fat plus vehicle; HFD plus orlistat (Xenical(®), Roche, Basel, Switzerland) (50 mg/kg); and HFD plus PBE (500 mg/kg). PBE was administered daily by oral gavage for 12 weeks. Oral administration of PBE (500 mg/kg) significantly reduced body weight gain, hepatic lipid concentrations, and fat accumulation in epididymal adipocytes compared with mice fed HFD alone ($P < .05$). mRNA expression of genes related to triglyceride (TG) synthesis was suppressed in the PBE groups, and fatty acid synthase activity was also significantly inhibited ($P < .05$). Furthermore, we evaluated the effect of PBE on TG absorption and detected marked reduction in TG absorption in Xenical- and PBE-treated mice compared with the control group ($P < .05$). To determine the active compound of PBE, fractionation was conducted, and interfungin A, davallialactone, and hypholomine B were identified as the main compounds. Among the three identified compounds, as a representative compound, davallialactone was also shown to suppress fat accumulation in an *in vitro* model system. These anti-obesity and hypolipidemic effects appear to be partly mediated by suppressing plasma and hepatic fat accumulation through the inhibition of enzymes associated with hepatic and intestinal lipid absorption and synthesis.

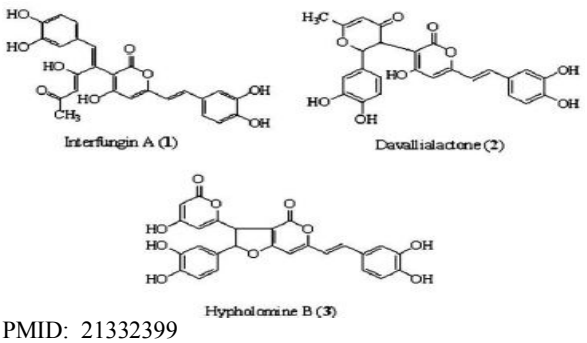

PMID: 21332399

Keywords : Anti-Obesity; Hepatic Lipid; *Phellinus baumii*; Triglyceride Absorption; Immunomodulating Activities; Linteus; Antioxidants; Inonotus; Orlistat

Article 158

An ethnomedicinal inventory of knotweeds of Indian Himalaya

J Med Plants Res. 2011; 5(10):2095-03.

Choudhary RK, Oh S, Lee J*

*Corresponding: joongku@kribb.re.kr
International Biological Material Research Center

The present study aims to highlight the current knowledge of the usefulness of Knotweeds (*Polygonum* L.) of India as to point out what species need careful consideration for conservation rather than eradication. The present study intends to produce an inventory of the important Polygonums that needs re-evaluation for cultivation and hence increasing our accessibility to natural medicinal products. Out of about 72 species reported to occur in India, we found 34 promising species that could be utilized for medicines, ornamentals, famine food and others. Many ethno-botanical data confined to a very small niche of ethnic people residing in Eastern Himalayan region are being reported here for the first time.

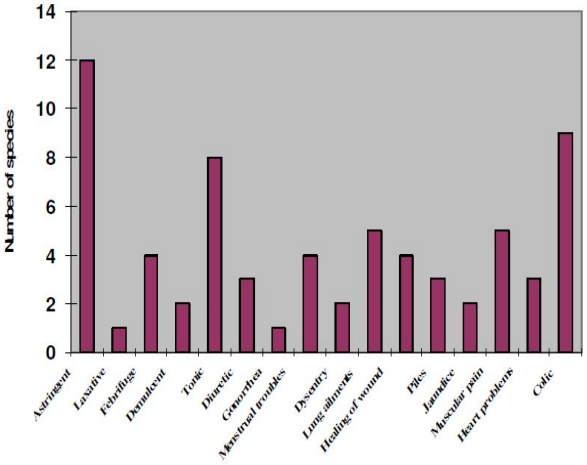

Keywords : Ethnomedicine; *Polygonum*; Himalaya; India; Medicinal-Plants; Phytoremediation; Weeds

Article 159

Bacillus manliponensis sp. nov., a new member of the *Bacillus cereus* group isolated from foreshore tidal flat sediment

J Microbiol. 2011 Dec; 49(6):1027-32.

Jung MY, Kim JS, Paek WK, Lim J, Lee H, Kim PI, Ma JY, Kim W, Chang YH*

*Corresponding: yhchang@kribb.re.kr
Biological Resource Center

A Gram-positive, endospore-forming, new *Bacillus* species, strain BL4-6^T, was isolated from tidal flat sediment of the Yellow Sea. Strain BL4-6^T is a straight rod, with motility by peritrichate flagella. The cell wall contains *meso*-diaminopimelic acid, and the major respiratory quinone is menaquinone-7. The major fatty acids are iso-$C_{15:0}$ and summed feature 3 (containing $C_{16:1}$ ω7c/iso-$C_{15:0}$ 2OH, and/or iso-$C_{15:0}$ 2OH/$C_{16:1}$ ω7c). Cells are catalase-positive and oxidase-negative. The G+C content of the genomic DNA is 38.0 mol%. Based on a comparative 16S rRNA gene sequence analysis, the isolate belongs to the genus *Bacillus*, forms a clade with the *Bacillus cereus* group, and is closely related to *Bacillus mycoides* (98.5%), *Bacillus cereus* (98.5%), *Bacillus anthracis* (98.4%), *Bacillus thuringiensis* (98.4%), *Bacillus weihenstephanensis* (98.1%), and *Bacillus pseudomycoides* (97.5%). The isolate showed less than 85% similarity of the *gyrA* gene sequence and below 95% similarity of the *rpoB* gene sequence to the members of this group. DNA-DNA relatedness between strain BL4-6^T and *B. cereus* group was found to be in a range of 22.8-42.3%, and thus BL4-6^{T}represents a unique species. On the basis of these studies, strain BL4-6^T (=KCTC 13319^T =JCM 15802^T) is proposed to represent the type strain of a novel species, *Bacillus manliponensis* sp. nov.
PMID: 22203569

Keywords : *Bacillus cereus* Group; *Bacillus manliponensis* sp nov.; Phylogenetic; New Species; Bacterial Systematics; Genus *Bacillus*; *Thuringiensis*; Resistance; Sequences

Article 160

Expressed sequence tag analysis of *Physa acuta*: a freshwater pulmonate in Korea

J Shellfish Res. 2011; 30(1):127-32.

Lee YS, Lee SG, Kang SW, Jeong JE, Baek MK, Choi SH, Chae SH, Jo YH, Han YS, Park HS*

*Corresponding: hspark@kribb.re.kr
Genome Resource Center

Physa acuta (left-handed shell) have strong natural growth activity not only in lentic waters but also in eutrophic environments. Therefore, it has been considered one of the candidate species that could evaluate the degree of water pollution by physiological and biochemical methods. In this study, we constructed a *P. acuta* cDNA library using the 5` oligo capping method, and determined the sequences of 2,282 clones by 5` end-single path sequencing. After trimming, clustering, and assembling these sequences, we finally obtained 575 distinctly available transcripts that were 718 bp in average length. These transcripts were annotated using the BLASTX search and were classified by function using KOG analysis. After comparison with biomarker genes already known in several organisms, we identified 27 potential biomarker candidates that were categorized into two groups strongly related to stress and defense genes by their functions. To the best of our knowledge, this is the first report of massive profiling of cDNA sequences and the characterizing of potential biomarker genes in *P. acuta*. Our study offers valuable information to scientists for developing new environmental biomonitoring markers, and for scientists studying the physiology, growth and development, immunity, genetic identification, and evolutional diversity in *P. acuta*.

Keywords : *Physa acuta*; EST; Biomarker; cDNA Library; Apoptosis-Linked Gene-2; Mytilus-Edulis; Crassostrea-Virginica; Blue Mussel; Metallothionein; Stress

Article 161

EST analysis predicts putatively causative genes underlying the pharmaceutical application of *Glycyrrhiza uralensis* Fisch

Plant Mol Biol Rep. 2011; 29(4):814-24.

Kim DW, Kim RN, Choi SH, Kim DW, Nam SH, Choi HS, Koh HD, Kim A, Chae SH, Ahn JC, Kang A, Park HS*

*Corresponding: hspark@kribb.re.kr
Genome Resource Center

Glycyrrhiza uralensis Fisch is an important medicinal plant used not only as a natural sweetener but also for a variety of pharmaceutical applications. Even though there have been previous reports of genes putatively associated with the biosynthesis of the sweet compound glycyrrhizin, the absence of genomic information and the insufficient transcriptomic data for this plant still hinder sufficient insight into the causative genes underlying the pharmaceutical and culinary applications of *Glycyrrhiza uralensis Fisch*. In this study, we sequenced 5,276 ESTs from *Glycyrrhiza uralensis Fisch*, established 2,353 unique sequences based on clustering and performed comparative analysis of them. Of the 2,353 unique sequences, we found homologs and orthologs for 1,499 of them with similarity searches against the non-redundant protein database at NCBI using the BLASTX algorithm and against the InterPro database using hidden Markove model (HMM) methods. We have functionally classified 749 unique sequences using Gene Ontology (GO) terms, mapped pathways for 248 unique sequences with the Kyoto Encyclopedia of Genes and Genomes (KEGG) and predicted 30 secreted proteins. Based on their expression levels, we have identified genes encoding a novel beta-D-xylosidase, glutathione-S-transferase and arabinogalactan protein 16 that may function in the glycyrrhizin biosynthesis, anti-tumor activity and detoxifying activity of this very promising medicinal plant. Furthermore, the EST sequence information described in this paper could be a valuable resource for future scientific research projects on this plant, including genome sequencing and annotation and genetic diversity as well as functional genomics and molecular functional studies.

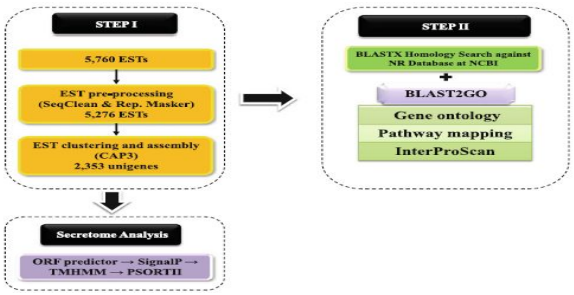

Keywords : *Glycyrrhiza Uralensis* Fisch; Glycyrrhizin; Pharmaceutical Application; EST; D-xylosidase; cDNA-Clones; Licorice; Arabinogalactan; Biosynthesis; Sequences

Article 162

Developmental transcriptomic features of the carcinogenic liver fluke, *Clonorchis sinensis*

PLoS Negl Trop Dis. 2011 Jun; 5(6):e1208.

Yoo WG, Kim DW, Ju JW, Cho PY, Kim TI, Cho SH, Choi SH, Park HS*, Kim TS, Hong SJ

*Co-corresponding: hspark@kribb.re.kr
Genome Resource Center

Clonorchis sinensis is the causative agent of the life-threatening disease endemic to China, Korea, and Vietnam. It is estimated that about 15 million people are infected with this fluke. *C. sinensis* provokes inflammation, epithelial hyperplasia, and periductal fibrosis in bile ducts, and may cause cholangiocarcinoma in chronically infected individuals. Accumulation of a large amount of biological information about the adult stage of this liver fluke in recent years has advanced our understanding of the pathological interplay between this parasite and its hosts. However, no developmental gene expression profiles of *C. sinensis* have been published. In this study, we generated gene expression profiles of three developmental stages of *C. sinensis* by analyzing expressed sequence tags (ESTs). Complementary DNA libraries were constructed from the adult, metacercaria, and egg developmental stages of *C. sinensis*. A total of 52,745 ESTs were generated and assembled into 12,830 *C. sinensis* assembled EST sequences, and then these assemblies were further categorized into groups according to biological functions and developmental stages. Most of the genes that were differentially expressed in the different stages were consistent with the biological and physical features of the particular developmental stage; high energy metabolism, motility and reproduction genes were differentially expressed in adults, minimal metabolism and final host adaptation genes were differentially expressed in metacercariae, and embryonic genes were differentially expressed in eggs. The higher expression of glucose transporters, proteases, and antioxidant enzymes in the adults accounts for active uptake of nutrients and defense against host immune attacks. The types of ion channels present in *C. sinensis* are consistent with its parasitic nature and phylogenetic placement in the tree of life. We anticipate that the transcriptomic information on essential regulators of development, bile chemotaxis, and physico-metabolic pathways in *C. sinensis* that presented in this study will guide further studies to identify novel drug targets and diagnostic antigens.
PMID: 21738807

Keywords : Heat-Shock Proteins; B-Cell Epitopes; Opisthorchis-Viverrini; Fasciola-Hepatica; Excretory/Secretory Products; Schistosoma-Mansoni; Hamster Liver; Tag

Article 163

Barcoding bugs: DNA-based identification of the true bugs (Insecta: Hemiptera: Heteroptera)

PLoS One. 2011 Apr; 6(4):e18749.

Park DS*, Foottit R, Maw E, Hebert PD

*First: dspark@kribb.re.kr
Biological Resource Center

BACKGROUND: DNA barcoding, the analysis of sequence variation in the 5' region of the mitochondrial cytochrome c oxidase I (COI) gene, has been shown to provide an efficient method for the identification of species in a wide range of animal taxa. In order to assess the effectiveness of barcodes in the discrimination of Heteroptera, we examined 344 species belonging to 178 genera, drawn from specimens in the Canadian National Collection of Insects.
METHODOLOGY/PRINCIPAL FINDINGS: Analysis of the COI gene revealed less than 2% intra-specific divergence in 90% of the taxa examined, while minimum interspecific distances exceeded 3% in 77% of congeneric species pairs. Instances where barcodes fail to distinguish species represented clusters of morphologically similar species, except one case of barcode identity between species in different genera. Several instances of deep intraspecific divergence were detected suggesting possible cryptic species.
CONCLUSIONS/SIGNIFICANCE: Although this analysis encompasses 0.8% of the described global fauna, our results indicate that DNA barcodes will aid the identification of Heteroptera. This advance will be useful in pest management, regulatory and environmental applications and will also reveal species that require further taxonomic research.

Table 3. Sequence divergences (K2P) at the COI barcode region for Hemiptera at varied taxonomic levels.

	Range (%)	Mean Dist (%)	SE (%)
within species	0–7.72	0.74 (0.8)	0.027
among species in genus	0–24.80	10.67 (12.6)	0.074
among genera in family	0–35.80	19.81 (19.9)	0.007
among families	12.15–36.67	23.66	0.005

PMID: 21526211

Keywords : DNA Barcoding; True Bugs; Hemiptera; Heteroptera; COI Gene; Fauna

Article 164

Mice lacking adenylyl cyclase type 5 (AC5) show increased ethanol consumption and reduced ethanol sensitivity

Psychopharmacology. 2011 May; 215(2):391-8.

Kim KS*, Kim H, Baek IS, Lee KW, Han PL

*First: kskim@kribb.re.kr
Laboratory Animal Center

RATIONALE: The adenylyl cyclase (AC)/cAMP system is believed to be a key component in regulating alcohol-drinking behavior. It was reported that adenylyl cyclase-5 (AC5) is expressed widely in the brain, with a preferential concentration in the dorsal striatum and nucleus accumbens, brain regions which are important for addiction and emotion. AC5 has been shown to be an essential mediator of morphine addiction and dopamine receptor function; however, it remains unknown whether or not AC5 plays a role in ethanol preference and sensitivity in animals.
OBJECTIVE: This work was carried out to determine the role of AC5 in alcohol consumption and the hypnotic response to alcohol using AC5 knockout (KO) mice.
RESULTS: In the test for ethanol preference employing a two-bottle free-choice paradigm, AC5 KO mice showed increased ethanol consumption and preference compared with the wild-type mice. Ethanol-induced hypothermia was weakly reduced in AC5 KO mice. AC5 KO mice exhibited sedation/behavioral sleep to high-dose ethanol, but their responses were greatly suppressed compared with the wild-type mice.
CONCLUSIONS: These results suggest that AC5 is an important signaling molecule regulating alcohol sensitivity and preference in animals. These data provide critical information for AC5 activation as a candidate target for the treatment of alcoholism.

PMID: 21193983

Keywords : Adenylyl Cyclase Type 5; Knockout Mice; Ethanol Consumption; Ethanol Sensitivity; Protein-Kinase; Nucleus-Accumbens; Induced Sedation; Antagonists

Article 165

Studies on genetic diversity among populations of *Persicaria barbata* (L.) H. Hara from India based on internal transcribed spacer sequences of nuclear ribosomal DNA

Saudi J Biol Sci. 2011; 18(2):123-7.

Choudhary RK, Ali MA, Lee J*

*Corresponding: joongku@kribb.re.kr
International Biological Material Research Center

Internal transcribed spacer (ITS) region of nuclear ribosomal DNA from 16 populations of *Persicaria barbata* (L.) H. Hara (Polygonaceae) belonging to five geographical locations of India (Arunachal Pradesh, Himachal Pradesh, Bihar, Karnataka and Andaman Island) was sequenced. Analysis of nucleotide sequences reveals polymorphism among the populations. UPGMA analysis conducted on the ITS datasets shows that the sampled populations of *P. barbata* are grouped according to their geographic locations and are supposed to be evolved under reproductive isolation which most probably is due to the long distance distribution and population fragmentation.

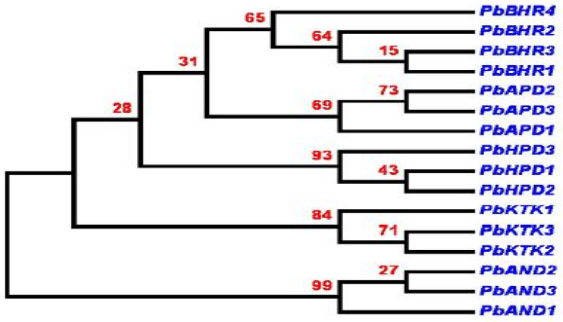

Keywords : *Persicaria barbata*; Genetic Diversity; ITS; nrDNA; rDNA; Polygonaceae; Evolution; Trees; Recombination; Polymorphism

Article 166

Halogranum salarium sp. nov., a halophilic archaeon isolated from sea salt

Syst Appl Microbiol. 2011 Dec; 34(8):576-80.

Kim KK, Lee KC, Lee JS*

*Corresponding: jslee@kribb.re.kr
Biological Resource Center

Three halophilic archaea, strains B-1^T, B-3 and B-4, were isolated from evaporitic salt crystals from Namhae, Korea. Cells of the strains were Gram-stain-negative, motile and pleomorphic, and colonies were red-pigmented. The three isolates had identical 16S rRNA gene sequences and formed a tight phylogenetic clade with *Halogranum rubrum* RO2-11^{T}in the genus *Halogranum*, showing 99.5% sequence similarity. The next most closely related species were *Halogranum amylolyticum* and *Halogranum gelatinilyticum* (97.4 and 96.3% similarity to the respective type strains). The phylogeny based on the full-length RNA polymerase subunit B' gene (*rpoB'*) was in agreement with the 16S rRNA gene sequence analysis, but allowed better discrimination. DNA-DNA hybridization between a representative strain (B-1^T) and the type strains of *Hgn. rubrum, Hgn. amylolyticum* and *Hgn. gelatinilyticum* revealed less than 40% relatedness. Polar lipid analysis showed that the three isolates contained phosphatidylglycerol, phosphatidylglycerol phosphate methyl ester and three glycolipids. Combined genotypic and phenotypic data supported the conclusion that strains B-1^T, B-3 and B-4 represent a novel species of the genus *Halogranum*, for which the name *Halogranum salarium* sp. nov. is proposed. The type strain is B-1^T (=KCTC 4066^T=DSM 23171^T).
PMID: 21616619

Keywords : *Halogranum salarium* sp nov.; Halophilic Archaea; *rpoB'* gene; Marine Solar Saltern; Family Halobacteriaceae; Emended Description; Bacterium; Sequences; Topology; China

Article 167

Association of the *adiponectin* gene variations with risk of ischemic stroke in a Korean population

Yonsei Med J. 2011 Jan; 52(1):20-5.

Cheong MY, Bang OS, Cha MH, Park YK, Kim SH, Kim YJ*

*Corresponding: yjkim8@kribb.re.kr
Genome Resource Center

PURPOSE: Stroke is the second leading cause of death and a major cause of morbidity and mortality worldwide. Evidence of variations in *adiponectin* (*AdipoQ*) genes that are associated with ischemic stroke has not been consistent, and it is unclear whether the same loci contribute to these associations in the Korean population. Using a Korean population, we tested ischemic stroke-associated *AdipoQ* markers.
MATERIALS AND METHODS: In a preliminary genome-wide association study using 320 250 k Affymetrix NSP chips, *AdipoQ* was found to be associated with ischemic stroke in Koreans. To study of *AdipoQ*, a further 673 ischemic stroke patients and 267 unrelated individuals without a history of stroke or transient ischemic attack were examined in a case-control study.
RESULTS: Six polymorphisms (rs182052G > A, rs16861205G > A, rs822391T > C, rs822396A > G, rs12495941G > T and rs3774261A > G) that had a minor allele frequency of over 1% were strongly associated with stroke ($p < 0.05$). Two of these, rs822391T > C and rs822396A > G showed this association on both dominant and additive logistic regression analysis after adjusting for age and sex. The haplotypes ht 1 (AGGCGG and AAGTAG) were significantly associated with susceptibility to stroke.
CONCLUSION: Our findings show that polymorphisms in *AdipoQ* are associated with risk for ischemic stroke in the Korean population. This study lends further support to the putative role of *AdipoQ* in stroke.

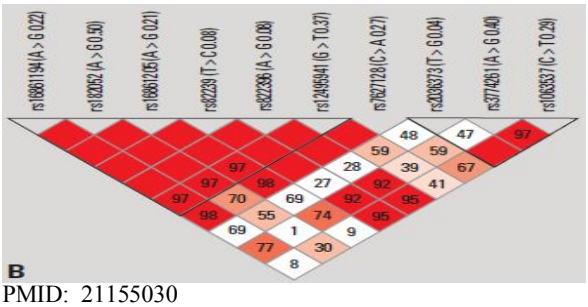

PMID: 21155030

Keywords : *AdipoQ*; Ischemic; Stroke; Koreans; Adipose-Specific Protein; Type-2 Diabetic-Patients; Plasma *Adiponectin*; Insulin Sensitivity; Metabolic Syndrome; Adipocytes

2011
KRIBB Article Abstracts
Corresponding Articles
Indexed in SCIE

Division of KRIBB Strategy Projects

- Viral Infectious Disease Research Center
- AI Control Material Research Center
- Kinomics Based Anticancer Research World Class Institute
- Cancer Biomarkers Development Research Center

Korea Research Institute of Bioscience and Biotechnology


KRIBB
www.kribb.re.kr

Article 168

Synthesis and high performance of magnetofluorescent polyelectrolyte nanocomposites as MR/near-infrared multimodal cellular imaging nanoprobes

ACS Nano. 2011 Oct; 5(10):8230-40.

Kim HM, Lee H, Hong KS, Cho MY, Sung MH, Poo H*, Lim YT

*Co-corresponding: haryoung@kribb.re.kr
Viral Infectious Disease Research Center

Here, we describe an easy but robust chemical strategy to synthesize high-performance magnetic resonance (MR)/near-infrared (NIR) multimodal imaging nanoprobes. Poly(γ-glutamic acid) was used for the convenient phase transfer of MnFe(2)O(4) nanoparticles dispersed in organic solvents into aqueous solutions and facilitated further ionic gelation with poly(l-lysine). During the gelation process, MnFe(2)O(4) nanoparticulate satellites were encapsulated in the ionic nanocomplex, which induced synergistic magnetism and resulted in huge T_2 relaxivity (r_2). The positively charged outer surfaces were assembled with other negatively charged NIR emitting fluorescent nanocrystals and enabled the highly efficient delivery of the magnetofluorescent polyelectrolyte nanocomposites (MagFL-PEN) into cancer cells. The enhancement of negative contrast of MagFL-PEN at 2 μg/mL concentration was similar to that of Resovist at 20 μg/mL concentration. The NIR fluorescence microscopy images of the MagFL-PEN-labeled cells even at 12.5 pM were able to be clearly observed. The labeling efficiency of MagFL-PEN was approximately 65-fold higher compared to that of the commercialized fluorescent nanocrystals, only after 3 h incubation period, even at the test concentration (100 pM). Due to the high-performance capabilities both in materials properties and cell labeling efficiency, the MagFL-PEN is expected to be used as a highly efficient MR/NIR dual-modality imaging nanoprobe in the detection of cancer cells and monitoring of therapeutic cells *in vivo*.

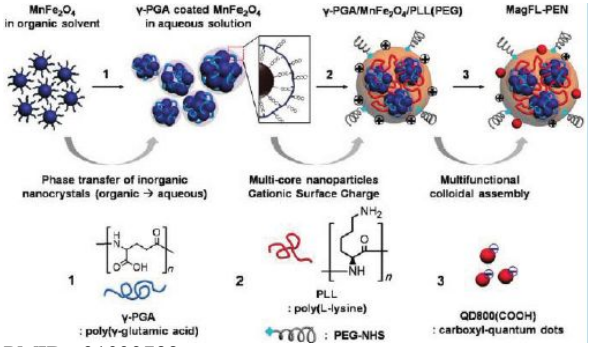

PMID: 21932788

Keywords : Imaging Agents; Nanostructures; Polyelectrolyte; Magnetic Resonance Imaging; Near-Infrared Imaging; Breast Cancer; Silica Nanoparticles; Gene Delivery; Fluorescent; Nanocrystals

Article 169

Galectin-3 binding protein promotes cell motility in colon cancer by stimulating the shedding of protein tyrosine phosphatase kappa by proprotein convertase 5

Biochem Biophys Res Commun. 2011 Jan; 404(1):96-102.

Kim YS, Jung JA, Kim HJ, Ahn YH, Yoo JS, Oh S, Cho C, Yoo HS, Ko JH*

*Corresponding: jhko@kribb.re.kr
Cancer Biomarkers Development Research Center

It has previously been reported that shedding of the PTPκ ectodomain drives enhanced motility of colon cancer cells. Herein, we provide mechanism underlying the regulation of PTPκ shedding by galectin-3 binding protein. PTPκ was inarguably scissored by the processed form of proprotein convertase 5 (subtilisin/kexin type 5), and galectin-3 binding protein which is over-produced in colon cancer cells and tissues contributed to increased cancer cell motility by acting as a negative regulator of galectin-3 at the cell surface. The high expression ratio of galectin-3 binding protein to galectin-3 was clinically correlated to lymphatic invasion. These results suggest that galectin-3 binding protein may be a potential therapeutic target for treatment of, at least, colon cancer patients with high expression of galectin-3 binding protein.

PMID: 21094132

Keywords : Galectin-3 Binding Protein; Proprotein Convertase 5; PTP Kappa Shedding; Tumor-Associated Antigen; Proteolytic Cleavage; Carcinoma; Ligands

Article 170

Asperlin induces G_2/M arrest through ROS generation and ATM pathway in human cervical carcinoma cells

Biochem Biophys Res Commun. 2011 Jun; 409(3):489-93.

He L, Nan MH, Oh HC, Kim YH, Jang JH, Erikson RL, Ahn JS*, Kim BY*

*Co-corresponding: jsahn@kribb.re.kr bykim@kribb.re.kr
Kinomics Based Anticancer Research World Class Institute

We exploited the biological activity of an antibiotic agent asperlin isolated from *Aspergillus nidulans* against human cervical carcinoma cells. We found that asperlin dramatically increased reactive oxygen species (ROS) generation accompanied by a significant reduction in cell proliferation. Cleavage of caspase-3 and PARP and reduction of Bcl-2 could also be detected after asperlin treatment to the cells. An anti-oxidant N-acetyl-L-cysteine (NAC), however, blocked all the apoptotic effects of asperlin. The involvement of oxidative stress in asperlin induced apoptosis could be supported by the findings that ROS- and DNA damage-associated G2/M phase arrest and ATM phosphorylation were increased by asperlin. In addition, expression and phosphorylation of cell cycle proteins as well as G2/M phase arrest in response to asperlin were significantly blocked by NAC or an ATM inhibitor KU-55933 pretreatment. Collectively, our study proved for the first time that asperlin could be developed as a potential anti-cancer therapeutics through ROS generation in HeLa cells.

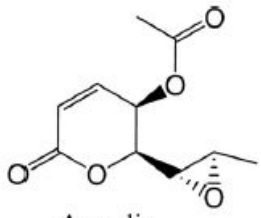

Asperlin

PMID: 21600879

Keywords : Asperlin; ROS; ATM; Double-Strand Breaks; DNA Damage; Cdc25 Phosphatases; Oxidative Stress; Apoptosis; Cancer; Kinase

Article 171

Optimization of phage-immobilized ELISA for autoantibody profiling in human sera

Biotechnol Lett. 2011 Apr; 33(4):655-61.

Woo MK, Heo CK, Hwang HM, Ko JH, Yoo HS, Cho EW*

*Corresponding: ewcho@kribb.re.kr
Cancer Biomarkers Development Research Center

Phage libraries displaying cDNA or random peptides have been used for profiling autoantibodies in cancer. The detection of autoantibodies in human sera using phages displaying specific epitopes is usually performed by phage-immobilized ELISAs which can detect specific antibodies without identification of whole antigens. However, these ELISAs can give feeble detection signals that are indistinguishable from background signals which are caused by human sera. To improve the usefulness of phage ELISA for human sera, the conditions for each step in phage ELISA were optimized. The antigenicity of phage antigens was maximal when using coating buffer of neutral pH. By using protein-free blocking buffer and pre-adsorbing human sera with phage host cell ER2738 extracts significantly decreased non-specific signals. Finally, when these conditions were applied to phage ELISA using K10P1, the values of the negative controls were concentrated near cutoff values, which made the assay more reliable. The optimized phage ELISA conditions described here would increase the efficacy of detection specific autoantibodies in human sera.

PMID: 21125414

Keywords : Blocking Buffer; Coating Buffer; Human Serum; Phage ELISA; Pre-Adsorption; Identification; Peptides; Library; Ligands

Article 172

Pros and cons of using aberrant glycosylation as companion biomarkers for therapeutics in cancer

BMB Rep. 2011 Dec; 44(12):765-71.

Kang JG, Ko JH, Kim YS*

*Corresponding: omsys1@kribb.re.kr
Cancer Biomarkers Development Research Center

Cancer treatment has been stratified by companion biomarker tests that serve to provide information on the genetic status of cancer patients and to identify patients who can be expected to respond to a given treatment. This stratification guarantees better efficiency and safety during treatment. Cancer patients, however, marginally benefit from the current companion biomarker-aided treatment regimens, presumably because companion biomarker tests are dependent solely on the mutation status of several genes *status quo*. In the true sense of the term, "personalized medicine", cancer patients are deemed to be identified individually by their molecular signatures, which are not necessarily confined to genetic mutations. Glycosylation is tremendously dynamic and shows alterations in cancer. Evidence is accumulating that aberrant glycosylation contributes to the development and progression of cancer, holding the promise for use of glycosylation status as a companion biomarker in cancer treatment. There are, however, several challenges derived from the lack of a reliable detection system for aberrant glycosylation, and a limited library of aberrant glycosylation. The challenges should be addressed if glycosylation status is to be used as a companion biomarker in cancer treatment and contribute to the fulfillment of personalized medicine.

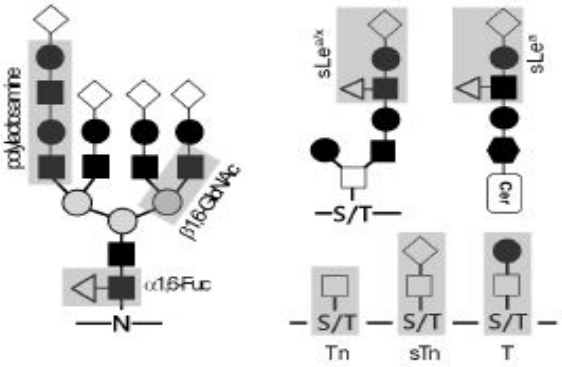

PMID: 22189678

Keywords : Aberrant Glycosylation; Cancer Diagnostics; Companion Biomarker; Tyrosine Kinase; Carcinoma Cells; Oncogene; Mutations; Kras; Phosphorylation

Article 173

Proteasome inhibitor-I enhances tunicamycin-induced chemosensitization of prostate cancer cells through regulation of NF-κB and CHOP expression

Cell Signal. 2011 May; 23(5):857-65.

Huong PT, Moon DO, Kim SO, Kim KE, Jeong SJ, Lee KW, Lee KS, Jang JH, Erikson RL, Ahn JS*, Kim BY*

*Co-corresponding: jsahn@kribb.re.kr bykim@kribb.re.kr
Kinomics Based Anticancer Research World Class Institute

Although endoplasmic reticulum (ER) stress induction by some anticancer drugs can lead to apoptotic death of cancer cells, combination therapy with other chemicals would be much more efficient. It has been reported that proteasome inhibitors could induce cancer cell death through ER-stress. Our study, however, showed a differential mechanism of proteasome inhibitor-I (Pro-I)-induced cell death. Pro-I significantly enhanced apoptotic death of PC3 prostate cancer cells pretreated with tunicamycin (TM) while other signaling inhibitors against p38, mitogen activated kinase (MEK) and phosphatidyl-inositol 3-kinase (PI3K) did not, as evidenced by cell proliferation and cell cycle analyses. NF-κB inhibition by Pro-I, without direct effect on ER-stress, was found to be responsible for the TM-induced chemosensitization of PC3 cells. Moreover, TM-induced/enhancer-binding protein (C/EBP) homologous protein (CHOP) expression was enhanced by Pro-I without change in GRP78 expression. CHOP knockdown by siRNA also showed a significant decrease in Pro-I chemosensitization. All these data suggest that although TM could induce both NF-κB activation and CHOP expression through ER-stress, both NF-κB inhibition and increased CHOP level by Pro-I are required for enhanced chemosensitization of PC3 prostate cancer cells. Thus, our study might contribute to the identification of anticancer targets against prostate cancer cells.

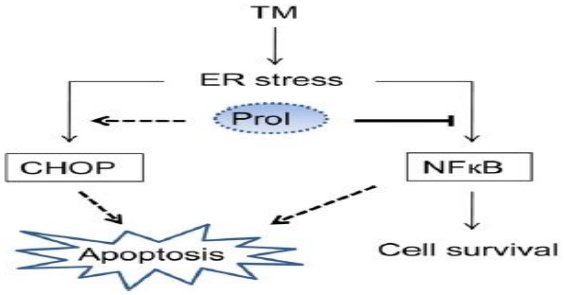

PMID: 21276850

Keywords : Proteasome Inhibitor-1; Tunicamycin; ER-Stress; NF-Kappa B; CHOP; Apoptosis; Phosphorylation; Stimulation; Caspase-12; Resistance

Article 174

Electrostatically assembled biocompatible polymer nanoparticles for MR/optical dual-modality imaging nanoprobes

Chem Commun (Camb). 2011 Aug; 47(31):8889-91.

Chung KH, Cho MY, Sung MH, Poo H*, Lim YT

*Co-corresponding: haryoung@kribb.re.kr
Viral Infectious Disease Research Center

Biocompatible dual-modality imaging nanoprobes were synthesized by the electrostatic assembly of poly(γ-glutamic acid)[Gd-DTPA] and chitosan[IRDye800] and applied for the imaging of immune cells (phagocytic) and cancer cells (non-phagocytic).

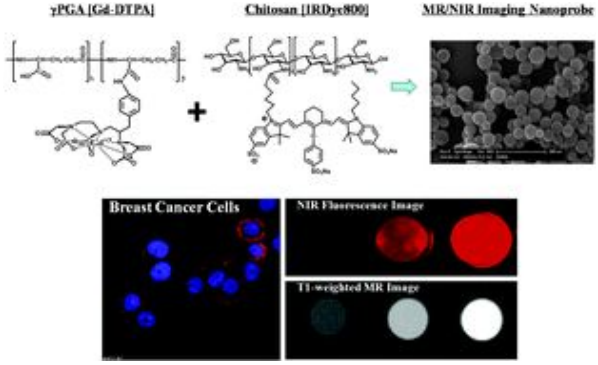

PMID: 21748163

Keywords : Dendritic Cells; Quantum Dots; Contrast Agents; Cancer; Probe; Imaging Nanoprobe; Immune Cells

Article 175

Interspecies transmission of the canine influenza H3N2 virus to domestic cats in South Korea, 2010

J Gen Virol. 2011 Oct; 92(10):2350-5.

Song DS*, An DJ, Moon HJ, Yeom MJ, Jeong HY, Jeong WS, Park SJ, Kim HK, Han SY, Oh JS, Park BK, Kim JK, Poo H, Webster RG, Jung K, Kang BK

*Co-first: sds1@kribb.re.kr
Viral Infectious Disease Research Center

In the past 4 years, incidences of endemic or epidemic respiratory diseases associated with canine influenza H3N2 virus in Asian dogs have been reported in countries such as South Korea and China. Canine species were considered to be the new natural hosts for this virus. However, at the beginning of 2010, influenza-like respiratory signs, such as dyspnoea, were also observed among cats as well as in dogs in an animal shelter located in Seoul, South Korea. The affected cats showed 100 % morbidity and 40 % mortality. We were able to isolate a virus from a lung specimen of a dead cat, which had suffered from the respiratory disease, in embryonated-chicken eggs. The eight viral genes isolated were almost identical to those of the canine influenza H3N2 virus, suggesting interspecies transmission of canine influenza H3N2 virus to the cat. Moreover, three domestic cats infected with intranasal canine/Korea/GCVP01/07 (H3N2) all showed elevated rectal temperatures, nasal virus shedding and severe pulmonary lesions, such as suppurative bronchopneumonia. Our study shows, for the first time, that cats are susceptible to canine influenza H3N2 infection, suggesting that cats may play an intermediate host role in transmitting the H3N2 virus among feline and canine species, which could lead to the endemic establishment of the virus in companion animals. Such a scenario raises a public health concern, as the possibility of the emergence of new recombinant feline or canine influenza viruses in companion animals with the potential to act as a zoonotic infection cannot be excluded.

PMID: 21715595

Keywords : H5N1; H3N2; Viruses; Dog; Cat; Respiratory Disease; Canine Influenza; Korea; China

Article 176

Emergence of mammalian species-infectious and -pathogenic avian influenza H6N5 virus with no evidence of adaptation

J Virol. 2011 Dec; 85(24):13271-7.

Nam JH, Kim EH, Song D, Choi YK, Kim JK, Poo H*

*Co-corresponding: haryoung@kribb.re.kr
Viral Infectious Disease Research Center

The migratory waterfowl of the world are considered to be the natural reservoir of influenza A viruses. Of the 16 hemagglutinin subtypes of avian influenza viruses, the H6 subtype is commonly perpetuated in its natural hosts and is of concern due to its potential to be a precursor of highly pathogenic influenza viruses by reassortment. During routine influenza surveillance, we isolated an unconventional H6N5 subtype of avian influenza virus. Experimental infection of mice revealed that this isolate replicated efficiently in the lungs, subsequently spread systemically, and caused lethality. The isolate also productively infected ferrets, with direct evidence of contact transmission, but no disease or transmission was seen in pigs. Although the isolate possessed the conserved receptor-binding site sequences of avian influenza viruses, it exhibited relatively low replication efficiencies in ducks and chickens. Our genetic and molecular analyses of the isolate revealed that its PB1 sequence showed the highest evolutionary relationship to those of highly pathogenic H5N1 avian influenza viruses and that its PA protein had an isoleucine residue at position 97 (a representative virulence marker). Further studies will be required to examine why our isolate has the virologic characteristics of mammalian influenza viruses but the archetypal receptor binding profiles of avian influenza viruses, as well as to determine whether its potential virulence markers (PB1 analogous to those of H5N1 viruses or isoleucine residue at position 97 within PA) could render it highly pathogenic in mice.
PMID: 21994462

Keywords : Viruses; Receptor Specificity; Virulence Marker; Molecular-Basis; Gene Pool; H5N1; Evolution; Duck; Erythrocytes; California; China

Article 177

Bioderived polyelectrolyte nanogels for robust antigen loading and vaccine adjuvant effects

Small. 2011 Dec; 7(23):3281-6.

Lim YT, Shim SM, Noh YW, Lee KS, Choi DY, Uyama H, Bae HH, Kim JH, Hong KS, Sung MH, Poo H*

*Co-corresponding: haryoung@kribb.re.kr
Viral Infectious Disease Research Center

An easy but robust strategy for the synthesis of bioderived polyelectrolyte nanogels for protein antigen loading and vaccine adjuvant systems that can improve both humoral (Th2) and cellular immunity (Th1) is presented. The synthesized polyelectrolyte nanogels promote the uptake of antigens into antigen-presenting cells and strongly induce ovalbumin-specific INF-γ producing cells, cytotoxic T cell activity, and antibody production.

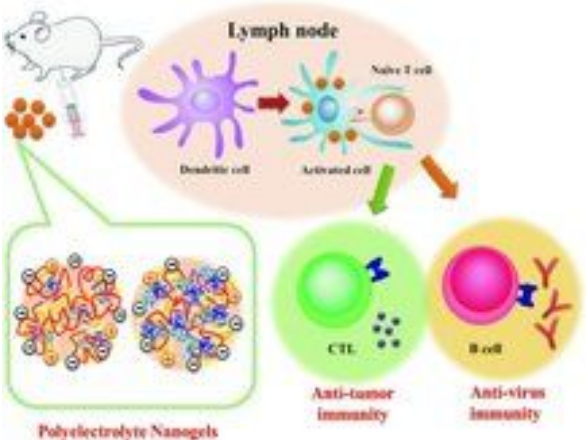

PMID: 22009658

Keywords : Polyelectrolyte Nanogels; Antigens; Drug Delivery; Vaccine Adjuvant; Dendritic Cells

Article 178

Association between nasal shedding and fever that influenza A (H3N2) induces in dogs

Virol J. 2011 Jan; 8:1.

Song D*, Moon H, Jung K, Yeom M, Kim H, Han S, An D, Oh J, Kim J, Park B, Kang B

*Co-first: sds1@kribb.re.kr
Viral Infectious Disease Research Center

BACKGROUND: Avian origin canine influenza virus was reported in Korea. The dog to dog contact transmission of the avian origin canine influenza virus (CIV) H3N2 and CIV H3N8 was shown by experimental contact transmission. This study was focused on viral excretion and fever in order to elucidate the epidemiological associations which might be helpful to control the disease transmissions in CIV outbreak in dogs.
METHODS: An influenza seronegative 10-week-old Beagle dog was experimentally inoculated with the canine influenza virus A/canine/01/2007, subtype H3N2. Eight hours after inoculation, the infected dog was cohoused with seven uninfected Beagle dogs. Clinical signs including fever were recorded for 14 days post inoculation.
RESULTS: The infected dog and four of seven contact dogs in the study showed clinical signs (sneezing, nasal discharge and coughing) during the study. Viral shedding occurred in all of the animals tested and began on 1 to 6 DPI in dogs with clinical signs. Elevated body temperatures above 39.5 °C (geometric mean temperature of 39.86 °C ± 0.49) were observed in all symptomatic dogs. The mean viral titer during fever was 2.99 log EID_{50}/ml, which was significantly higher than the viral titer detected in the non fever.
CONCLUSIONS: The data show that contact dogs with a canine influenza infected dog shed different levels of virus in their nasal excretions and demonstrate that clinical signs, including fever, significantly correlate with the viral shedding.
PMID: 21205327

Keywords : Virus-Infection; Transmission; Humans; Influenza A; Canine Influenza Virus; H3N2; Dog

Article 179

Experimental infection of a newly emerging Korean type I porcine reproductive and respiratory syndrome virus isolate in colostrum-deprived pigs

Virol J. 2011 Apr; 8:177.

Kim HK, Lee CS, Kang BK, Yeom MJ, Moon HJ, Park SJ, Nguyen VG, Song DS*, Park BK

*Co-corresponding: sds1@kribb.re.kr
Viral Infectious Disease Research Center

BACKGROUND: Recently, new emergence of type I PRRSV has been reported in Korea by several research groups. Although specific subgroups of type I PRRSVs in Korea were observed in the previous phylogenetic analysis, there is a lack of information about the virulence of type I PRRSV recently isolated in Korea.
METHODS: One type I PRRSV isolate (G2446, 3 times passaged in primarily cultured pulmonary macrophages) in Korea was experimentally infected in colostrum-deprived pigs. The pathological and serological evaluations were performed and compared to type II PRRSV strain (CP07-401-9, 5 times passaged in MARC-145 cell lines)-infected pigs, for 21 days post challenge (dpc).
RESULTS: The pneumonia found in gross examination was more severe in type I PRRSV-infected pigs than type II PRRSV-infected pigs. Both groups showed bronchointerstitial pneumonia, mild multifocal perivascular lymphohistiocytic myocarditis and lymphadenopathy at 14 dpc. However, the unique histopathologic lesions were not found in the pigs experimentally infected with a Korean type I PRRSV isolate, when compared to previous data about classical pathology of PRRSV. The PRRS-specific antibodies were detected in the first week after challenge and viremia continued at least until 21 dpc in both groups.
CONCLUSION: The gross and histopathologic lesion in this study indicated that Korean type I PRRSV strain (G2446) caused classical PRRSV-specific lesions. Although this study evaluated one representative strain of Korean type I PRRSV, the results may provide information regarding the pathogenicity of type I PRRSV recently emerged in Korea.
PMID: 21496335

Keywords : Type I PRRSV Korea; Infection; Emerging; Swine Infertility; Lelystad Virus; PRRS Viruses; Pathogenicity; Replication; Sequences; Vr-2332; Strains; Europe

Article 180

The assessment of efficacy of porcine reproductive respiratory syndrome virus inactivated vaccine based on the viral quantity and inactivation methods

Virol J. 2011 Jun; 8:323.

Kim H, Kim HK, Jung JH, Choi YJ, Kim J, Um CG, Hyun SB, Shin S, Lee B, Jang G, Kang BK, Moon HJ, Song DS*

*Corresponding: sds1@kribb.re.kr
Viral Infectious Disease Research Center

BACKGROUND: There have been many efforts to develop efficient vaccines for the control of porcine reproductive and respiratory syndrome virus (PRRSV). Although inactivated PRRSV vaccines are preferred for their safety, they are weak at inducing humoral immune responses and controlling field PRRSV infection, especially when heterologous viruses are involved.
RESULTS: In all groups, the sample to positive (S/P) ratio of IDEXX ELISA and the virus neutralization (VN) titer remained negative until challenge. While viremia did not reduce in the vaccinated groups, the IDEXX-ELISA-specific immunoglobulin G increased more rapidly and to significantly greater levels 7 days after the challenge in all the vaccinated groups compared to the non-vaccinated groups ($p < 0.05$). VN titer was significantly different in the 106 PFU/mL PRRSV vaccine-inoculated and binary ethylenimine (BEI)-inactivated groups 22 days after challenge ($p < 0.05$). Consequently, the inactivated vaccines tested in this study provided weak memory responses with sequential challenge without any obvious active immune responses in the vaccinated pigs.
CONCLUSIONS: The inactivated vaccine failed to show the humoral immunity, but it showed different immune response after the challenge compared to mock group. Although the 10^6 PFU/mL-vaccinated and BEI-inactivated groups showed significantly greater VN titers 22 days after challenge, all the groups were already negative for viremia.
PMID: 21703032

Keywords : PRRSV Vaccine; Neutralizing Antibodies; Swine Infertility; Protection; Pig; Immunity; Failure; Strain

Korean Bioinformation Center

Korea Research Institute of Bioscience and Biotechnology


KRIBB
www.kribb.re.kr

Article 181

Whole-exome sequencing identifies mutations of *KIF22* in spondyloepimetaphyseal dysplasia with joint laxity, leptodactylic type

Am J Hum Genet. 2011 Dec;8 9(6):760-6.

Min BJ, Kim N*, Chung T, Kim OH, Nishimura G, Chung CY, Song HR, Kim HW, Lee HR, Kim J, Kang TH, Seo ME, Yang SD, Kim DH, Lee SB, Kim JI, Seo JS, Choi JY, Kang D, Kim D, Park WY, Cho TJ

*Co-first: deepreds@kribb.re.kr
Korean Bioinformation Center

Spondyloepimetaphyseal dysplasia with joint laxity (SEMDJL), leptodactylic (lepto-SEMDJL) or Hall type, is an autosomal-dominant skeletal dysplasia manifesting with short stature, joint laxity with dislocation(s), limb malalignment, and spinal deformity. Its causative gene mutation has not yet been discovered. We captured and sequenced the exomes of eight affected individuals in six unrelated kindreds (three individuals in a family and five simplex individuals). Five novel sequence variants in *KIF22*, which encodes a member of the kinesin-like protein family, were identified in seven individuals. Sanger sequencing of *KIF22* confirmed that c.443C>T (p.Pro148Ser) cosegregated with the phenotype in the affected individuals in the family; c.442C>T (p.Pro148Leu) or c.446G>A (p.Arg149Gln) was present in four of five simplex individuals, but was absent in unaffected individuals in their family and 505 normal cohorts. *KIF22* mRNA was detected in human bone, cartilage, joint capsule, ligament, skin, and primary cultured chondrocytes. *In silico* analysis of KIF22 protein structure indicates that Pro148 and Arg149 are important in maintaining hydrogen bonds in the ATP binding and motor domains of KIF22. We conclude that these mutations in *KIF22* cause lepto-SEMDJL.

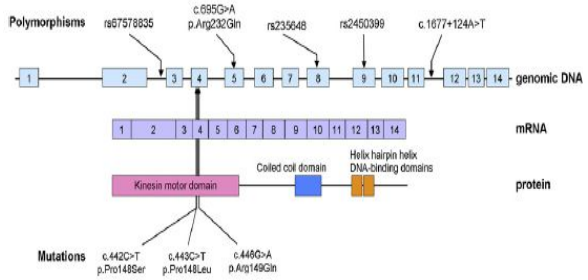

PMID: 22152677

Keywords : Dislocations Hall Type; Genetic Skeletal Disorders; Dominant Inheritance; Diagnostic Feature; Distinct Form; Kinesin; DNA; Classification; Alignment

Article 182

Genome-wide expression patterns associated with oncogenesis and sarcomatous transdifferentation of cholangiocarcinoma

BMC Cancer. 2011 Feb; 11:78.

Seol MA, Chu IS*, Lee MJ, Yu GR, Cui XD, Cho BH, Ahn EK, Leem SH, Kim IH, Kim DG

*Co-first: chu@kribb.re.kr
Korean Bioinformation Center

BACKGROUND: The molecular mechanisms of CC (cholangiocarcinoma) oncogenesis and progression are poorly understood. This study aimed to determine the genome-wide expression of genes related to CC oncogenesis and sarcomatous transdifferentiation.
METHODS: Genes that were differentially expressed between CC cell lines or tissues and cultured normal biliary epithelial (NBE) cells were identified using DNA microarray technology. Expressions were validated in human CC tissues and cells.
RESULTS: Using unsupervised hierarchical clustering analysis of the cell line and tissue samples, we identified a set of 342 commonly regulated (>2-fold change) genes. Of these, 53, including tumor-related genes, were upregulated, and 289, including tumor suppressor genes, were downregulated (<0.5 fold change). Expression of *SPP1, EFNB2, E2F2, IRX3, PTTG1, PPARγ, KRT17, UCHL1, IGFBP7* and *SPARC* proteins was immunohistochemically verified in human and hamster CC tissues. Additional unsupervised hierarchical clustering analysis of sarcomatoid CC cells compared to three adenocarcinomatous CC cell lines revealed 292 differentially upregulated genes (>4-fold change), and 267 differentially downregulated genes (<0.25 fold change). The expression of 12 proteins was validated in the CC cell lines by immunoblot analysis and immunohistochemical staining. Of the proteins analyzed, we found upregulation of the expression of the epithelial-mesenchymal transition (EMT)-related proteins *VIM* and *TWIST1*, and restoration of the methylation-silenced proteins *LDHB, BNIP3, UCHL1,* and *NPTX2* during sarcomatoid transdifferentiation of CC.
CONCLUSION: The deregulation of oncogenes, tumor suppressor genes, and methylation-related genes may be useful in identifying molecular targets for CC diagnosis and prognosis.

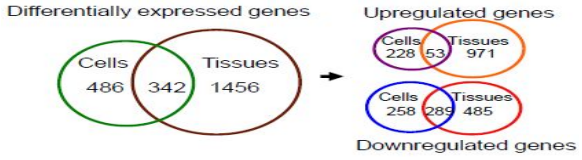

PMID: 21333016

Keywords : Activated-Receptor-Gamma; Hepatocellular-Carcinoma; Intrahepatic Cholangiocarcinoma; Pancreatic-Cancer; Tumor-Suppressor; Gene-Expression; Cell-Lines

Article 183

The proteomic complexity and rise of the primordial ancestor of diversified life

BMC Evol Biol. 2011 May; 11:140.

Kim KM*, Caetano-Anollés G*

*First: kmkim@kribb.re.kr
Korean Bioinformation Center

BACKGROUND: The last universal common ancestor represents the primordial cellular organism from which diversified life was derived. This urancestor accumulated genetic information before the rise of organismal lineages and is considered to be either a simple 'progenote' organism with a rudimentary translational apparatus or a more complex 'cenancestor' with almost all essential biological processes. Recent comparative genomic studies support the latter model and propose that the urancestor was similar to modern organisms in terms of gene content. However, most of these studies were based on molecular sequences, which are fast evolving and of limited value for deep evolutionary explorations.
RESULTS: Here we engage in a phylogenomic study of protein domain structure in the proteomes of 420 free-living fully sequenced organisms. Domains were defined at the highly conserved fold superfamily (FSF) level of structural classification and an iterative phylogenomic approach was used to reconstruct *max_set* and *min_set* FSF repertoires as upper and lower bounds of the urancestral proteome. While the functional make up of the urancestral sets was complex, they represent only 5-11% of the 1,420 FSFs of extant proteomes and their make up and reuse was at least 5 and 3 times smaller than proteomes of free-living organisms, repectively. Trees of proteomes reconstructed directly from FSFs or from molecular functions, which included the *max_set* and *min_set* as articial taxa, showed that urancestors were always placed at their base and rooted the tree of life in Archaea. Finally, a molecular clock of FSFs suggests the *min_set* reflects urancestral genetic make up more reliably and confirms diversified life emerged about 2.9 billion years ago during the start of planet oxygenation.
CONCLUSIONS: The minimum urancestral FSF set reveals the urancestor had advanced metabolic capabilities, was especially rich in nucleotide metabolism enzymes, had pathways for the biosynthesis of membrane *sn1,2* glycerol ester and ether lipids, and had crucial elements of translation, including a primordial ribosome with protein synthesis capabilities. It lacked however fundamental functions, including transcription, processes for extracellular communication, and enzymes for deoxyribonucleotide synthesis. Proteomic history reveals the urancestor is closer to a simple progenote organism but harbors a rather complex set of modern molecular functions.
PMID: 21612591

Keywords : Universal Common Ancestor; Horizontal Gene-Transfer; Protein Fold Architecture; Elongation-Factor G; Transfer-RNA; *Methanococcus jannaschii*; *Methanogenic archaeon*; Phylogenomic Analysis; Comparative Genomics

Article 184

Liverome: a curated database of liver cancer-related gene signatures with self-contained context information

BMC Genomics. 2011 Nov; 12(S3):S3.

Lee L, Wang K, Li G, Xie Z, Wang Y, Xu J, Sun S, Pocalyko D, Bhak J, Kim C, Lee
KH, Jang YJ, Yeom YI, Yoo HS*, Hwang S*

*Co-corresponding: yoohyang@kribb.re.kr swhwang@kribb.re.kr
Korean Bioinformation Center

BACKGROUND: Hepatocellular carcinoma (HCC) is the fifth most common cancer worldwide. A number of molecular profiling studies have investigated the changes in gene and protein expression that are associated with various clinicopathological characteristics of HCC and generated a wealth of scattered information, usually in the form of gene signature tables. A database of the published HCC gene signatures would be useful to liver cancer researchers seeking to retrieve existing differential expression information on a candidate gene and to make comparisons between signatures for prioritization of common genes. A challenge in constructing such database is that a direct import of the signatures as appeared in articles would lead to a loss or ambiguity of their context information that is essential for a correct biological interpretation of a gene's expression change. This challenge arises because designation of compared sample groups is most often abbreviated, *ad hoc*, or even missing from published signature tables. Without manual curation, the context information becomes lost, leading to uninformative database contents. Although several databases of gene signatures are available, none of them contains informative form of signatures nor shows comprehensive coverage on liver cancer. Thus we constructed Liverome, a curated database of liver cancer-related gene signatures with self-contained context information.
DESCRIPTION: Liverome's data coverage is more than three times larger than any other signature database, consisting of 143 signatures taken from 98 HCC studies, mostly microarray and proteome, and involving 6,927 genes. The signatures were post-processed into an informative and uniform representation and annotated with an itemized summary so that all context information is unambiguously self-contained within the database. The signatures were further informatively named and meaningfully organized according to ten functional categories for guided browsing. Its web interface enables a straightforward retrieval of known differential expression information on a query gene and a comparison of signatures to prioritize common genes. The utility of Liverome-collected data is shown by case studies in which useful biological insights on HCC are produced.
CONCLUSION: Liverome database provides a comprehensive collection of well-curated HCC gene signatures and straightforward interfaces for gene search and signature comparison as well. Liverome is available at http://liverome.kobic.re.kr.
PMID: 22369201

Keywords : Hepatocellular-Carcinoma; Expression; Inhibition; Glypican-3; Deficient; Proteins; Network; Growth; Rat

Article 185

Sulfatase 1 and sulfatase 2 in hepatocellular carcinoma: associated signaling pathways, tumor phenotypes, and survival

Gene Chromosom Canc. 2011 Feb; 50(2):122-35.

Yang JD, Sun Z, Hu C, Lai J, Dove R, Nakamura I, Lee JS, Thorgeirsson SS, Kang KJ, Chu IS*, Roberts LR

*Co-corresponding: chu@kribb.re.kr
Korean Bioinformation Center

The heparin-degrading endosulfatases sulfatase 1 (SULF1) and sulfatase 2 (SULF2) have opposing effects in hepatocarcinogenesis despite structural similarity. Using mRNA expression arrays, we analyzed the correlations of SULF expression with signaling networks in human hepatocellular carcinomas (HCCs) and the associations of SULF expression with tumor phenotype and patient survival. Data from two mRNA microarray analyses of 139 and 36 HCCs and adjacent tissues were used as training and validation sets. Partek and Metacore software were used to identify SULF correlated genes and their associated signaling pathways. Associations between SULF expression, the hepatoblast subtype of HCC, and survival were examined. Both SULF1 and 2 had strong positive correlations with periostin, IQGAP1, TGFB1, and vimentin and inverse correlations with HNF4A and IQGAP2. Genes correlated with both SULFs were highly associated with the cell adhesion, cytoskeletal remodeling, blood coagulation, TGFB, and Wnt/β-catenin and epithelial mesenchymal transition signaling pathways. Genes uniquely correlated with SULF2 were more associated with neoplastic processes than genes uniquely correlated with SULF1. High SULF expression was associated with the hepatoblast subtype of HCC. There was a bimodal effect of SULF1 expression on prognosis, with patients in the lowest or highest tertile having a worse prognosis than those in the middle tertile. SULFs have complex effects on HCC signaling and patient survival. There are functionally similar associations with cell adhesion, ECM remodeling, TGFB, and WNT pathways, but also unique associations of SULF1 and SULF2. The roles and targeting of the SULFs in cancer require further investigation.
PMID: 21104785

Keywords : IQGAP1 Integrates Ca2+/Calmodulin; Heparan-Sulfate; Transforming Growth-Factor-Beta-1; Breast-Cancer; Expression; HSULF-1; SULF1; SULF2

Article 186

The effect of thiobarbituric acid on tyrosinase: inhibition kinetics and computational simulation

J Biomol Struct Dyn. 2011 Dec; 29(3):463-70.

Yin SJ, Si YX, Wang ZJ, Wang SF, Oh S, Lee S, Sim SM, Yang JM, Qian GY, Lee J*, Park YD

*Co-corresponding: jinhyuk@kribb.re.kr
Korean Bioinformation Center

Tyrosinase plays various roles in organisms and much research has focused on the regulation of tyrosinase activity. We studied the inhibitory effect of thiobarbituric acid (TBA) on tyrosinase. Our kinetic study showed that TBA inhibited tyrosinase in a reversible noncompetitive manner (K_i = 14.0 ± 8.5 mM and IC_{50} = 8.0 ± 1.0 mM). Intrinsic and ANS-binding fluorescences studies were also performed to gain more information regarding the binding mechanism. The results showed that no tertiary structural changes were obviously observed. For further insight, we predicted the 3D structure of tyrosinase and simulated the docking between tyrosinase and TBA. The docking simulation was successful with significant scores (binding energy for AutoDock4: -5.52 kcal/mol) and suggested that TBA was located in the active site. The 11 ns molecular dynamics simulation convinced that the four HIS residues (residue numbers: 57, 90, 250, and 282) were commonly responsible for the interaction with TBA. Our results provide a new inhibition strategy that works using an antioxidant rather than targeting the copper ions within the tyrosinase active site.

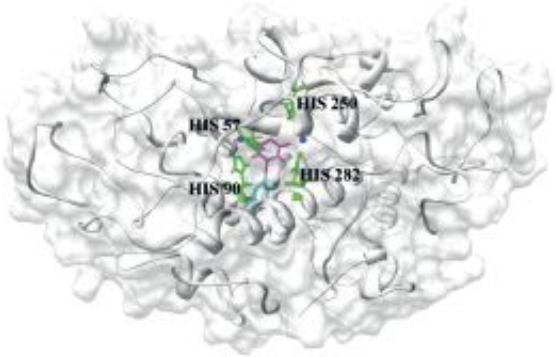

PMID: 22066533

Keywords : Mushroom Tyrosinase; Inhibition Kinetics; Thiobarbituric Acid; Docking Simulation; Lipid-Peroxidation; Induced Melanogenesis; Manduca-Sexta; Prophenoloxidase

Article 187

A genome-wide identification of genes potentially associated with host specificity of *Brucella* species

J Microbiol. 2011 Oct; 49(5):768-75.

Kim KM*, Kim KW, Sung S, Kim H

*First: kmkim@kribb.re.kr
Korean Bioinformation Center

Brucella species are facultative intracellular pathogenic α -Proteobacteria that can cause brucellosis in humans and domestic animals. The clinical and veterinary importance of the bacteria has led to well established studies on the molecular mechanisms of *Brucella* infection of host organisms. However, to date, no genome-wide study has scanned for genes related to the host specificity of *Brucella* spp. The majority of bacterial genes related to specific environmental adaptations such as host specificity are well-known to have evolved under positive selection pressure. We thus detected signals of positive selection for individual orthologous genes among *Brucella* genomes and identified genes related to host specificity. We first determined orthologous sets from seven completely sequenced *Brucella* genomes using the Reciprocal Best Hits (RBH). A maximum likelihood analysis based on the branch-site test was accomplished to examine the presence of positive selection signals, which was subsequently confirmed by phylogenetic analysis. Consequently, 12 out of 2,033 orthologous genes were positively selected by specific *Brucella* lineages, each of which belongs to a particular animal host. Extensive literature reviews revealed that half of these computationally identified genes are indeed involved in *Brucella* host specificity. We expect that this genome-wide approach based on positive selection may be reliably used to screen for genes related to environmental adaptation of a particular species and that it will provide a set of appropriate candidate genes.

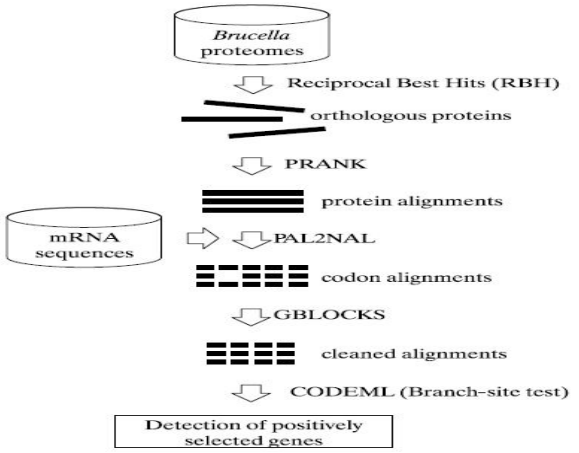

PMID: 22068493

Keywords : Genus *Brucella*; Evolution; Genome; Host Specificity; Positive Selection; *Staphylococcus aureus*; Phylogenetic Analysis; Sequence; Melitensis; Suis

Article 188

Controlling transcriptional programs for cellular adaptation by chromatin regulation

Mol Biosyst. 2011 May; 7(5):1713-9.

Kim SC*, Choi JK

*First: sckim@kribb.re.kr
Korean Bioinformation Center

Gene expression is dynamically reprogrammed during growth control and stress responses, which are two key processes of cellular adaptation. Single-gene studies suggest that gene regulatory patterns of the two processes commonly show high environmental responsiveness, but contrast in terms of regulatory flexibility. Our whole-genome analysis shows that the growth and stress genes are associated with activated and repressed chromatin, respectively, which can modulate the responsiveness of promoters and help balance regulatory flexibility and fidelity. Stochastic modeling of critical nucleosomes at specific promoter regions enables rapid induction of genes during stress responses by activating repressed chromatin. Conversely, activating histone modifications may contribute to regulatory fidelity for precise growth control by common transcription factors. Nucleosome eviction and modification loss lead to an intermediate chromatin state. The combinatorial role of nucleosome organization and modification is central to the balanced control of gene expression programs for stress responses and efficient growth. These regulatory mechanisms can also contribute to evolutionary adaptation.

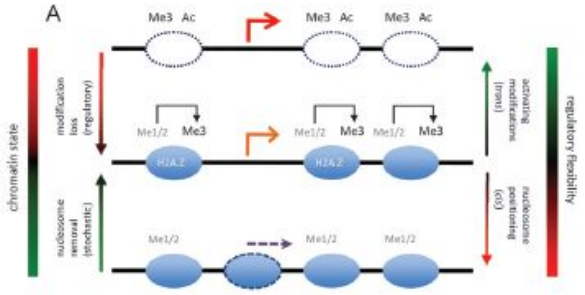

PMID: 21412562

Keywords : Stochastic Gene-Expression; *Saccharomyces cerevisiae*; Fluctuating Environments; Yeast; Genome; Noise; Variability; DNA

Article 189

Accurate quantification of transcriptome from RNA-Seq data by effective length normalization

Nucleic Acids Res. 2011 Jan; 39(2):e9.

Lee S, Seo CH, Lim B, Yang JO, Oh J, Kim M, Lee S, Lee B, Kang C, Lee S*

*Corresponding: sanghyuk@kribb.re.kr
Korean Bioinformation Center

We propose a novel, efficient and intuitive approach of estimating mRNA abundances from the whole transcriptome shotgun sequencing (RNA-Seq) data. Our method, NEUMA (Normalization by Expected Uniquely Mappable Area), is based on effective length normalization using uniquely mappable areas of gene and mRNA isoform models. Using the known transcriptome sequence model such as RefSeq, NEUMA pre-computes the numbers of all possible gene-wise and isoform-wise informative reads: the former being sequences mapped to all mRNA isoforms of a single gene exclusively and the latter uniquely mapped to a single mRNA isoform. The results are used to estimate the effective length of genes and transcripts, taking experimental distributions of fragment size into consideration. Quantitative RT-PCR based on 27 randomly selected genes in two human cell lines and computer simulation experiments demonstrated superior accuracy of NEUMA over other recently developed methods. NEUMA covers a large proportion of genes and mRNA isoforms and offers a measure of consistency ('consistency coefficient') for each gene between an independently measured gene-wise level and the sum of the isoform levels. NEUMA is applicable to both paired-end and single-end RNA-Seq data. We propose that NEUMA could make a standard method in quantifying gene transcript levels from RNA-Seq data.

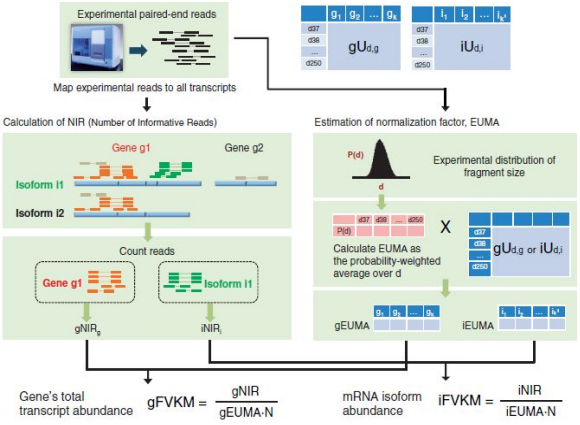

PMID: 21059678

Keywords : Transcriptome; RNA-Seq; mRNA Abundance; RT-PCR; Expression; Expected Uniquely Mappable Area

Article 190

miRGator v2.0: an integrated system for functional investigation of microRNAs

Nucleic Acids Res. 2011 Jan; 39(D):D158-62.

Cho S, Jun Y, Lee S, Choi HS, Jung S, Jang Y, Park C, Kim S, Lee S*, Kim W

*Co-corresponding: sanghyuk@kribb.re.kr
Korean Bioinformation Center

miRGator is an integrated database of microRNA (miRNA)-associated gene expression, target prediction, disease association and genomic annotation, which aims to facilitate functional investigation of miRNAs. The recent version of miRGator v2.0 contains information about (i) human miRNA expression profiles under various experimental conditions, (ii) paired expression profiles of both mRNAs and miRNAs, (iii) gene expression profiles under miRNA-perturbation (e.g. miRNA knockout and overexpression), (iv) known/predicted miRNA targets and (v) miRNA-disease associations. In total, >8000 miRNA expression profiles, ~300 miRNA-perturbed gene expression profiles and ~2000 mRNA expression profiles are compiled with manually curated annotations on disease, tissue type and perturbation. By integrating these data sets, a series of novel associations (miRNA-miRNA, miRNA-disease and miRNA-target) is extracted via shared features. For example, differentially expressed genes (DEGs) after miRNA knockout were systematically compared against miRNA targets. Likewise, differentially expressed miRNAs (DEmiRs) were compared with disease-associated miRNAs. Additionally, miRNA expression and disease-phenotype profiles revealed miRNA pairs whose expression was regulated in parallel in various experimental and disease conditions. Complex associations are readily accessible using an interactive network visualization interface. The miRGator v2.0 serves as a reference database to investigate miRNA expression and function (http://miRGator.kobic.re.kr).

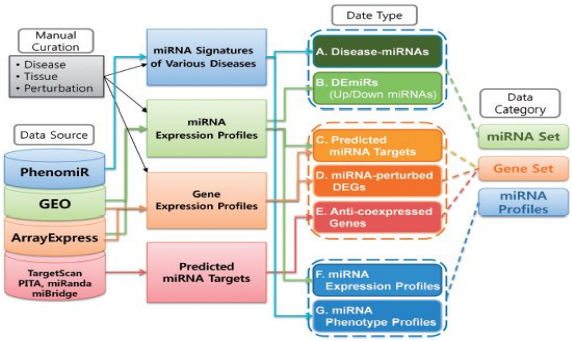

PMID: 21062822

Keywords : Target Recognition; Expression; Genomics; Database; Archive; Tool; microRNA; miRNA

Article 191

VnD: a structure-centric database of disease-related SNPs and drugs

Nucleic Acids Res. 2011 Jan; 39(D):D939-44.

Yang JO, Oh S, Ko G, Park SJ, Kim WY, Lee B*, Lee S*

*Corresponding: bulee@kribb.re.kr sanghyuk@kribb.re.kr
Korean Bioinformation Center

Numerous genetic variations have been found to be related to human diseases. Significant portion of those affect the drug response as well by changing the protein structure and function. Therefore, it is crucial to understand the trilateral relationship among genomic variations, diseases and drugs. We present the variations and drugs (VnD), a consolidated database containing information on diseases, related genes and genetic variations, protein structures and drug information. VnD was built in three steps. First, we integrated various resources systematically to deduce catalogs of disease-related genes, single nucleotide polymorphisms (SNPs), protein mutations and relevant drugs. VnD contains 137,195 disease-related gene records (13,940 distinct genes) and 16,586 genetic variation records (1790 distinct variations). Next, we carried out structure modeling and docking simulation for wild-type and mutant proteins to examine the structural and functional consequences of non-synonymous SNPs in the drug-related genes. Conformational changes in 590 wild-type and 4437 mutant proteins from drug-related genes were included in our database. Finally, we investigated the structural and biochemical properties relevant to drug binding such as the distribution of SNPs in proximal protein pockets, thermo-chemical stability, interactions with drugs and physico-chemical properties. The VnD database, available at http://vnd.kobic.re.kr:8080/VnD/ or vandd.org, would be a useful platform for researchers studying the underlying mechanism for association among genetic variations, diseases and drugs.

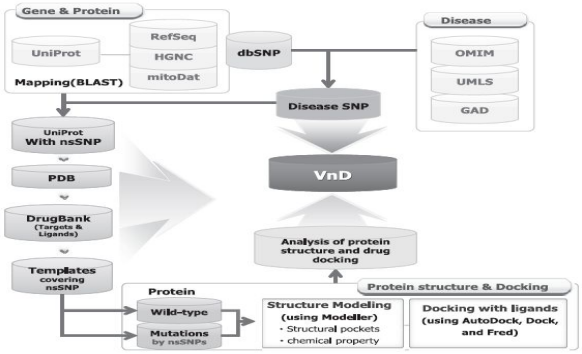

PMID: 21051351

Keywords : Single Nucleotide Polymorphisms; Japanese Population; National-Center; Genome Browser; Human Genes; Knowledgebase; Resources; Alignment

Article 192

Gene expression pattern in transmitochondrial cytoplasmic hybrid cells harboring type 2 diabetes-associated mitochondrial DNA haplogroups

PLoS One. 2011; 6(7):e22116.

Hwang S*, Kwak SH, Bhak J, Kang HS, Lee YR, Koo BK, Park KS, Lee HK, Cho YM

*Co-first: swhwang@kribb.re.kr
Korean Bioinformation Center

Decreased mitochondrial function plays a pivotal role in the pathogenesis of type 2 diabetes mellitus (T2DM). Recently, it was reported that mitochondrial DNA (mtDNA) haplogroups confer genetic susceptibility to T2DM in Koreans and Japanese. Particularly, mtDNA haplogroup N9a is associated with a decreased risk of T2DM, whereas haplogroups D5 and F are associated with an increased risk. To examine functional consequences of these haplogroups without being confounded by the heterogeneous nuclear genomic backgrounds of different subjects, we constructed transmitochondrial cytoplasmic hybrid (cybrid) cells harboring each of the three haplogroups (N9a, D5, and F) in a background of a shared nuclear genome. We compared the functional consequences of the three haplogroups using cell-based assays and gene expression microarrays. Cell-based assays did not detect differences in mitochondrial functions among the haplogroups in terms of ATP generation, reactive oxygen species production, mitochondrial membrane potential, and cellular dehydrogenase activity. However, differential expression and clustering analyses of microarray data revealed that the three haplogroups exhibit a distinctive nuclear gene expression pattern that correlates with their susceptibility to T2DM. Pathway analysis of microarray data identified several differentially regulated metabolic pathways. Notably, compared to the T2DM-resistant haplogroup N9a, the T2DM-susceptible haplogroup F showed down-regulation of oxidative phosphorylation and up-regulation of glycolysis. These results suggest that variations in mtDNA can affect the expression of nuclear genes regulating mitochondrial functions or cellular energetics. Given that impaired mitochondrial function caused by T2DM-associated mtDNA haplogroups is compensated by the nuclear genome, we speculate that defective nuclear compensation, under certain circumstances, might lead to the development of T2DM.

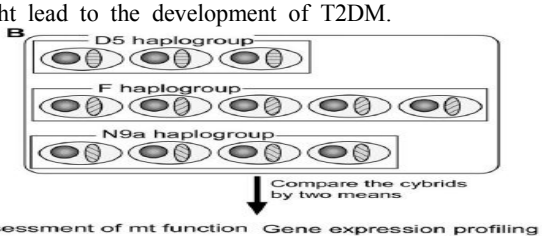

PMID: 21765942

Keywords : Set Enrichment Analysis; Korean Population; mtDNA; Mitochondrial DNA; Mellitus; Polymorphisms; Resistance; Profiles; Mutation

2011
KRIBB Article Abstracts
Corresponding Articles
Indexed in SCIE

Division of Bio-Therapeutics Research

- Immunotherapy Research Center
- Regenerative Medicine Research Center
- Chemical Biology Research Center
- Natural Medicine Research Center

Korea Research Institute of Bioscience and Biotechnology


KRIBB
www.kribb.re.kr

Article 193

Highly sensitive biosensing using arrays of plasmonic Au nanodisks realized by nanoimprint lithography

ACS Nano. 2011 Feb; 5(2):897-904.

Lee SW, Lee KS, Ahn J, Lee JJ, Kim MG, Shin YB*

*Co-corresponding: ybshin@kribb.re.kr
Immunotherapy Research Center

We describe the fabrication of elliptical Au nanodisk arrays as a localized surface plasmon resonance (LSPR) sensing substrate for clinical immunoassay *via* thermal nanoimprint lithography (NIL) and enhancement in the sensitivity of the detection of the prostate-specific antigen (PSA) using the precipitation of 5-bromo-4-chloro-3-indolyl phosphate *p*-toluidine/nitro blue tetrazolium (BCIP/NBT), catalyzed by alkaline phosphatase. Au nanodisks were fabricated on glass through an unconventional tilted evaporation, which could preserve the thickness of imprinted resists and create an undercut beneficial to the subsequent lift-off process without any damage to pattern dimension and the glass while removing the residual polymers. To investigate the optically anisotropic property of the LSPR sensors, a probe light with linear polarization parallel to and perpendicular to the long axis of the elliptical nanodisk array was utilized, and their sensitivity to the bulk refractive index (RI) was measured as 327 and 167 nm/RIU, respectively. To our knowledge, this is the first application of enzyme-substrate reaction to sandwich immunoassay-based LSPR biosensors that previously suffered from a low sensitivity due to the short penetration depth of the plasmon field, especially when large-sized antibodies were used as bioreceptors. As a result, a large change in local refractive index because of the precipitation on the Au nanodisks amplified the wavelength shift of the LSPR peak in the vis-NIR spectrum, resulting in femtomolar detection limits, which was ~10^5-fold lower than the label-free detection without the enzyme precipitation. This method can be extended easily to the other clinical diagnostics with a high sensitivity.

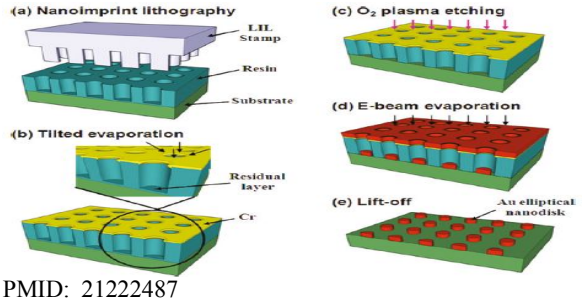

PMID: 21222487

Keywords : Nanodisk Arrays; Nanoimprint Lithography; Localized Surface Plasmon Resonance; LSPR; Prostate-Specific Antigen; Enzymatic Precipitation; Gold; Nanoparticles; Nanosensors

Article 194

Eudesmanolides from *Taraxacum mongolicum* and their inhibitory effects on the production of nitric oxide

Arch Pharm Res. 2011 Jan; 34(1):37-41.

Kim YH, Choo SJ, Ryoo IJ, Ahn JS, Yoo ID*

*Corresponding: idyoo@kribb.re.kr
Chemical Biology Research Center

A new eudesmanolide, 1β,3β-dihydroxy-eudesman-11(13)-en-6α,12-olide (1) was isolated and identified from *Taraxacum mongolicum*, together with two known compounds, 1β,3β-dihydroxyeudesman-6α,12-olide (2) and loliolide (3). The structure of 1 was established by analysis of its physical and spectroscopic data. 1 was found to have an inhibitory activity on nitric oxide production with an IC_{50} of 38.9 μM in activated RAW 264.7 cells.

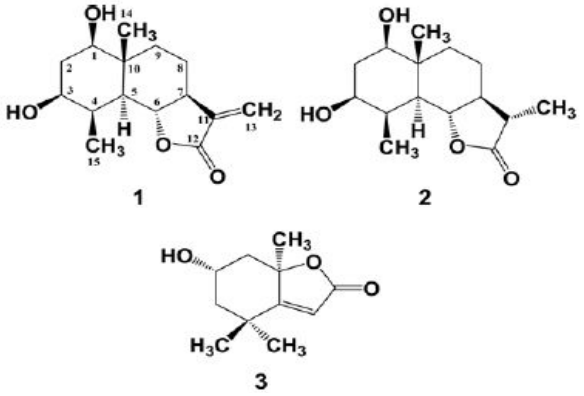

PMID: 21468913

Keywords : *Taraxacum mongolicum*; Eudesmanolide; Nitric Oxide; Macrophage; Synthases; Sesquiterpenoids; Derivatives; Phenolics

Article 195

The conformation and CETP inhibitory activity of [10]-dehydrogingerdione isolated from *Zingiber officinale*

Arch Pharm Res. 2011 May; 34(5):727-31.

Choi SY, Park GS, Lee SY, Kim JY, Kim YK*

*Corresponding: kimyk@kribb.re.kr
Chemical Biology Research Center

In the course of searching for cholesteryl ester transfer protein (CETP) inhibitors from natural sources, a new type of CETP inhibitor, [10]-dehydrogingerdione (1), was isolated from the extract of rhizomes of *Zingiber officinale* Roscoe. By NMR spectroscopic analysis of its (1)HNMR, (13)C-NMR, and (1)H-(1)H COSY, HMBC, HMQC and NOESY, more precise structure, compared with its originally proposed structures, of [10]-dehydrogingerdione has been elucidated. This active compound inhibited human plasma CETP with IC_{50} values of 35 μM.

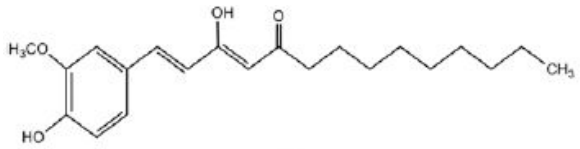

A

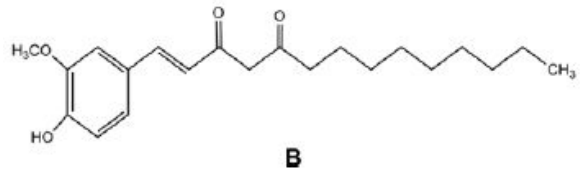

B

PMID: 21656357

Keywords : Cholesteryl Ester Transfer Protein; Gingiber Officinale; Inhibitor; Ginger; Mechanism; Disease

Article 196

Synthesis of grandisol, the sexual attracting insect pheromone

Arch Pharm Res. 2011 Sep; 34(9):1399-402.

Kwak YS*, Jeong BS

*Co-corresponding: yskwak@kribb.re.kr
Chemical Biology Research Center

In this issue, Suh's group reported a new formal total synthesis of (±)-grandisol featuring a palladium-catalyzed 4-exo-trig cyclization. Grandisol's interesting cyclobutane structure has been a popular test model for various cyclization methods over the years. This report summarizes Suh's formal synthesis of grandisol along with a concise review of the four-membered ring cyclization strategies employed in the synthesis of grandisol.

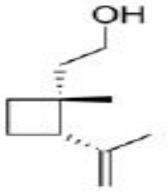

(+)-grandisol (1)

PMID: 21975799

Keywords : Enantioselective Synthesis; (+)- Grandisol; Efficient; Cyclization Method; Insect Pheromone

Article 197

Generation of human induced pluripotent stem cells from osteoarthritis patient-derived synovial cells

Arthritis Rheum. 2011 Oct; 63(10):3010-21.

Kim MJ, Son MJ, Son MY, Seol B, Kim J, Park J, Kim JH, Kim YH, Park SA, Lee CH, Lee KS, Han YM, Chang JS, Cho YS*

*Corresponding: june@kribb.re.kr
Regenerative Medicine Research Center

OBJECTIVE: This study was undertaken to generate and characterize human induced pluripotent stem cells (PSCs) from patients with osteoarthritis (OA) and to examine whether these cells can be developed into disease-relevant cell types for use in disease modeling and drug discovery.
METHODS: Human synovial cells isolated from two 71-year-old women with advanced OA were characterized and reprogrammed into induced PSCs by ectopic expression of 4 transcription factors (Oct-4, SOX2, Klf4, and c-Myc). The pluripotency status of each induced PSC line was validated by comparison with human embryonic stem cells (ESCs).
RESULTS: We found that OA patient-derived human synovial cells had human mesenchymal stem cell (MSC)-like characteristics, as indicated by the expression of specific markers, including CD14-, CD19-, CD34-, CD45-, CD44+, CD51+, CD90+, CD105+, and CD147+. Microarray analysis of human MSCs and human synovial cells further determined their unique and overlapping gene expression patterns. The pluripotency of established human induced PSCs was confirmed by their human ESC-like morphology, expression of pluripotency markers, gene expression profiles, epigenetic status, normal karyotype, and *in vitro* and *in vivo* differentiation potential. The potential of human induced PSCs to differentiate into distinct mesenchymal cell lineages, such as osteoblasts, adipocytes, and chondrocytes, was further confirmed by positive expression of markers for respective cell types and positive staining with alizarin red S (osteoblasts), oil red O (adipocytes), or Alcian blue (chondrocytes). Functional chondrocyte differentiation of induced PSCs in pellet culture and 3-dimensional polycaprolactone scaffold culture was assessed by chondrocyte self-assembly and histology.
CONCLUSION: Our findings indicate that patient-derived synovial cells are an attractive source of MSCs as well as induced PSCs and have the potential to advance cartilage tissue engineering and cell-based models of cartilage defects.
PMID: 21953087

Keywords : Articular-Cartilage; X Collagen; Progenitor Cells; Hypertrophy; Expression; Plasma; Growth; Differentiation; Transplantation; Pluripotent Stem Cell

Article 198

Epigenetic regulation of the transcription factor Foxa2 directs differential elafin expression in melanocytes and melanoma cells

Biochem Biophys Res Commun. 2011 Apr; 408(1):160-6.

Yu KS, Jo JY, Kim SJ, Lee Y, Bae JH, Chung YH, Koh SS*

*Corresponding: sskoh@kribb.re.kr
Immunotherapy Research Center

Elafin, a serine protease inhibitor, induces the intrinsic apoptotic pathway in human melanoma cells, where its expression is transcriptionally silenced. However, it remains unknown how the elafin gene is repressed in melanoma cells. We here demonstrate that elafin expression is modulated *via* epigenetically regulated expression of the transcription factor Foxa2. Treatment of melanoma cells with a DNA methyltransferase inhibitor induced elafin expression, which was specifically responsible for reduced proliferation and increased apoptosis. Suppression of Foxa2 transcription, mediated by DNA hypermethylation in its promoter region, was released in melanoma cells upon treatment with the demethylating agent. Luciferase reporter assays indicated that the Foxa2 binding site in the elafin promoter was critical for the activation of the promoter. Chromatin immunoprecipitation assays further showed that Foxa2 bound to the elafin promoter *in vivo*. Analyses of melanoma cells with varied levels of Foxa2 revealed a correlated expression between Foxa2 and elafin and the ability of Foxa2 to induce apoptosis. Our results collectively suggest that, in melanoma cells, Foxa2 expression is silenced and therefore elafin is maintained unexpressed to facilitate cell proliferation in the disease melanoma.
PMID: 21466784

Keywords : Elafin; Foxa2; Melanoma; Epigenetics; DNA Methylation; Apoptosis; Factor-Kappa-B; Epithelial-Cells; Prostate-Cancer; Carcinoma; Inhibitor

Article 199

Evaluation of immunotoxicity of Shizukaol B isolated from *Chloranthus japonicus*

Biomol Ther. 2011; 19(1):59-64.

Kwon SW, Kim YK*, Kim JY, Ryu HS, Lee HK, Kang JS, Kim HM, Hong JT, Kim Y, Han SB

*Co-first: kimyk@kribb.re.kr
Natural Medicine Research Center

Dimeric sesquiterpenoid shizukaol B (SKB) was isolated from *Chloranthus japonicus* Sieb. Except that SKB inhibited adhesion molecule expression in monocytes and endothelial cells, no more biological and pharmacological activity of SKB had been reported until now. In this study, we examined immunosuppressive activity of SKB. SKB strongly inhibited lipopolysaccharide (LPS)-induced B cell proliferation with IC(50) of 137 ng/ml, but slightly or not concanavalin A-induced T cell proliferation, LPS-induced macrophage NO production, and LPS-induced dendritic cell maturation. As a mechanism, SKB strongly induced apoptotic death of B cells, but not other cell types. These results suggested that SKB induced toxicity-mediated immunosuppression against B cells.

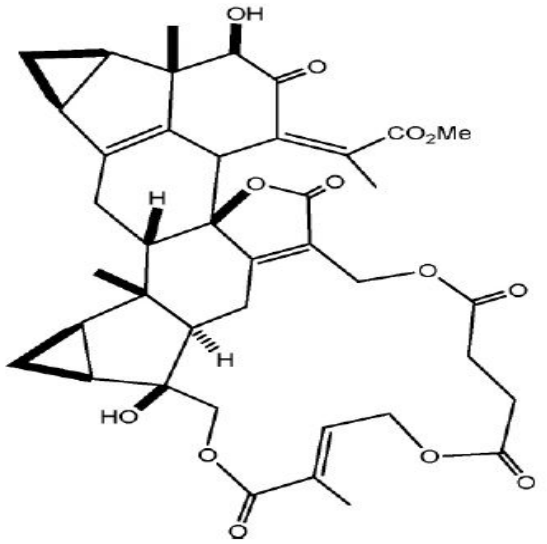

Keywords : Shizukaol B; *Chloranthus japonicus*; Immunosuppression; Cytotoxicity; B cells; Dendritic Cells; Apoptosis; Expression; Maturation; Sieb

Article 200

Protein expression analysis in hematopoietic stem cells during osteopontin-induced differentiation of natural killer cells

Biomol Ther. 2011; 19(2):206-10.

Kim MS, Bae KS, Kim HJ, Yoon SR, Oh DB, Hwang KW, Jun WJ, Shim SI, Kim KD, Jung YW, Park SY, Kwon KS, Choi I*, Chung JW

*Co-corresponding: ipchoi@kribb.re.kr
Immunotherapy Research Center

Natural Killer (NK) cells are the lymphocytes that are derived from hematopoietic stem cells, developed in the bone marrow from hematopoietic stem cells (HSC) by sequential acquisition of functional surface receptors, and express the repertoire of inhibitory and activating receptors. Recently, Osteopontin (OPN) has been identified as a critical factor for differentiation of natural killer cells. However, the detailed mechanism of OPN-induced NK differentiation has been still to be elucidated. Here, we determined the signaling pathway and possible receptor for OPN in NK differentiation. OPN induced expression of Bcl-2 and activation of Erk kinase. Inhibition of Erk pathway decreased the effect of OPN on NK differentiation. In addition, the expression of integrin alpha 9 was significantly increased by OPN during NK differentiation, suggesting the possible role of a major signaling molecule for OPN- induced NK differentiation.

Keywords : Osteopontin; Natural Killer Cells; Hematopoietic Stem Cells; ERK; Bcl-2; Activation; Apoptosis; Component; Promotes; Niche

Article 201

Electrical immunosensor based on a submicron-gap interdigitated electrode and gold enhancement

Biosens Bioelectron. 2011 Aug; 26(12):4690-6.

Ahn J, Lee TH, Li T, Heo K, Hong S, Ko J, Kim Y, Shin YB*, Kim MG

*Co-corresponding: ybshin@kribb.re.kr
Immunotherapy Research Center

We demonstrated that the detection of human interleukin 5 (IL5) with a higher sensitivity than the enzyme-linked immunosorbent assay (ELISA) was possible using mass-producible submicron-gap interdigitated electrodes (IDEs) combined with signal amplification by a gold nanoparticle (AuNP) and gold enhancement. IDEs, facing comb-shape electrodes, can act as simple and miniaturized devices for immunoassay. An IDE with a gap size of 400nm was fabricated by a stepper photolithography process and was applied for the immunoassay of human IL5. A biotinylated anti-human IL5 was immobilized on the streptavidin-modified IDE, and biotin-bovine serum albumin (BSA) and BSA were added sequentially to reduce non-specific binding between the streptavidin-immobilized IDE surface and other proteins. The immunoassay procedure included three main steps: the reaction of human IL5 to form antigen-antibody complexes, the binding of AuNP conjugation with an antibody against human IL5 for the sandwich immunoassay, and gold enhancement for electrical signal amplification. The measurement of electrical current at each step showed that the gold enhancement step was very critical in detection of the concentration of human IL5. Analysis by scanning electron microscope (SEM) showed that close to 1μm particles were formed from 10nm AuNP by the gold enhancement reaction using gold ions and hydroxylamine. Under optimized conditions, human IL5 could be analyzed at 1pgmL^{-1} with a wide dynamic range (from 10^{-3} to 100ngmL^{-1} concentrations).

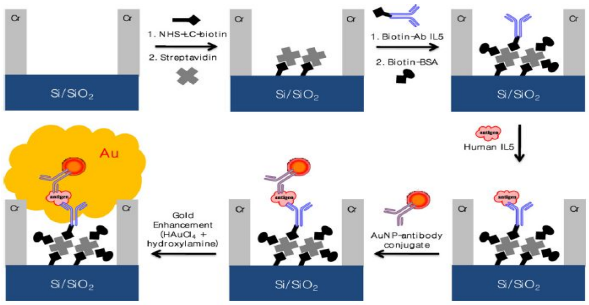

PMID: 21684145

Keywords : Immunosensor; Lnterdigitated Electrode; Gold Nanoparticle; Interleukin 5; Nanogap Electrodes; Surfaces; Immunoassay; Fabrication; Biosensor

Article 202

Human microRNA-27a* targets Prf1 and GzmB expression to regulate NK-cell cytotoxicity

Blood. 2011 Nov; 118(20):5476-86.

Kim TD, Lee SU, Yun S, Sun HN, Lee SH, Kim JW, Kim HM, Park SK, Lee CW, Yoon SR, Greenberg PD, Choi I*

*Corresponding: ipchoi@kribb.re.kr
Immunotherapy Research Center

Perforin (Prf1) and granzyme B (GzmB) are essential effector molecules for natural killer (NK)-cell cytotoxicity, but how Prf1 and GzmB expression is regulated during arming of NK cells is poorly defined. We show that human microRNA (miR)-27a* is a negative regulator of NK-cell cytotoxicity by silencing Prf1 and GzmB expression. Human miR-27a* specifically bound to the 3' untranslated regions of Prf1 and GzmB, down-regulating expression in both resting and activated NK cells, and it functioned as a fine-tuner for homeostasis of the net amount of the effector proteins. Consistent with miR-27a* having an inhibitory role, knockdown of miR-27a* in NK cells dramatically increased cytotoxicity *in vitro* and decreased tumor growth in a human tumor xenograft model. Thus, NK-cell cytotoxicity is regulated, in part, by microRNA, and modulating endogenous miR-27a* levels in NK cells represents a potential immunotherapeutic strategy.

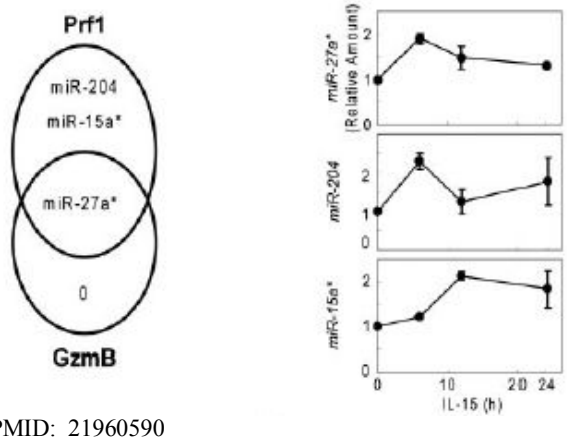

PMID: 21960590

Keywords : Natural-Killer-Cells; Granzyme-B; Immune-System; T-Cells; Differential Expression; microRNA Pathway; Dicer; Interleukin-15; Immunotherapy

Article 203

Facile synthesis of *trans*-S-1-propenyl-L-cysteine sulfoxide (isoalliin) in onions (*Allium cepa*)

Bull Korean Chem Soc. 2011; 32(1):319-320.

Lee S*, Kim JN, Choung DH, Lee HK*

*Co-corresponding: sangku@kribb.re.kr hykylee@kribb.re.kr
Natural Medicine Research Center

Trans-S-1-propenyl-L-cystein sulfoxide (isoalliin) has been shown to be the precursor of the lachrymatory properties of *Allium cepa*. The unusual amino acid *trans*-S-1-propenyl-L-cystein sulfoxide is in demand in the field of *Allium* chemistry including metabolism and biological studies, and serves as a standard for determination of S-alk(en)yl-Lcystein sulfoxides.

A natural amino acid, *trans*-S-1-propenyl-Lcystein sulfoxide was synthesized from (*E*)-1-bromo-1-propene in a concise way, via the sequential (i) the formation of vinylsulfide from lithiated propene and disulfide, (ii) reductive cleavage/alkylation of vinylsulfide, (iii) sulfide oxidation to sulfoxide. This compound is widely used as a reference for studies on *Allium* chemistry including biosynthesis of S-alkenyl-L-cystein sulfoxides, metabolism studies and biological investigations.

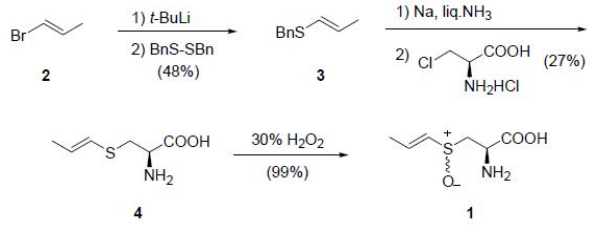

Keywords : Natural Product; Amino Acid; Isoalliin; Sulfoxide; Onion; *Allium cepa*; Antioxidant Activity; Garlic Extract

Article 204

Sequential conjugation of 6-aminohexanoic acids and L-arginines to poly(amidoamine) dendrimer to modify hydrophobicity and flexibility of the polymeric gene carrier

Bull Korean Chem Soc. 2011; 32(2):651-5.

Yu GS, Yu HN, Choe YH, Son SJ, Ha TH*, Choi JS

*Co-corresponding: taihwan@kribb.re.kr
Immunotherapy Research Center

We synthesized a novel cationic dendrimer consisting of a poly(amidoamine) dendrimer (PAMAM, generation 4) backbone with both L-arginine (Arg) at the termini and 6-aminohexanoic acid (Ahx) between the original core polymer and the peripheral Arg units. The sequential chemical modification of PAMAM G4 with Ahx and Arg resulted in higher transfection efficiency with much less cytotoxicity. PAMAM G4-Ahx-Arg formed stable polyplexes at weight ratios of 8:1 or higher (polymer: plasmid DNA), and the mean polyplex diameter was 180 ± 20 nm. PAMAM G4-Ahx-Arg showed much higher transfection ability than PAMAM G4 or PAMAM G4-Ahx. Furthermore, PAMAM G4-Ahx-Arg was much less cytotoxic than PEI25KD and PAMAM G4-Arg. In addition to Arg grafting of the PAMAM dendrimer, which endows a higher transfection capability, the addition of Ahx spacer increased dendrimer hydrophobicity, introduced flexibility into the conjugated amino acids, and reduced cytotoxicity. Overall, it appears that the concomitant modification of PAMAM with Ahx and Arg could lead to new PAMAM conjugates with better performances.

Keywords : Pamam Dendrimer; Gene Delivery; Polyplex; Transfection Efficiency; Gene Carrier; Biological Applications; Lipids

Article 205

Isolation of protein tyrosine phosphatase 1B inhibitory constituents from the sclerotia of *Polyporus umbellatus* Fries

Bull Korean Chem Soc. 2011; 32(2):697-700.

Lee HS, Hwang IH, Kim JA, Choi JY, Jang TS, Osada H, Ahn JS*, Na M, Lee SH

*Co-corresponding: jsahn@kribb.re.kr
Chemical Biology Research Center

Using *in vitro* PTP1B enzyme assay, a MeOH extract of the sclerotia of *Polyporus umbellatus* Fries (Polyporaceae) showed PTP1B inhibitory activity at a level of 30 μg/mL. The sclerotia of *P. umbellatus* is a saprophytic mushroom that grows on the roots of *Alnus* sp., *Quercus* sp., and *Betula* sp. We found out that some steroids and a new ceramide isolated from the sclerotia of *P. umbellatus* had the PTP1B

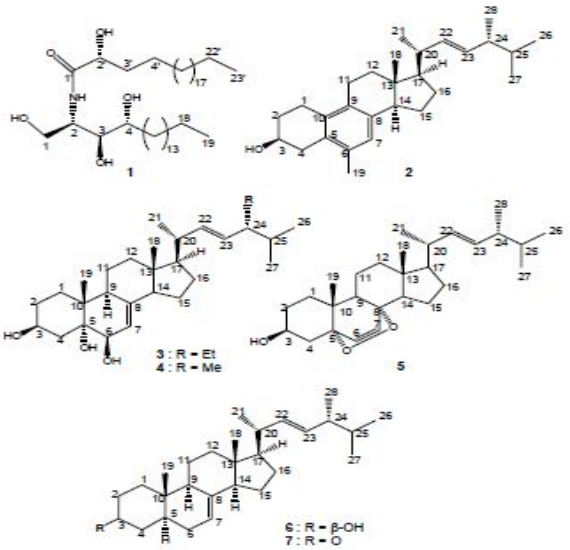

inhibitory activity. The results indicate that active steroidal compounds from the sclerotia of *P. umbellatus* can be regarded as sources for the PTP1B inhibitors, which are prompted by previous reports on steroids of their pharmacological actions. This study suggests that the components from the sclerotia of *P. umbellatus* may be considerable for development as PTP1B inhibiting agents.

Keywords : Protein Tyrosine Phosphatase 1B; *Polyporus umbellatus*; Ceramide; Steroid; Insulin-Resistance; Fruiting Bodies; Cell-Line; Sterols; Obesity; Plant

Article 206

Synthesis of 2,4,6-tripyridyl pyridines, and evaluation of their antitumor cytotoxicity, topoisomerase I and II inhibitory activity, and structure-activity relationship

Bull Korean Chem Soc. 2011; 32(10):3566-70.

Jeong BS, Choi H, Kwak YS*, Lee ES

*Co-corresponding: yskwak@kribb.re.kr
Chemical Biology Research Center

A series of 2,4,6-tripyridyl pyridines were synthesized, and evaluated for their antitumor cytotoxicity, topoisomerase I and II inhibitory activity. From the eighteen prepared compounds, compounds 10-12 have shown better or similar cytotoxicity against several human cancer cell lines as compared to 2,2:6,2"-terpyridine and doxorubicin. Especially, compound 10 exhibited the most potent cytotoxicity better than positive controls. Structure-activity relationship study indicated that 2,2':6',2"-terpyridine skeleton has an important role in displaying significant cytotoxicity against several human cancer cell lines.

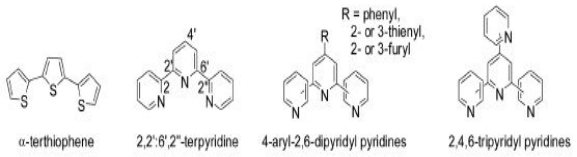

Keywords : Terpyridine; 2,4,6-Tripyridyl Pyridine; Topoisomerase Inhibition; Cytotoxicity; SAR Study; Kinase C Inhibitors; DNA Topoisomerases; Derivatives; Intercalation; Moiety

Article 207

Anti-inflammatory diterpene from *Thyrsanthera suborbicularis*

Chem Pharm Bull. 2011; 59(3):382-4.

Khiev P, Oh SR, Chae HS, Kwon OK, Ahn KS, Chin YW, Lee HK*

*Corresponding: hykylee@kribb.re.kr
Natural Medicine Research Center

Bioactivity-guided isolation on a *n*-hexane-soluble fraction of *Thyrsanthera suborbicularis* led to the isolation of a new rosane-type diterpene, 19-hydroxy-1(10), 15-rosadiene (1), along with three known compounds, taraxerol, acetyl aleuritolic acid, and spathulenol. The structures of isolated compounds were determined by interpretation of NMR spectroscopic data and mass spectrometry. Compound 1 demonstrated significantly inhibitory activity on nitric oxide production in RAW264.7 lipopolysaccharide (LPS)-activated mouse macrophages with an IC_{50} value of 2.91 μg/ml via the suppression of inducible nitric oxide synthase (iNOS) mRNA expression.

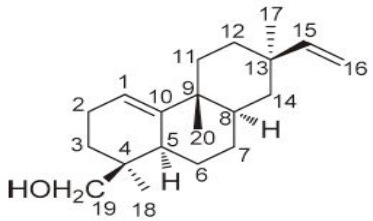

PMID: 21372422

Keywords : *Thyrsanthera suborbicularis*; Euphorbiaceae; Rosane Diterpenoid; Inducible Nitric Oxide Synthase; Constituents; Terpenoids

Article 208

Coordination power adjustment of surface-regulating polymers for shaping gold polyhedral nanocrystals

Chemistry. 2011 Jul; 17(30):8466-71.

Lee SJ, Park G, Seo D, Ka D, Kim SY, Chung IS*, Song H

*Co-corresponding: cis123@kribb.re.kr
Immunotherapy Research Center

PVP (poly(vinyl pyrrolidone)) is a common polymer that behaves as a surface-regulating agent that shapes metal nanocrystals in the polyol process. We have used different polymers containing tertiary amide groups, namely PVCL (poly(vinyl caprolactam)) and PDMAm (poly(*N,N*-dimethyl acrylamide)), for the synthesis of gold polyhedrons, including octahedrons, cuboctahedrons, cubes, and higher polygons, under the present polyol reaction conditions. The basicity and surface coordination power of the polymers are in the order of PVCL, PVP, and PDMAm. A correlation is observed between the coordination power of the polymers and the resulting gold nanocrystal size. Strong coordination and electron donation from the polymer functional groups to the gold surface restrict particle growth rates, which leads to small nanocrystals. The use of PVCL can yield gold polyhedral structures with small sizes, which cannot be achieved in the reactions with PVP. Simultaneous hydrolysis of the amide group in PDMAm leads to carboxylate functionality, which is very useful for generating chemical and bioconjugates through the formation of ester and amide bonds.

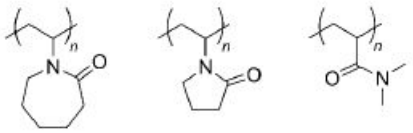

PMID: 21656861

Keywords : Coordination; Gold; Morphology; Polymers; Platinum Nanoparticles; Metal Nanoparticles; Silver Nanoparticles; Nanostructures; Nanorods; Stability

Article 209

Inhibition of ganglioside GD1a synthesis suppresses the differentiation of human mesenchymal stem cells into osteoblasts

Dev Growth Differ. 2011 Apr; 53(3):323-32.

Yang HJ, Jung KY, Kwak DH, Lee SH, Ryu JS, Kim JS, Chang KT, Lee JW*, Choo YK

*Co-corresponding: jwlee@kribb.re.kr
Regenerative Medicine Research Center

In this study, we investigated the regulatory role of ganglioside GD1a in the differentiation of osteoblasts from human mesenchymal stem cells (hMSCs) by using lentivirus-containing short hairpin (sh)RNA to knockdown ST3 β-galactoside α-2, 3-sialyltransferase 2 (ST3Gal II) mRNA expression. After hMSCs were infected for 72 h with the lentivirus constructed with ST3Gal II shRNAs, the puromycin-resistant cells were selected and subcultured to produce hMSCs with ST3Gal II mRNA knockdown. The hMSCs established from human dental papilla abundantly expressed CD44 and CD105, but not CD45 and CD117. Osteoblasts that differentiated from normal hMSCs showed a significant increase in alkaline phosphatase (ALP) activity and ganglioside GD1a expression level compared with those in hMSCs. Lentiviral infection of hMSCs successfully induced a marked inhibition of ST3Gal II mRNA expression and caused a significant decrease in ALP activity and ganglioside GD1a expression. During osteoblastic differentiation, the increased ALP activity remarkably reduced by suppression of ganglioside GD1a expression by ST3Gal II shRNA. Ganglioside GD1a and ALP were mainly expressed in the cell body of hMSCs and osteoblasts with colocalization. The phosphorylation of extracellular signal-regulated kinases (ERK) 1/2 mitogen-activated protein (MAP) kinase and epidermal growth factor receptor (EGFR) was significantly reduced in the osteoblasts that had differentiated from the hMSCs with ST3Gal II mRNA knockdown. These results suggest that ganglioside GD1a plays an important role in the regulation of osteoblastic differentiation of hMSCs through the activation of ERK 1/2 MAP kinase and EGFR.
PMID: 21492147

Keywords : Epidermal Growth Factor Receptor; Mesenchymal Stem Cells; Osteogenesis; ST3Gal II; Signaling Pathway; Osteogenic Differentiation; Progenitor Cells; EGF Receptor; Phosphorylation; Chondrogenesis

Article 210

Pancreatic adenocarcinoma up-regulated factor (PAUF) enhances the expression of β-catenin, leading to a rapid proliferation of pancreatic cells

Exp Mol Med. 2011 Feb; 43(2):82-90.

Cho IR, Koh SS*, Min HJ, Kim SJ, Lee Y, Park EH, Ratakorn S, Jhun BH, Oh S, Johnston RN, Chung YH

*Co-first: sskoh@kribb.re.kr
Immunotherapy Research Center

It is not yet understood how the enhanced expression of pancreatic adenocarcinoma up-regulated factor (PAUF; a novel oncogene identified in our recent studies), contributes to the oncogenesis of pancreatic cells. We herein report that PAUF up-regulates the expression and transcriptional activity of β-catenin while the suppression of PAUF by shRNA down-regulates β-catenin. The induction of b-catenin by PAUF is mediated by the activities of Akt and GSK-3β, but inhibition of downstream ERK does not reduce β-catenin expression. To test whether PAUF emulates either the Wnt3a-mediated or the protein kinase A-mediated signaling pathway for the stabilization of β-catenin, we examined the phosphorylation status of β-catenin in the presence of PAUF compared with that of β-catenin during treatment with Wnt3a or dibutyryl cAMP, a cell permeable cyclic AMP analogue. PAUF expression induces phosphorylation at Ser-33/37/Thr-41 and Ser-675 of β-catenin but no phosphorylation at Ser-45, indicating that a unique phosphorylation pattern of b-catenin is caused by PAUF. Finally, the expression of PAUF up-regulates both *cyclin-D1* and *c-Jun*, target genes of β-catenin, leading to a rapid proliferation of pancreatic cells; conversely decreased PAUF expression (by shRNA) results in the reduced proliferation of pancreatic cells. Treatment with hexachlorophene (an inhibitor of β-catenin) reduces the proliferation of pancreatic cells despite the presence of PAUF. Taken together, we propose that PAUF can up-regulate and stabilize β-catenin *via* a novel pattern of phosphorylation, thereby contributing to the rapid proliferation of pancreatic cancer cells.
PMID: 21196815

Keywords : Beta Catenin; Carcinoma, Pancreatic Ductal; Cyclic AMP-Dependent Protein Kinases; PAUF Protein, Human; Wnt Proteins; Phosphorylation; Transcription

Article 211

PAUF promotes adhesiveness of pancreatic cancer cells by modulating focal adhesion kinase

Exp Mol Med. 2011 May; 43(5):291-7.

Lee YS, Kim SJ, Min HJ, Jo JY, Park EH, Koh SS*

*Corresponding: sskoh@kribb.re.kr
Immunotherapy Research Center

Pancreatic cancer is a notorious disease with a poor prognosis and low survival rates, which is due to limited advances in understanding of the molecular mechanism and inadequate development of effective treatment options over the decades. In previous studies, we demonstrated that a novel soluble protein named pancreatic adenocarcinoma up-regulated factor (PAUF) acts on tumor and immune cells and plays an important role in metastasis and progression of pancreatic cancer. Here we show that PAUF promotes adhesiveness of pancreatic cancer cells to various extracellular matrix (ECM). Our results further support a positive correlation of activation and expression of focal adhesion kinase (FAK), a key player in tumor cell metastasis and survival, with PAUF expression. PAUF-mediated adhesiveness was significantly attenuated upon blockade of the FAK pathway. Moreover, PAUF appeared to enhance resistance of pancreatic cancer cells to anoikis via modulation of FAK. Our results suggest that PAUF-mediated FAK activation plays an important role in pancreatic cancer progression.
PMID: 21464589

Keywords : Adhesion; Anoikis; FAK; PAUF; Pancreatic Cancer; Signaling

Article 212

Modulation of exosome-mediated mRNA turnover by interaction of GTP-binding protein 1 (GTPBP1) with its target mRNAs

FASEB J. 2011 Aug; 25(8):2757-69.

Woo KC, Kim TD*, Lee KH, Kim DY, Kim S, Lee HR, Kang HJ, Chung SJ, Senju S, Nishimura Y, Kim KT

*Co-first: tdkim@kribb.re.kr
Immunotherapy Research Center

Eukaryotic mRNA turnover is among most critical mechanisms that affect mRNA abundance and are regulated by mRNA-binding proteins and the cytoplasmic exosome. A functional protein, guanosine-triphosphate-binding protein 1 (GTPBP1), which associates with both the exosome and target mRNAs, was identified. The overexpression of GTPBP1 accelerated the target mRNA decay, whereas the reduction of the GTPBP1 expression with RNA interference stabilized the target mRNA. GTPBP1 has a putative guanosine-triphosphate (GTP)-binding domain, which is found in members of the G-protein family and Ski7p, a well-known core factor of the exosome-mediated mRNA turnover pathway in yeast. Analyses of protein interactions and mRNA decay demonstrated that GTPBP1 modulates mRNA degradation *via* GTP-binding-dependent target loading. Moreover, GTPBP1-knockout models displayed multiple mRNA decay defects, including elevated nocturnal levels of Aanat mRNA in pineal glands, and retarded degradation of TNF-α mRNA in lipopolysaccharide-treated splenocytes. The results of this study suggest that GTPBP1 is a regulator and adaptor of the exosome-mediated mRNA turnover pathway.

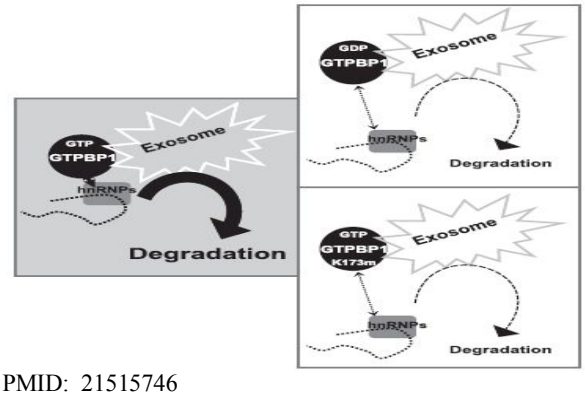

PMID: 21515746

Keywords : Circadian Rhythm; Untranslated Region; Serotonin N-Acetyltransferase; *Saccharomyces cerevisiae*; Rich Elements; Ski Complex; Mouse; Decay; GTPBP1

Article 213

TOX regulates the differentiation of human natural killer cells from hematopoietic stem cells *in vitro*

Immunol Lett. 2011 Apr; 136(1):29-36.

Yun S, Lee SH, Yoon SR, Kim MS, Piao ZH, Myung PK, Kim TD, Jung H, Choi I*

*Corresponding: ipchoi@kribb.re.kr
Immunotherapy Research Center

Natural killer (NK) cells act important roles in innate immunity and adaptive immunity. However, the mechanisms governing NK cell development have not been clearly elucidated. Previous studies have shown that an HMG (high-mobility group) protein, TOX, is important for regulating the differentiation program of developing T cells in mice. In this study, we examined the role of TOX in differentiation of human NK cells. Knockdown of TOX in differentiating cells decreased the NK cell population identified by expression of NK surface markers and receptors. In addition, over-expression of TOX enhanced the differentiation of NK cells which give rise to a population showing effector functions of mature NK cells. Moreover, TOX influenced expression of T-bet (T-box expressed in T cells, also as known as Tbx21) during NK cell development. Overall, these results suggest that TOX is required for IL-15-mediated NK cell differentiation and affected expression of T-bet that plays critical roles in NK differentiation and maturation.
PMID: 21126536

Keywords : High-Mobility Group Protein Tox; Natural Killer Cell; Differentiation; T-Bet; Developmental Pathways; NK Cells; Maturation; Transcription; Commitment; Lineages

Article 214

Oxygen tension regulates NK cells differentiation from hematopoietic stem cells *in vitro*

Immunol Lett. 2011 Jun; 137(1-2):70-7.

Yun S, Lee SH, Yoon SR, Myung PK, Choi I*

*Corresponding: ipchoi@kribb.re.kr
Immunotherapy Research Center

Natural killer (NK) cells are differentiated from hematopoietic stem cells (HSCs) which are located at the lowest end of an oxygen gradient within the bone marrow (BM). In this report, we investigated whether oxygen tension could affect NK cell differentiation from hematopoietic cells *in vitro*. We found that hypoxia led to an inhibition of differentiation in NK cells, and increased oxygen supply alleviated this inhibition and restored NK cell differentiation under hypoxic condition. Hypoxia-treated cells demonstrated reduced mRNA expression of transcription factors (TFs) that have important roles in NK cell differentiation, such as EOMES, T-bet, GATA-3 and ETS-1. Moreover, hypoxia-pretreated cells recovered mRNA expression of TFs when the oxygen tension was changed to normoxia. Our findings suggest that oxygen tension modulates *in vitro* differentiation of NK cells through the regulation of TF expression.
PMID: 21354208

Keywords : Hypoxia; NK Cells; Differentiation; Transcription Factor; Hematopoietic Stem Cells; Natural-Killer-Cell; Leukemic-Cells; Developmental Pathways; Cytotoxicity Receptors

Article 215

IL-22 producing NKp46+ innate lymphoid cells can differentiate from hematopoietic precursor cells

Immunol Lett. 2011 Dec; 141(1):61-7.

Kim MS, Kim WS, Piao ZH, Yun S, Lee SH, Lee S, Jeong M, Sun HN, Park YJ, Jung H, Yoon SR, Choi I*

*Corresponding: ipchoi@kribb.re.kr
Immunotherapy Research Center

The IL-22 NKp46$^+$ innate lymphoid cells, NCR22 cells, are very important for the early host defense against microbial pathogens. We show here that NCR22 cells were differentiated from Lin(-)CD127$^+$CD117$^+$ cells that were derived from hematopoietic precursor cells (HPCs) of mouse bone marrow cells. The combination CD127$^+$CD117$^+$ cells. NCR22 cells expressed a large amount of IL-22 and RORγt, and they had poor cytolytic activity and produced little IFN-γ. Lin(-)CD127$^+$CD117$^+$ cells were very similar to intestinal lamina propria LTi-like cells; both cells dominantly expressed RORγt and IL-22. Meanwhile, Lin(-)CD127(-)CD117$^+$ cells that were also derived from HPCs did not express RORγt and IL-22, and they developed into conventional NK cells, not into NCR22 cells. These findings revealed that NCR22 cells can be differentiated from Lin(-)CD127$^+$CD117$^+$ cells which are derived from HPCs.

PMID: 21835206

Keywords : NCR22; IL-22; ROR gamma t; NK cells; Differentiation; Natural-Killer-Cells; Distinct; Defense; IL-17

Article 216

Effects of astilbic acid on airway hyperresponsiveness and inflammation in a mouse model of allergic asthma

Int Immunopharmacol. 2011 Feb; 11(2):266-73.

Yuk JE, Lee MY, Kwon OK, Cai XF, Jang HY, Oh SR, Lee HK, Ahn KS*

*Corresponding: ksahn@kribb.re.kr
Natural Medicine Research Center

Bronchial asthma is characterized by chronic lung inflammation, airway hyperresponsiveness (AHR), and airway remodeling. Astilbic acid, extracted from the medicinal herb *Astilbe chinensis*, is used as a headache remedy in traditional medicine and has anti-pyretic and analgesic effects. However, the effect of astilbic acid on asthma remains to be established. In the present study, we therefore examined the effect of astilbic acid in a mouse model in which asthma was established by sensitization and challenge with ovalbumin (OVA). Astilbic acid inhibited OVA-induced AHR to inhaled methacholine and significantly suppressed the levels of T-helper 2-type cytokines (including IL [interleukin]-4, IL-5, and IL-13) and inflammatory cells (including eosinophils) in bronchoalveolar lavage (BAL) fluid. Histochemical analysis revealed reduced goblet cell hyperplasia and mucus production, as well as attenuated eosinophil-rich leukocyte infiltration, in the astilbic acid-treated group, compared with OVA-challenged mice. Moreover, the compound significantly inhibited synthesis of IL-4-, IL-5-, IL-13-, IL-17-, and eotaxin-encoding mRNA following asthma induction in lung tissue, in addition to suppressing the immunoglobulin E (IgE) response to asthma in both BAL fluid and serum. Our results indicate that astilbic acid has great potential as a therapeutic candidate for the treatment of asthma.

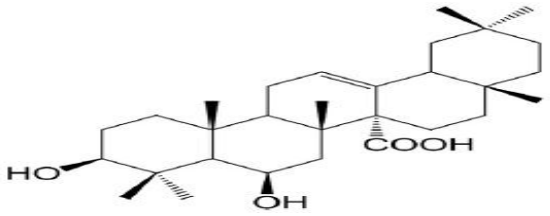

PMID: 21168540

Keywords : Astilbic Acid; Asthma; Cytokine; Factor-Kappa-B; Deficient Mice; T-Cells; Interleukin-17; Pathogenesis; Fibroblasts; Receptors

Article 217

Fusarisetin A, an acinar morphogenesis inhibitor from a soil fungus, *Fusarium* sp. FN080326

J Am Chem Soc. 2011 May; 133(18):6865-7.

Jang JH, Asami Y, Jang JP, Kim SO, Moon DO, Shin KS, Hashizume D, Muroi M, Saito T, Oh H, Kim BY, Osada H, Ahn JS*

*Co-corresponding: jsahn@kribb.re.kr
Chemical Biology Research Center

An acinar morphogenesis inhibitor named fusarisetin A (1) that possesses both an unprecedented carbon skeleton and a new pentacyclic ring system has been identified from an in-house fractionated fungal library using a three-dimensional matrigel-induced acinar morphogenesis assay system. The structure of 1 was determined in detail by NMR and circular dichroism spectroscopy, X-ray analysis, and chemical reaction experiments.

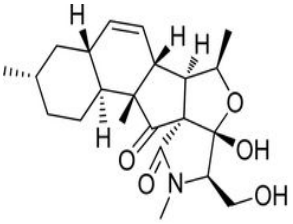

Fusarisetin A

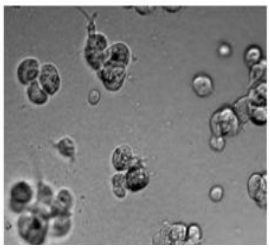

PMID: 21500849

Keywords : Basement-Membrane Cultures; Drug Discovery; Epithelial Acini; Natural Product; Cancer-Cells; Proliferation; Libraries; *Fusarium*

Article 218

New non-quinone geldanamycin analogs from genetically engineered *Streptomyces hygroscopicus*

J Antibiot. 2011 Jun; 64(6):461-3.

Wu CZ, Moon AN, Jang JH, Lee D, Kang SY, Park JT, Ahn JS, Hwang BY, Kim YH, Lee HS, Hong YS*

*Corresponding: hongsoo@kribb.re.kr
Chemical Biology Research Center

We reported the development of non-quinone 1 analogs by a mutasynthetic approach and directed biosynthetic method. Of these non-quinone 1 analogs, DHQ3 (3), a 15-hydroxyl-17-demethoxy non-quinone analog, was found to inhibit Hsp90 ATPase activity more than 1. Moreover, during these studies, novel tricyclic 1 analogs were prepared from a genetically engineered strain (AC15) of *Streptomyces hygroscopicus*. We describe the fermentation of mutant AC15, and the isolation, structural determination and bioactivity of new non-quinone 1 analogs produced by the mutant: DHQ7 (4) and DHQ8 (5). All isolated compounds (3, 4 and 5) were tested for the ability to inhibit yeast Hsp90 activity using a malachite green ATPase assay. Compounds 4 and 5 showed potent activity of ATPase inhibition with IC_{50} values of 1.75 and 5.87 μM, respectively. But, the 3 showed stronger ATPase inhibition activity (0.68 μM) compared with the original Hsp90 inhibitor 1 (3.19 μM). The non-quinone 1 analogs interact with the nucleotide-binding site of Hsp90. The analogs were evaluated for their anti-proliferation activity using tumor cell growth inhibition assays in human ovarian A2780 and breast SK-Br3 and BT474 cancer cell lines. These non-quinone 1 derivatives showed favorable potency in the ATPase assay.

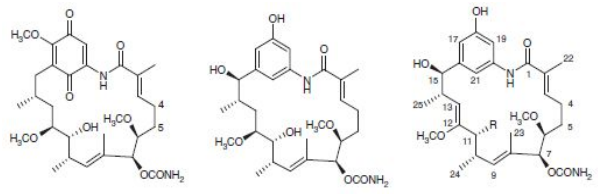

PMID: 21448187

Keywords : Biosynthetic Engineering; Geldanamycin; Hsp90 Inhibitor; Non-Quinone Geldanamycin; Cancer; Derivatives; Disruption; Ansamycins; Affinity

Article 219

Pleurone, a novel human neutrophil elastase inhibitor from the fruiting bodies of the mushroom *Pleurotus eryngii* var. *ferulae*

J Antibiot. 2011 Aug; 64(8):587-9.

Lee IS, Ryoo IJ, Kwon KY, Ahn JS, Yoo ID*

*Corresponding: idyoo@kribb.re.kr
Chemical Biology Research Center

The genus *Pleurotus* (Jacq.: Fr.) Kumm. (Pleurotaceae, higher Basidiomycetes) comprises a diverse group of cultivated mushroom species with high nutritional value and significant pharmacological properties. We found that the EtOAc-soluble fraction of a methanol (MeOH) extract of *P. eryngii* var. *ferulae* sporocarps has considerable HNE-inhibitory activity (IC_{50}, 62.9 μg ml^{-1}). Further investigation of this fraction resulted in the isolation of one new compound (1), together with three known compounds (2–4). Compound 1, designated 'pleurone,' was obtained as an amorphous white powder and established as 4H-1,3-dioxine-2,4-dione (1). The inhibitory mechanism of pleurone on HNE is a mixed-type, a combination of noncompetitive and uncompetitive inhibition against HNE. Our findings suggest that *P. eryngii* var. *ferulae* and its components might be beneficial for the prevention or treatment of skin aging.

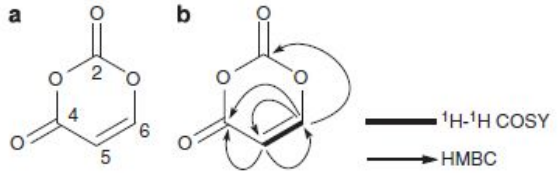

PMID: 21673713

Keywords : Human Neutrophil Elastase, Kinetics; Pleurotaceae; *Pleurotus eryngii* Var. *Ferulae*; Ostreatus; Polysaccharides; Cancer; Glucan

Article 220

JHDM3A module as an effector molecule in guide-directed modification of target chromatin

J Biol Chem. 2011 Feb; 286(6):4461-70.

Jeong YS, Park JS, Ko Y, Kang YK*

*Corresponding: ykkang@kribb.re.kr
Regenerative Medicine Research Center

With the objective of returning cells to their undifferentiated state through alteration of epigenetic states, small molecules have been used that specifically inhibit proteins involved in sustaining the epigenetic system. However, this chemical-based approach can cause chaotic epigenomic states due to random actions of the inhibitors. We investigated whether JHDM3A/JMJD2A, a trimethylated histone H3-lysine 9 (H3K9me3)-specific demethylase, could function as an effector molecule to selectively demethylate target chromatin, with the aid of a guide protein to serve as a delivery vehicle. JHDM3A, which normally locates in euchromatin, spread out to heterochromatin when it was fused to heterochromatin protein-1α (HP1α) or HP1β; in these cells, demethylation efficiency was also markedly increased. Two truncated modules, JHDM3A(GFP)(406) and JHDM3A(GFP)(701), had contrasting modes and efficiencies of H3K9me3 demethylation; JHDM3A(GFP)(406) showed a very uniform rate (~80%) of demethylation, whereas JHDM3A(GFP)(701) had a broad methylation range of 4-80%. The methylation values were highly dependent on the presence of the guide proteins OCT4, CTCF, and HP1. Chromatin immunoprecipitation detected reduced H3K9me3 levels at OCT4 regulatory loci in the cells expressing OCT4-tagged JHDM3A(GFP)(701). Derepression of the *Sox2* gene was observed in JHDM3A(GFP)(701)OCT4-expressing cells, but not in cells that expressed the JHDM3A(GFP)(701) module alone. JHDM3A(GFP)(701)-assisted OCT4 more efficiently turned on stem cell-related microRNAs than GFP-OCT4 itself. These results suggest that JHDM3A(GFP)(701) is a suitable catalytic module that can be targeted, under the control of a guide protein, to specific loci where the chromatin H3K9me3 status and the milieu of gene expression are to be modified.

PMID: 21148561

Keywords : Pluripotent Stem-Cells; Histone H3 Lysine-9; Silenced Genes; JMJD2 Family; Genome; Methylation; Demethylation; Cancer; 5-Aza-2'-Deoxycytidine; Trichostatin

Article 221

Dual functions of histone-lysine N-methyltransferase Setdb1 protein at promyelocytic leukemia-nuclear body (PML-NB): maintaining PML-NB structure and regulating the expression of its associated genes

J Biol Chem. 2011 Nov; 286(47):41115-24.

Cho S, Park JS, Kang YK*

*Corresponding: ykkang@kribb.re.kr
Regenerative Medicine Research Center

Setdb1/Eset is a histone H3 lysine 9 (H3K9)-specific methyltransferase that associates with various transcription factors to regulate gene expression via chromatin remodeling. Here, we report that Setdb1 associates with promyelocytic leukemia (Pml) protein from the early stage of mouse development and is a constitutive member of promyelocytic leukemia (PML)-nuclear bodies (PML-NBs) that have been linked to many cellular processes such as apoptosis, DNA damage responses, and transcriptional regulation. Arsenic treatment, which induces Pml degradation, caused Setdb1 signals to disappear. Setdb1 knockdown resulted in dismantlement of PML-NBs. Immunoprecipitation results demonstrated physical interactions between Setdb1 and Pml. Chromatin immunoprecipitation revealed that, within the frame of PML-NBs, Setdb1 binds the promoter of *Id2* and suppresses its expression through installing H3K9 methylation. Our findings suggest that Setdb1 performs dual, but inseparable, functions at PML-NBs to maintain the structural integrity of PML-NBs and to control PML-NB-associated genes transcriptionally.

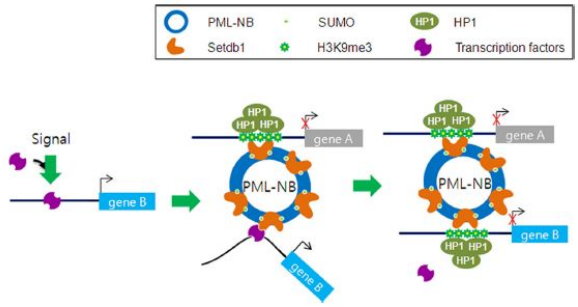

PMID: 21921037

Keywords : Cell Cycle; Bodies; Chromatin; H3; Heterochromatin; Methylation; DNA; Transcription; Domain; Interacts

Article 222

Generation of antibodies recognizing an aberrant glycoform of human tissue inhibitor of metalloproteinase-1 (TIMP-1) using decoy immunization and phage display

J Biotechnol. 2011 Jan; 151(2):225-30.

Ahn HJ, Kim YS, Lee CH, Cho EW, Yoo HS, Kim SH, Ko JH*, Kim SJ*

*Co-corresponding: jhko@kribb.re.kr sjick@kribb.re.kr
Immunotherapy Research Center

Aberrant glycosylation of human tissue inhibitor of metalloproteinase-1 (TIMP-1) by *N*-acetylglucosaminyltransferase-V (GnT-V) was previously reported to be related to cancer progression. Here, we report on the antibodies recognizing the structural features initiated by an addition of N-linked β(1,6)-*N*-acetylglucosamine (GlcNAc) branch by GnT-V on TIMP-1. Two glycoforms of TIMP-1, TIMP1-L produced in Lec4 cells without GnT-V activity and TIMP1-B in GnT-V overexpressing transfectant cells, were purified from culture supernatant and used for generation of antibodies. TIMP1-L was injected in the left hind footpad of mice as decoy and TIMP1-B in the right hind footpad as immunogen. Phage-displayed scFv library was constructed from the B cells retrieved from the right popliteal lymph nodes and subjected to panning and screening. Phage ELISA of individual clones revealed the scFv clones with preferential binding activity to TIMP1-B, and they were converted into an scFv-Fc format for further characterization of binding specificity. Glycan binding assay of an antibody, 1-9F, revealed its differential specificity toward an extension of glycan structure initiated with β (1,6)-GlcNAc linkage and terminally decorated with a sialic acid. This study demonstrates feasibility of a new strategy combining decoy immunization with phage display for the efficient generation of antibodies tracking down structural features of different glycoforms.

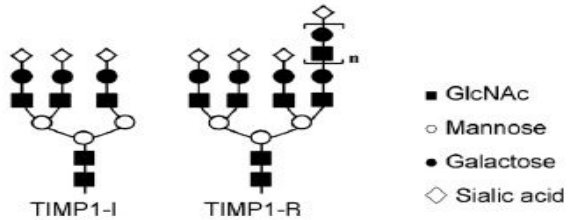

PMID: 21167221

Keywords : Phage Display; Antibody Library; Decoy Immunization; Glycan; N-Linked Beta(1,6)-Glcnac Branch; Single-Chain Antibodies; Carbohydrate Antigens; Glycosylation

Article 223

Involvement of neuropeptide Y and its Y1 and Y5 receptors in maintaining self-renewal and proliferation of human embryonic stem cells

J Cell Mol Med. 2011 Jan; 15(1):152-65.

Son MY, Kim MJ, Yu K, Koo DB, Cho YS*

*Corresponding: june@kribb.re.kr
Regenerative Medicine Research Center

Neuropeptide Y (NPY) and NPY receptors are widely expressed in various organs and cell types and have been shown to have pleiotropic functions. However, their presence or role in human embryonic stem cells (hESCs) remains unknown. We now show that undifferentiated hESCs primarily express NPY and its Y1 and Y5 receptors. Inhibition of NPY signalling using either the selective NPY Y1 or Y5 receptor antagonist reduces the maintenance of self-renewal and proliferation of undifferentiated hESCs. We also provide compelling evidence that exogenous NPY supports the long-term growth of undifferentiated hESCs in the absence of feeder cell factors using only knockout serum replacement media. Further, NPY facilitates the use of chemically defined medium made up of N2/B27 supplement and basic fibroblast growth factor (bFGF) for hESC feeder-free culture. Our results indicate that both Y1 and Y5 receptors appear to be involved in the NPY-mediated activation of AKT/protein kinase B and extracellular signal-regulated kinase 1/2 (ERK1/2) in hESCs. Notably, only Y1 receptor, but not Y5 receptor, is responsible for the NPY-induced activation of cAMP-response element binding (CREB) in hESCs. These results provide the first evidence that NPY and its Y1 and Y5 receptors have potential role in maintaining hESC self-renewal and pluripotency. We demonstrate the underlying importance of NPY signalling and its usefulness in the development of a defined and xeno-free culture condition for the large-scale propagation of undifferentiated hESCs.

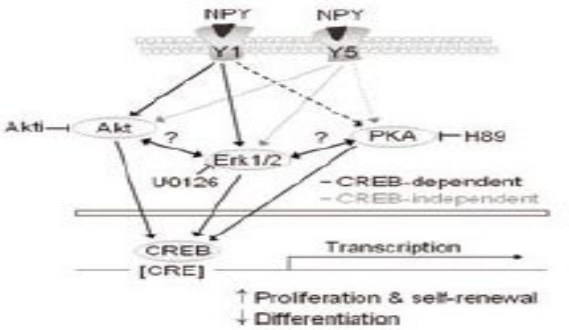

PMID: 19874423

Keywords : Human Embryonic Stem Cells; Self-Renewal; NPY Y1 Receptor; NPY Y5 Receptor; Stimulates Proliferation; Signaling Pathways; Brain Peptide; Growth-Factor; Neurotrophins

Article 224

Cucurbitacin B suppresses the transactivation activity of RelA/p65

J Cell Biochem. 2011 Jun; 112(6):1643-50.

Jin HR, Jin X, Dat NT, Lee JJ*

*Corresponding: jjlee@kribb.re.kr
Chemical Biology Research Center

Cucurbitacin B, a natural triterpenoid is well-known for its strong anticancer activity, and recent studies showed that the compound inhibits JAK/STAT3 pathway. In this study, we demonstrate for the first time that cucurbitacin B is also a potent inhibitor of NF-κB activation. Our results showed that cucurbitacin B inhibited TNF-α-induced expression of NF-κB reporter gene and NF-κB target genes in a dose-dependent manner, however, it did not prevent either stimuli-induced degradation of IκBα or nuclear translocation and DNA-binding activity of NF-κB. On the other hand, cucurbitacin B dose-dependently suppressed not only NF-κB activation induced by overexpression of RelA/p65 but also transactivation activity of RelA/p65 subunit of NF-κB. Consistently, treatment of HeLa cells with the compound significantly suppressed TNF-α-induced activation of Akt and phosphorylation of Ser536 in RelA/p65, which is required for transactivation activity. Consequently, cucurbitacin B inhibited TNF-α-induced expression of NF-κB-dependent anti-apoptotic proteins such as c-IAP1, c-IAP2, XIAP, TRAF1, and TRAF2 and sensitized TNF-α-induced cell death. Taken together, our results demonstrated that cucurbitacin B could be served as a valuable candidate for the intervention of NF-κB-dependent pathological condition such as cancer.

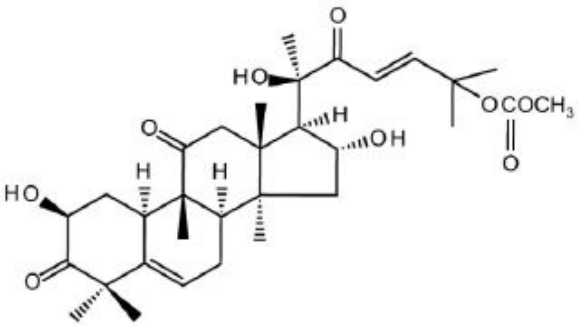

PMID: 21344491

Keywords : Cucurbitacin B; NF-Kappa B; RelA/p65; Akt; Transactivation; Anti-Apoptosis; Immune-System; Cancer Cells; Ikk-Beta; Phosphorylation; Inflammation; Apoptosis

Article 225

The WNT antagonist Dickkopf2 promotes angiogenesis in rodent and human endothelial cells

J Clin Invest. 2011 May; 121(5):1882-93.

Min JK*, Park H, Choi HJ, Kim Y, Pyun BJ, Agrawal V, Song BW, Jeon J, Maeng YS, Rho SS, Shim S, Chai JH, Koo BK, Hong HJ, Yun CO, Choi C, Kim YM, Hwang KC, Kwon YG

*Co-first: jekmin@kribb.re.kr
Immunotherapy Research Center

Neovessel formation is a complex process governed by the orchestrated action of multiple factors that regulate EC specification and dynamics within a growing vascular tree. These factors have been widely exploited to develop therapies for angiogenesis-related diseases such as diabetic retinopathy and tumor growth and metastasis. WNT signaling has been implicated in the regulation and development of the vascular system, but the detailed mechanism of this process remains unclear. Here, we report that Dickkopf1 (DKK1) and Dickkopf2 (DKK2), originally known as WNT antagonists, play opposite functional roles in regulating angiogenesis. DKK2 induced during EC morphogenesis promoted angiogenesis in cultured human endothelial cells and in *in vivo* assays using mice. Its structural homolog, DKK1, suppressed angiogenesis and was repressed upon induction of morphogenesis. Importantly, local injection of DKK2 protein significantly improved tissue repair, with enhanced neovascularization in animal models of both hind limb ischemia and myocardial infarction. We further showed that DKK2 stimulated filopodial dynamics and angiogenic sprouting of ECs via a signaling cascade involving LRP6-mediated APC/Asef2/Cdc42 activation. Thus, our findings demonstrate the distinct functions of DKK1 and DKK2 in controlling angiogenesis and suggest that DKK2 may be a viable therapeutic target in the treatment of ischemic vascular diseases.
PMID: 21540552

Keywords : Growth-Factor; Signaling Pathway; Vascular Morphogenesis; Hindlimb Ischemia; Exchange Factor; Head Induction; Stem-Cells; Notch; Receptor; Dickkopf2

Article 226

A FLT3-inhibitory constituent from the rhizomes of *Anemarrhena asphodeloides*

J Enzyme Inhib Med Chem. 2011 Jun; 26(3):445-8.

Han SY, Chin YW*

*Corresponding: f2744@kribb.re.kr
Natural Medicine Research Center

Bioactivity-guided investigation for the rhizomes of *Anemarrhena asphodeloides* using the Fms-like tyrosine kinase 3 (FLT3) inhibition assay led to the identification of an active xanthone, mangiferin. Mangiferin was found to inhibit activity of the FLT3 wild type and a mutated form of FLT3 with IC_{50} values of 0.7 and 1.2 μM, respectively. Furthermore, this compound was assessed with a small panel of select kinases anaplastic lymphoma kinase (ALK), insulin receptor, and epidermal growth factor receptor) and was also found to be active in ALK assay.
PMID: 20846091

Keywords : *Anemarrhena asphodeloides*; Mangiferin; FLT3; Alk; Xanthone; Acute Myeloid-Leukemia; Factor-Kappa-B; Identification

Article 227

Biosynthesis of plant-specific phenylpropanoids by construction of an artificial biosynthetic pathway in *Escherichia coli*

J Ind Microbiol Biotechnol. 2011 Oct; 38(10):1657-65.

Choi O, Wu CZ, Kang SY, Ahn JS, Uhm TB, Hong YS*

*Corresponding: hongsoo@kribb.re.kr
Chemical Biology Research Center

Biological synthesis of plant secondary metabolites has attracted increasing attention due to their proven or assumed beneficial properties and health-promoting effects. Phenylpropanoids are the precursors to a range of important plant metabolites such as the secondary metabolites belonging to the flavonoid/stilbenoid class of compounds. In this study, engineered *Escherichia coli* containing artificial phenylpropanoid biosynthetic pathways utilizing tyrosine as the initial precursor were established for production of plant-specific metabolites such as ferulic acid, naringenin, and resveratrol. The construction of the artificial pathway utilized tyrosine ammonia lyase and 4-coumarate 3-hydroxylase from *Saccharothrix espanaensis*, cinnamate/4-coumarate:coenzyme A ligase from *Streptomyces coelicolor*, caffeic acid O-methyltransferase and chalcone synthase from *Arabidopsis thaliana*, and stilbene synthase from *Arachis hypogaea*.

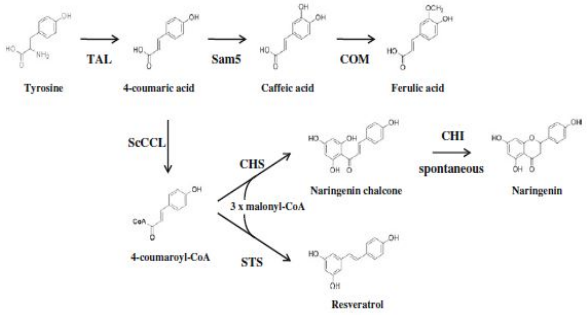

PMID: 21424580

Keywords : Flavonoid Biosynthesis; Phenylpropanoid; Heterologous Expression; Artificial Pathway; Gene-Cluster; Resveratrol; Flavanones

Article 228

Anticomplement activity of compounds isolated from the roots of *Euphorbia kansui*

J Korean Soc Appl Biol Chem. 2011; 54(2):159-162.

Li G, Kim JH, Shen GH, Lee J, Lee HK, Oh SR*

*Corresponding: seiryang@kribb.re.kr
Natural Medicine Research Center

The anticomplement activity-guided fractionation of the methanol extract of *Euphorbia kansui* L. resulted in isolation of three diterpenes, two triterpenes, and two sterols (1-7) from ethyl acetate fraction. By spectroscopic analysis, their chemical structures were elucidated as: beta-amyrin (1); kansuiphorin C (2); 3-*O*-(2'E,4'Z-decadienoyl)-ingenol (3); 3-*O*-(2,3-dimethylbutyryl)-13-0-n-dodecanoyl-13-hydroxyi ngenol (4); P-sitosterol (5); a-euphol (6); beta-sitosterol-3-*O*-P-D-glucopyranoside (7). These compounds were investigated *in vitro* for their anticomplement activily against the classical pathway of the complement system, with compounds 2-4 exhibiting significant anticomplement activity with respective 50% inhibitory concentration values of 44.1 +/- 3.8, 89.5 +/- 5.5, and 152.1 +/- 6.2 μM.

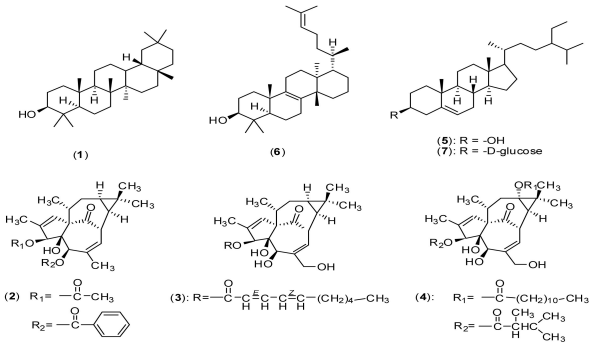

Keywords : Anticomplement Activity; *Euphorbia kansui*; Kansuiphorin C; Antitumor Agents; Cell-Division; Triterpenes; Diterpenes; Xenopus

Article 229

(-)-Pinoresinol monomethyl ether inhibits LPS-induced iNOS and COX-2 expression *via* the attenuation of NF-kappa B in Raw 264.7 macrophage cells

J Korean Soc Appl Biol Chem. 2011; 54(2):163-168.

Park BY, Lee MY, Ahn KS, Chin YW, Lee HK, Oh SR*

*Corresponding: seiryang@kribb.re.kr
Natural Medicine Research Center

Anti-inflammatory effects of (-)-pinoresinol monomethyl ether (PME) were evaluated on lipopolysaccharide (LPS)-treated Raw 264.7 macrophage cells. PME inhibited translocation of p65-nuclear factor-kappa B (NF-kappa B) into the nucleus in immunocytochemical analysis for NF-kappa B activation, expression of inducible nitric oxide synthase (iNOS) and cyclooxygenase-2 (COX-2) in Western blotting, as well as production of pro-inflammatory mediators, such as nitric oxide (NO), tumor necrosis factor (TNF-alpha), and prostaglandin E_2 (PGE_2) in LPS-induced Raw 264.7 cells. These results suggest the anti-inflammatory activity of PME could be due to the down-regulation of iNOS, COX-2, TNF-alpha, and PGE_2 in activated Raw 264.7 cells through NF-kappa B-dependent pathways.

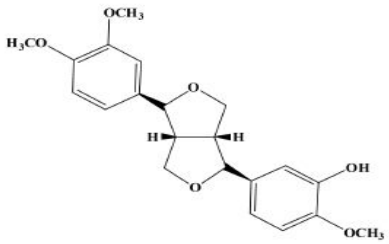

Keywords : COX-2; Inducible Nitric Oxide Synthase; Nuclear Factor-Kappa B; Prostaglandin E(2); (-)-Pinoresinol Monomethyl Ether; Tumor Necrosis Factor; Cyclooxygenase; Inflammation

Article 230

Capsicum annuum L. methanolic extract inhibits ovalbumin-induced airway inflammation and oxidative stress in a mouse model of asthma

J Med Food. 2011 Oct; 14(10):1144-51.

Jang HY, Kim SM, Yuk JE, Kwon OK, Oh SR, Lee HK, Jeong H, Ahn KS*

*Corresponding: ksahn@kribb.re.kr
Natural Medicine Research Center

The pepper fruit of *Capsicum annuum* L. is used as a food, spice, and topical medicine. Here, we investigated the effect of a methanolic *C. annuum* L. extract (CAE) in a mouse model of ovalbumin-induced allergic airway inflammation. Animals were treated with CAE by oral gavage before ovalbumin challenge. After ovalbumin challenge, airway responsiveness to methacholine, influx of inflammatory cells into the lung, cytokine levels in bronchoalveolar lavage fluid and lung, nuclear factor-κB (NF-κB) activity in lungs, and lung histopathology were assessed. Oral treatment with CAE significantly reduced the pathophysiological signs of allergic airway disease, including increased inflammatory cell recruitment to the airways, airway hyperresponsiveness, and increased levels of T-helper type 2 cytokines. Reactive oxygen species were also decreased in cells from bronchoalveolar lavage fluid. In addition, we found that administration of CAE attenuated ovalbumin-induced increases in NF-κB activity in lungs. Collectively, these results suggest that CAE may be an effective oral treatment for allergic airway inflammation by virtue of its antioxidant activity.
PMID: 21875363

Keywords : Airway Hyperresponsiveness; Antioxidant Activity; Asthma; *Capsicum Annuum* L.; Kappa-B Activation; Murine Model; Capsaicin; Cancer

Article 231

Protuboxepins A and B and protubonines A and B from the marine-derived fungus *Aspergillus* sp. SF-5044

J Nat Prod. 2011 May; 74(5):1284-7.

Lee SU, Asami Y, Lee D, Jang JH, Ahn JS*, Oh H

*Co-corresponding: jsahn@kribb.re.kr
Chemical Biology Research Center

Two new oxepin-containing (1 and 2) and two diketopiperazine-type alkaloids (3 and 4) have been isolated from an EtOAc extract of the marine-derived fungus *Aspergillus* sp. SF-5044. The structures of these metabolites were determined through analysis of NMR and MS data, along with Marfey's method. Compound 1 showed weak growth inhibitory activity against a small panel of cell lines.

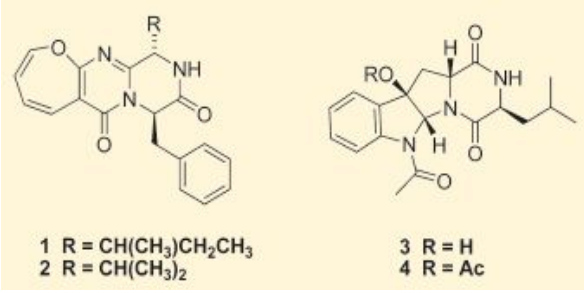

PMID: 21366228

Keywords : Metabolites; Protuboxepins; Protubonines; Alkaloids; EtOAc Extract; Marfey Method; *Aspergillus*;

Article 232

IL-15-induced IL-10 increases the cytolytic activity of human natural killer cells

Mol Cells. 2011 Sep; 32(3):265-72.

Park JY, Lee SH, Yoon SR, Park YJ, Jung H, Kim TD*, Choi I*

*Co-corresponding: tdkim@kribb.re.kr ipchoi@kribb.re.kr
Immunotherapy Research Center

Interleukin 10 (IL-10) is a multifunctional cytokine that regulates diverse functions of immune cells. Natural killer (NK) cells express the IL-10 and IL-10 receptor, but little is known about the function of IL-10 on NK cell activation. In this study, we show the expression and role of IL-10 in human NK cells. Among the cytokines tested, IL-15 was the most potent inducer of IL-10, with a maximal peak expression at 5 h after treatment. Furthermore, IL-10 receptor was shown to be expressed in NK cells. IL-10 alone had a significant effect on NK cytotoxicity which additively increased NK cell cytotoxicity in the presence of IL-15. Neutralizing IL-10 with anti-IL-10 antibody suppressed the inductive effect of IL-10 on NK cell cytotoxicity; however, IL-10 had no effect on IFN-γ or TNF-α production or NK cell activatory receptor expression. STAT signals are implicated as a key mediator of IL-10/IL-15 cytotoxicity response. Thus, the effect of IL-10 on NK cells is particularly interesting with regard to the STAT3 signal that was enhanced by IL-10 or IL-15.

PMID: 21809216

Keywords : Cytotoxicity; IL-10; IL-15; Natural Killer Cell; Interferon-Gamma-Production; Human NK Cells; T-Cells; Toxoplasma-Gondii; Resistance; Proliferation

Article 233

Pancreatic adenocarcinoma upregulated factor promotes metastasis by regulating TLR/CXCR4 activation

Oncogene. 2011 Jan; 30(2):201-11.

Park HD, Lee Y, Oh YK, Jung JG, Park YW, Myung K, Kim KH, Koh SS*, Lim DS

*Co-corresponding: sskoh@kribb.re.kr
Immunotherapy Research Center

Pancreatic adenocarcinoma upregulated factor (PAUF) is overproduced in certain types of cancer. However, little is known of the tumorigenic function of PAUF. In this study, we report the X-ray crystal structure of PAUF and reveal that PAUF is a mammalian lectin normally found in plant lectins. We also identify PAUF as an endogenous ligand of Toll-like receptor 2 (TLR2) and TLR4 by screening extracellular domain receptor pools. We further confirmed the specificity of the PAUF-TLR2 interaction. PAUF induces extracellular signal-regulated kinase (ERK) phosphorylation and activates the IKK-β-mediated TPL2/MEK/ERK signaling pathway through TLR2. In agreement with the result of TLR2-mediated ERK activation by PAUF, PAUF induces increased expression of the protumorigenic cytokines RANTES and MIF in THP-1 cells. However, PAUF does not fully activate Iκ-B-α signaling pathways in THP-1 cells, and fails to translocate the p65 subunit of the nuclear factor-κ B (NF-κB) complex into the nucleus, resulting in no NF-κB activation. Surprisingly, we found that PAUF also associated with the CXC chemokine receptor (CXCR4)-TLR2 complex and inhibited CXCR4-dependent, TLR2-mediated NF-κB activation. Together, these findings suggest that the new cancer-associated ligand, PAUF, may activate TLR-mediated ERK signaling to produce the protumorigenic cytokines, but inhibits TLR-mediated NF-κB signaling, thereby facilitating tumor growth and escape from innate immune surveillance.

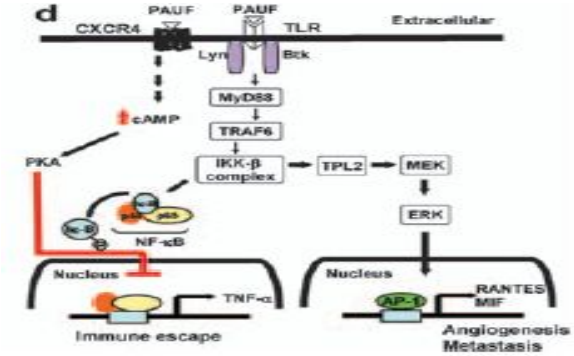

PMID: 20802527

Keywords : PAUF; TLR; CXCR4; TPL2; ERK; NF-kappa B; Tumor-Growth; Carbohydrate Specificities; Cancer-Cells; Angiogenesis; Lipopolysaccharide; Inflammation

Article 234

The cell adhesion molecule L1 promotes gallbladder carcinoma progression *in vitro* and *in vivo*

Oncol Rep. 2011 Apr; 25(4):945-52.

Jung J, Son YS, Park H, Jeon SK, Lee JW, Choi SY, Kim JM, Kwon YG, Hong HJ, Min JK*

*Co-corresponding: jekmin@kribb.re.kr
Immunotherapy Research Center

Recent studies have demonstrated that the cell adhesion molecule, L1, is expressed in several malignant tumor types and its expression correlates with tumor progression and metastasis. However, the role of L1 in gallbladder carcinoma (GBC) remains unclear. Here, we demonstrate that L1 is expressed in GBC cells and plays an important role in the growth, motility, invasiveness, and adhesiveness of GBC cells. Specific depletion or overexpression of L1 in the GBC cell lines JCRB1033 and SNU-308, respectively, was achieved by lentivirus-mediated transduction and expression of an L1 mRNA-specific short hairpin RNA or full-length human L1. Stable depletion of L1 led to a significant decrease in GBC cell proliferation, migration and invasion, as well as decreased intracellular signaling through AKT and FAK. Overexpression of L1 in GBC cells enhanced these cellular activities. In a GBC xenograft nude mouse model, suppression of L1 markedly reduced tumor growth and increased the survival of tumor-bearing mice whereas L1 overexpression stimulated tumorigenicity. Taken together, these results suggest that L1 plays a crucial role in GBC progression and may be a novel therapeutic target in GBC treatment.

PMID: 21318226

Keywords : Gallbladder Carcinoma; L1 Cell Adhesion Molecule; Therapeutic Target; Ovarian Carcinomas; Cancer Cells; Tumor-Growth; Metastasis; Antibodies

Article 235

Syntheses of sulfur and selenium analogues of pachastrissamine *via* double displacements of cyclic sulfate

Org Biomol Chem. 2011 Oct; 9(20):7237-42.

Jeon H, Bae H, Baek DJ, Kwak YS*, Kim D, Kim S

*Co-corresponding: yskwak@kribb.re.kr
Chemical Biology Research Center

Bioisosteric analogues of pachastrissamine that contain sulfur and selenium atoms replacing the oxygen in the ring system, were efficiently prepared from a cyclic sulfate intermediate by sequential intermolecular and intramolecular S_N2 displacement reactions of the dianions. The analogues exhibited cytotoxicities comparable to that of pachastrissamine.

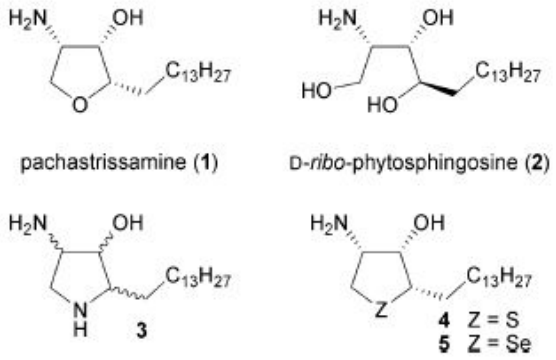

PMID: 21879131

Keywords : Jaspine-B Pachastrissamine; Stereoselective-Synthesis; Marine Sponge; Vic-Diols; Derivatives; Sphingosine; Episulfides; Olefins

Article 236

Physical passaging of embryoid bodies generated from human pluripotent stem cells

PLoS One. 2011 May; 6(5):e19134.

Son MY, Kim HJ, Kim MJ, Cho YS*

*Corresponding: june@kribb.re.kr
Regenerative Medicine Research Center

Spherical three-dimensional cell aggregates called embryoid bodies (EBs), have been widely used in *in vitro* differentiation protocols for human pluripotent stem cells including human embryonic stem cells (hESCs) and human induced pluripotent stem cells (hiPSCs). Recent studies highlight the new devices and techniques for hEB formation and expansion, but are not involved in the passaging or subculture process. Here, we provide evidence that a simple periodic passaging markedly improved hEB culture condition and thus allowed the size-controlled, mass production of human embryoid bodies (hEBs) derived from both hESCs and hiPSCs. hEBs maintained in prolonged suspension culture without passaging (>2 weeks) showed a progressive decrease in the cell growth and proliferation and increase in the apoptosis compared to 7-day-old hEBs. However, when serially passaged in suspension, hEB cell populations were significantly increased in number while maintaining the normal rates of cell proliferation and apoptosis and the differentiation potential. Uniform-sized hEBs produced by manual passaging using a 1 : 4 split ratio have been successfully maintained for over 20 continuous passages. The passaging culture method of hEBs, which is simple, readily expandable, and reproducible, could be a powerful tool for improving a robust and scalable *in vitro* differentiation system of human pluripotent stem cells.

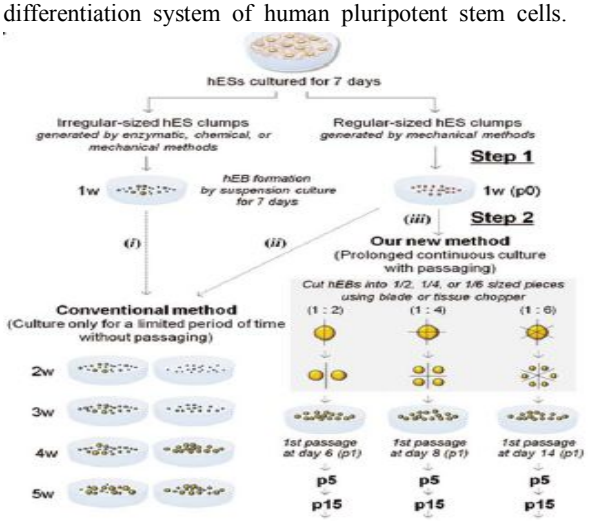

PMID: 21559272

Keywords : Stress Defense-Mechanisms; Differentiation; Propagation; Cultivation; Suspension; Efficiency; Lines; Human Embryonic Stem Cells

Article 237

Direct reprogramming of mouse fibroblasts to neural progenitors

Proc Natl Acad Sci U S A. 2011 May; 108(19):7838-43.

Kim J*, Efe JA, Zhu S, Talantova M, Yuan X, Wang S, Lipton SA, Zhang K, Ding S

*First: janghwan.kim@kribb.re.kr
Regenerative Medicine Research Center

The simple yet powerful technique of induced pluripotency may eventually supply a wide range of differentiated cells for cell therapy and drug development. However, making the appropriate cells via induced pluripotent stem cells (iPSCs) requires reprogramming of somatic cells and subsequent redifferentiation. Given how arduous and lengthy this process can be, we sought to determine whether it might be possible to convert somatic cells into lineage-specific stem/progenitor cells of another germ layer in one step, bypassing the intermediate pluripotent stage. Here we show that transient induction of the four reprogramming factors (Oct4, Sox2, Klf4, and c-Myc) can efficiently transdifferentiate fibroblasts into functional neural stem/progenitor cells (NPCs) with appropriate signaling inputs. Compared with induced neurons (or iN cells, which are directly converted from fibroblasts), transdifferentiated NPCs have the distinct advantage of being expandable *in vitro* and retaining the ability to give rise to multiple neuronal subtypes and glial cells. Our results provide a unique paradigm for iPSC-factor-based reprogramming by demonstrating that it can be readily modified to serve as a general platform for transdifferentiation.

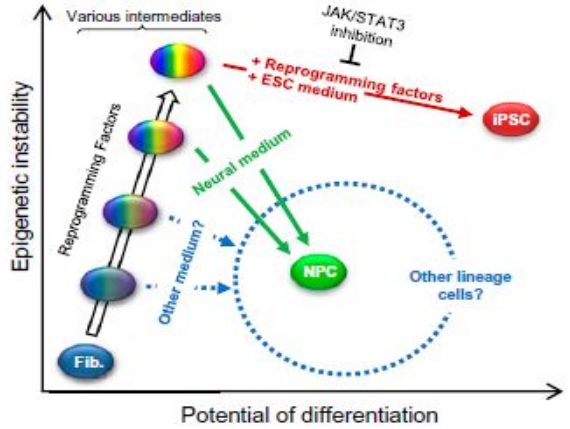

PMID: 21521790

Keywords : Direct Conversion; Direct Reprogramming; Transdifferentiation; Neural Stem Cells; Induced Pluripotent Stem Cells; Reprogramming Factors

Article 238

L1 cell adhesion molecule, a novel surface molecule of human embryonic stem cells, is essential for self-renewal and pluripotency

Stem Cells. 2011 Dec; 29(12):2094-9.

Son YS, Seong RH, Ryu CJ, Cho YS, Bae KH, Chung SJ, Lee B, Min JK*, Hong HJ

*Co-corresponding: jekmin@kribb.re.kr
Immunotherapy Research Center

Despite the recent identification of surface markers of undifferentiated human embryonic stem cells (hESCs), the crucial cell-surface molecules that regulate the self-renewal capacity of hESCs remain largely undefined. Here, we generated monoclonal antibodies (MAbs) that specifically bind to undifferentiated hESCs but not to mouse embryonic stem cells. Among these antibodies, we selected a novel MAb, 4-63, and identified its target antigen as the L1 cell adhesion molecule (L1CAM) isoform 2. Notably, L1CAM expressed in hESCs lacked the neuron-specific YEGHH and RSLE peptides encoded by exons 2 and 27, respectively. L1CAM colocalized with hESC-specific cell-surface markers, and its expression was markedly downregulated on differentiation. Stable L1CAM depletion markedly decreased hESC proliferation, whereas L1CAM overexpression increased proliferation. In addition, the expression of octamer-binding transcription factor 4, Nanog, sex-determining region Y-box 2, and stage-specific embryonic antigen (SSEA)-3 was markedly downregulated, whereas lineage-specific markers and SSEA-1 were upregulated in L1CAM-depleted hESCs. Interestingly, the actions of L1CAM in regulating the proliferation and differentiation of hESCs were exerted predominantly through the fibroblast growth factor receptor 1 signaling pathway. Taken together, our results suggest that L1CAM is a novel cell-surface molecule that plays an important role in the maintenance of self-renewal and pluripotency in hESCs.
PMID: 21957033

Keywords : L1 Cell Adhesion Molecule; L1CAM; Cell-Surface Marker; Human Embryonic Stem Cells; Monoclonal Antibody; Fibroblast Growth Factor Receptor 1; Human Blastocysts

Article 239

Combinatorial activin receptor-like kinase/Smad and basic fibroblast growth factor signals stimulate the differentiation of human embryonic stem cells into the cardiac lineage

Stem Cells Dev. 2011 Sep; 20(9):1479-90.

Yook JY, Kim MJ, Son MJ, Lee S, Nam Y, Han YM, Cho YS*

*Corresponding: june@kribb.re.kr
Regenerative Medicine Research Center

The transforming growth factor beta/bone morphogenetic protein-activated Smad signaling pathway plays a complicated role in the maintenance of human embryonic stem cell (hESC) pluripotency and in the cell fate decision of hESCs. Here, we report that sustained inhibition of the transforming growth factor beta type I receptor (also termed activin receptor-like kinase or ALK) using a chemical inhibitor selective for ALK4/5/7 (ALKi) leads to the cardiac differentiation of hESCs under feeder-free and serum-free conditions. Treatment with ALKi reduced Smad2/3 phosphorylation and increased Smad1/5/8 phosphorylation in hESCs, suggesting a requirement for active Smad1/5/8 signaling for cardiac induction in these cells when ALK/Smad2/3 is inhibited. Importantly, active basic fibroblast growth factor (bFGF) signaling was also required for ALKi-mediated cardiac differentiation of monolayer-cultured hESCs. The FGF receptor inhibitor SU5402 blocked ALKi-mediated cardiac induction in hESCs, whereas bone morphogenetic protein-4 enhanced the ALKi-induced increase in phospho-Smad1/5/8 levels but failed to induce the cardiac differentiation of hESCs and instead promoted trophoblastic differentiation. We also confirmed that ALKi potentially enhanced the cardiac differentiation of human embryoid bodies, as determined by expression of cardiac-specific markers, increased beating areas, and action potential recorded from beating areas. These results demonstrate that an ALKi could be used as a potential cardiac-inducing agent and that the development of culture conditions that provide an appropriate balance between ALK/Smad and bFGF signaling is necessary to direct the fate of hESCs into the cardiac lineage.

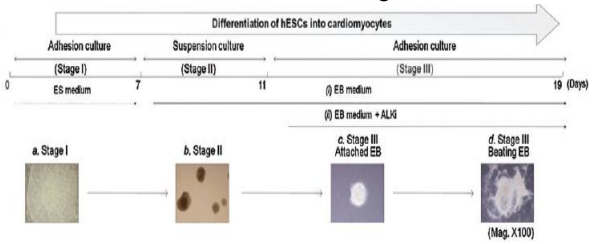

PMID: 21208046

Keywords : Cardiomyocyte Differentiation; Self-Renewal; Heart Development; Feeder Layers; Human Embryonic Stem Cells; FGF; Pluripotency; Pathways; Mesoderm; BMP

Article 240

Expedient synthesis of 4-*O*-methylhonokiol via Suzuki-Miyaura cross-coupling

Tetrahedron. 2011; 67(48):9401-4.

Kwak JH, Cho YA, Jang JY, Seo SY, Lee H, Hong JT, Han SB, Lee K, Kwak YS*, Jung JK

*Co-corresponding: yskwak@kribb.re.kr
Chemical Biology Research Center

Concise and practical synthesis of 4-*O*-methylhonokiol was achieved in 34% overall yield. The key features of our synthesis include chemoselective *ortho*-mono bromination of phenol as well as biaryl formation via Suzuki-Miyaura cross-coupling, in which bromophenol was reacted with potassium aryltrifluoroborate using $Pd(OAc)_2$ and RuPhos under microwave conditions. Further efforts are in progress for the synthesis of 4-O-methylhonokiol derivatives in light of the structureeactivity relationship for anti-inflammatory and neurotropic effects.

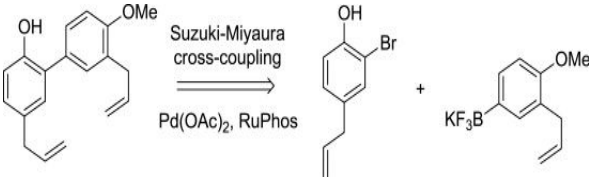

Keywords : Neolignan; 4-O-Methylhonokiol; Suzuki-Miyaura Cross-Coupling; Potassium Aryltrifluoroborate; Concise Synthesis; Honokiol

2011
KRIBB Article Abstracts
Corresponding Articles
Indexed in SCIE

Division of Biomedical Infrastructure

- Biotechnology Process Engineering Center
- Bio-Evaluation Center
- National Primate Research Center
- Biomedical Mouse Resource Center

Korea Research Institute of Bioscience and Biotechnology


KRIBB
www.kribb.re.kr

Article 241

Do transgenic chili pepper plants producing viral coat protein affect the structure of a soil microbial community?

Appl Soil Ecol. 2011; 51:130-8.

Chun YJ, Kim DY, Kim HJ, Park KW, Jeong SC, Park S, Lee B, Harn CH, Kim HM, Kim CG*

*Co-corresponding: cgkim@kribb.re.kr
Bio-Evaluation Center

We used field trials to study the potential non-target effects of transgenic chili pepper on the composition of a rhizosphere microbial community. These plants expressed a viral coat protein (CP) gene that confers resistance to cucumber mosaic virus (CMV). For comparison, we included a non-transgenic parental cultivar (wild type) and another non-transgenic commercial variety. Soil samples were collected at the time of flowering (June) and twice during the fruit-ripening stage (August and September). The microbial community was characterized by analyzing levels of phospholipid fatty acids (PLFAs) as well as the terminal restriction fragment length polymorphism (T-RFLP) of bacterial 16S-rRNA and the fungal internal transcribed spacer (ITS) region. Although the amounts of PLFAs and their diversity indices did not differ among pepper lines, they did vary significantly over the growing season. We also used non-metric multidimensional scaling (NMDS) and permutational multivariate analysis of variance (PerMANOVA) to evaluate microbial assemblages from these plants. Overall, no differences were found among pepper lines. However, a significant difference was found between wild type and transgenic peppers, with regard to their bacterial composition based on the T-RFLP profile from *HhaI* digest. We conclude that the impact of CMV-resistant transgenic pepper on soil microbial assemblages is weak and minor, compared with the dominating natural variations associated with plant growth stages.

Keywords : Chili Pepper; Cucumber Mosaic Virus; PLFA; Soil Microbial Community; T-RFLP; Transgenic Crop; Genetically-Modified Crops; *Bacillus thuringiensis*; Extracellular DNA

Article 242

Intra-host competition and interactions between *Soybean mosaic virus* (SMV) strains in mixed-infected soybean

Aust J Crop Sci. 2011; 5(11):1379-87.

Hwang TY, Jeong SC*, Kim O, Park HM, Lee SK, Seo MJ, Choi MS, Lee YY, Yun HT, Kwon YU, Kim WH, Kim YH

*Co-first: scjeong@kribb.re.kr
Bio-Evaluation Center

Over the past two decades, the dominant *Soybean mosaic virus* (SMV) strain in South Korea has changed from G5 to G7H. To examine the dominance of G7H, intra-host competition between G7H and G5 was evaluated in soybean plants infected with a mixture of SMV strains. The distribution patterns of the two SMV strains in soybean plants inoculated with G7H, G5 and G7H/G5 were investigated at designated time points by RT-PCR/RFLP analysis, which enables the specific differentiation of low concentrations of SMV strains and the detection of mixed infection at any given time. When leaves of 'Kwangankong' and 'Tawonkong' were infected with both strains, the upper leaves had only the G7H strain in simultaneous infections. In sequential inoculations, the leaves exhibited mosaic symptoms caused by G7H, and the G5 strain was not detected in plants pre-inoculated with the G7H strain before inoculation with the G5 strain. In the reverse treatment, both G5 and G7H were present at every vegetative stage. In addition, interactions between the virulence and dominance of G7H, G5, and G1, a less virulent strain, were investigated. Three landrace soybeans were co-inoculated with G7H/G5, G7H/G1, G5/G1, and G7H/G5/G1 sets. There was no significant difference between virulence and dominance. These results demonstrate the dominance of G7H in mixed infections and could explain the prevalence of G7H in South Korea.

Keywords : Intra-Host Competition; Mixed Infection; RT-PCR/RFLP; Seed Mottling; *Soybean mosaic virus*; SMV strain G5; SMV strain G7H

Article 243

Instability of toxin A subunit of AB_5 toxins in the bacterial periplasm caused by deficiency of their cognate B subunits

Biochim Biophys Acta. 2011 Oct; 1808(10):2359-65.

Kim SH, Ryu SH, Lee SH, Lee YH, Lee SR, Huh JW, Kim SU, Kim E, Kim S, Jon S, Bishop RE, Chang KT*

*Co-corresponding: changkt@kribb.re.kr
National Primate Research Center

Shiga toxin (STx) belongs to the AB_5 toxin family and is transiently localized in the periplasm before secretion into the extracellular milieu. While producing outer membrane vesicles (OMVs) containing only A subunit of the toxin (STxA), we created specific STx1B- and STx2B-deficient mutants of *E. coli* O157:H7. Surprisingly, STxA subunit was absent in the OMVs and periplasm of the STxB-deficient mutants. In parallel, the A subunit of heat-labile toxin (LT) of enterotoxigenic *E. coli* (ETEC) was absent in the periplasm of the LT-B-deficient mutant, suggesting that instability of toxin A subunit in the absence of the B subunit is a common phenomenon in the AB_5 bacterial toxins. Moreover, STx2A was barely detectable in the periplasm of *E. coli* JM109 when *stx2A* was overexpressed alone, while it was stably present when *stxB* was co-expressed. Compared with STx2 holotoxin, purified STx2A was degraded rapidly by periplasmic proteases when assessed for *in vitro* proteolytic susceptibility, suggesting that the B subunit contributes to stability of the toxin A subunit in the periplasm. We propose a novel role for toxin B subunits of AB_5 toxins in protection of the A subunit from proteolysis during holotoxin assembly in the periplasm.
PMID: 21762677

Keywords : Shiga Toxin; Heat-Labile Enterotoxin; Outer Membrane; Periplasm; Biomedical Applications; Vibrio-Cholerae; Hybrid Toxins; Secretion

Article 244

Phenotypic plasticity of introduced versus native purple loosestrife: univariate and multivariate reaction norm approaches

Biol Invasions. 2011; 13(4):819-829.

Chun YJ*

*Corresponding: youngjinchun@gmail.com
Bio-Evaluation Center

The plastic responses to environmental change by *Lythrum salicaria* (purple loosestrife) were compared between native plants derived from seeds collected in Europe and those introduced into North America. Plants from nine populations each were grown under two levels of water and nutrient conditions. At the end of the growing season, samples were evaluated for eight traits related to their life history, plant size/architecture, and reproduction. Genetic (G), environmental (E), and G x E interactions were assessed by restricted maximum likelihood (REML) analysis of covariance (ANCOVA) and multivariate analysis of covariance (MANCOVA). Both univariate and multivariate reaction norm analyses were used to test for differences in the magnitude and direction of phenotypic plasticity between introduced and native plants. Under high-nutrient conditions, introduced plants were taller and had more branches and greater aboveground biomass. They also exhibited significantly greater amounts of phenotypic plasticity for aboveground biomass than did the natives in response to changing nutrient levels in standing water. This difference in univariate plasticity contributed to the general contrast in multivariate plasticity between introduced and native plants. These results support the idea that introduced plants may successfully invade a habitat and grow better than native plants in response to increased resources.

Keywords : Common Garden; Genetic x Environment (G x E) Interaction; Introduced Species; *Lythrum salicaria*; Reaction Norm; Invasive Plants; Nutrient; Evolution; Commelinaceae

Article 245

Immunostimulatory effect by aqueous extract of *Hizikia fusiforme* in RAW 264.7 macrophage and whole spleen cells

Biotechnol Bioproc Eng. 2011; 16(6):1099-1105.

Yoon YD*, Lee ES, Park JP, Kim MR, Lee JW, Kim TH, Na MK, Kim JH

*First: yunyd76@kribb.re.kr
Bio-Evaluation Center

Hizikia fusiforme is a commonly used food that possesses potent anti-bacterial, anti-fungal, and anti-inflammatory activities. The immunostimulatory activities of aqueous extract of *Hizikia fusiforme* (HFAE) in RAW 264.7 macrophages and whole spleen cells were investigated. HFAE activated RAW 264.7 macrophages to produce cytokines such as nitric oxide (NO), tumor necrosis factor-alpha (TNF-alpha), interleukin-1 beta (IL-1 beta), and interleukin-6 (IL-6) in a dose-dependent manner. In addition, HFAE induced the mRNA expression of TNF-alpha, IL-1 beta, and IL-6 in RAW 264.7 macrophages. Moreover, HFAE stimulated proliferation of whole spleen cells and reference mitogen. Taken together, the results demonstrate that HFAE potently activates the immune function by regulating NO, TNF-alpha, IL-1 beta, and IL-6 in RAW 264.7 macrophage and promoting spleen cell proliferation.

Keywords : *Hizikia fusiforme*; Immunostimulatory Activity; Nitric Oxide; Spleen Cells; Acanthopanax-Obovatus Roots; Tumor Necrosis Factor; Polysaccharide; Fucoidan; Seaweed

Article 246

Effect of constitutively active Ras overexpression on cell growth in recombinant Chinese hamster ovary cells

Biotechnol Prog. 2011 Mar; 27(2):577-80.

Kim YG*, Han YK, Kim JY, Lee EG, Lee HW, Lee GM

*First: ygkim@kribb.re.kr
Biotechnology Process Engineering Center

Constitutively active Ras (CA-Ras) is known to enhance cell growth through the induction of various signaling cascades including the phosphoinositide 3-kinase (PI3K)/Akt and mitogen-activated protein kinase (MAPK)/ERK signaling pathways, although the cellular response is highly dependent on the cell type. To evaluate the effect of CA-Ras overexpression on cell growth in recombinant Chinese hamster ovary (rCHO) cells, an erythropoietin (EPO)-producing rCHO cell line with regulated CA-Ras overexpression (EPO-off-CA-Ras) was established using the Tet-off system. The CA-Ras expression level in EPO-off-CA-Ras cells was tightly regulated by doxycycline addition. Although CA-Ras overexpression slightly increased the viable cell concentration during the late exponential phase, it did not increase the maximum viable cell concentration or specific growth rate to a significant degree. Unexpectedly, CA-Ras overexpression in rCHO cells led only to the enhancement in the activation of the MAPK/ERK signaling pathway and not the PI3K/Akt signaling pathway. Taken together, CA-Ras overexpression in rCHO cells did not significantly affect cell growth; it also had no critical impact on viable cell concentration or EPO production, possibly due to a failure to activate the PI3K/Akt signaling pathway.
PMID: 21438179

Keywords : rCHO cells; Ras; Cell Growth; Inducible Expression; Erythropoietin; Factor-I; Apoptosis; Pathways; Insulin; Antibodies

Article 247

Regulatory roles of ganglioside GQ1b in neuronal cell differentiation of mouse embryonic stem cells

BMB Rep. 2011 Dec; 44(12):799-804.

Kwak DH, Jin JW, Ryu JS, Ko K, Lee SD, Lee JW, Kim JS, Jung KY, Ko K, Ma JY, Hwang KA, Chang KT*, Choo YK

*Co-corresponding: changkt@kribb.re.kr
National Primate Research Center

Gangliosides play an important role in neuronal differentiation processes. The regulation of ganglioside levels is related to the induction of neuronal cell differentiation. In this study, the ST8Sia5 gene was transfected into mESCs and then differentiated into neuronal cells. Interestingly, ST8Sia5 gene transfected mESCs expressed GQ1b by HPTLC and immunofluorescence analysis. To investigate the effects of GQ1b over-expression in neurogenesis, neuronal cells were differentiated from GQ1b expressing mESCs in the presence of retinoic acid. In GQ1b expressing mESCs, increased EBs formation was observed. After 4 days, EBs were co-localized with GQ1b and nestin, and GFAP. Moreover, GQ1b co-localized with MAP-2 expressing cells in GQ1b expressing mESCs in 7-day-old EBs. Furthermore, GQ1b expressing mESCs increased the ERK1/2 MAP kinase pathway. These results suggest that the ST8Sia5 gene increases ganglioside GQ1b and improves neuronal differentiation via the ERK1/2 MAP kinase pathway.
PMID: 22189683

Keywords : Ganglioside GQ1b; MAP Kinase; Mouse Embryonic Stem Cells; Neural Differentiation; ST8Sia5; Activated Protein-Kinases; Pc12 Cells; ERK1/2; Glycosphingolipids

Article 248

Proteomics analysis of salt-induced leaf proteins in two rice germplasms with different salt sensitivity

Can J Plant Sci. 2011; 91(2):337-49.

Lee DG, Park KW*, An JY, Sohn YG, Ha JK, Kim HY, Bae DW, Lee KH, Kang NJ, Lee BH, Kang KY, Lee JJ

*Co-corresponding: park@kribb.re.kr
Bio-Evaluation Center

This study was conducted to investigate salt-stress-related physiological responses and proteomics changes in the leaves of two rice (*Oryza saliva* L.) cultivars. Shoot growth and water content of rice leaves were more severely reduced in Dalseongaengmi-44 than in Dongjin under salt stress. The salt-sensitive Dalseongaengmi-44 exhibited a greater increase in sodium ion accumulation in its leaves than the salt tolerant Dongjin. Comparative analysis of the rice leaf proteins using two-dimensional gel electrophoresis (2-DGE) revealed that a total of 23 proteins were up-regulated under salt stress. Based on matrix-assisted laser desorption ionization-time of flight mass spectrometry and/or electrospray ionization-tandem mass spectrometry analyses, the 23 protein spots were found to represent 16 different proteins. Ten of the identified proteins were previously reported to be salt-responsive proteins, while six, class III peroxidase 29 precursor, beta-1,3-glucanase precursor, OSJNBa0086A10.7 (putative transcription factor), putative chaperon 21 precursor, Rubisco activase small isoform precursor and drought-induced S-like ribonuclease, were novel salt-induced proteins. Under salt stress, fragmentation was increased in several proteins containing the Rubisco large chain. The results of these physiological and proteomics analyses provide useful information that can lead to a better understanding of the molecular basis of salt-stress responses in rice.

Keywords : Polyethylene Glycol Fractionation; Proteomics; Rice Leaf; Na(+) Accumulation; Salt Tolerance; Antioxidant Responses; Oxidative Stress; Salinity

Article 249

Mouse model for hemolytic uremic syndrome induced by outer membrane vesicles of *Escherichia coli* O157:H7

FEMS Immunol Med Microbiol. 2011 Dec; 63(3):427-34.

Kim SH, Lee YH, Lee SH, Lee SR, Huh JW, Kim SU, Chang KT*

*Corresponding: changkt@kribb.re.kr
National Primate Research Center

Hemolytic uremic syndrome (HUS) is characterized by acute renal failure in children and is typically complicated with thrombocytopenia and hemolytic anemia. Although mouse models of HUS have been evaluated using Shiga toxin (STx) combined with or without lipopolysaccharide (LPS), no HUS model has been tested using purified outer membrane vesicles (OMVs) from STx-producing *Escherichia coli* (STEC) O157:H7. Accordingly, we investigated whether OMVs of STEC O157:H7 conveying STx2 and LPS can cause HUS-like symptoms in mice inoculated intraperitoneally. Three types of OMVs differing in LPS acylation status and STx2 amount were used to compare their ability to induce HUS-like symptoms. Native OMVs (nOMV) with fully hexa-acylated LPS caused HUS-like symptoms at 72-96 h after dually divided injections of 1 μg nOMV per animal. However, elevated doses of modified OMVs (mOMV) carrying mainly penta-acylated LPS were required to induce similar HUS signs. Moreover, mitomycin-C-induced OMVs (mcOMV) that were enriched with STx2 induced HUS-like symptoms similar to those of nOMV at the same dose. These results suggest that the OMVs of STEC O157:H7 potentiated with STx2 and fully hexa-acylated LPS can be utilized for inducing HUS-like symptoms in mice and could be the causative material involved in the development of HUS.
PMID: 22029600

Keywords : Hemolytic Uremic Syndrome; Lipopolysaccharide; Outer Membrane Vesicles; Shiga Toxin; O157-H7 Infection; Translocation; Strains; Mutant

Article 250

NADPH-dependent *pgi*-gene knockout *Escherichia coli* metabolism producing shikimate on different carbon sources

FEMS Microbiol Lett. 2011 Nov; 324(1):10-6.

Ahn J*, Chung BK, Lee DY, Park M, Karimi IA, Jung JK, Lee H

*First: ahnjo@kribb.re.kr
Biotechnology Process Engineering Center

We explored the physiological and metabolic effects of different carbon sources (glucose, fructose, and glucose/fructose mixture) in phosphoglucose isomerase (*pgi*) knockout *Escherichia coli* mutant producing shikimic acid (SA). It was observed that the *pgi*(-) mutant grown on glucose exhibited significantly lower cell growth compared with the *pgi*(+) strain and its mixed glucose/fructose fermentation grew well. Interestingly, when fructose was used as a carbon source, the *pgi*(-) mutant showed the enhanced SA production compared with the *pgi*(+) strain. *In silico* analysis of a genome-scale *E. coli* model was then conducted to characterize the cellular metabolism and quantify NAPDH regeneration, which allowed us to understand such experimentally observed attenuated cell growth and enhanced SA production in glucose- and fructose-consuming *pgi*(-) mutant, respectively with respect to cofactor regeneration.

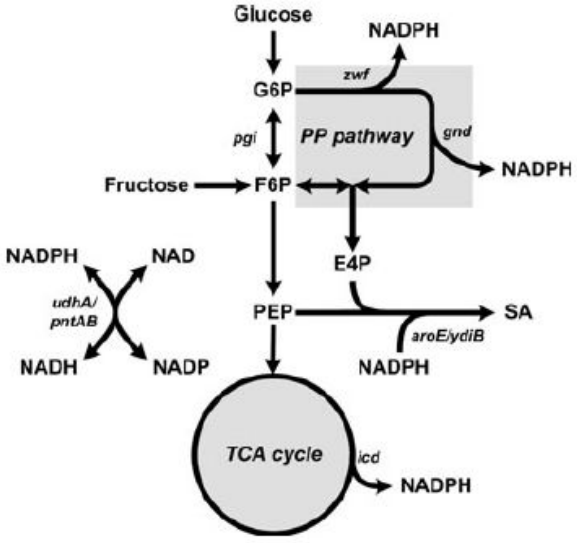

PMID: 22092758

Keywords : Phosphoglucose Isomerase; *Escherichia coli*; Shikimic Acid; NAPDH Regeneration; Genome-Scale *In silico* Model; Predictions; Network

Article 251

Supplementation with estradiol-17β improves porcine oocyte maturation and subsequent embryo development

Fertil Steril. 2011 Jun; 95(8):2582-4.

Kim JS, Song BS, Lee SR, Yoon SB, Huh JW, Kim SU, Kim E, Kim SH, Choo YK, Koo DB, Chang KT*

*Co-corresponding: changkt@kribb.re.kr
National Primate Research Center

Metaphase II oocyte production was significantly increased by treatment with E_2 during the first half of the total *in vitro* maturation (IVM) period, which was further evidenced by an increase in monospermic fertilization, blastocyst formation, or blastomere viability of IVF- or somatic cell nuclear transfer-derived embryos. Thus, we concluded that transient E_2 supplementation could improve the IVM rate and subsequent developmental competence in pigs.

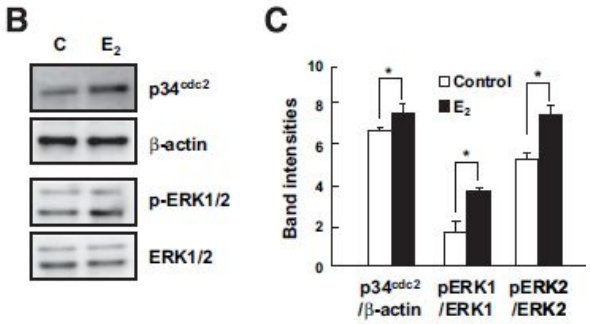

PMID: 21459376

Keywords : IVM; Pig Oocytes; Estradiol-17 beta; Embryo Development; IVF; SCNT; Fertilization; Nuclear

Article 252

Improvement of high-fat diet-induced obesity by a mixture of red grape extract, soy isoflavone and L-carnitine: implications in cardiovascular and non-alcoholic fatty liver diseases

Food Chem Toxicol. 2011 Sep; 49(9):2453-8.

Kang JS*, Lee WK, Lee CW*, Yoon WK, Kim N, Park SK, Lee HS, Park HK, Han SB, Yun J, Lee K, Lee KH, Park SK, Kim HM

*Co-first: kanjon@kribb.re.kr changwoo@kribb.re.kr
Bio-Evaluation Center

In the present study, we examined the effect of a mixture of dietary components, including red grape extract, soy isoflavone and L-carnitine (RISC), on obesity. RISC substantially inhibited high-fat diet (HFD)-induced increase in body weight in a dose-dependent manner in C57BL/6 mice. The amount of subcutaneous and mesenteric fat was also significantly decreased by RISC treatment in HFD-fed C57BL/6 mice, whereas epididymal fat was not affected. Moreover, HFD-induced plasma leptin levels were down-regulated by RISC treatment. In these mice, RISC treatment significantly increased the plasma level of high density lipoprotein cholesterol without affecting the level of low density lipoprotein cholesterol and triglycerides. In addition, HFD-induced increase in liver weight and lipid accumulation in liver was significantly suppressed by RISC treatment in C57BL/6mice. Plasma level of glutamic-oxaloacetic transaminase and glutamic-pyruvic transaminase was also inhibited by RISC treatment. These results demonstrate that RISC suppresses HFD-induced obesity and suggest that RISC supplementation might be a promising adjuvant therapy for the treatment of obesity and its complications, such as cardiovascular and non-alcoholic fatty liver diseases.

PMID: 21745528

Keywords : Red Grape; Soy Isoflavone; L-Carnitine; Obesity; 3T3-L1 Adipocytes; Mitochondrial-Function; Gene-Expression; Resveratrol; Genistein; Mice; Adipogenesis; Rats

Article 253

Identification and characterization of full-length *vps29* gene in five mammalian species

Genes Genom. 2011; 33(5):505-12.

Kim YH, Park SJ, Huh JW, Kim KM, Lee SR, Imakawa K, Chang KT*

*Corresponding: changkt@kribb.re.kr
National Primate Research Center

Retromer is a heteropentameric complex associated with retrograde transport of cargo protein from the endosome to the *trans*-Golgi network. The mammalian retromer complex consists of three *vps* genes (*vps26, vps35*, and *vps29*) and two sorting nexin genes (*snx1* and *snx2*). Previous studies had reported the protein sorting functions of retromer in the intracellular compartment. However, individual genes of retromer complex have not yet been fully characterized. In this study, we identified full-length *vps29* gene in human, crab-eating macaque, mouse, rat, and dog species. Total forty-four novel transcripts of *vps29*, including two actively expressed major transcripts, were identified by 5'-and 3'-RACE. Comparative analysis indicated that functionally important sites of the *vps29* gene were well conserved in the eukaryotic genome. However, two major transcript variants were occurred in the vertebrate genome only. From our results, we assumed that there are many different transcripts variants of *vps29* gene and specifically two major transcripts could play important roles in the protein sorting mechanism.

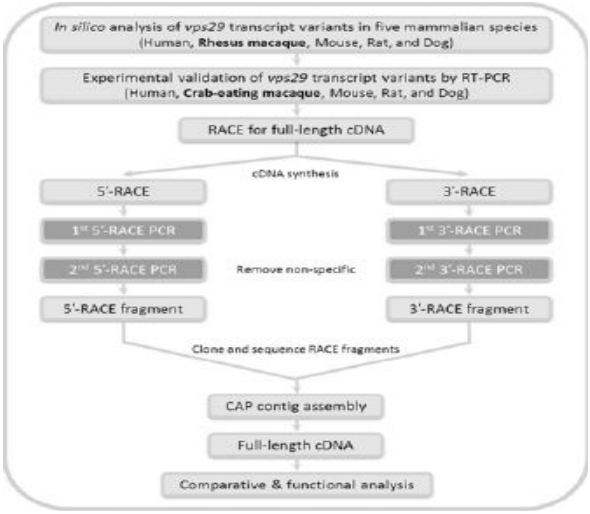

Keywords : *Vps29* Gene; Retromer Complex; Protein Sorting; Transcript Variants; Trans-Golgi Network; Retrograde Transport; Sorting Nexin-1; Shiga Toxin; Endosome; Yeast

Article 254

Novel major quantitative trait loci regulating the content of isoflavone in soybean seeds

Genes Genom. 2011; 33(6):685-92.

Yang K, Moon JK, Jeong N, Chun HK, Kang ST, Back K, Jeong SC*

*Corresponding: scjeong@kribb.re.kr
Bio-Evaluation Center

Despite their medicinal, pharmaceutical, and nutritional importance of isoflavones, the genetic basis controlling the amounts of isoflavones in soybean seeds is still not well understood. The main obstacle is the great variability in the content of isoflavone in seeds harvested from different environments. In this study, quantitative trait loci (QTL) for the content of different isoflavones including daidzein, genistein, and glycitein were investigated in a population of recombinant inbred lines derived from the cross of "Hwangkeum" (*Glycine max*) by "IT182932" (*Glycine soja*). Seeds analyzed were harvested in three different experimental environments. QTL analyses for isoflavone content were conducted by composite interval mapping across a genomewide genetic map. Two major QTL were mapped to soybean chromosomes 5 and 8, which were designated *QDZGT1* and *QDZGT2*, respectively. Both loci have not been previously reported in other isoflavone sources. The results from this study will be useful in cloning genes that can control the contents of isoflavones in soybean and for the development of soybean lines containing a high or low isoflavone content.

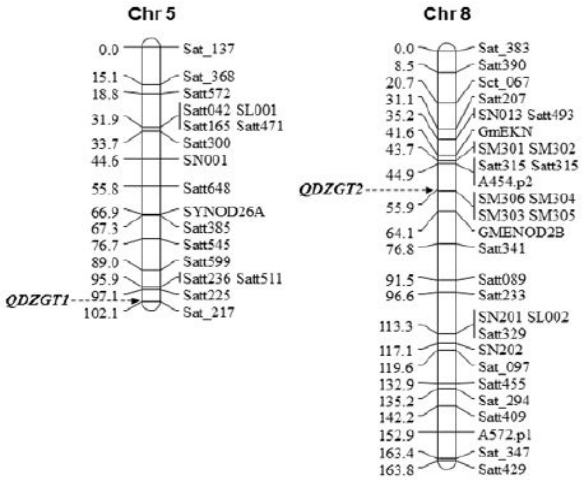

Keywords : Environment; Isoflavone; Quantitative Trait Locus; Seed; Soybean; Glycine-Max; QTL; Biosynthesis; Inoculation; Genotype; Variety

Article 255

Spatial distribution of glucose hypometabolism induced by intracerebroventricular streptozotocin in monkeys

J Alzheimers Dis. 2011; 25(3):517-23.

Heo JH, Lee SR, Lee ST, Lee KM, Oh JH, Jang DP, Chang KT*, Cho ZH

*Co-corresponding: changkt@kribb.re.kr
National Primate Research Center

Intracerebroventricular injection of streptozotocin (icv-STZ) in rodents induces cellular and behavioral features mimicking Alzheimer's disease (AD). However, the effect of icv-STZ in terms of regional cerebral glucose metabolism has not yet been examined *in vivo*. Given that regionally specific hypometabolism of glucose is a consistent neuroimaging marker in early AD, we monitored 18F-deoxyglucose uptake using a high-resolution micro-PET after icv-STZ in non-human primates. Two cynomolgus monkeys (Macaca fascicularis) received STZ (2 mg/kg), and another two were given normal saline as controls, at the cerebellomedullary cistern (CM) three times (day 1, 7, and 14). FDG-PET, as well as MRI for structural evaluation, was performed immediately before, six weeks after, and 12 weeks after the first icv injection. In the STZ group, FDG uptake decreased significantly in comparison to the pre-injection baseline, at the precuneus, the posterior cingulate, and medial temporal cortices. Increase in sulcal markings suggesting brain atrophy was observed by MRI at six weeks post-injection. The structural changes normalized at 12 weeks, but the reduced FDG uptake persisted at the same loci. The cortical distribution of glucose hypometabolism was similar to that at early stages of AD patients. The findings demonstrate that the effect of icv-STZ is regionally specific, lending further support for the method as a model of AD pathogenesis.
PMID: 21471644

Keywords : Sporadic Alzheimers Disease; Cynomolgus; Streptozotocin-Induced AD Model; Hyperphosphorylated Tau-Protein; Insulin; Pet

Article 256

Ependymal cyst in the cerebrum of an African green monkey (*Chlorocebus aethiops*)

J Comp Pathol. 2011 Aug; 145(2-3):235-9.

Chang KS, Lee SR, Kim SW, Cho ZH, Son HY, Kim D, Chang KT*

*Corresponding: changkt@kribb.re.kr
National Primate Research Center

A focal lesion was detected by magnetic resonance imaging in the right caudal occipital lobe of the cerebrum in an African green monkey (*Chlorocebus aethiops*). Neurological signs were not observed in this animal. At necropsy examination, an 8mm wedge-shaped intracranial cavity was found, which apparently did not communicate with the ventricles. Microscopically, the inner surface of the cavity was lined by ciliated cuboidal epithelium with positive immunoreactivity for S100 protein, glial fibrillary acidic protein and cytokeratin. Based on the gross, microscopical and immunohistochemical findings the lesion was classified as an ependymal cyst. To the best of our knowledge, this is the first report of an ependymal cyst in an African green monkey.
PMID: 21388637

Keywords : African Green Monkey; *Chlorocebus aethiops*; Cerebrum; Ependymal Cyst; Necropsy Examination

Article 257

Vitamin D3 up-regulated protein 1 deficiency accelerates liver regeneration after partial hepatectomy in mice

J Hepatol. 2011 Jun; 54(6):1168-76.

Kwon HJ, Won YS, Yoon YD, Yoon WK, Nam KH, Choi IP, Kim DY, Kim HC*

*Co-corresponding: hckim@kribb.re.kr
Biomedical Mouse Resource Center

BACKGROUND & AIMS: Liver regeneration is a complicated process involving a variety of interacting factors. Vitamin D3 up-regulated protein 1 (VDUP1) is a potent growth suppressor that, upon over-expression, inhibits tumor cell proliferation and cell-cycle progression. Here, we investigated the function of VDUP1 in liver regeneration following hepatectomy in mice.
METHODS: Liver regeneration after 70% partial hepatectomy (PH) was compared in *VDUP1* knockout (KO) and wild-type (WT) mice, and the activities of proliferative- and cell-cycle-related signaling pathways were measured.
RESULTS: Compared with WT mice, liver recovery was significantly accelerated in *VDUP1* KO mice during the first day after PH, in association with increased DNA synthesis. Consistent with this observation, the expression levels of key cell-cycle regulatory proteins, including cyclin D, cyclin E, cyclin-dependent kinase 4 (CDK4), p21, and p27, were markedly altered in the livers of *VDUP1* KO mice. Induction of growth factors and activation of proliferative signaling pathway components including extracellular signal-regulated kinase 1/2 (ERK1/2), Akt, glycogen synthase kinase 3β (GSK3β), mammalian target of rapamycin (mTOR), and p70S6 kinase ($p70^{S6K}$), occurred much earlier and to a greater extent in *VDUP1* KO mouse livers. In addition, primary hepatocytes isolated from *VDUP1* KO mice displayed increased activation of ERK1/2 and Akt in response to HGF and TGF-α.
CONCLUSIONS: Our results reveal an important role for VDUP1 in the regulation of proliferative signaling during liver regeneration. Altered activation of genes involved in ERK1/2 and Akt signaling pathways may explain the accelerated growth responses seen in *VDUP1* KO mice.
PMID: 21145821

Keywords : Akt; ERK1/2; Growth Factor; Liver Regeneration; VDUP1; Hepatocellular-Carcinoma; Oxidative Stress; Kinase; Progression; Proliferation

Article 258

High Genetic Differentiation in Endangered *Sedum ussuriense* and Implications for Its Conservation in Korea

J Plant Biol. 2011; 54(4):262-8.

Ku YB, Oh HK, Chun YJ*, Cho KH

*Co-corresponding: youngjinchun@gmail.com
Bio-Evaluation Center

Sedum ussuriense Kom. (Crassulaceae) is a succulent perennial herb localized to rocky valleys in southeastern Korea. Although it is an important natural resource with high economic value as an ornamental plant, it is currently endangered because of land-use changes and illegal exploitation. To initiate a proper conservation plan, we selected four populations (Juwang, Okgye, Jeolgol, and Haok) around Mt. Juwang, characterized their phenotypic traits, and evaluated patterns of random amplified polymorphic DNA variation. Despite its small population size, Okgye had the greatest proportion of flowering plants and higher seed production than from the other populations. This population also harbored the greatest genetic diversity. However, recent fragmentation between Okgye and Haok appeared to cause genetic divergence, leading to close genetic relationships of Okgye to Juwang vs. Haok to Jeolgol. In the long term, this raises concerns about the loss of genetic variation and the possibility of a demographic crash in those fragmented populations. Because our results indicated a high degree of divergence among populations, we suggest that conservation activities should focus on maintaining and propagating all populations throughout this species' range.

Keywords : Genetic Diversity; Habitat Fragmentation; RAPD; Rare Species; Population-Size; Inbreeding Depression; Diversity; Plant; Fitness

Article 259

Adaptive divergence for a fitness-related trait among invasive *Ambrosia artemisiifolia* populations in France

Mol Ecol. 2011 Apr; 20(7):1378-88.

Chun YJ*, LE Corre V, Bretagnolle F

*Corresponding: youngjinchun@gmail.com
Bio-Evaluation Center

The impact of natural selection on the adaptive divergence of invasive populations can be assessed by testing the null hypothesis that the extent of quantitative genetic differentiation (Q_{ST}) would be similar to that of neutral molecular differentiation (F_{ST}). Using eight microsatellite loci and a common garden approach, we compared Q_{ST} and F_{ST} among ten populations of an invasive species *Ambrosia artemisiifolia* (common ragweed) in France. In a common garden study with varying water and nutrient levels, we measured Q_{ST} for five traits (height, total biomass, reproductive allocation, above- to belowground biomass ratio, and days to flowering). Although low F_{ST} indicated weak genetic structure and strong gene flow among populations, we found significant diversifying selection (Q_{ST} > F_{ST}) for reproductive allocation that may be closely related to fitness. It suggests that abiotic conditions may have exerted selection pressure on *A. artemisiifolia* populations to differentiate adaptively, such that populations at higher altitude or latitude evolved greater reproductive allocation. As previous studies indicate multiple introductions from various source populations of *A. artemisiifolia* in North America, our results suggest that the admixture of introduced populations may have increased genetic diversity and additive genetic variance, and in turn, promoted the rapid evolution and adaptation of this invasive species.
PMID: 21306459

Keywords : Diversifying Selection; F_{ST} And Q_{ST}; Invasive Species; Quantitative Trait; Common Ragweed; Genetic Differentiation; Local Adaptation; Clinal Variation

Article 260

Quantitative analysis of retromer complex-related genes during embryo development in the mouse

Mol Cells. 2011 May; 31(5):431-6.

Park SJ, Huh JW, Kim YH, Kim JS, Song BS, Lee SR, Kim SU, Kim HS, Imakawa K, Chang KT*

*Corresponding: changkt@kribb.re.kr
National Primate Research Center

The retromer complex is a heteropentameric protein unit associated with retrograde transport of cargo proteins from endosomes to the *trans*-Golgi network. Functional silencing study of the Vps26a gene indicated the important role of the retromer complex during early developmental stages in the mouse. However, individual expression patterns and quantitative analysis of individual members of the retromer complex during the early developmental stages has not been investigated. In this study, we conducted quantitative expression analysis of six retromer complex genes (*Vps26a, Vps26b, Vps29, Vps35, Snx1*, and *Snx2*) and one related receptor gene (*Ci-mpr*) during the eleven embryonic stages with normal MEF (mouse embryonic fibroblast) and Vps26a(-/-) MEF cells. Remarkably, except for *Vps26a* (maternal expression pattern), all tested genes showed maternal-zygotic expression patterns. And five genes (*Vps26b, Vps29, Vps35, Snx2*, and *Ci-mpr*) showed a pattern of decreased expression in Vps26a(-/-) MEF cells by comparative analysis between normal MEF and Vps26a(-/-) MEF cells. However, the *Snx1* gene showed a pattern of increased expression in Vps26a(-/-) MEF cells. From our results, we could assume that retromer complex-related genes have important roles during oocyte development. However, in the preimplantation stage, they did not have significant roles.
PMID: 21359680

Keywords : Mouse Embryonic Fibroblast; rt-PCR; Retromer Complex; Mammalian Retromer; Sorting Nexin-1; Alzheimers Disease; Yeast; Endosomes

Article 261

Proteomic analysis of phosphotyrosyl proteins in human embryonic stem cell-derived neural stem cells

Neurosci Lett. 2011 Jul; 499(3):158-63.

Kim J, Kim JS*, Kim HE, Jeon YJ, Kim DW, Soh Y, Seo KS, Lee HK, Choi NJ, Chung HM, Lee DS, Chae JI

*Co-first: vjman@kribb.re.kr
National Primate Research Center

Phosphorylation can reveal essential cell functions, such as cell differentiation, signal transduction, metabolic maintenance and cell division. The aim of this study was to investigate phosphorylated protein expression changes during neuronal lineage differentiation from hESCs. To measure the phosphorylated protein expression change during neuronal differentiation, we performed a comparative phosphoproteome analysis using 2-DE after MALDI-TOF MS and an MS/MS protein identification method, making a comparison between neural lineage differentiating cells and normal embryoid bodies (EBs) differentiated from human embryonic stem cells (hESCs) and profiling constituent phosphorylated proteins. Of 36 differentially expressed protein spots, 12 spots were shown to be up-regulated in differentiating neural cells. Specifically, the 7 up-regulated proteins of the 12 have potential roles in neuronal differentiation or neuronal damage recovery, including ACTB, heterogeneous nuclear ribonucleoprotein A2B1 (hnRNP A2B1), heterogeneous nuclear ribonucleoprotein L (hnRNP L), SET, chaperonin-containing TCP-1, vimentin and voltage-dependent anion channel protein 1 (VDAC1). These proteins are discussed further below.

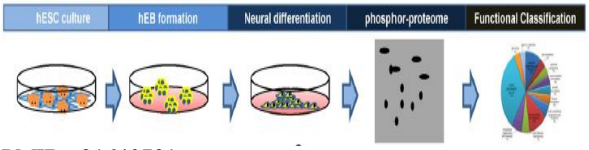

PMID: 21640791

Keywords : Human Embryonic Stem Cell; Neural Stem Cell; Proteomic Analysis; Phosphotyrosyl Protein; Chaperonin; TCP-1

Article 262

A combination of grape extract, green tea extract and L-carnitine improves high-fat diet-induced obesity, hyperlipidemia and non-alcoholic fatty liver disease in mice

Phytother Res. 2011 Dec; 25(12):1789-95.

Kang JS*, Lee WK, Yoon WK*, Kim N, Park SK, Park HK, Ly SY, Han SB, Yun J, Lee CW, Lee K, Lee KH, Park SK, Kim HM

*Co-first: kanjon@kribb.re.kr ykyoon@kribb.re.kr
Bio-Evaluation Center

To develop a therapeutic agent for obesity-related metabolic disorders, a mixture of dietary components was prepared, including grape extract, green tea extract and L-carnitine (RGTC), and its effects on obesity, hyperlipidemia and non-alcoholic fatty liver disease examined. The RGTC dramatically inhibited the high-fat diet (HFD)-induced increase in body weight and fat in C57BL/6 mice, whereas food consumption was not affected by RGTC treatment. The RGTC also concentration-dependently suppressed the HFD-induced increase in plasma lipids, such as low-density lipoprotein cholesterol and triglycerides. In addition, increases in liver weight and liver steatosis were returned to normal by RGTC treatment in HFD-fed C57BL/6 mice. The plasma levels of glutamic-oxaloacetic transaminase and glutamic-pyruvic transaminase were also significantly down-regulated by RGTC treatment. These results suggest that RGTC suppressed HFD-induced obesity, hyperlipidemia and non-alcoholic fatty liver disease, suggesting that RGTC supplementation might be a promising adjuvant therapy for the treatment of these metabolic disorders.

PMID: 21480410

Keywords : Grape Extract; Green Tea Extract; L-Carnitine; High-Fat Diet; Hyperlipidemia; Fatty Liver Disease; Metabolic Syndrome; Resveratrol; Catechins; Adipogenesis; Quercetin

Article 263

Gene flow from herbicide-tolerant GM rice and the heterosis of GM rice-weed F2 progeny

Planta. 2011 Apr; 233(4):807-15.

Chun YJ, Kim DI, Park KW, Kim HJ, Jeong SC, An JH, Cho KH, Back K, Kim HM, Kim CG*

*Co-corresponding: cgkim@kribb.re.kr
Bio-Evaluation Center

Gene flow from genetically modified (GM) crops to non-GM cultivars or weedy relatives may lead to the development of more aggressive weeds. We quantified the amount of gene flow from herbicide-tolerant GM rice (*Protox* GM, derived from the cultivar Dongjin) to three cultivars (Dongjin, Aranghyangchal and Hwaseong) and a weedy rice line. Gene flow frequency generally decreased with increasing distance from the pollen donor. At the shortest distance (0.5 m), we observed a maximum frequency (0.039%) of gene flow. We found that the cultivar Dongjin received the greatest amount of gene flow, with the second being weedy rice. Heterosis of F2 inbred progeny was also examined between *Protox* GM and weedy rice. We compared growth and reproduction between F2 progeny (homozygous or hemizygous for the *Protox* gene) and parental rice lines (GM and weedy rice). Here, transgene-homozygous F2 progeny was significantly taller and produced more seeds than the transgene-hemizygous F2 progeny and parental lines. Although the gene flow frequency was generally low, our results suggest that F2 progeny between GM and weedy relatives may exhibit heterosis.
PMID: 21212977

Keywords : Genetically Modified; Heterosis; Transgenic Rice; Risk Assessment; Transgene; Xanthus Protoporphyrinogen Oxidase; *Oryza sativa* L.; Bifunctional Fusion; Field-Evaluation

Article 264

Effect of Bcl-xL overexpression on erythropoietin production in recombinant Chinese hamster ovary cells treated with dimethyl sulfoxide

Process Biochem. 2011; 46(11):2201-4.

Kim YG, Kim JY, Park B, Ahn JO, Jung JK, Lee HW, Lee GM, Lee EG*

*Co-corresponding: eglee@kribb.re.kr
Biotechnology Process Engineering Center

Dimethyl sulfoxide (DMSO) can increase the specific productivity (q) of foreign proteins in mammalian cells, while it can also induce cell death, particularly apoptosis. Bcl-xL is a typical anti-apoptotic protein that inhibits the apoptosis in recombinant Chinese hamster ovary (rCHO) cell culture. To evaluate the potential role of Bcl-xL overexpression on DMSO-mediated erythropoietin (EPO) production, we used EPO-producing rCHO cells with regulated Bcl-xL overexpression (EPO-off-Bcl-xL) by doxycycline. Although DMSO addition enhanced specific EPO productivity (q_{EPO}), it also induced cell death in EPO-off-Bcl-xL cells. Bcl-xL overexpression reduced the DMSO-induced cell death followed by release of various enzymes from plasma membrane-damaged cells as evidenced from LDH assay, resulting in delayed loss of EPO. However, it did not significantly improve the maximum EPO production. In addition, Bcl-xL overexpression suppressed DMSO-induced apoptosis, characterized by DNA fragmentation and Annexin V staining. Taken together, Bcl-xL overexpression could inhibit DMSO-induced apoptosis, thereby delaying the loss of EPO.

Keywords : Dimethyl Sulfoxide; Bcl-xL; Apoptosis; rCHO Cells; Inducible Expression; Surface-Antigen Expression; Antithrombin-Iii; Kinetics; Antibody

Article 265

Identification of maturation and protein synthesis related proteins from porcine oocytes during *in vitro* maturation

Proteome Sci. 2011 Jun; 9:28.

Kim J, Kim JS*, Jeon YJ, Kim DW, Yang TH, Soh Y, Lee HK, Choi NJ, Park SB, Seo KS, Chung HM, Lee DS, Chae JI

*Co-first: vjman@kribb.re.kr
National Primate Research Center

BACKGROUND: *In vitro* maturation (IVM) of mammalian oocytes is divided into the GV (germinal vesicle stage), MI (metaphase I stage) and MII (metaphase II stage) stages, and only fully mature oocytes have acquired the ability to be fertilized and initiate zygotic development. These observations have been mostly based on morphological evaluations, but the molecular events governing these processes are not fully understood.The aim of the present study was to better understand the processes involved in the molecular regulation of IVM using 2-DE analysis followed by mass spectrometry to identify proteins that are differentially expressed during oocyte IVM.
RESULT: A total of 16 up-regulated and 12 down-regulated proteins were identified. To investigate the IVM process, we specifically focused on the proteins that were up-regulated during the MII stage when compared with the GV stage, which included PRDX 2, GST, SPSY, myomegalin, PED4D, PRKAB 1, and DTNA. These up-regulated proteins were functionally involved in redox regulation and the cAMP-dependent pathway, which are essential for the intracellular signaling involved in oocyte maturation. Interestingly, the PDE4D and its partner, myomegalin, during the MII stage was consistently confirmed up-regulation by western blot analyses.
CONCLUSION: These results could be used to better understand some aspects of the molecular mechanisms underlying porcine oocyte maturation. This study identified some regulatory proteins that may have important roles in the molecular events involved in porcine oocyte maturation, particularly with respect to the regulation of oocyte meiotic resumption, MII arrest and oocyte activation. In addition, this study may have beneficial applications not only to basic science with respect to the improvement of oocyte culture conditions but also to mammalian reproductive biotechnology with potential implications.
PMID: 21649931

Keywords : Porcine Oocytes; Pig Oocytes; *In vitro* Maturation; Proteomics; Meiotic Maturation; Kinase A; Expression; Phosphodiesterase; Subunits

Article 266

Inactivated Sendai-virus-mediated fusion improves early development of cloned bovine embryos by avoiding endoplasmic-reticulum-stress-associated apoptosis

Reprod Fertil Dev. 2011; 23(6):826-36.

Song BS, Kim JS, Yoon SB, Lee KS, Koo DB, Lee DS, Choo YK, Huh JW, Lee SR, Kim SU, Kim SH, Kim HM, Chang KT*

*Corresponding: changkt@kribb.re.kr
National Primate Research Center

Somatic cell nuclear transfer (SCNT) is a powerful tool, not only for producing cloned animals, but also in revealing various early developmental events. However, relatively little is known regarding the biological events and underlying mechanism(s) directly associated with early development of SCNT embryos. Here, we show that production of high-quality bovine SCNT blastocysts is dependent on the method used for fusion and the associated reduction in endoplasmic reticulum (ER) stress. During fusion between the donor cell and the enucleated oocyte, electrofusion triggers spontaneous oocyte activation, accompanied by an increase in intracellular Ca^{2+} and improper nuclear remodelling. These events can be greatly reduced by the use of Sendai virus (SV)-mediated fusion. Moreover, SV-SCNT improves the blastulation rate and blastocyst quality, defined by the number and ratio of inner cell mass and trophectoderm cells in each blastocyst, in comparison with electrofusion-mediated SCNT (E-SCNT). Interestingly, expression of ER-stress-associated genes and blastomere apoptosis were significantly increased in E-SCNT embryos. These increases could be reversed by inhibition of ER stress or by using the SV-mediated fusion method. Collectively, these results indicate that SV-mediated fusion improves the developmental competence and quality of SCNT blastocysts, by reducing ER-stress-associated apoptosis.
PMID: 21791184

Keywords : Electrofusion; Somatic Cell Nuclear Transfer; Unfolded Protein Response; Inner Cell Mass; Enucleated Oocytes; Pig Embryos; Stem Cell; Fertilization

Article 267

Fine genetic mapping of the genomic region controlling leaflet shape and number of seeds per pod in the soybean

Theor Appl Genet. 2011 Mar; 122(5):865-74.

Jeong N, Moon JK, Kim HS, Kim CG, Jeong SC*

*Corresponding: scjeong@kribb.re.kr
Bio-Evaluation Center

Narrow leaflet cultivars tend to have more seeds per pod than broad leaflet cultivars in soybean [*Glycine max* (L.) Merr.], which suggests that the leaflet-shape trait locus is tightly linked to or cosegregates with the trait locus controlling the number of seeds per pod (NSPP). Here, we attempted to further elucidate the relationship between leaflet shape and NSPP. A BC(3)F(2) population from a cross between the 'Sowon' (narrow leaflets and high NSPP) and 'V94-5152' (broad leaflets and low NSPP) variants was used. The results of the molecular genetic analyses indicated that, although the NSPP characteristic, in particular, the occurrence of 4-seeded pods, is governed by additional modifying genes that are likely present in Sowon, the two traits cosegregate in the BC_3F_2 population. The mapping results generated using public markers demonstrated that the narrow leaflet-determining gene in Sowon is an allele of the previously highly studied *ln* gene on chromosome 20. A high-resolution map delimited the genomic region controlling both the leaflet shape and NSPP traits to a sequence length of 66 kb, corresponding to 0.7 cM. Among the three genes annotated in this 66 kb region, Glyma20g25000.1 appeared to be a good candidate for the *Ln*-encoding gene, owing to its 47.8% homology with the protein encoding for the *JAGGED* gene that regulates lateral organ development in *Arabidopsis*. Taken together, our results suggested that phenotypic variations for narrow leaflet and NSPP are predominantly from the pleiotropic effects of the *ln* gene. Thus, our results should provide a molecular framework for soybean breeding programs with the objective of improving soybean yield.

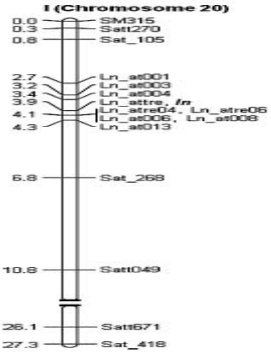

PMID: 21104397

Keywords : Linkage Map; Yield; Inheritance; Population; Mutant; PEA; Soybean; Number of Seeds Per Pod (NSPP)

Article 268

Glycine max non-nodulation locus *rj1*: a recombinogenic region encompassing a SNP in a lysine motif receptor-like kinase (*GmNFR1α*)

Theor Appl Genet. 2011 Mar; 122(5):875-84.

Lee WK, Jeong N, Indrasumunar A, Gresshoff PM, Jeong SC*

*Corresponding: scjeong@kribb.re.kr
Bio-Evaluation Center

The *rj1* mutation of soybean is a simple recessive allele in a single line that arose as a spontaneous mutation in a population; it exhibits non-nodulation with virtually all *Bradyrhizobium* and *Sinorhizobium* strains. Here, we described fine genetic and physical mapping of the *rj1* locus on soybean chromosome 2. The initial mapping of the *rj1* locus using public markers indicated that A343.p2, a sequence-based marker that contains sequence similar to a part of the *LjNFR1* gene regulating nodule formation as a member of lysin motif-type receptor-like kinase (LYK) family, maps very close to or cosegregates with the *rj1* locus. The sequence of A343.p2 is 100% identical to parts of two BAC clone sequences (GM_WBb0002O19 and GM_WBb098N11) that contain three members of the *LYK* family. We analyzed the sequence contig (262 kbp) of the two BAC clones by resequencing and subsequent fine genetic and physical mapping. The results indicated that *rj1* is located in a gene-rich region with a recombination rate of 120 kbp/cM: several fold higher than the genome average. Among the *LYK* genes, *NFR1α* is most likely the gene encoded at the *Rj1* locus. The non-nodulating *rj1* allele was created by a single base-pair deletion that results in a premature stop codon. Taken together, the fine genetic and physical mapping of the *Rj1*-residing chromosomal region, combined with the unexpected observation of a putative recombination hotspot, allowed us to demonstrate that the *Rj1* locus most likely encodes the *NFR1α* gene.

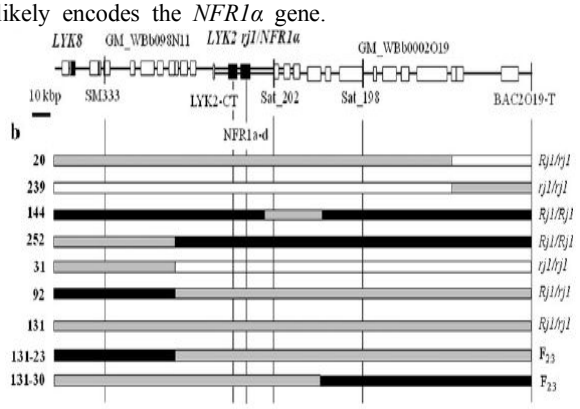

PMID: 21104396

Keywords : Genetic-Linkage Map; Meiotic Recombination; *Medicago truncatula*; *Rhizobium japonicum*; *Lotus japonicus*; Est Databases; Lysm Domain; L Merr; Mutants; Resistance

Article 269

Adjuvant effect of bacterial outer membrane vesicles with penta-acylated lipopolysaccharide on antigen-specific T cell priming

Vaccine. 2011 Oct; 29(46):8293-301.

Lee DH, Kim SH, Kang W, Choi YS, Lee SH, Lee SR, You S, Lee HK, Chang KT*, Shin EC

*Co-corresponding: changkt@kribb.re.kr
National Primate Research Center

Outer membrane vesicles (OMV) are nano-sized spherical blebs shed by Gram-negative bacteria and have been utilized in vaccine development. In the present study, we evaluated T cell adjuvant activity of OMV with strictly penta-acylated LPS produced by Δ*msbB*/Δ*pagP* mutant of non-pathogenic *Escherichia coli* W3110 (mOMV) compared to OMV with hexa-acylated LPS produced by wild-type *E. coli* W3110 (wOMV). Penta-acylation of LPS renders mOMV less endotoxic than wOMV in *in vitro* and *in vivo* toxicity assays. In mice, mOMV has adjuvant activity on T cell priming not only in KLH protein immunization but also in SIINFEKL peptide immunization. The T-cell adjuvant activity of mOMV was comparable to that of wOMV and LPS and was abrogated in TLR4 K/O mice. In innate immunity, mOMV stimulated BMDCs to up-regulate co-stimulatory and antigen-presenting molecules and to produce pro-inflammatory cytokines in a TLR4-dependent manner. Of note, mOMV induced cytokine production at a significantly less extent compared with wOMV. Taken together, we propose that mOMV with penta-acylated LPS is a safe vaccine adjuvant for T cell priming and can be used in vaccine development against viral diseases and cancer.
PMID: 21893142

Keywords : Adjuvant; Outer Membrane Vesicles; Penta-Acylated Lps; T Cells; O157-H7; *Neisseria meningitidis*; Mutant Strains; Shiga Toxin; Vaccine; Typhimurium

Article 270

Identification of novel immunogenic proteins in pathogenic *Haemophilus parasuis* based on genome sequence analysis

Vet Microbiol. 2011 Feb; 148(1):89-92.

Hong M, Ahn J, Yoo S, Hong J, Lee E, Yoon I, Jung JK, Lee H*

*Corresponding: hwlee12@kribb.re.kr
Biotechnology Process Engineering Center

Haemophilus parasuis causes contagious porcine Glässer's disease, which is occurring worldwide and leads to severe losses in the pig industry. To identify novel antigen candidates against this disease, 22 surface-exposed or secreted proteins were selected from the annotated *H. parasuis* genome by reverse vaccinology strategy. Expression of these proteins in *Escherichia coli* was attempted. Immunogenicity of the expressed candidates was assessed using Western blot analysis with mouse-derived antiserum prepared with whole bacteria of *H. parasuis* serovar 4 or 5. Three ABC-type transporters (OppA, YfeA and PlpA) and 1 curli protein assembly (CsgG) were identified as potent immunogenic proteins. The proteins show cross-reactions when tested with sera raised against serovars 4 and 5 of *H. parasuis*.
PMID: 20817421

Keywords : *Haemophilus parasuis*; Reverse Vaccinology; Antigenic Protein; Outer Membrane Proteins; Virulence; Iron

Article 271

Herbicidal action of clove oil on cucumber seedlings

Weed Biol Manag. 2011; 11(4):235-40.

Park KW*, Choi SH, Ahn JY, Sohn YG, Kim CG, Lee JJ

*First: park@kribb.re.kr
Bio-Evaluation Center

The herbicidal action of clove oil on cucumber seedlings was characterized under light and dark conditions. Paraquat showed herbicidal activity only under the light condition, whereas the clove oil displayed herbicidal activity in both the light and the dark condition. Specifically, wilting and water content reduction progressed rapidly under both the light and the dark condition 1 h after the clove oil treatment, whereas the paraquat damage occurred only under the light condition 5 h after treatment. The malondialdehyde concentration increased more with the clove oil treatment than with the paraquat treatment under the light and dark conditions. The superoxide dismutase (SOD) activity was stimulated, but the catalase activity decreased in the clove oil treatment. In contrast, both the SOD and catalase activity decreased in the paraquat treatment. These results suggest that clove oil exerts herbicidal effects through a mechanism that is different from that of paraquat.

Keywords : Catalase; Clove Oil; Malondialdehyde; Reactive Oxygen Species; Superoxide Dismutase; Stress; Phytotoxicity; Chloroplasts; Antioxidants; Metabolism; Enzymes

2011
KRIBB Article Abstracts
Corresponding Articles
Indexed in SCIE

Bio-Materials Research Institute

- Applied Microbiology Research Center
- Infection Control Material Research Center
- Bioindustrial Process Research Center

Korea Research Institute of Bioscience and Biotechnology


KRIBB
www.kribb.re.kr

Article 272

Production of lipids containing high levels of docosahexaenoic acid by a newly isolated microalga, *Aurantiochytrium* sp. KRS101

Appl Biochem Biotechnol. 2011 Aug; 164(8):1468-80.

Hong WK, Rairakhwada D, Seo PS, Park SY, Hur BK, Kim CH, Seo JW*

*Corresponding: jwseo@kribb.re.kr
Applied Microbiology Research Center

In the present study, a novel oleaginous Thraustochytrid containing a high content of docosahexaenoic acid (DHA) was isolated from a mangrove ecosystem in Malaysia. The strain identified as an *Aurantiochytrium* sp. by 18S rRNA sequencing and named KRS101 used various carbon and nitrogen sources, indicating metabolic versatility. Optimal culture conditions, thus maximizing cell growth, and high levels of lipid and DHA production, were attained using glucose (60 g l^{-1}) as carbon source, corn steep solid (10 g l^{-1}) as nitrogen source, and sea salt (15 g l^{-1}). The highest biomass, lipid, and DHA production of KRS101 upon fed-batch fermentation were 50.2 g l^{-1} (16.7 g l^{-1} day^{-1}), 21.8 g l^{-1} (44% DCW), and 8.8 g l^{-1} (40% TFA), respectively. Similar values were obtained when a cheap substrate like molasses, rather than glucose, was used as the carbon source (DCW of 52.44 g l^{-1}, lipid and DHA levels of 20.2 and 8.83 g l^{-1}, respectively), indicating that production of microbial oils containing high levels of DHA can be produced economically when the novel strain is used.
PMID: 21424706

Keywords : *Aurantiochytrium* sp.; Heterotrophic Microalga; Lipid; Docosahexaenoic Acid; Yeast Rhodosporidium Toruloides; *Schizochytrium limacinum* SR21; Biodiesel Production

Article 273

Identification and characterization of the propanediol utilization protein PduP of *Lactobacillus reuteri* for 3-hydroxypropionic acid production from glycerol

Appl Microbiol Biotechnol. 2011 Feb; 89(3):697-703.

Luo LH, Seo JW, Baek JO, Oh BR, Heo SY, Hong WK, Kim DH, Kim CH*

*Corresponding: kim3641@kribb.re.kr
Applied Microbiology Research Center

Although the de novo biosynthetic mechanism of 3-hydroxypropionic acid (3-HP) in glycerol-fermenting microorganisms is still unclear, the propanediol utilization protein (PduP) of *Lactobacillus* species has been suggested to be a key enzyme in this regard. To verify this hypothesis, a pduP gene from *Lactobacillus reuteri* was cloned and expressed, and the encoded protein was characterized. Recombinant *L. reuteri* PduP exhibited broad substrate specificity including 3-hydroxypropionaldehyde and utilized both NAD^+ and $NADP^+$ as a cofactor. Among various aldehyde substrates tested, the specific activity was highest for propionaldehyde, at pH 7.8 and 37 °C. The K_m and V_{max} values for propionaldehyde in the presence of NAD^+ were 1.18 mM and 0.35 U mg^{-1}, respectively. When *L. reuteri* pduP was overexpressed in *Klebsiella pneumoniae*, 3-HP production remarkably increased as compared to the wild-type strain (from 0.18 g L^{-1} to 0.72 g L^{-1}) under shake-flask culture conditions, and the highest titer (1.38 g L^{-1} 3-HP) was produced by the recombinant strain under batch fermentation conditions in a bioreactor. This is the first report stating the enzymatic properties of PduP protein and the probable role in biosynthesis of 3-HP in glycerol fermentation.

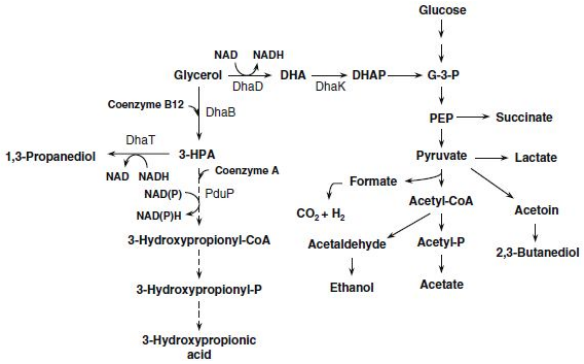

PMID: 20890600

Keywords : Glycerol; 3-Hydroxypropionic Acid; *Klebsiella pneumoniae*; *Lactobacillus reuteri*; Propanediol Utilization Protein Pdup; 1,3-Propanediol; Strain

Article 274

A novel bifunctional endo-/exo-type cellulase from an anaerobic ruminal bacterium

Appl Microbiol Biotechnol. 2011 Mar; 89(5):1453-62.

Ko KC, Han Y, Choi JH, Kim GJ, Lee SG, Song JJ*

*Corresponding: jjsong@kribb.re.kr
Applied Microbiology Research Center

An anaerobic microorganism termed *AN-C16-KBRB* was isolated from the bovine rumen and demonstrated cellulolytic activity on a NB agar plate containing azo-carboxymethyl cellulose. The 16S rRNA gene of the strain was 98% similar to that of Clostridiaceae bacterium SK082 (AB298754) as the highest homology. A novel *celEdx16* gene encoding a bifunctional endo-/exocellulase (CelEdx16) was cloned by the shotgun method from *AN-C16-KBRB*, and the enzyme was characterized. The *celEdx16* gene had an open reading frame of 1,104-base pairs, which encoded 367 amino acids to yield a protein of molecular mass 40.4 kDa. The amino acid sequence was 53% identical to that of an endoglucanase from *Clostridium thermocellum*. CelEdx16 was overexpressed in *Escherichia coli* and purified using Ni-NTA affinity chromatography. The specific endocellulase and exocellulase activities of CelEdx16 were 15.9 and 3.6 x 10^{-2} U mg^{-1}, respectively. The Michaelis-Menten constant (K_m values) and the maximal reaction velocities (V_{max} *values*) of CelEdx16 were 47.1 μM and 9.6 x 10^{-3} μmole min^{-1} when endocellulase activity was measured and 106.3 μM and 2.1 x 10^{-5} μmol min^{-1} when exocellulase activity was assessed. CelEdx16 was optimally active at pH 5.0 and 40 °C.
PMID: 21046376

Keywords : Screening; Korean Bovine Ruminal Bacterium; Bifunctional Endo-/Exo-Type Cellulase; Cloning; *Trichoderma reesei*; *Clostridium cellulovorans*; *Orpinomyces joyonii*; Endoglucanase Gene

Article 275

Truncation of N- and C-terminal regions of *Streptococcus mutans* dextranase enhances catalytic activity

Appl Microbiol Biotechnol. 2011 Jul; 91(2):329-39.

Kim YM*, Shimizu R, Nakai H, Mori H, Okuyama M, Kang MS, Fujimoto Z, Funane K, Kim D, Kimura A

*Co-corresponding: u9897854@kribb.re.kr
Infection Control Material Research Center

Multiple forms of native and recombinant endo-dextranases (Dexs) of the glycoside hydrolase family (GH) 66 exist. The GH 66 Dex gene from *Streptococcus mutans* ATCC 25175 (SmDex) was expressed in *Escherichia coli*. The recombinant full-size (95.4 kDa) SmDex protein was digested to form an 89.8 kDa isoform (SmDex90). The purified SmDex90 was proteolytically degraded to more than seven polypeptides (23-70 kDa) during long storage. The protease-insensitive protein was desirable for the biochemical analysis and utilization of SmDex. GH 66 Dex was predicted to comprise four regions from the N- to C-termini: N-terminal variable region (N-VR), conserved region (CR), glucan-binding site (GBS), and C-terminal variable region (C-VR). Five truncated SmDexs were generated by deleting N-VR, GBS, and/or C-VR. Two truncation-mutant enzymes devoid of C-VR (TM-NCGΔ) or N-VR/C-VR (TM-ΔCGΔ) were catalytically active, thereby indicating that N-VR and C-VR were not essential for the catalytic activity. TM-ΔCGΔ did not accept any further protease-degradation during long storage. TM-NCGΔ and TM-ΔCGΔ enhanced substrate hydrolysis, suggesting that N-VR and C-VR induce hindered substrate binding to the active site.
PMID: 21479716

Keywords : Endo-Dextranase; Glycoside Hydrolase Family 66; Limited Proteolysis; Truncation; Sequence-Analysis; Hydrolyzing Enzymes; *Bacillus* sp; T-3040

Article 276

Rice *OsERG3* encodes an unusual small C2-domain protein containing a Ca(2+)-binding module but lacking hospholipid-binding properties

Biochim Biophys Acta. 2011 Dec; 1810(12):1317-22.

Kang CH, Moon BC, Park HC, Koo SC, Jeon JM, Cheong YH, Chung WS, Lim CO, Kim JY, Yoon BD, Lee SY, Kim CY*

*Corresponding: kimcy@kribb.re.kr
Infection Control Material Research Center

BACKGROUND: The C2 domain is a Ca(2+)/phospholipid-binding motif found in many proteins involved in signal transduction or membrane trafficking. *OsERG3* is a homolog of *OsERG1*, a gene encoding a small C2-domain protein in rice.
METHODS: OsERG3 Ca(2+)-binding and phospholipid-binding assays were carried out using (3)H-labeled phospholipid liposomes and a (45)Ca(2+) overlay assay, respectively. Cytosolic expression of OsERG3 was investigated by Western blot analysis and the *OsERG3*::*smGFP* transient expression assay.
RESULTS: *OsERG3* transcript levels were greatly enhanced by treatment with a fungal elicitor and Ca(2+)-ionophore. OsERG3 protein proved unable to interact with phospholipids regardless of the presence or absence of Ca(2+) ions. Nonetheless, OsERG3 displayed calcium-binding activity in an *in vitro*(45)Ca(2+)-binding assay, a property not observed with OsERG1. The cytosolic location of OsERG3 was not altered by the presence of fungal elicitor or Ca(2+)-ionophore.
CONCLUSIONS: *OsERG3* encodes a small C2-domain protein consisting of a single C2 domain. OsERG3 binds Ca(2+) ions but not phospholipids. OsERG3 is a cytosolic soluble protein. The OsERG3 gene may play a role in signaling pathway involving Ca(2+) ions.
GENERAL SIGNIFICANCE: The data demonstrate that OsERG3 is an unusual small C2-domain protein containing a Ca(2+)-binding module but lacking phospholipid-binding properties.

PMID:21756975

Keywords : Rice; Signal Transduction; Small C2 domain Protein; Ca2+/Phospholipid Binding; Membrane-Binding; Fungal Elicitor; Kinase C; Synaptotagmin; Phloem; Motif

Article 277

Characteristic of alkylated chalcones from *Angelica keiskei* on influenza virus neuraminidase inhibition

Bioorg Med Chem Lett. 2011 Sep; 21(18):5602-4.

Park JY, Jeong HJ, Kim YM, Park SJ, Rho MC, Park KH, Ryu YB*, Lee WS*

*Co-corresponding: ybryu@kribb.re.kr wslee@kribb.re.kr
Infection Control Material Research Center

As part of our ongoing effort to develop influenza virus neuraminidase (NA) inhibitors from various medicinal plants, we utilized bioassay-guided fractionation to isolated six alkylated chalcones (1-6) from *Angelica keiskei*. Xanthokeistal A (1) emerged as new compound containing the rare alkyl substitution, *6,6-dimethoxy-3-methylhex-2-enyl*. When we tested the ability of these individual alkyl substituted chalcones to inhibit influenza virus NA hydrolysis, we found that 2-hydroxy-3-methyl-3-butenyl alkyl (HMB) substituted chalcone (3, IC_{50}=12.3 μM) showed most potent inhibitory activity. The order of potency of substituted alkyl groups on for NA inhibition was HMB>6-hydroxyl-3,7-dimethyl-octa-2,7-dienyl>dimethylallyl>geranyl. All NA inhibitors screened were found to be reversible noncompetitive inhibitors.

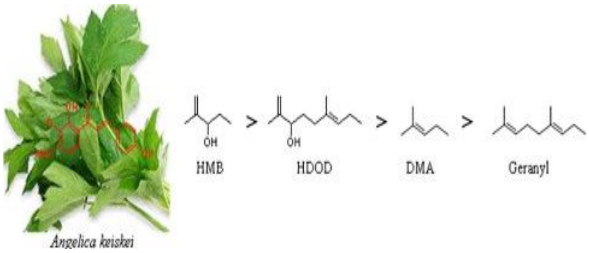

PMID: 21824777

Keywords : *Angelica keiskei*; Alkylated Chalcone; Neuraminidase; H1N1; Oseltamivir; Flavonoids

Article 278

1,3-Propandiol production by engineered *Hansenula polymorpha* expressing *dha* genes from *Klebsiella pneumoniae*

Bioprocess Biosyst Eng. 2011 Feb; 34(2):231-6.

Hong WK, Kim CH, Heo SY, Luo LH, Oh BR, Rairakhwada D, Seo JW*

*Corresponding: jwseo@kribb.re.kr
Applied Microbiology Research Center

Currently, 1,3-propanediol (1,3-PD) is an important chemical widely used in polymer production, but its availability is being restricted owing to its expensive chemical synthesis. A methylotrophic yeast *Hansenula polymorpha* was engineered by expression of *dhaB1, dhaB2, dhaB3, dhaB*$_{RA1}$ and *dhaB*$_{RA2}$ encoding glycerol dehydratase complex and *dhaT* encoding 1,3-PD oxidoreductase from *Klebsiella pneumoniae* under direction of promoter of glyceraldehyde-3 phosphate dehydrogenase (GAPDH). The engineered recombinant yeast strain can produce 1,3-PD from glucose (2.4 g L^{-1}) as well as glycerol (0.8 g L^{-1}), which might lead to a safe and cost-effective method for industrial production of 1,3-PD from various biomass resources.

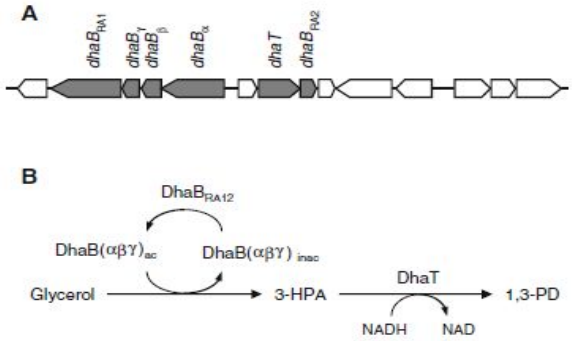

PMID: 20820806

Keywords : *Hansenula polymorpha*; Glycerol Dehydratase; 1,3-Propanediol; *Klebsiella pneumoniae*; Microbial-Production

Article 279

Efficient production of ethanol from crude glycerol by a *Klebsiella pneumoniae* mutant strain

Bioresour Technol. 2011 Feb; 102(4):3918-22.

Oh BR, Seo JW, Heo SY, Hong WK, Luo LH, Joe MH, Park DH, Kim CH*

*Corresponding: kim3641@kribb.re.kr
Applied Microbiology Research Center

A mutant strain of *Klebsiella pneumoniae*, termed GEM167, was obtained by γ irradiation, in which glycerol metabolism was dramatically affected on exposure to γ rays. Levels of metabolites of the glycerol reductive pathway, 1,3-propanediol (1,3-PD) and 3-hydroxypropionic acid (3-HP), were decreased in the GEM167 strain compared to a control strain, whereas the levels of metabolites derived from the oxidative pathway, 2,3-butanediol (2,3-BD), ethanol, lactate, and succinate, were increased. Notably, ethanol production from glycerol was greatly enhanced upon fermentation by the mutant strain, to a maximum production level of 21.5 g/l, with a productivity of 0.93 g/l/h. Ethanol production level was further improved to 25.0 g/l upon overexpression of *Zymomonas mobilis pdc* and *adhII* genes encoding pyruvate decarboxylase (Pdc) and aldehyde dehydrogenase (Adh), respectively in the mutant strain GEM167.

PMID: 21186120

Keywords : Glycerol; Ethanol Production; Anaerobic Fermentation; *Klebsiella pneumoniae*; Mutant; *Saccharomyces cerevisiae*; 1,3-Propanediol; Inactivation; Pathway

Article 280

Regioselective deglycosylation of onion quercetin glucosides by *Saccharomyces cerevisiae*

Biotechnol Lett. 2011 Apr; 33(4):783-6.

Chung DM, Chung YC, Maeng PJ, Chun HK*

*Corresponding: hkchun@kribb.re.kr
Infection Control Material Research Center

Bioconversion of quercetin glucosides using four generally recognized as safe (GRAS) organisms (*Aspergillus oryzae, Bacillus subtilis, Lactobacillus plantarum,* and *Saccharomyces cerevisiae*) was evaluated by measuring changes in the levels of quercetin compounds of onion. Of the four organisms, *S. cerevisiae* increased the content of quercetin-3-O-β-D-glucoside (III; isoquercitrin) and quercetin (IV), whereas decreasing quercetin-3,4'-O-β-D-glucoside (I) and quercetin-4'-O-β-D-glucoside (II). Also, *S. cerevisiae* converted authentic compound I to III, and II to IV, respectively. These results suggest that *S. cerevisiae* can be used to increase the levels of isoquercitrin (III), the most bioavailable quercetin compound in onion.

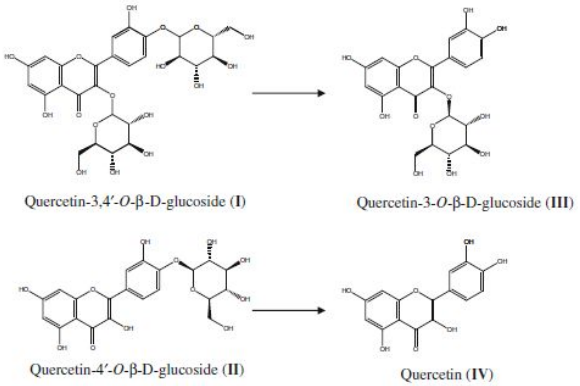

PMID: 21188617

Keywords : Bioconversion; Isoquercitrin; Onion; Quercetin; *Saccharomyces cerevisiae*; Allium-Cepa; Glycosides

Article 281

Silver-stained fibrin zymography: separation of proteases and activity detection using a single substrate-containing gel

Biotechnol Lett. 2011 Aug; 33(8):1663-6.

Chung DM, Kim KE, Ahn KH, Park CS, Kim DH, Koh HB, Chun HK, Yoon BD, Kim HJ, Kim MS*, Choi NS

*Co-corresponding: ms5732@kribb.re.kr
Bioindustrial Process Research Center

A new zymogram method, silver-stained fibrin zymography, for separation of protease bands and activity detection using a single substrate gel, was developed. The method takes advantage of the nanoscale sensitivity of both zymography and silver staining. After SDS-PAGE in a gel containing fibrin, the gel was incubated in enzyme reaction buffer and the zymogram was silver-stained. Bands with protease activity were stained with silver in clear areas where the protein substrate had been degraded. The molecular sizes of proteases were accurately determined. Furthermore, proteases of high molecular weight were clearly and sharply resolved.

PMID: 21487781

Keywords : Protease; Silver Staining; Fibrin Zymography; Zymogram Method; Proteolytic-Enzymes; SDS-PAGE

Article 282

Phenolic compounds isolated from *Zingiber officinale* roots inhibit cell adhesion

Food Chem. 2011; 128(3):778-82.

Lee SW, Lim JH, Kim MS, Jeong JH, Song GY, Lee WS, Rho MC*

*Corresponding: rho-m@kribb.re.kr
Bioindustrial Process Research Center

Inhibitors of celladhesion molecule-mediated celladhesion might be novel therapeutic agents for the treatment of various inflammatory diseases. In this study, nine phenoliccompounds were isolated from the methanol extracts of *Zingiber officinale* roots by bioactivity-guided fractionation. The structures of the compounds were determined by spectroscopic analysis (1H, 13C NMR and MS), to be 6-gingerol (1), 8-gingerol (2), 10-gingerol (3), 6-shogaol (4), 8-shogaol (5), 10-shogaol (6), dehydro-6-gingerdione (7), dehydro-10-gingerdione (8) and 6-paradol (9). Compounds3, 4, 5 and 7 inhibited direct binding between sICAM-1 and LFA-1 of the THP-1 cells in a dose-dependent manner with IC50 values of 57.6, 27.1, 65.4 and 62.0 μM, respectively. Compounds4 and 7 had an inhibitory effect on direct binding between sVCAM-1 and VLA-4 of THP-1 cells. These results suggest that the phenoliccompounds from *Z. officinaleroots* are good candidates for therapeutic strategies aimed at inflammation.

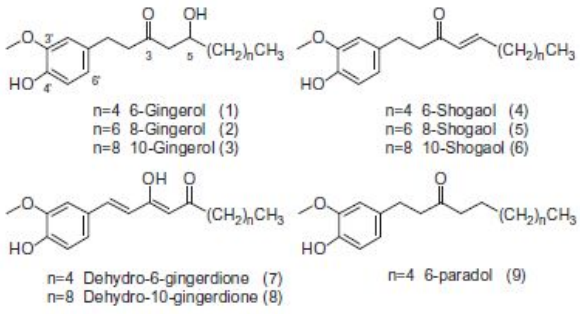

Keywords : *Zingiber officinale*; Zingiberaceae; Gingerols; Shogaols; Cell Adhesion Molecules; THP-1 Cells; Antibody; Macrophages; Antagonists; Psoriasis

Article 283

Novel quantitative method for the degree of branching in dextran

Food Sci Biotech. 2011; 20(2):537-41.

Kim YM*, Kimura A, Kim D

*First : u9897854@kribb.re.kr
Infection Control Material Research Center

A novel quantitative method for the determination of degree of branching in *Leuconostoc mesenteroides* B-512F dextran was developed by using the combination of 3 dextran-degrading enzymes. First, *Paenibacillus* sp. endo-dextranase was randomly degraded B-512F dextran into linear or branched isomalto-oligosaccharides with various degree of polymerization (2–8). Second, *Streptococcus mutans* dextran glucosidase hydrolyzed linear or branched isomalto-oligosaccharides into glucose and branched isomalto-penta-saccharides. Third, the branched isomaltopenta-saccharide was degraded into glucose by using *Bacteroides thetaimicron* α-glucosidase. The number of branching points in B-512F dextran (5.42%) was determined by the difference in the amount of glucose in the reaction digest between BTGase-PDex and DGase-PDex treatments.

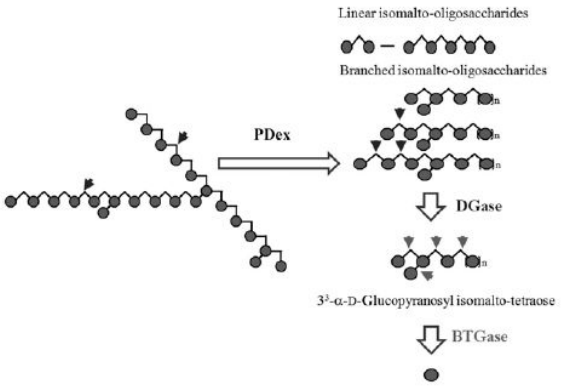

Keywords : Dextran; Endo-Dextranase; Exo-Dextranase; Degree of Branching; Lipomyces-Starkeyi; Glucanhydrolase; Polysaccharides; Reagent; Cloning; Enzyme

Article 284

Isolation of cholinesterase-inhibiting flavonoids from *Morus lhou*

J Agric Food Chem. 2011 May; 59(9):4589-96.

Kim JY, Lee WS*, Kim YS, Curtis-Long MJ, Lee BW, Ryu YB, Park KH

*Co-first: wslee@kribb.re.kr
Infection Control Material Research Center

Cholinesterases are key enzymes that play important roles in cholinergic transmission. Nine flavonoids displaying cholinesterase inhibitory activity were isolated from the root bark of *Morus lhou* L., a cultivated edible plant. The isolated compounds were identified as a new flavone (1), 5'-geranyl-5,7,2',4'-tetrahydroxyflavone (2), kuwanon U (3), kuwanon E (4), morusin (5), morusinol (6), cyclomorusin (7), neocyclomorusin (8), and kuwanon C (9). All compounds apart from compound 6 inhibited cholinesterase enzyme in a dose-dependent manner with K_i values ranging between 3.1 and 37.5 μM and between 1.7 and 19.1 μM against acetylcholinesterase (AChE) and butyrylcholinesterase (BChE) enzymes, respectively. The new compound was charactierized as 5'-geranyl-4'-methoxy-5,7,2'-trihydroxyflavone (1). It showed the most potent inhibitory activity (K_i = 3.1 μM for AChE, K_i = 1.74 μM for BChE). Lineweaver-Burk and Dixon plots and their secondary replots indicated that flavones (5-9) with prenyl substitution on C-3 were noncompetitive inhibitors, whereas those unsubstituted (1-4) at C-3 were mixed inhibitors of both AChE and BChE. In conclusion, this is the first study to demonstrate that alkylated flavonoids of *M. lhou* have potent inhibitory activities against AChE and BChE.

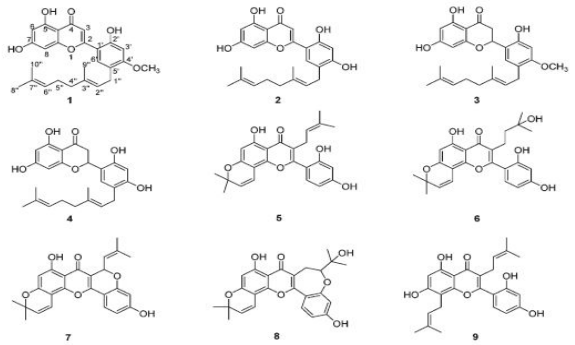

PMID: 21434689

Keywords : Alzheimer's Disease; Acetylcholinesterase; Butyrylcholinesterase; Cholinesterase Inhibitors; *Morus lhou*; Cultivated Mulberry Tree; Alba L; Polyphenols; Tyrosinase

Article 285

Influenza virus neuraminidase inhibitory activity of phlorotannins from the edible brown alga *Ecklonia cava*

J Agric Food Chem. 2011 Jun; 59(12):6467-73.

Ryu YB, Jeong HJ, Yoon SY, Park JY, Kim YM, Park SJ, Rho MC, Kim SJ, Lee WS*

*Corresponding: wslee@kribb.re.kr
Infection Control Material Research Center

Influenza A virus infections continue to pose a major threat to humans and several animal species. Neuraminidase (NA) is one of the most promising targets for the development of drugs against influenza viruses because of its critical role in the viral life cycle. During the course of a search for NA inhibitors from edible natural sources, we found that the ethyl acetate layer of ethanol extracts of *Ecklonia cava* showed extremely high NA-inhibitory activity (72.1% inhibition at 30 μg/mL). Bioactivity-guided fractionation of the ethyl acetate layer yielded five phlorotannins, identified as phloroglucinol (1), eckol (2), 7-phloroeckol (3), phlorofucofuroeckol (4), and dieckol (5). The inhibitory activities of these compounds (1-5) against NAs from group-1 (A/Bervig_Mission/1/18 [H1N1], A/PR/8/34 [H1N1]) and group-2 (A/Hong Kong/8/68 [H3N2], A/Chicken/Korea/MS96/96 [H9N2]) influenza A were evaluated to determine potencies and kinetic behavior. Analyses using various *in vitro* influenza A virus NA assays showed that all five phlorotannin derivatives were selective NA inhibitors. Of the phlorotannins, phlorofucofuroeckol (4) exhibited the most potent inhibitory activities toward group-1 NAs (IC_{50} values, 4.5 and 14.7 μM), whereas dieckol (5) potently inhibited group-2 NAs. Kinetic analyses indicated that compounds 1-5 were all noncompetitive. Notably, these noncompetitive inhibitors synergized with oseltamivir to enhance the NA-inhibitory effects of oseltamivir.

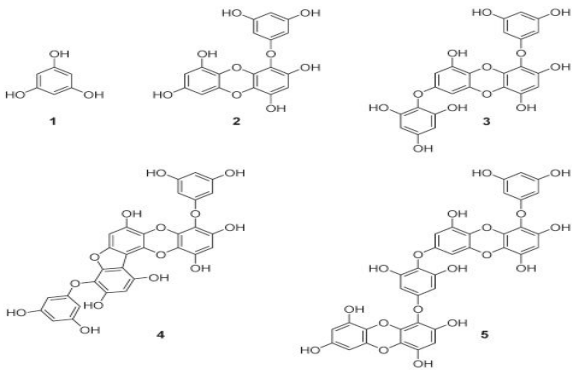

PMID: 21585204

Keywords : Influenza Virus; Neuraminidase; *Ecklonia cava*; Phlorotannin; DNA-Damage; H1N1; ESR

Article 286

Expression and characterization of a second L-amino acid deaminase isolated from *Proteus mirabilis* in *Escherichia coli*

J Basic Microbiol. 2011 Apr; 51(2):129-35.

Baek JO, Seo JW, Kwon O, Seong SI, Kim IH, Kim CH*

*Co-corresponding: kim3641@kribb.re.kr
Applied Microbiology Research Center

L-amino acid deaminases catalyze the deamination of natural L-amino acids. Two types of L-amino acid deaminase have been identified in *Proteus* species. One exhibits high levels of activity toward a wide range of aliphatic and aromatic L-amino acids, typically L-phenylalanine, whereas the other acts on a relatively narrow range of basic L-amino acids, typically L-histidine. In this study, we cloned, expressed, and characterized a second amino acid deaminase, termed Pm1, from *P. mirabilis* KCTC 2566. Homology alignment of the deduced amino acid sequence of Pm1 demonstrated that the greatest similarity (96%) was with the L-amino acid deaminase (LAD) of *P. vulgaris*, and that homology with Pma was relatively low (72%). Also, similar to LAD, Pm1 was most active on L-histidine, indicating that Pm1 belongs to the second type of amino acid deaminase. In agreement with this conclusion, the V_{max} and K_m values of Pm1 were 119.7 (μg phenylpyruvic acid/mg/min) and 31.55 mM phenylalanine, respectively, values lower than those of Pma. The Pml deaminase will be very useful industrially in the preparation of commercially valuable materials including urocanic acid and α-oxoglutarate.

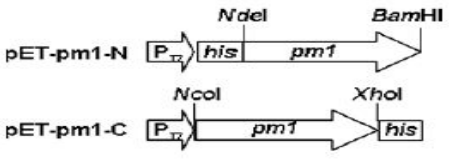

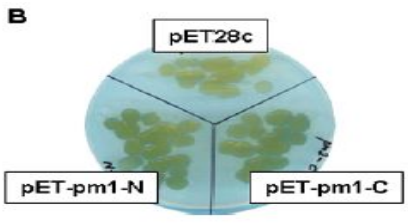

PMID: 21298676

Keywords : *Proteus mirabilis*; Amino Acid Deaminase; Phenylpyruvic Acid; Phenyllactic Acid; Ferric Chloride; *Rhodococcus opacus*; Sequence; Oxidases; Metabolism; Vulgaris

Article 287

Stimulation of reductive glycerol metabolism by overexpression of an aldehyde dehydrogenase in a recombinant *Klebsiella pneumoniae* strain defective in the oxidative pathway

J Ind Microbiol Biotechnol. 2011 Aug; 38(8):991-9.

Luo LH, Seo JW, Oh BR, Seo PS, Heo SY, Hong WK, Kim DH, Kim CH*

*Corresponding: kim3641@kribb.re.kr
Applied Microbiology Research Center

Previously, we constructed a glycerol oxidative pathway-deficient mutant strain of *Klebsiella pneumoniae* by inactivation of glycerol dehydrogenase (*dhaD*) to eliminate by-product synthesis during production of 1,3-propanediol (1,3-PD) from glycerol. Although by-product formation was successfully blocked in the resultant strain, the yield of 1,3-PD was not enhanced, probably because *dhaD* disruption resulted in insufficient regeneration of the cofactor NADH essential for the activity of 1,3-PD oxidoreductase (DhaT). To improve cofactor regeneration, in the present study we overexpressed an NAD^+-dependent aldehyde dehydrogenase in the recombinant strain. To this end, an aldehyde dehydrogenase AldHk homologous to *E. coli* AldH but with NAD^+-dependent propionaldehyde dehydrogenase activity was identified in *K. pneumoniae*. Functional analysis revealed that the substrate specificity of AldHk embraced various aldehydes including propionaldehyde, and that NAD^+ was preferred over $NADP^+$ as a cofactor. Overexpression of AldHk in the glycerol oxidative pathway-deficient mutant AK/pVOTHk resulted in a 3.6-fold increase (0.57 g l^{-1} to 2.07 g l^{-1}) in the production of 3-hydroxypropionic acid (3-HP), and a 1.1-fold enhancement (8.43 g l^{-1} to 9.65 g l^{-1}) of 1,3-PD synthesis, when glycerol was provided as the carbon source, compared to the levels synthesized by the control strain (AK/pVOT). Batch fermentation using AK/pVOTHk showed a significant increase (to 70%, w/w) in conversion of glycerol to the reductive metabolites, 1,3-PD and 3-HP, with no production of by-products except acetate.

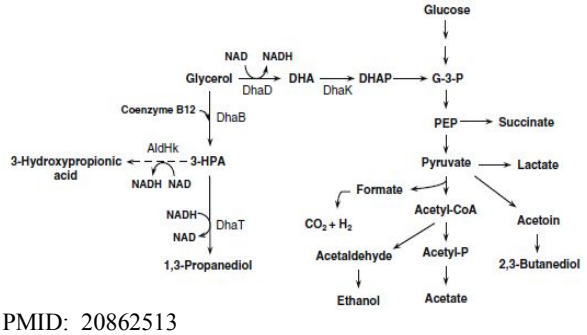

PMID: 20862513

Keywords : Glycerol; *Klebsiella pneumoniae*; Aldehyde Dehydrogenase; 3-Hydroxypropionic Acid; 1,3-Propanediol; Fermentation; Bacteria

Article 288

A phosphorylation assay using [γ-^{32}P]ATP: A highly sensitive detection of protein kinase C

J Labelled Comp Radiopharm. 2011; 54(2):105–9.

Ko KC*, Choi MH, Park SH

*First: kcko@kribb.re.kr
Applied Microbiology Research Center

The involvement of protein kinase C (PKC) in many biological processes such as development, memory, cell differentiation and proliferation, and carcinogenesis has been demonstrated. Using the *mep45* gene encoding the 45-kDa major envelope protein (Mep45) of *Selenomonas ruminantium*, a protein-fused substrate (neurogranin-Mep45, MFS-PKC) was cloned, which is a highly selective substrate for PKC. The recombinant protein-fused substrate can be constantly produced in reasonable quantities with a small outlay. In this study, a suitable strategy for the detection of the phosphorylation of a peptide-type substrate and a Mep45-fused substrate catalyzed by PKC by using a sensitive radiodetection is described. This strategy can be applicable to the development of protein microarray, which can be a useful tool for high-throughput screening in biological and medical research.

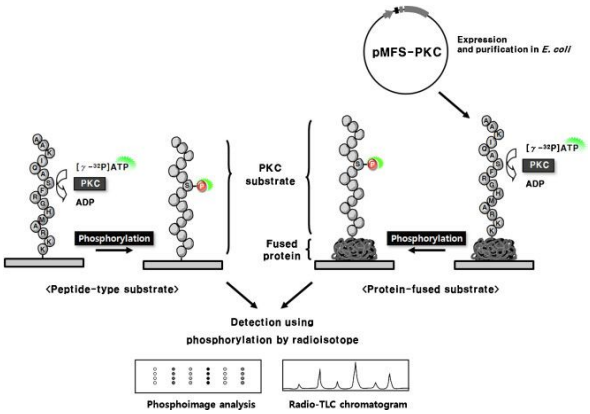

Keywords : Radiodetection; Radioisotope Detection Technique; Protein Kinase C; Phosphorylation Detection; Biomolecule Interactions; Biochip; Arrays

Article 289

Manassantin A and B from *Saururus chinensis* inhibit interleukin-6-induced signal transducer and activator of transcription 3 activation in Hep3B cells

J Pharmacol Sci. 2011; 115(1):84-8.

Chang JS, Lee SW, Kim MS, Yun BR, Park MH, Lee SG, Park SJ, Lee WS, Rho MC*

*Corresponding: rho-m@kribb.re.kr
Bioindustrial Process Research Center

Inhibition of interleukin-6 (IL-6) has been postulated to be an effective therapy in the pathogenesis of several inflammatory diseases. The current study was performed to examine potential effects of manassantin A and B isolated from *Saururus chinensis* on the IL-6-induced response to human hepatoma cells. We found that manassantin A and B inhibit signal transducer and activator of transcription 3 (Stat3) activity stimulated by IL-6. We also found that both compounds decreased IL-6-induced Stat3 phosphorylation and nuclear translocation. Both compounds blocked suppressor of cytokine signaling 3 (SOCS-3)-mRNA expression induced by IL-6. In addition, we found that Stat3 inhibitory effects of these compounds could be related to protein tyrosine phosphatase. These findings suggest that manassantin A and B could be useful remedies for treatment of inflammatory diseases by inhibiting IL-6 action.

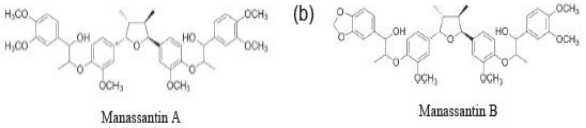

Manassantin A　　Manassantin B

PMID: 21258167

Keywords : Manassantin; Interleukin-6; Signal Transducer and Activator of Transcription 3 (Stat3); NF-Kappa-B; Endothelial Cells; Gene Expression; Cancer Cells; Pathway

Article 290

Hypouricemic effects of anthocyanin extracts of purple sweet potato on potassium oxonate-induced hyperuricemia in mice

Phytother Res. 2011; 25(9):1415-7.

Hwa KS, Chung DM, Chung YC, Chun HK*

*Corresponding: hkchun@kribb.re.kr
Infection Control Material Research Center

Gout is a clinical syndrome in which tissue damage is induced by a chronic metabolic disorder associated with increased concentrations of uric acid in the blood. The study investigated the hypouricemic effects of anthocyanin extracts from purple sweet potato (APSP), and allopurinol, on serum uric acid levels in hyperuricemic mice. It was found that administration of a single oral dose of 100 mg/kg APSP to such animals reduced the serum uric acid concentration to 4.10 ± 0.04 mg/dL, compared with a concentration of 10.25 ± 0.63 mg/dL in the hyperuricemic control group.

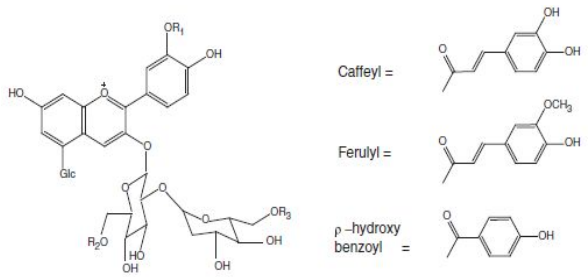

PMID: 21433153

Keywords : Allopurinol; Anthocyanins; Gout; Hyperuricemia; Purple Sweet Potato; Xanthine-Oxidase; Uric Acid; Serum

Article 291

Production and purification of human papillomavirus type 33 L1 virus-like particles from *Spodoptera frugiperda* 9 cells using two-step column chromatography

Protein Expr Purif. 2011 Feb; 75(2):211-7.

Baek JO, Seo JW, Kim IH, Kim CH*

*Co-corresponding: kim3641@kribb.re.kr
Applied Microbiology Research Center

The major capsid protein L1 of human papillomavirus (HPV) is essential in construction of recombinant antigen vaccines against cervical cancer. HPV type 33 accounts for about 10% of all HPV infections in Asia. The gene encoding the major capsid protein L1 of the high-risk HPV type 33 was isolated from a Korean patient and expressed in *Sf*-9 insect cells using a baculovirus expression system. HPV33 L1 protein was isolated by two-step chromatographic purification using strong-cation exchange and ceramic hydroxyapatite chromatography. Strong-cation-exchange chromatography was performed to achieve initial purification of HPV33 L1 and to remove most contaminating proteins, and secondary ceramic hydroxyapatite chromatography yielded pure HPV33 L1 virus-like particles (VLPs). Ceramic hydroxyapatite columns are particularly useful in the purification of antibodies, antigens, human viruses, and VLPs, and we thus used this system. The expression of HPV L1 protein in *Sf*-9 cells was examined by SDS-PAGE, Western-blotting, and ELISA analyses, and the data showed that HPV33 L1 VLPs were determined to > 98% purity and 58.7% recovery by a quantitative immuno-ELISA assay. Transmission electron microscopy analysis revealed that the HPV VLPs were approximately 50-60 nm in diameter and created by self-assembly of HPV L1 protein. The efficient and simple purification process described here should be useful in production of a cervical cancer vaccine.

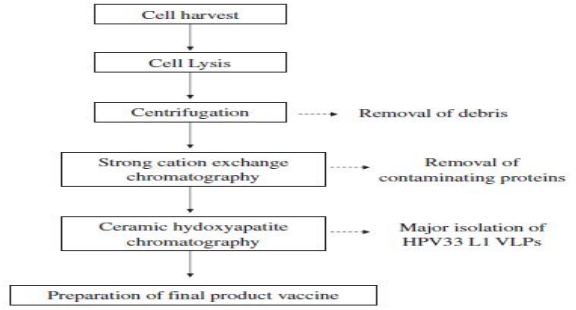

PMID: 20716445

Keywords : Human Papillomavirus (HPV); Baculovirus System; Virus-like Particle (VLP); Strong-Cation Exchange; Ceramic Hydroxyapatite; *Saccharomyces cerevisiae*; Infection; Vaccine

2011
KRIBB Article Abstracts
Corresponding Articles
Indexed in SCIE

Indexes

Korea Research Institute of Bioscience and Biotechnology


KRIBB
www.kribb.re.kr

Corresponding Author Index

Journal Index

Keyword Index

한국생명공학연구원
Korea Research Institute of Bioscience and Biotechnology
305-806 대전광역시 유성구 과학로 125
Tel. 042)860-4114 Fax. 042)861-1759 http://www.kribb.re.kr